GRAVITATIONAL WAVES: A NEW WINDOW TO THE UNIVERSE

EDITED BY: Rosalba Perna and Bruno Giacomazzo
PUBLISHED IN: Frontiers in Astronomy and Space Sciences and Frontiers in Physics

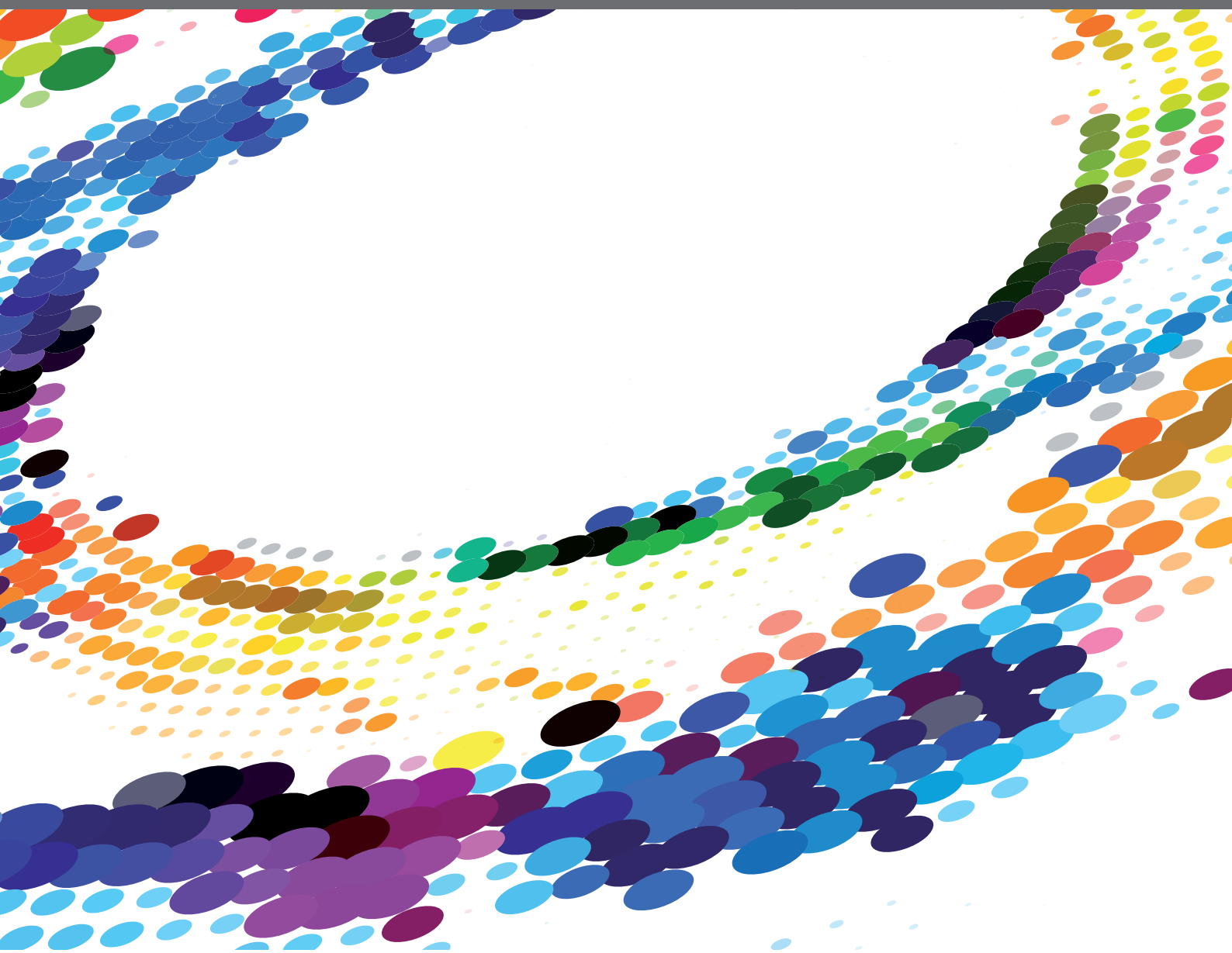

frontiers Research Topics

frontiers

ISSN 1664-8714
ISBN 978-2-88966-941-7
DOI 10.3389/978-2-88966-941-7

About Frontiers

Frontiers is more than just an open-access publisher of scholarly articles: it is a pioneering approach to the world of academia, radically improving the way scholarly research is managed. The grand vision of Frontiers is a world where all people have an equal opportunity to seek, share and generate knowledge. Frontiers provides immediate and permanent online open access to all its publications, but this alone is not enough to realize our grand goals.

Frontiers Journal Series

The Frontiers Journal Series is a multi-tier and interdisciplinary set of open-access, online journals, promising a paradigm shift from the current review, selection and dissemination processes in academic publishing. All Frontiers journals are driven by researchers for researchers; therefore, they constitute a service to the scholarly community. At the same time, the Frontiers Journal Series operates on a revolutionary invention, the tiered publishing system, initially addressing specific communities of scholars, and gradually climbing up to broader public understanding, thus serving the interests of the lay society, too.

Dedication to Quality

Each Frontiers article is a landmark of the highest quality, thanks to genuinely collaborative interactions between authors and review editors, who include some of the world's best academicians. Research must be certified by peers before entering a stream of knowledge that may eventually reach the public - and shape society; therefore, Frontiers only applies the most rigorous and unbiased reviews.
Frontiers revolutionizes research publishing by freely delivering the most outstanding research, evaluated with no bias from both the academic and social point of view. By applying the most advanced information technologies, Frontiers is catapulting scholarly publishing into a new generation.

What are Frontiers Research Topics?

Frontiers Research Topics are very popular trademarks of the Frontiers Journals Series: they are collections of at least ten articles, all centered on a particular subject. With their unique mix of varied contributions from Original Research to Review Articles, Frontiers Research Topics unify the most influential researchers, the latest key findings and historical advances in a hot research area! Find out more on how to host your own Frontiers Research Topic or contribute to one as an author by contacting the Frontiers Editorial Office: frontiersin.org/about/contact

GRAVITATIONAL WAVES: A NEW WINDOW TO THE UNIVERSE

Topic Editors:
Rosalba Perna, Stony Brook University, United States
Bruno Giacomazzo, University of Milano-Bicocca, Italy

Citation: Perna, R., Giacomazzo, B., eds. (2021). Gravitational Waves: A New Window to the Universe. Lausanne: Frontiers Media SA. doi: 10.3389/978-2-88966-941-7

Table of Contents

frontiers in Astronomy and Space Sciences

EDITORIAL
published: 30 April 2021
doi: 10.3389/fspas.2021.681919

Editorial: Gravitational Waves: A New Window to the Universe

Rosalba Perna[1] *and Bruno Giacomazzo*[2,3]*

[1] Department of Physics and Astronomy, Stony Brook University, Stony Brook, NY, United States, [2] Department of Physics "Giuseppe Occhialini", University of Milano-Bicocca, Milan, Italy, [3] INFN, Division of Milano-Bicocca, Milan, Italy

Keywords: gravitational waves, gamma-ray burst, kilonovae, numerical relativity, neutron star, black hole

Editorial on the Research Topic

Gravitational Waves: A New Window to the Universe

This Research Topic focuses on gravitational waves, and their role in advancing knowledge in research areas ranging from cosmology to high energy physics to nuclear physics.

The first article of this Research Topic (Palenzuela) provides a short introduction to the field of numerical relativity, including also a summary of the 3+1 decomposition of Einstein's equations, allowing the reader to get a broad overview of the equations and numerical methods used in this field. Numerical relativity is one of the fundamental tools for the study of compact binary mergers and it has allowed for the study of gravitational wave sources, such as the ones discussed in the following articles.

Ciolfi and Foucart present an overview of the state of the art in the field of binaries composed of two neutron stars (NSs) or of an NS and a black hole (BH). Neutron star binaries have gained a lot of attention since the detection of the first gravitational wave (GW) signal emitted by one of such systems (GW170817). Observations of an electromagnetic counterpart have provided evidence for the presence of a relativistic jet and for the ejection of high-density NS material. The formation of a jet, and the properties of the ejecta have been the subject of numerous investigations, and they are reviewed in Ciolfi.

Similarly, in Foucart the reader will find an overview of NS-BH mergers and in particular of what theoretical models predict for their GW and electromagnetic (EM) emission. In the case of NS-BH mergers it is critical for the NS to be tidally disrupted by the companion BH in order to be able to produce bright EM signals and this is strongly correlated with the binary properties, including the NS equation of state.

One of the most detected sources of GWs is given by binary BH mergers and these are discussed in detail in Schmidt. This review describes both how these sources can be modeled from a theoretical point of view as well as the properties, such as masses and spins, of the many binary BH systems detected by the LIGO-Virgo Collaboration.

Among the GW sources detected by LIGO/Virgo to date, GW170817 was especially important since it was accompanied by electromagnetic radiation covering a very broad spectrum, from gamma-rays to radio. Detailed modeling of both the prompt (gamma-ray) emission and the following longer-wavelength radiations demonstrated that the properties of this source were consistent with those of a classical short gamma-ray burst (SGRB), hence firmly establishing the link between those and an NS-NS merger. Given the importance of this finding, Lazzati is specifically devoted to a review of the source GW170817 and its connection to SGRBs.

Another important source of EM emission from a binary NS merger is given by the so-called kilonova, described in Barnes. With respect to SGRBs, kilonovae have the advantage of being isotropic emitters and therefore may be detected with most binary NS mergers. They also constitute the site for the production of heavy elements. Barnes provides a review of the theoretical models

OPEN ACCESS

Edited and reviewed by:
Gianluca Calcagni, Consejo Superior de Investigaciones Científicas (CSIC), Spain

***Correspondence:**
Bruno Giacomazzo
bruno.giacomazzo@unimib.it

Specialty section:
This article was submitted to Cosmology, a section of the journal Frontiers in Astronomy and Space Sciences

Received: *17 March 2021*
Accepted: *25 March 2021*
Published: *30 April 2021*

Citation:
Perna R and Giacomazzo B (2021) Editorial: Gravitational Waves: A New Window to the Universe. Front. Astron. Space Sci. 8:681919. doi: 10.3389/fspas.2021.681919

used to predict the heavy element production and observational appearance, and what we have learned from their first observation associated with GW170817.

The last two articles are dedicated to an overview of the formation channels of solar mass binary BH systems (Mapelli) and of future detections of supermassive BHs with LISA (Sesana). More specifically, Mapelli reviews the two main channels of BH-BH formation, that is the isolated one resulting from standard binary evolution, and the dynamical one, in which binaries are formed as a results of gravitational interactions in dense environments.

Looking into the future of gravitational wave science, Sesana provides a broad overview of the potential science with the Laser Interferometer Space Antenna (LISA). Expected to be launched in the 30s, GW detections with this instrument are expected to open an additional window into the Universe, and especially in the way the enigmatic supermassive BHs lurking in the center of galaxies were assembled.

AUTHOR CONTRIBUTIONS

RP and BG are the editors of this Research Topic.

FUNDING

RP acknowledged the support by NSF award #AST-2006839.

Conflict of Interest: The authors declare that the research was conducted in the absence of any commercial or financial relationships that could be construed as a potential conflict of interest.

frontiers in Astronomy and Space Sciences

MINI REVIEW
published: 10 September 2020
doi: 10.3389/fspas.2020.00058

Introduction to Numerical Relativity

*Carlos Palenzuela**

Departament de Fisica & IAC3, Universitat de les Illes Balears, Palma, Spain

Numerical Relativity is a multidisciplinary field including relativity, magneto-hydrodynamics, astrophysics and computational methods, among others, with the aim of solving numerically highly-dynamical, strong-gravity scenarios where no other approximations are available. Here we describe some of the foundations of the field, starting from the covariant Einstein equations and how to write them as a well-posed system of evolution equations, discussing the different formalisms, coordinate conditions, and numerical methods commonly employed nowadays for the modeling of gravitational wave sources.

Keywords: numerical relativity, Einstein equations, 3+1 decomposition, formulations, gauge conditions, numerical methods

1. INTRODUCTION

General Relativity is the theory that identifies gravity as the curvature of a four dimensional space-time manifold. The consequences of this identification deeply changed our conception of Nature. From the physics point of view, Relativity introduced new ideas, like that time and space are not absolute but depend on the observer, that the effects of gravity propagate at the speed of light, or that energy and matter are equivalent and can modify the structure of both space and time, among others. From the mathematical point of view, the main consequence is that gravity can be described by using the tools of differential geometry, where the basic object to represent a manifold is the metric g_{ab} that allow us to compute distances between neighboring points. The famous Einstein equations describe the dynamics of the four-dimensional space-time metric and how it is deformed by a given mass-energy distribution. On the other hand, the Bianchi identities from differential geometry ensure that the divergence of the Einstein tensor vanishes, implying the conservation of the stress-energy tensor (i.e., corresponding to energy and linear momentum conservation), which describes how matter moves in a curved spacetime.

One of the greatest achievements of General Relativity was the prediction of gravitational waves, space-time deformations produced by acceleration of masses which behave like waves as they propagate away from the sources. Gravitational waves are essentially unscattered between emission and detection, thereby giving direct information about the sources powering these phenomena. Precisely due to the weak interaction of these waves with matter, their existence was initially only confirmed indirectly by observations of the orbital dynamics of binary pulsars (Hulse and Taylor, 1975; Will, 2014). However, current kilometer-scale interferometric gravitational wave (GW) detectors, such as Advanced LIGO (aLIGO) (Abramovici et al., 1992) and Advanced Virgo (adVirgo) (Caron et al., 1997) facilities, since 2015 have directly detected gravitational waves on the kiloHertz frequency regime, consistent with the merger of binary black holes and binary neutron stars (Abbott et al., 2019). Further improvements on these detectors, as well as new ones added to the array of GW observatories, will allow to establish many routinary GW observations in the next few years. These new observations allow us a new way to study some of the most energetic and exotic processes in the universe and start a new era of gravitational wave astronomy that will inevitably lead to unprecedented discoveries and breakthroughs not only in Astrophysics

OPEN ACCESS

Edited by:
Bruno Giacomazzo,
University of Milano-Bicocca, Italy

Reviewed by:
Davood Momeni,
Sultan Qaboos University, Oman
Thomas Baumgarte,
Bowdoin College, United States

***Correspondence:**
Carlos Palenzuela
carlos.palenzuela@uib.es

Specialty section:
This article was submitted to Cosmology, a section of the journal Frontiers in Astronomy and Space Sciences

Received: *19 February 2020*
Accepted: *30 July 2020*
Published: *10 September 2020*

Citation:
Palenzuela C (2020) Introduction to Numerical Relativity. Front. Astron. Space Sci. 7:58. doi: 10.3389/fspas.2020.00058

and Cosmology, but also in fundamental theories like gravity and nuclear physics. The detection, identification, and accurate determination of the physical parameters of sources is crucial to validate (and challenge) not only our theories but also our astrophysical models, which rely both on precise experimental data and on the availability of template banks of theoretical waveforms. For the slow inspiral, when the neutron stars (NSs) or black holes (BHs) are widely separated, analytical approximations for the gravitational waveforms are provided by perturbative post-Newtonian (PN) expansion techniques (Blanchet, 2014). For the last orbits and merger, where the fields are particularly strong and most might be gained in terms of insight on fundamental physics, the PN expansion breaks down and the full Einstein equations have to be solved numerically. This has only become possible after a series of breakthroughs in the field of Numerical Relativity (Pretorius, 2005a; Baker et al., 2006b; Campanelli et al., 2006a), calling for an incorporation of this new type of information into data analysis strategies and methods. Since then, outstanding progress has been made to explore the late stage of binary coalescence with numerical methods. The next sections summarize some of the foundations of Numerical Relativity, with a view on the modeling of gravitational sources, from the construction of a well-posed evolution system to the numerical methods commonly employed to solve them. Notice that this review focus on Cauchy formulations, excluding other alternatives. For a wider overview of all the possible formulations, please see Lehner (2001).

2. EVOLUTION SYSTEMS

2.1. Einstein Equations

The equations of motion of a classical theory like General Relativity can be derived directly from a suitable action by using the Euler-Lagrange equations, leading to the well-known Einstein equations (Misner et al., 1973),

$$G_{ab} \equiv R_{ab} - \frac{R}{2} g_{ab} = 8\pi\, T_{ab}, \tag{1}$$

where G_{ab} is the Einstein tensor, R_{ab} is the Ricci tensor of the spacetime represented by the metric g_{ab}, $R \equiv g^{ab} R_{ab}$ is the Ricci or curvature scalar, and T_{ab} is the stress-energy tensor describing generically the matter-energy distributions in the spacetime. We have chosen geometric units such that $G = c = 1$ and adopt the convention where roman indices $a, b, c, \ldots$ denote space-time components (i.e., from 0 to 3), while $i, j, k, \ldots$ denote spatial ones (i.e., from 1 to 3).

The Ricci tensor can be written in terms of the Christophel symbols Γ^a_{bc} as follows

$$\begin{aligned} R_{ab} &\equiv \partial_c \Gamma^c_{ab} - \partial_a \Gamma^c_{cb} + \Gamma^c_{cd}\Gamma^d_{ab} - \Gamma^c_{da}\Gamma^d_{cb}, \\ \Gamma^c_{ab} &= \frac{1}{2} g^{cd}\left(\partial_a g_{bd} + \partial_b g_{ad} - \partial_d g_{ab}\right), \end{aligned} \tag{2}$$

Notice that Equations (1–2) form a system of ten non-linear partial differential equations (PDEs) for the spacetime metric components g_{ab}, which are coupled to the matter fields by means of the stress-energy tensor.

On the other hand, an important relation in differential geometry, known as the (contracted) Bianchi identities, implies the covariant conservation law for the Einstein tensor and, consequently, for the stress-energy tensor,

$$\begin{aligned} \nabla_a G^{ab} &= 0 \Longrightarrow \nabla_a T^{ab} = 0, \\ \nabla_a T^{ab} &= \partial_a T^{ab} + \Gamma^a_{ac} T^{cb} + \Gamma^b_{ac} T^{ac} \end{aligned} \tag{3}$$

where ∇_a is the covariant derivative, the generalization of the partial derivative on a manifold. These covariant equations correspond to conservation laws for both the energy and linear momentum, which are the basic physical equations to describe any matter field. Notice also that the Bianchi identities imply that four of the ten components of Einstein's equations cannot be independent. This redundancy gives rise to both the four coordinate degrees freedom and the four constraint equations, which will be clearly manifested in the 3+1 decomposition described in the next section.

2.2. The 3+1 Decomposition

Despite its elegance and compactness, the covariant form of the four-dimensional Einstein equations is not suitable to describe how the gravity fields evolve from an initial configuration toward the future. In such case, it is more intuitive to consider instead a time succession of three-dimensional spatial slice geometries, called foliation, where the evolution of a given slice is given by the Einstein equations (for more detailed treatments see for instance; Gourgoulhon, 2007; Alcubierre, 2008; Bona et al., 2009; Baumgarte and Shapiro, 2010; Shibata, 2015). This 3+1 decomposition, in which the four-dimensional manifold is splitted into "space+time" components and the covariant Einstein equations are converted into evolution equations for three-dimensional geometric fields, can be summarized in the following steps:

- *specify the choice of coordinates.* The covariance of Einstein equations implies that they can be written in the same generic way on any system of coordinates, which can be defined by a set of observers. The spacetime can be foliated by a family of spacelike hypersurfaces Σ, which are intersected by a congruence of time lines that will determine our observers (i.e., our system of coordinates). This congruence is described by the vector field $t^a = \alpha n^a + \beta^a$, where n^a is the timelike unit vector normal to the spacelike hypersurfaces, α is the lapse function which measures the proper time of the Eulerian (orthogonal) observers and β^a is the shift vector that measures the displacement, between consecutive hypersurfaces, of the time line t^a followed by the observers with respect to the normal n^a (see **Figure 1**).
- *decompose every 4D object into its 3+1 components.* The choice of coordinates allows for the definition of a spatial projection tensor $\gamma^a{}_b \equiv \delta^a_b + n^a n_b$. Any four-dimensional tensor can be decomposed into 3+1 pieces using either the spatial projector to obtain the spatial components, or contracting with n^a for the time components. For instance, the line element measuring the distance between neighboring points can be written by

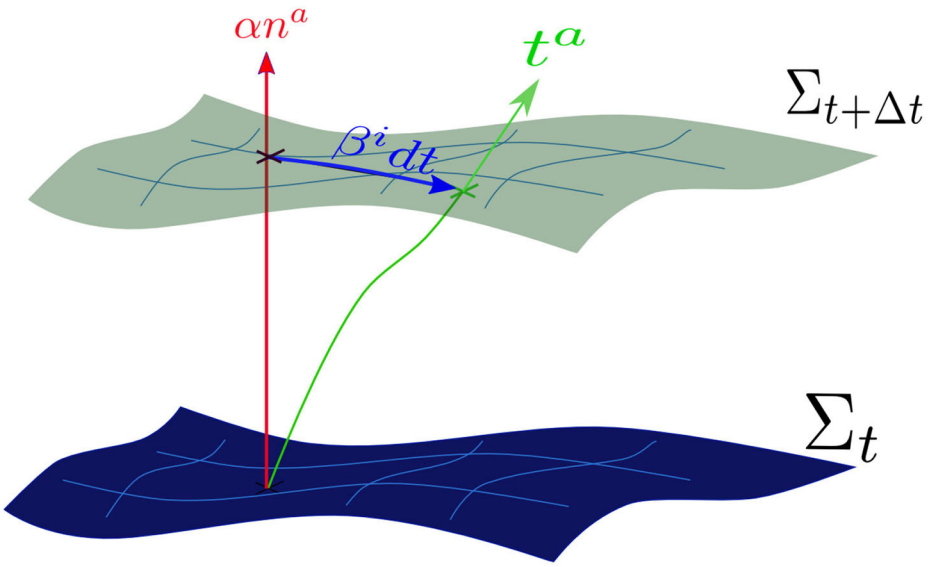

FIGURE 1 | Foliation of the spacetime manifold. The lapse function α measures the proper time along the normal n^a to the hypersurface Σ_t, which is equipped with an induced metric γ_{ij}. The shift vector β^i measures the displacement, on consecutive hypersurfaces, between the observer time lines t^a and the normal lines n^a.

using these generic 3+1 coordinates as

$$ds^2 = g_{ab}dx^a dx^b = -\alpha^2\, dt^2 + \gamma_{ij}(dx^i + \beta^i dt)\,(dx^j + \beta^j dt), \quad (4)$$

where the spatial three-dimensional induced metric γ_{ij} is just the projection of the four-dimensional metric g_{ab} into the space-like hypersurface Σ. Other objects, like the stress-energy tensor, can also be decomposed into its various components, namely

$$\tau \equiv T^{ab}\, n_a\, n_b, \;\; S_i \equiv -T_{ab}\, n^a\, \gamma^b{}_i, \;\; S_{ij} \equiv T_{ab}\, \gamma^a{}_i\, \gamma^b{}_j. \quad (5)$$

- *write down the field equations in terms of the 3+1 components.* Within the framework outlined here, the induced metric γ_{ij} is the only unknown, since both lapse and shift are set by our choice of coordinates. In differential geometry it is also common to define an additional tensor K_{ij} with a strong geometrical meaning, as it describes the change of the induced metric along the congruence of normal observers. This definition involves the Lie derivative $\mathcal{L}_{\mathbf{n}}$, a generalization of the directional derivative along the vector $\mathbf{n}$ in a manifold. Therefore, the definition of the extrinsic curvature and the 3+1 decomposition of Einstein equations form an hyperbolic-elliptic system of PDEs, commonly known as the Arnowitt-Deser-Misner (ADM) formalism (Witten, 1962; York, 1979), which can be written as

$$\begin{aligned} K_{ij} &\equiv -\frac{1}{2}\mathcal{L}_{\mathbf{n}}\gamma_{ij} = -\frac{1}{2\alpha}\left(\partial_t - \mathcal{L}_\beta\right)\gamma_{ij}, \\ \mathcal{L}_\beta \gamma_{ij} &= \beta^k \partial_k \gamma_{ij} + \gamma_{ik}\partial_j \beta^k + \gamma_{kj}\partial_i \beta^k, \quad (6) \\ \left(\partial_t - \mathcal{L}_\beta\right) K_{ij} &= -\nabla_i \nabla_j \alpha + \alpha\left(R_{ij} - 2K_i{}^k K_{jk} + \mathrm{trK}\, K_{ij}\right. \\ &\quad \left. - 8\pi\left[S_{ij} - \frac{\gamma_{ij}}{2}\left(\mathrm{trS} - \tau\right)\right]\right), \quad (7) \end{aligned}$$

$$\mathcal{H} = R_i{}^i + (\mathrm{trK})^2 - K_i{}^j K_j{}^i - 16\pi\,\tau = 0, \quad (8)$$

$$\mathcal{M}_i = \nabla_j\left(K_i{}^j - \mathrm{trK}\,\delta_i{}^j\right) - 8\pi\, S_i = 0. \quad (9)$$

where we have defined the trace of any three-dimensional tensor C_{ij} as $trC = \gamma^{ij}C_{ij}$. The evolution hyperbolic Equations (6,7) for the evolved fields $\{\gamma_{ij}, K_{ij}\}$ are complemented with the energy and momentum constraint Equations (8,9), that have to be satisfied at each hypersurface. This system of equations needs to be completed with a specification of the coordinate system, that is, by a choice of lapse and shift $\{\alpha, \beta^i\}$. The ADM formalism still preserves the covariance under spatial or time coordinate transformations (i.e., 3+1 covariance). Notice that, although manifest four-dimensional covariance is lost when performing the 3+1 decomposition, the solution space is still invariant under general coordinate transformations.

One can take advantage of the contracted Bianchi identities to prove that the constraint Equations (8,9) are just first integrals of the evolution ones (6,7), so that if the constraints are satisfied on an initial hypersurface (i.e., $\mathcal{H} = \mathcal{M}_i = 0$ at Σ_t), they will remain satisfied for all times. This redundancy of the equations allows for different evolution approaches. The most straightforward choice, the *constrained evolution* approach, involves solving simultaneously both the evolution equations and the constraints, but it presents several difficulties. From the theoretical point of view, it is not clear how to split the dynamical modes, solved through evolution equations, from the constrained ones, enforced by elliptic equations. From the computational point of view, elliptic equations are computationally more expensive and difficult to solve efficiently than hyperbolic ones. A simpler alternative is given by the *free evolution* approach, where the fields are obtained uniquely from the evolution equations, while the constraints are enforced only

at the initial time (i.e., although they can be computed during the evolution to estimate the validity of the solution). Notice however that discarding the constraint equations breaks the underlying invariance of the solutions. Due to its simplicity, the free evolution approach has traditionally been the most common choice in Numerical Relativity applications without symmetry assumptions, particularly in efforts associated to the modeling of gravitational wave sources.

It is important to stress that any astrophysical scenario, except those including only black holes, involves some type of matter, which will evolve on a curved spacetime as described by Equation (3). We can also perform the 3+1 decomposition on this equation to obtain the evolution for the matter energy density τ and the momentum density S_i, namely

$$(\partial_t - \mathcal{L}_\beta)\tau \; + \; \alpha \nabla_k S^k = \alpha \left(\tau \; trK - 2 S^k \; \partial_k \ln \alpha + K_{ij} S^{ij} \right), \qquad (10)$$

$$(\partial_t - \mathcal{L}_\beta) S_i \; + \; \alpha \nabla_k S^k{}_i = \alpha \left(S_i \; trK - S^k{}_i \; \partial_k \ln \alpha - \tau \; \partial_i \ln \alpha \right). \qquad (11)$$

Notice that these equations need a closure relation $S^k{}_i = S^k{}_i(\tau, S_i)$ that will depend on the type of matter considered.

2.3. Formulations of the Einstein Equations

Any mathematical model representing a physical system must be described by a well-posed system of equations, meaning that there exists a unique bounded solution that depends continuously on the initial data. Such requirement is relevant not only from a conceptual point of view, but it is of crucial importance in computational applications: a numerical solution solving an ill-posed problem is not enforced to converge to its corresponding continuum solution. A clear example of this undesired behavior can be observed in the ADM free evolution system resulting directly from the 3+1 decomposition of Einstein equations. Although the ADM formalism was extensively used at the dawn of Numerical Relativity due to its simplicity, the presence of several numerical instabilities in the three-dimensional case made it unsuitable for computational applications. The reason behind these instabilities, as it was shown in the nineties, was the ill posedness of the ADM system in 3+1 dimensions when supplemented with standard gauge conditions.

Since then, there have been several attempts to construct well-posed free-evolution formalisms, either by selecting a particular gauge or by mixing the constraints with the evolution equations to modify the principal part of the system. The mathematical structure of the Einstein field equations was first investigated on a specific coordinate choice, called the harmonic gauge, in which the spacetime coordinates follow wave equations and can be written as $\Gamma^a \equiv g^{bc}\Gamma^a_{bc} = 0$ (Witten, 1962). This choice allowed to greatly simplify Einstein equations, which could then be written as a set of (well-posed) generalized wave equations, $g^{cd}\partial_c\partial_d g_{ab} = H_{ab}(g, \partial g)$, where H_{ab} is a quadratic function in the metric first derivatives. This Harmonic formalism, written for different set of fields and for generalized harmonic conditions (Pretorius, 2005b; Lindblom et al., 2006), was used successfully to model the coalescence of compact objects, like black holes (Pretorius, 2006; Szilágyi et al., 2009), boson stars (Palenzuela et al., 2007), and neutron stars (Anderson et al., 2008).

Another very convenient way to write down Einstein equations is the Baumgarte-Shapiro-Shibata-Nakamura (BSSN) formalism (Shibata and Nakamura, 1995; Baumgarte and Shapiro, 1999), which relies in three important modifications of the ADM system. First, it applies a conformal decomposition on the evolved fields, partially motivated by the fact that the Schwarschild black hole solution is conformally flat. Therefore, a conformal metric $\tilde{\gamma}_{ij}$, with unit determinant, and a conformal, trace-less, extrinsic curvature $\tilde{A}_{ij}$ can be introduced as

$$\tilde{\gamma}_{ij} = \chi \; \gamma_{ij}, \;\; \tilde{A}_{ij} = \chi \left(K_{ij} - \frac{1}{3} \gamma_{ij} \; trK \right). \qquad (12)$$

These new definitions involve the appearance of two new constraints, $\tilde{\gamma} = 1$ and $tr\tilde{A} \equiv \tilde{\gamma}^{ij}\tilde{A}_{ij} = 0$, which will be denoted as *conformal constraints* from now on to distinguish them from the energy-momentum *physical constraints*. The second modification consists on extending the space of solutions by introducing a new evolved field $\tilde{\Gamma}^i = \tilde{\gamma}^{jk}\tilde{\Gamma}^i{}_{jk} = -\partial_j\tilde{\gamma}^{ij}$, namely the contraction of the Christoffel symbols associated to the conformal metric. The third modification, which is essential to achieve a well-posed system, is to add the momentum constraint in a specific way to the evolution equation for this new quantity $\tilde{\Gamma}^i$ (i.e., which is originally calculated, as usual, by taking the time derivative of its definition). Notice that the last two modifications are analogous to rewrite the momentum constraint as an evolution equation and affect strongly the principal part of the system (i.e., the terms with derivatives of highest order), transforming the free-evolution ADM ill-posed system into a well-posed one, when supplemented with appropriate gauge conditions (Sarbach et al., 2002; Gundlach and Martín-García, 2006). This formalism, with the 1+log slicing and the gamma-freezing shift conditions described below, has been used successfully to model the coalescence of black holes without the need of excising the interior of the apparent horizons to remove the physical singularity from the computational domain (van Meter et al., 2006; Brügmann et al., 2008), making them especially convenient for black hole simulations (Baker et al., 2006a; Campanelli et al., 2006b; Sperhake, 2007). Notice however that the BSSN formalism was already being used successfully to model the coalescence of binary neutron stars (Shibata and Uryū, 2000, 2002), although the lack of advanced computational techniques like Adaptive Mesh Refinement (AMR) prevented the calculation of accurate waveforms until several years later.

An asymmetry of the BSSN formalism is manifested on the different ways to treat the physical constraints, since the momentum constraint is mixed with the evolution equations but the energy constraint is not. Related to this, and like many other contemporary formalisms, BSSN does not include any mechanism to control dynamically unavoidable constraint violations, which could grow significantly during a numerical simulation, even if they are only seeded by tiny discretization errors (Lindblom and Scheel, 2002). The Z4 formalism, which was introduced as a extension of the Einstein equations to achieve a well posed, hyperbolic evolution system free of

constraints (Bona et al., 2003, 2004), allowed to address these issues in an elegant general-covariant way. The equations of motion can be derived from a suitable action via a Palatini-type variation (Bona et al., 2010), obtaining

$$R_{ab} + \nabla_a Z_b + \nabla_b Z_a = 8\pi \left(T_{ab} - \frac{1}{2} g_{ab}\, trT\right) + \kappa_z \left(n_a Z_b + n_b Z_a - g_{ab} n^c Z_c\right), \quad (13)$$

where Z_a is introduced as a new four-vector measuring the deviation from Einstein's solutions, which are those satisfying the algebraic condition $Z_a = 0$. Although the original formulation, corresponding to the choice $\kappa_z = 0$, is completely covariant, additional damping terms were included to enforce dynamically the decay of the physical constraint violations associated to Z_a (Brodbeck et al., 1999). As it is shown in Gundlach et al. (2005), all the physical constraint modes are exponentially damped if $\kappa_z > 0$. However, since the damping terms are proportional to the unit normal of the time slicing n_a, the full covariance of the system is lost due to the presence of this privileged time vector. The 3+1 decomposition of the Z4 formalism given by Equation (13) leads to evolution equations for the evolved fields $\{\gamma_{ij}, K_{ij}, Z_i, \Theta\}$, where we have defined the normal projection $\Theta \equiv -n_a Z^a$. Notice that now there are ten evolution equations to solve ten unknowns; the original elliptic constraints in the Einstein Equations have been converted into evolution equations for the new four-vector Z_a, which can be understood roughly as the time integral of the energy and momentum constraints. Einstein's solutions are recovered when the algebraic constraint $Z_a = 0$ is satisfied. Finally, the most important feature is that the evolution system, when combined with suitable gauge conditions, is directly well-posed, without the need of further modifications (Bona and Palenzuela, 2004).

The Z4 formalism has also been useful to understand also the constraint evolution system (i.e., subsidiary system) and the connection among different formalisms. For instance, the Harmonic formalism can be recovered from the Z4 one by substituting the harmonic condition with $\Gamma^a = -2Z^a$ (Bona et al., 2003), and a version of the BSSN by a symmetry-breaking mechanism (Bona et al., 2004). Along these lines, one can take advantage of the Z4 formalism flexibility to incorporate the ability to deal with black hole singularities without excision. The conformal and covariant Z4 (CCZ4) formalism (Alic et al., 2012) was constructed by performing the same conformal transformations as in the BSSN formalism (i.e., see also Bernuzzi and Hilditch, 2010 for other conformal but non-covariant Z4 formulations) but using, instead of trK and Z_i, the following quantities as evolved fields,

$$tr\hat{K} \equiv trK - 2\,\Theta, \hat{\Gamma}^i \equiv \tilde{\Gamma}^i + \frac{2}{\chi} Z^i, \quad (14)$$

so that the evolution equations are closer to those in the BSSN formulation. The full list of evolved fields is then given by $\{\chi, \tilde{\gamma}_{ij}, tr\hat{K}, \tilde{A}_{ij}, \hat{\Gamma}^i, \Theta\}$ and follow the evolution equations (Bezares et al., 2017),

$$\begin{aligned}
\partial_t \tilde{\gamma}_{ij} &= \beta^k \partial_k \tilde{\gamma}_{ij} + \tilde{\gamma}_{ik}\,\partial_j \beta^k + \tilde{\gamma}_{kj} \partial_i \beta^k - \frac{2}{3}\,\tilde{\gamma}_{ij} \partial_k \beta^k \\
&\quad - 2\alpha \left(\tilde{A}_{ij} - \frac{1}{3}\tilde{\gamma}_{ij}\, tr\tilde{A}\right) - \frac{\kappa_c}{3}\,\alpha \tilde{\gamma}_{ij} \ln \tilde{\gamma}, \quad (15)\\
\partial_t \tilde{A}_{ij} &= \beta^k \partial_k \tilde{A}_{ij} + \tilde{A}_{ik} \partial_j \beta^k + \tilde{A}_{kj} \partial_i \beta^k - \frac{2}{3}\,\tilde{A}_{ij} \partial_k \beta^k \quad (16)\\
&\quad - \frac{\kappa_c}{3}\,\alpha\,\tilde{\gamma}_{ij}\, tr\tilde{A} + \chi \left[\alpha \left({}^{(3)}\hat{R}_{ij} + \hat{R}^{\chi}_{ij} - 8\pi\, S_{ij}\right) - \nabla_i \nabla_j \alpha\right]^{\rm TF} \\
&\quad + \alpha \left(tr\hat{K}\,\tilde{A}_{ij} - 2\tilde{A}_{ik}\tilde{A}^k{}_j\right),\\
\partial_t \chi &= \beta^k \partial_k \chi + \frac{2}{3}\,\chi \left[\alpha(tr\hat{K} + 2\,\Theta) - \partial_k \beta^k\right], \quad (17)\\
\partial_t tr\hat{K} &= \beta^k \partial_k tr\hat{K} - \nabla_i \nabla^i \alpha \\
&\quad + \alpha \left[\frac{1}{3}\left(tr\hat{K} + 2\Theta\right)^2 + \tilde{A}_{ij}\tilde{A}^{ij} + 4\pi\left(\tau + trS\right) + \kappa_z \Theta\right] \\
&\quad + 2\, Z^i \nabla_i \alpha, \quad (18)\\
\partial_t \Theta &= \beta^k \partial_k \Theta + \frac{\alpha}{2}\left[{}^{(3)}R + 2\nabla_i Z^i \right. \\
&\quad \left. + \frac{2}{3}\, tr^2\hat{K} + \frac{2}{3}\,\Theta\left(tr\hat{K} - 2\Theta\right) - \tilde{A}_{ij}\tilde{A}^{ij}\right] - Z^i \nabla_i \alpha \\
&\quad - \alpha \left[8\pi\,\tau + 2\kappa_z\,\Theta\right], \quad (19)\\
\partial_t \hat{\Gamma}^i &= \beta^j \partial_j \hat{\Gamma}^i - \hat{\Gamma}^j \partial_j \beta^i + \frac{2}{3}\hat{\Gamma}^i \partial_j \beta^j + \tilde{\gamma}^{jk} \partial_j \partial_k \beta^i + \frac{1}{3}\,\tilde{\gamma}^{ij} \partial_j \partial_k \beta^k \\
&\quad - 2\tilde{A}^{ij} \partial_j \alpha + 2\alpha \left[\tilde{\Gamma}^i{}_{jk} \tilde{A}^{jk} - \frac{3}{2\chi}\,\tilde{A}^{ij} \partial_j \chi - \frac{2}{3}\,\tilde{\gamma}^{ij} \partial_j tr\hat{K} \right. \\
&\quad \left. - 8\pi\,\tilde{\gamma}^{ij}\, S_i\right] + 2\alpha \left[-\tilde{\gamma}^{ij}\left(\frac{1}{3}\partial_j \Theta + \frac{\Theta}{\alpha}\,\partial_j \alpha\right)\right. \\
&\quad \left. - \frac{1}{\chi} Z^i \left(\kappa_z + \frac{2}{3}\left(tr\hat{K} + 2\Theta\right)\right)\right], \quad (20)
\end{aligned}$$

where the expression $[\ldots]^{\rm TF}$ indicates the trace-free part with respect to the metric $\tilde{\gamma}_{ij}$. The non-trivial terms inside this expression can be written as

$$\begin{aligned}
\hat{R}^{\chi}_{ij} &= \frac{1}{2\chi}\,\partial_i \partial_j \chi - \frac{1}{2\chi}\,\tilde{\Gamma}^k_{ij} \partial_k \chi - \frac{1}{4\chi^2}\,\partial_i \chi\, \partial_j \chi + \frac{2}{\chi^2} Z^k \tilde{\gamma}_{k(i} \partial_{j)} \chi \\
&\quad + \frac{1}{2\chi}\tilde{\gamma}_{ij}\left[\tilde{\gamma}^{km}\left(\partial_k \partial_m \chi - \frac{3}{2\chi}\,\partial_k \chi\, \partial_m \chi\right) - \hat{\Gamma}^k \partial_k \chi\right],\\
{}^{(3)}\hat{R}_{ij} &= -\frac{1}{2}\,\tilde{\gamma}^{mn} \partial_m \partial_n \tilde{\gamma}_{ij} + \tilde{\gamma}_{k(i} \partial_{j)} \hat{\Gamma}^k + \hat{\Gamma}^k \tilde{\Gamma}_{(ij)k} \\
&\quad + \tilde{\gamma}^{mn}\left(\tilde{\Gamma}^k_{mi}\tilde{\Gamma}_{jkn} + \tilde{\Gamma}^k_{mj}\tilde{\Gamma}_{ikn} + \tilde{\Gamma}^k{}_{mi}\tilde{\Gamma}_{knj}\right),\\
\nabla_i \nabla_j \alpha &= \partial_i \partial_j \alpha - \tilde{\Gamma}^k_{ij} \partial_k \alpha \\
&\quad + \frac{1}{2\chi}\left(\partial_i \alpha\, \partial_j \chi + \partial_j \alpha\, \partial_i \chi - \tilde{\gamma}_{ij}\, \tilde{\gamma}^{km}\, \partial_k \alpha\, \partial_m \chi\right),
\end{aligned}$$

Notice that damping terms proportional to a free parameter κ_c have been included in order to dynamically control the conformal constraints, exactly in the same way as it is done with the physical ones.

2.4. Gauge Conditions

The principle of general covariance implies that the laws of physics, and in particular Einstein equations, must take the same form for all observers. This implies that they have to be written in a generic tensor form for any system of coordinates. The choice

of coordinates is commonly referred as gauge freedom, and it corresponds to define the congruence of our observers, i.e., the time vector t^a by setting the lapse and shift. Notice that setting gauge conditions is not only necessary to close the system of equations: these additional degrees of freedom can also be useful both to avoid coordinate or physical singularities and to adapt to the underlying symmetries appearing in our simulations. Besides the summary presented here, further details on the different gauge conditions can be found for instance in Gourgoulhon (2007), Alcubierre (2008), Bona et al. (2009), Baumgarte and Shapiro (2010), and Shibata (2015).

The simplest gauge conditions, known as geodesic coordinates, are obtained setting $\alpha = 1$ and $\beta^i = 0$, so that the time coordinate coincides with the proper timer of the Eulerian observers (i.e., those following timelike geodesics). A simple perturbation analysis shows however that any formalism supplemented with this choice of coordinates might suffer of unstable non-physical modes. Even worse, this gauge condition might also lead to coordinate singularities, since Eulerian observers will focus into a single point such that the spatial volume $\sqrt{\gamma} \to 0$. Coordinate pathologies can be prevented by imposing suitable geometrical conditions, which usually involve some type of elliptic equations (Smarr and York, 1978). This is the case, for instance, in the *maximal slicing condition* $trK = 0$, which, when imposed at all times, implies

$$\nabla^i \nabla_i \alpha = \alpha \left[K_{ij} K^{ij} + 4\pi(\tau + S) \right]. \tag{21}$$

This slicing condition is called *singularity-avoiding* condition because the lapse function α goes to zero when the spatial volume $\sqrt{\gamma}$ goes to zero, avoiding the coordinate singularities during the evolution by slowing-down the proper time of the observers near strong-gravity regions. Another interesting geometrical property to be satisfied would be the *minimal distortion condition*, which can be written as

$$\nabla^j \nabla_j \beta^i + \frac{1}{3} \nabla^i \nabla_j \beta^j + R^i{}_j \beta^j = 2 \nabla_j \left[\alpha (K^{ij} - \frac{1}{3} \gamma^{ij} trK) \right]. \tag{22}$$

This shift condition minimizes the changes in the shape of the volume elements, independently of their size. Both the maximal slicing and the minimal distortion conditions (21, 22) are elliptic equations. These type of equations are computationally much more expensive than hyperbolic evolution ones, and are usually avoided or transformed into hyperbolic ones in the context of free evolution formalisms.

Indeed, hyperbolic evolution equations are preferred and were already adopted to enforce some interesting property, like for instance the harmonic coordinates, which ensured the well-posedness of the Harmonic formalism (Witten, 1962). A suitable family of evolution equations for the lapse is given by the *Bona-Massó slicing condition* (Bona et al., 1995),

$$\partial_t \alpha = \beta^i \partial_i \alpha - \alpha^2 f(\alpha)\, trK, \tag{23}$$

which, for any $f(\alpha) \geq 1$, is not only singularity avoiding, but also maintains the well-posedness of the formalism. The case $f(\alpha) = 1$ correspond to the harmonic slicing condition, while that $f(\alpha) \to \infty$ mimics the maximal slicing condition Equation (21). A common choice in numerical applications, especially those involving black holes, is to use the so-called $1 + \log$ *slicing condition*, corresponding to $f(\alpha) = 2/\alpha$. This choice has excellent singularity avoidance conditions, since near the physical singularity $\alpha \to 0$, mimicking the maximal slicing condition.

A suitable family of hyperbolic dynamical equations for the shift-vector β^i is given by the *Gamma-driver condition* (Alcubierre et al., 2003),

$$\partial_t \beta^i = \beta^j \partial_j \beta^i + g(\alpha)\, \hat{\Gamma}^i - \eta \beta^i, \tag{24}$$

where $g(\alpha)$ is an arbitrary function depending on the lapse function and η a constant damping parameter introduced to avoid strong oscillations during the shift evolution. This gauge condition not only maintains the well posedness of BSSN and CCZ4 formalisms, but also mimics the minimal distortion condition Equation (22), trying then to minimize the stretching of the spatial coordinates. For numerical simulations involving black holes and neutron stars, standard values are $g(\alpha) = 3/4$ and $\eta \approx 2/M$, being M the mass of the compact object. Notice that in most of the literature the evolution of the shift is written in terms of an auxiliary field B^i, which however does not seem necessary for most of the relevant numerical scenarios (van Meter et al., 2006).

3. NUMERICAL METHODS

In the same way that any reasonable physical model must be described by a well-posed PDE system, any numerical solution must satisfy the following three conditions: (i) *consistency*, meaning that the discrete derivative operators reduce to the continuum ones as the resolution (i.e., the amount of discrete points sampling the continuum domain) increases; (ii) *stability*, such that the numerical solution is bounded and depends continuously on the initial data, and (iii) *convergence*, that is, the numerical solution tends to the continuum one as resolution increases.

Fortunately, it is not necessary to prove these three conditions, since Lax-Richtmyer equivalence theorem states that the numerical approximation of well-posed problems is convergent if and only if the scheme is stable and consistent (Lax and Richtmyer, 1956). Since consistency can be obtained quite trivially, the relevant question here is how to discretize the equations such that the well-posedness at the continuum problem translate into stability at the discrete one. Let us consider the following generic set of hyperbolic PDE at the continuum,

$$\partial_t u = \mathcal{P}(u, \partial u) \tag{25}$$

where $\mathcal{P}$ is the evolution operator, which can depend on arbitrary spatial derivatives of u. A popular technique to discretize this continuum problem is by using the *Method of Lines* (MoL), which decouples the treatment of space and time coordinates (Schiesser, 1991). In the first step, only the spatial dimensions are discretized, while leaving the time continuous. This semi-discrete problem consist on a set of ordinary differential equations for $U_i(t) =$

$u(t, x_i)$, one for each discrete spatial point x_i, separated by a mesh size Δx. The semi-discrete equations can formally be written by substituting $\mathcal{P} \rightarrow P$, a discrete version of the evolution operator, written in terms of discrete derivative operators D. In the second step, the fully discrete problem is obtained after discretizing in time, such that the fully discrete solution is given by $U_i^n = u(t^n, x_i)$ at each discrete time t^n, separated by a time-step Δt. The discrete equations can formally be written again by substituting ∂_t by a discrete time integrator D_t. As it is shown in Gustafsson et al. (1995), the fully discrete problem preserves the stability of the semi-discrete problem if it is integrated with a locally-stable time integrator, as for instance any Runge-Kutta of at least 3rd order. Thus, the problem is then reduced to ensure the stability of the semi-discrete problem by choosing a suitable space derivative discretization.

3.1. Smooth Solutions

For sufficiently smooth solutions, the full procedure to ensure convergence of the numerical solution can be found in Gustafsson et al. (1995) and summarized as follows: starting from a well-posed system at the continuum, apply the MoL, discretize in space with derivative operators satisfying certain conditions and then integrate with a Runge-Kutta of third order or higher. A problem at the continuum is well-posed if the solution satisfies an energy estimate which bounds some norm of the solution at some fixed time. A tool that is used in the derivation of such energy estimates is the integration by parts rule. Analogously, a semi-discrete problem can be shown to be stable if the discrete difference operators D satisfies the summation by parts rule, which is the discrete version of the integration by parts (see Calabrese et al., 2004 and references within for early works introducing these techniques in Numerical Relativity). For non-linear equations it is usually necessary to remove the high-frequency (unphysical) modes not accurately represented in the grid, which can grow continuously in time at any fixed resolution. The easiest way to damp these modes is by adding a filtering operator $Q_d U$ to the right-hand-side of the semi-discrete equations, like for instance the Kreiss-Oliger dissipation operator (Kreiss and Oliger, 1973). This operator vanishes at infinite resolution, such that the semi-discrete problem is still consistent, and it is designed not to spoil the accuracy of the numerical scheme. Notice that not only Einstein equations, but any hyperbolic system of non-linear PDEs without the presence of either shocks or discontinuities, can be solved with these methods.

3.2. Non-smooth Solutions

Although it is not the case with Einstein evolution systems, if the equations are genuinely non-linear like in fluid dynamics, discontinuities and shocks (i.e., a region with a crossing of the characteristics of the system) might appear even from smooth initial data. Discrete operators based on Taylor expansions, assuming smoothness of the solution, are going to fail near these regions and will produce artificial oscillations leading to unphysical solutions. Therefore, any spatial discretization able to handle shocks needs to take advantage of the integrated or weak-form of the equations (LeVeque, 1990). Let us consider a system of non-linear PDEs, like the conservation of energy and momentum given by Equations (10, 11), which can be written in the balance law form (Font et al., 2000)

$$\partial_t u + \partial_k F^k(u) = S(u) \tag{26}$$

where the fluxes $F^k(u)$ and the sources $S(u)$ depend on the fields but not on their derivatives. There are two popular different schemes to discretize these equations, based either on finite volumes or on finite differences (Shu, 1998). The starting point of the finite-volume approach is the integral of the previous balance law equation in a spatial volume element dV,

$$\partial_t \bar{u} + \oint F^k dS_k = \bar{S} \tag{27}$$

where $\bar{u}$ and $\bar{S}$ are the volume integrals of the corresponding quantity in the cell and we have used Gauss theorem to convert the volume integral of the fluxes into a surface one, being dS_k the surface element. This weak form can be easily discretized with a conservative scheme, namely

$$\partial_t \bar{U}_i = -\frac{1}{\Delta x}\left[F_{i+1/2} - F_{i-1/2}\right] + \bar{S}_i. \tag{28}$$

The problem is then reduced to compute (i) the solution at the grid points U_i from the volume averages $\bar{U}_i$, and (ii) the numerical flux at the interfaces $F_{i\pm1/2}$. These two steps must be performed in such a way that the semi-discrete solution is Total Variation Diminishing (TVD), or at least Total Variation Bounded (TVB), meaning essentially that no new extremes are allowed in the solution, which prevents the appearance of artificial oscillations. Notice that these conditions are more restrictive than stability, where the solution can still grow under certain tolerant bounds. The procedure to construct a shock-capturing scheme is the following. First, one needs to reconstruct the fields at the interfaces $x_{i\pm1/2}$ using information either from the right (R) or from the left (L) to the interface (see **Figure 2**), namely $(u^R_{i\pm1/2}, u^L_{i\pm1/2})$. Commonly used high-order reconstructions, preserving the monotonicity of the solution to prevent spurious oscillations, are for example the Weighted-Essentially-Non-Oscillatory (WENO) reconstructions (Jiang and Shu, 1996; Shu, 1998) and MP5 (Suresh and Huynh, 1997). Then, a suitable flux-formula is required to solve, at least approximately, the jump on the fields at each interface (i.e., Riemann problem), by combining information from the right and from the left, namely $F_{i\pm1/2} = F(u^R_{i\pm1/2}, u^L_{i\pm1/2})$. This flux-formula usually requires information on the characteristic structure of the system (i.e., eigenvectors and eigenvalues). This approach has been the most commonly employed in binary neutron star simulations, see for instance (Shibata and Uryū, 2002; Anderson et al., 2008; Baiotti et al., 2008; Liu et al., 2008; Yamamoto et al., 2008; Mösta et al., 2014).

Higher-order schemes are relatively easy to achieve with the finite-difference approach, providing an efficient approach to high-order shock-capturing methods (Shu and Osher, 1988). However, high-order finite-difference numerical schemes applied to the magneto-hydrodynamics (MHD) equations have not been

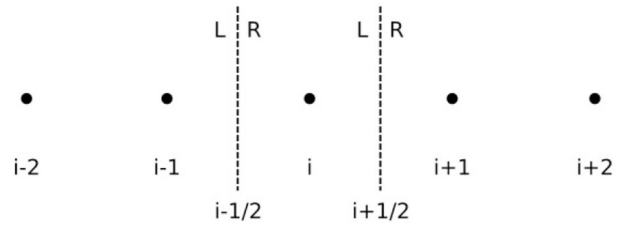

FIGURE 2 | The computational uniform grid x_i. The left (L) and right (R) states reconstructed at the interfaces $x_{i\pm1/2}$ are required to calculate the numerical flux $F_{i\pm1/2}$.

as robust as those based on finite-volume. Nowadays that is not a great inconvenient, and the possibility to achieve high order accuracy is leading to more efforts on implementing these methods on computational MHD codes (Radice et al., 2014; Bernuzzi and Dietrich, 2016). Although the derivation is different, the conservative scheme given by Equation (28) is still valid, where now $\bar{U}$ means just U_i, the value of the field in the grid point. Again, the problem is reduced to compute a suitable numerical flux at the interfaces such that solution is essentially non-oscillatory and preserves, or at least bounds, the Total Variation. The procedure starts by performing a Lax-Friedrichs splitting, where it is introduced the following combination of fluxes and fields $F_i^{\pm} = 1/2(F_i \pm \lambda U_i)$, being λ the maximum eigenvalue in the neighborhood of the point. These combinations are interpolated at the interfaces by using a monotonic reconstruction, like the high-order ones discussed before. The flux at the left of the interface $F^L_{i+1/2}$ is reconstructed using the values $\{F^+\}$, while that the flux at the right $F^R_{i+1/2}$ is reconstructed using the values $\{F^-\}$. The final numerical-flux is obtained just as $F_{i+1/2} = F^R_{i+1/2} + F^L_{i+1/2}$. At the lowest order reconstruction, $F^L_{i+1/2} = F^+_i$ and $F^R_{i+1/2} = F^-_{i+1}$, so that the final numerical-flux reduces to the popular and robust Local-Lax-Friedrichs flux (LeVeque, 1990).

Finally, notice that efforts considering other techniques to solve self-gravitation neutron stars, like the discontinuous Galerkin methods (Hébert et al., 2018), are underway and might be an interesting option in the near future.

AUTHOR CONTRIBUTIONS

The author confirms being the sole contributor of this work and has approved it for publication.

FUNDING

I acknowledge support from the Spanish Ministry of Economy and Competitiveness grant AYA2016-80289-P (AEI/FEDER, UE).

ACKNOWLEDGMENTS

It is my pleasure to thank Carles Bona, Miguel Bezares, Luis Lehner, and Joan Massó for their critical reading and helpful comments on the manuscript.

REFERENCES

Abbott, B. P., Abbott, R., Abbott, T. D., Abraham, S., Acernese, F., Ackley, K., et al. (2019). GWTC-1: a gravitational-wave transient catalog of compact binary mergers observed by LIGO and Virgo during the first and second observing runs. *Phys. Rev. X* 9:031040. doi: 10.1103/PhysRevX.9.031040

Abramovici, A., Althouse, W. E., Drever, R. W. P., Gürsel, Y., Kawamura, S., Raab, F. J., et al. (1992). Ligo: The laser interferometer gravitational-wave observatory. *Science* 256, 325–333. doi: 10.1126/science.256.5055.325

Alcubierre, M. (2008). *Introduction to 3+1 Numerical Relativity*, OUP Oxford. doi: 10.1093/acprof:oso/9780199205677.001.0001

Alcubierre, M., Brügmann, B., Diener, P., Koppitz, M., Pollney, D., Seidel, E., et al. (2003). Gauge conditions for long-term numerical black hole evolutions without excision. *Phys. Rev. D* 67:084023. doi: 10.1103/PhysRevD.67.084023

Alic, D., Bona-Casas, C., Bona, C., Rezzolla, L., and Palenzuela, C. (2012). Conformal and covariant formulation of the Z4 system with constraint-violation damping. *Phys. Rev. D* 85:064040. doi: 10.1103/PhysRevD.85.064040

Anderson, M., Hirschmann, E. W., Lehner, L., Liebling, S. L., Motl, P. M., Neilsen, D., et al. (2008). Simulating binary neutron stars: dynamics and gravitational waves. *Phys. Rev. D* 77:024006. doi: 10.1103/PhysRevD.77.024006

Baiotti, L., Giacomazzo, B., and Rezzolla, L. (2008). Accurate evolutions of inspiralling neutron-star binaries: Prompt and delayed collapse to a black hole. *Phys. Rev. D* 78:084033. doi: 10.1103/PhysRevD.78.084033

Baker, J. G., Centrella, J., Choi, D.-I., Koppitz, M., and van Meter, J. (2006a). Binary black hole merger dynamics and waveforms. *Phys. Rev. D* 73:104002. doi: 10.1103/PhysRevD.73.104002

Baker, J. G., Centrella, J., Choi, D.-I., Koppitz, M., and van Meter, J. (2006b). Gravitational-wave extraction from an inspiraling configuration of merging black holes. *Phys. Rev. Lett.* 96:111102. doi: 10.1103/PhysRevLett.96.111102

Baumgarte, T. W., and Shapiro, S. L. (1999). Numerical integration of Einstein's field equations. *Phys. Rev. D* 59:024007. doi: 10.1103/PhysRevD.59.024007

Baumgarte, T. W., and Shapiro, S. L. (2010). *Numerical Relativity: Solving Einstein's Equations on the Computer* (Cambridge: Baumgarte and Shapiro). doi: 10.1017/CBO9781139193344

Bernuzzi, S., and Dietrich, T. (2016). Gravitational waveforms from binary neutron star mergers with high-order weighted-essentially-nonoscillatory schemes in numerical relativity. *Phys. Rev. D* 94:064062. doi: 10.1103/PhysRevD.94.064062

Bernuzzi, S., and Hilditch, D. (2010). Constraint violation in free evolution schemes: comparing the BSSNOK formulation with a conformal decomposition of the Z4 formulation. *Phys. Rev. D* 81:084003. doi: 10.1103/PhysRevD.81.084003

Bezares, M., Palenzuela, C., and Bona, C. (2017). Final fate of compact boson star mergers. *Phys. Rev. D* 95:124005. doi: 10.1103/PhysRevD.95.124005

Blanchet, L. (2014). Gravitational radiation from post-newtonian sources and inspiralling compact binaries. *Living Rev. Relativ.* 17:2. doi: 10.12942/lrr-2014-2

Bona, C., Bona-Casas, C., and Palenzuela, C. (2010). Action principle for numerical-relativity evolution systems. *Phys. Rev. D* 82:124010. doi: 10.1103/PhysRevD.82.124010

Bona, C., Ledvinka, T., Palenzuela, C., and Žáček, M. (2003). General-covariant evolution formalism for numerical relativity. *Phys. Rev. D* 67:104005. doi: 10.1103/PhysRevD.67.104005

Bona, C., Ledvinka, T., Palenzuela, C., and Žáček, M. (2004). Symmetry-breaking mechanism for the Z4 general-covariant evolution system. *Phys. Rev. D* 69:064036. doi: 10.1103/PhysRevD.69.064036

Bona, C., Massó, J., Seidel, E., and Stela, J. (1995). New formalism for numerical relativity. *Phys. Rev. Lett.* 75, 600–603. doi: 10.1103/PhysRevLett.75.600

Bona, C., and Palenzuela, C. (2004). Dynamical shift conditions for the Z4 and BSSN formalisms. *Phys. Rev. D* 69:104003. doi: 10.1103/PhysRevD.69.104003

Bona, C., Palenzuela-Luque, C., and Bona-Casas, C. (2009). *Elements of Numerical Relativity and Relativistic Hydrodynamics*, Vol. 783. Berlin; Heidelberg: Springer-Verlag. doi: 10.1007/978-3-642-01164-1

Brodbeck, O., Frittelli, S., Hübner, P., and Reula, O. A. (1999). Einstein's equations with asymptotically stable constraint propagation. *J. Math. Phys.* 40, 909–923. doi: 10.1063/1.532694

Brügmann, B., González, J. A., Hannam, M., Husa, S., Sperhake, U., and Tichy, W. (2008). Calibration of moving puncture simulations. *Phys. Rev. D* 77:024027. doi: 10.1103/PhysRevD.77.024027

Calabrese, G., Lehner, L., Reula, O., Sarbach, O., and Tiglio, M. (2004). Summation by parts and dissipation for domains with excised regions. *Class. Quant. Grav.* 21, 5735–5757. doi: 10.1088/0264-9381/21/24/004

Campanelli, M., Lousto, C. O., Marronetti, P., and Zlochower, Y. (2006a). Accurate evolutions of orbiting black-hole binaries without excision. *Phys. Rev. Lett.* 96:111101. doi: 10.1103/PhysRevLett.96.111101

Campanelli, M., Lousto, C. O., and Zlochower, Y. (2006b). Last orbit of binary black holes. *Phys. Rev. D* 73:061501. doi: 10.1103/PhysRevD.73.061501

Caron, B., Dominjon, A., Drezen, C., Flaminio, R., Grave, X., Marion, F., et al. (1997). The Virgo interferometer. *Class. Quant. Grav.* 14, 1461–1469.

Font, J. A., Miller, M., Suen, W.-M., and Tobias, M. (2000). Three-dimensional numerical general relativistic hydrodynamics: formulations, methods, and code tests. *Phys. Rev. D* 61:044011. doi: 10.1103/PhysRevD.61.044011

Gourgoulhon, E. (2007). *3+1 Formalism in General Relativity. Lecture Notes in Physics*, Vol. 846. Berlin; Heidelberg: Springer-Verlag.

Gundlach, C. and Martín-García, J. M. (2006). Well-posedness of formulations of the Einstein equations with dynamical lapse and shift conditions. *Phys. Rev. D* 74:024016. doi: 10.1103/PhysRevD.74.024016

Gundlach, C., Martin-Garcia, J. M., Calabrese, G., and Hinder, I. (2005). Constraint damping in the Z4 formulation and harmonic gauge. *Class. Quant. Grav.* 22, 3767–3774. doi: 10.1088/0264-9381/22/17/025

Gustafsson, B., Kreiss, H.-O., and Oliger, J. (1995). *Time-Dependent Problems and Difference Methods, 2nd Edn* (Wiley).

Hébert, F., Kidder, L. E., and Teukolsky, S. A. (2018). General-relativistic neutron star evolutions with the discontinuous Galerkin method. *Phys. Rev. D* 98:044041. doi: 10.1103/PhysRevD.98.044041

Hulse, R. A., and Taylor, J. H. (1975). Discovery of a pulsar in a binary system. *Astrophys. J. Lett.* 195, L51–L53. doi: 10.1086/181708

Jiang, G.-S., and Shu, C.-W. (1996). Efficient implementation of weighted eno schemes. *J. Comput. Phys.* 126, 202–228. doi: 10.1006/jcph.1996.0130

Kreiss, H., and Oliger, J. (1973). *Methods for the Approximate Solution of Time Dependent Problems*. WMO-ICSU; Joint Organizing Committee.

Lax, P. D., and Richtmyer, R. D. (1956). Survey of the stability of linear finite difference equations. *Commun. Pure Appl. Math.* 9, 267–293. doi: 10.1002/cpa.3160090206

Lehner, L. (2001). TOPICAL REVIEW: numerical relativity: a review. *Class. Quant. Grav.* 18, R25–R86. doi: 10.1088/0264-9381/18/17/202

LeVeque, R. J. (1990). *Numerical Methods for Linear Equations*. Basel: Birkhäuser Basel. doi: 10.1007/978-3-0348-5116-9_10

Lindblom, L., and Scheel, M. A. (2002). Energy norms and the stability of the Einstein evolution equations. *Phys. Rev. D* 66:084014. doi: 10.1103/PhysRevD.66.084014

Lindblom, L., Scheel, M. A., Kidder, L. E., Owen, R., and Rinne, O. (2006). A new generalized harmonic evolution system. *Class. Quant. Grav.* 23, S447–S462. doi: 10.1088/0264-9381/23/16/S09

Liu, Y. T., Shapiro, S. L., Etienne, Z. B., and Taniguchi, K. (2008). General relativistic simulations of magnetized binary neutron star mergers. *Phys. Rev. D* 78:024012. doi: 10.1103/PhysRevD.78.024012

Misner, C. W., Thorne, K. S., and Wheeler, J. A. (1973). *Gravitation, 2nd Edn*. San Francisco, CA:W H Freeman and Company.

Mösta, P., Mundim, B. C., Faber, J. A., Haas, R., Noble, S. C., Bode, T., et al. (2014). GRHydro: a new open-source general-relativistic magnetohydrodynamics code for the Einstein toolkit. *Class. Quant. Grav.* 31:015005. doi: 10.1088/0264-9381/31/1/015005

Palenzuela, C., Olabarrieta, I., Lehner, L., and Liebling, S. L. (2007). Head-on collisions of boson stars. *Phys. Rev. D* 75:064005. doi: 10.1103/PhysRevD.75.064005

Pretorius, F. (2005a). Evolution of binary black-hole spacetimes. *Phys. Rev. Lett.* 95:121101. doi: 10.1103/PhysRevLett.95.121101

Pretorius, F. (2005b). Numerical relativity using a generalized harmonic decomposition. *Class. Quant. Grav.* 22, 425–451. doi: 10.1088/0264-9381/22/2/014

Pretorius, F. (2006). Simulation of binary black hole spacetimes with a harmonic evolution scheme. *Class. Quant. Grav.* 23, S529–S552. doi: 10.1088/0264-9381/23/16/S13

Radice, D., Rezzolla, L., and Galeazzi, F. (2014). High-order fully general-relativistic hydrodynamics: new approaches and tests. *Class. Quant. Grav.* 31:075012. doi: 10.1088/0264-9381/31/7/075012

Sarbach, O., Calabrese, G., Pullin, J., and Tiglio, M. (2002). Hyperbolicity of the Baumgarte-Shapiro-Shibata-Nakamura system of Einstein evolution equations. *Phys. Rev. D* 66:064002. doi: 10.1103/PhysRevD.66.064002

Schiesser, W. E. (1991). *The Numerical Method of Lines: Integration of Partial Differential Equations*. Academic Press.

Shibata, M. (2015). *Numerical Relativity*. World Scientific Publishing Co., Inc. doi: 10.1142/9692

Shibata, M., and Nakamura, T. (1995). Evolution of three-dimensional gravitational waves: Harmonic slicing case. *Phys. Rev. D* 52, 5428–5444. doi: 10.1103/PhysRevD.52.5428

Shibata, M., and Uryū, K. (2002). Gravitational waves from merger of binary neutron stars in fully general relativistic simulation. *Prog. Theor. Phys.* 107, 265–303. doi: 10.1143/PTP.107.265

Shibata, M., and Uryū, K. ō. (2000). Simulation of merging binary neutron stars in full general relativity: Γ=2 case. *Phys. Rev. D* 61:064001. doi: 10.1103/PhysRevD.61.064001

Shu, C.-W. (1998). "Essentially non-oscillatory and weighted essentially non-oscillatory schemes for hyperbolic conservation laws," in *Advanced Numerical Approximation of Nonlinear Hyperbolic Equations*, ed Q. Alfio (Berlin; Heidelberg: Springer), 325–432. doi: 10.1007/BFb0096355

Shu, C.-W., and Osher, S. (1988). Efficient implementation of essentially non-oscillatory shock-capturing schemes. *J. Comput. Phys.* 77, 439–471. doi: 10.1016/0021-9991(88)90177-5

Smarr, L., and York, J. W. Jr. (1978). Kinematical conditions in the construction of spacetime. *Phys. Rev. D* 17, 2529–2551. doi: 10.1103/PhysRevD.17.2529

Sperhake, U. (2007). Binary black-hole evolutions of excision and puncture data. *Phys. Rev. D* 76:104015. doi: 10.1103/PhysRevD.76.104015

Suresh, A., and Huynh, H. (1997). Accurate monotonicity-preserving schemes with Runge-Kutta time stepping. *J. Comput. Phys.* 136, 83–99. doi: 10.1006/jcph.1997.5745

Szilágyi, B., Lindblom, L., and Scheel, M. A. (2009). Simulations of binary black hole mergers using spectral methods. *Phys. Rev. D* 80:124010. doi: 10.1103/PhysRevD.80.124010

van Meter, J. R., Baker, J. G., Koppitz, M., and Choi, D.-I. (2006). How to move a black hole without excision: Gauge conditions for the numerical evolution of a moving puncture. *Phys. Rev. D* 73:124011. doi: 10.1103/PhysRevD.73.124011

Will, C. M. (2014). The confrontation between general relativity and experiment. *Living Rev. Relat.* 17:4. doi: 10.12942/lrr-2014-4

Witten, L. (1962). *Gravitation: An Introduction to Current Research* (Wiley).

Yamamoto, T., Shibata, M., and Taniguchi, K. (2008). Simulating coalescing compact binaries by a new code (SACRA). *Phys. Rev. D* 78:064054. doi: 10.1103/PhysRevD.78.064054

York, J. W. (1979). "Kinematics and dynamics of general relativity," in *Sources of Gravitational Radiation*, ed L. L. Smarr (Cambridge: Cambridge University Press), 83–126.

Conflict of Interest: The author declares that the research was conducted in the absence of any commercial or financial relationships that could be construed as a potential conflict of interest.

frontiers in Astronomy and Space Sciences

MINI REVIEW
published: 30 June 2020
doi: 10.3389/fspas.2020.00027

Binary Neutron Star Mergers After GW170817

Riccardo Ciolfi [1,2]*

[1] INAF–Osservatorio Astronomico di Padova, Padova, Italy, [2] INFN–Sezione di Padova, Padova, Italy

The first combined detection of gravitational waves and electromagnetic signals from a binary neutron star (BNS) merger in August 2017 (an event named GW170817) represents a major landmark in the ongoing investigation of these extraordinary systems. In this short review, we discuss BNS mergers as events of utmost importance for astrophysics and fundamental physics and survey the main discoveries enabled by this first multimessenger observation, including compelling evidence that such mergers produce a copious amount of heavy r-process elements and can power short gamma-ray bursts. We further discuss some remaining key open questions regarding this event and BNS mergers in general, focusing on the current status and limitations of theoretical models and numerical simulations.

Keywords: neutron stars, compact binary mergers, gravitational waves, multimessenger astrophysics, gamma-ray burst, kilonova

OPEN ACCESS

Edited by:
Bruno Giacomazzo,
University of Milano-Bicocca, Italy

Reviewed by:
Brian Metzger,
Columbia University, United States
Wen-Biao Han,
Chinese Academy of Sciences, China

***Correspondence:**
Riccardo Ciolfi
riccardo.ciolfi@inaf.it

Specialty section:
This article was submitted to Cosmology, a section of the journal Frontiers in Astronomy and Space Sciences

Received: *19 March 2020*
Accepted: *06 May 2020*
Published: *30 June 2020*

Citation:
Ciolfi R (2020) Binary Neutron Star Mergers After GW170817. Front. Astron. Space Sci. 7:27. doi: 10.3389/fspas.2020.00027

INTRODUCTION

Binary neutron star (BNS) mergers are among the most intriguing events known in the universe, with impressive scientific potential spanning many different research fields in physics and astrophysics. Investigating these mergers offers a unique opportunity to understand hadronic interactions at supranuclear densities and the equations of state (EOS) of matter in such extreme conditions while gaining crucial insights into the strong gravity regime, high-energy astrophysical phenomena of primary importance, such as gamma-ray bursts (GRBs), the origin of heavy elements in the local universe, formation channels of compact object binaries, and cosmology (see e.g., Faber and Rasio, 2012; Baiotti and Rezzolla, 2017 and references therein).

The merger of two neutron stars (NSs) is accompanied by a strong emission of gravitational waves (GWs) and a rich variety of electromagnetic (EM) signals covering the entire spectrum, from gamma-rays to radio. Such a unique combination of signals makes these systems ideal multimessenger sources and allows us to observe them up to cosmological distances. Moreover, among their EM "counterparts," BNS mergers have long been thought to be responsible for short gamma-ray bursts (SGRBs) (Paczynski, 1986; Eichler et al., 1989; Narayan et al., 1992; Barthelmy et al., 2005; Fox et al., 2005; Gehrels et al., 2005; Berger, 2014) as well as radioactively powered "kilonova" transients associated with r-process nucleosynthesis of heavy elements (Li and Paczyński, 1998; Rosswog, 2005; Metzger et al., 2010)[1].

[1]Merging mixed binaries, each composed of an NS and a black hole (BH), share most of the above features, also being promising GW sources, potential SGRB central engines, and potential sources of radioactively powered kilonovae. However, the properties of the emitted signals could be very different. Here we focus on BNS mergers only and refer the reader to other reviews (e.g., Shibata and Taniguchi, 2011) for the case of NS-BH binary mergers.

A major step forward in the study of BNS mergers was made possible by the first GW detection for this type of event by the LIGO and Virgo Collaboration in August 2017 (an event known as GW170817) (Abbott et al., 2017d). This merger was also observed in the EM spectrum, via a collection of gamma-ray, X-ray, ultraviolet (UV), optical, infrared (IR), and radio signals, thus also providing the first multimessenger observation of a GW source (Abbott et al., 2017e). This breakthrough led to a number of key discoveries, including a striking confirmation that BNS mergers can launch SGRB jets (Abbott et al., 2017c; Alexander et al., 2017, 2018; Goldstein et al., 2017; Hallinan et al., 2017; Margutti et al., 2017; Savchenko et al., 2017; Troja et al., 2017; Lazzati et al., 2018; Lyman et al., 2018; Mooley et al., 2018a,b; Ghirlanda et al., 2019) and are ideal sites for r-process nucleosynthesis (e.g., Arcavi et al., 2017; Coulter et al., 2017; Kasen et al., 2017; Pian et al., 2017; Smartt et al., 2017; see also Metzger, 2019 and references therein), the first GW-based constraints on the NS EOS (Abbott et al., 2019) and the Hubble constant (Abbott et al., 2017b), and more. The most important lessons learned from this event are discussed in section .

Besides the remarkable results mentioned above, the GW170817 event also raised a number of questions, some relating to details of the merging process that remained only poorly constrained. For instance, the remnant object resulting from the merger appears most likely to be a metastable massive NS that eventually collapsed into a BH, but the lack of clear indications of its survival time until collapse leaves doubts regarding the nature of the SGRB central engine, which could have been either the massive NS or the accreting BH (see e.g., Ciolfi, 2018 for a recent review). Theoretical modeling of the merger process via general relativistic magnetohydrodynamics (GRMHD) simulations (see **Figure 1**) offers the best chance to tackle the open questions and to establish a reliable connection between the merger and post-merger dynamics and the observable GW and EM emission (e.g., Ciolfi, 2020b and references therein). In section , we briefly report on the status of the research in this direction, with reference to specific challenges posed by the GW170817 event. Finally, concluding remarks are given in section .

THE BNS MERGER OF AUGUST 2017

The characteristic "chirp" signal of GW170817, with both frequency and amplitude increasing over time up to a maximum, leaves no doubt that the source was a merging compact binary with component masses fully consistent with two NSs (Abbott et al., 2017d). In addition, the BNS nature of the source is arguably reinforced by the EM counterparts observed along with GWs (Abbott et al., 2017e). Under the BNS assumption, this single detection significantly improved our estimate for the corresponding local coalescence rate (the value reported in Abbott et al., 2017d being $R = 1540^{+3200}_{-1220}\,\mathrm{Gpc^{-3}\,yr^{-1}}$)[2].

For this event, most of the information inferred from GWs came from the inspiral phase up to merger, while the lower detector sensitivity at frequencies above 1 kHz did not allow for a confident detection of the post-merger signal (Abbott et al., 2017d). Despite such limitations, it was possible to start placing the first limits on the NS tidal deformability and thus constrain the range of NS EOS compatible with the event (see e.g., Abbott et al., 2019; Kastaun and Ohme, 2019) by measuring finite-size effects (i.e., deviations from the point-mass waveform) in the last orbits of the inspiral. Moreover, by combining the luminosity distance derived from GWs with the EM redshift measurement that the identification of the host galaxy (NGC 4993) allowed, it was possible to obtain the first constraints on the Hubble constant based on a GW standard siren determination (Abbott et al., 2017b).

The observation of a gamma-ray signal emerging about 1.74 s after the estimated time of merger enabled us to confirm that GWs propagate at the speed of light with a precision better than 10^{-14} (Abbott et al., 2017c), which excluded a whole range of gravitational theories beyond general relativity. At the same time, this high-energy signal (called GRB 170817A) was found to be potentially consistent with an SGRB, albeit orders of magnitude less energetic than any other known SGRB (Abbott et al., 2017c). Combining the prompt gamma-ray emission with the multiwavelength afterglows (in X-ray, optical, and radio) monitored for several months, it was possible to eventually converge to the following picture (Abbott et al., 2017c; Alexander et al., 2017, 2018; Goldstein et al., 2017; Hallinan et al., 2017; Margutti et al., 2017; Savchenko et al., 2017; Troja et al., 2017; Lazzati et al., 2018; Lyman et al., 2018; Mooley et al., 2018a,b; Ghirlanda et al., 2019): (i) the merger remnant launched a highly relativistic jet (Lorentz factor > 10), in agreement with the consolidated GRB paradigm (e.g., Piran, 2004; Kumar and Zhang, 2015); (ii) the burst was observed off-axis by 15–30°, and the low-energy gamma-ray signal detected was not produced by the jet core but rather by a mildly relativistic outflow moving along the line of sight; (iii) the on-axis observer would have seen a burst energetically consistent with the other known SGRBs. This provided the long-awaited compelling evidence that *BNS mergers can generate SGRBs*. Furthermore, the off-axis view of a nearby ($\sim$ 40 Mpc distance) SGRB jet gave us an unprecedented opportunity to study its full angular structure.

The other major result related to GW170817 is the first clear photometric and spectroscopic identification of a kilonova, i.e., a UV/optical/IR transient powered by the radioactive decay of heavy r-process elements synthesized within the matter ejected by the merger process (e.g., Arcavi et al., 2017; Coulter et al., 2017; Kasen et al., 2017; Pian et al., 2017; Smartt et al., 2017; see also Metzger, 2019 and references therein). This confirmed that *BNS mergers produce a significant amount of elements heavier than iron, up to very large atomic mass numbers* ($A > 140$).

OPEN QUESTIONS AND ONGOING RESEARCH

The discoveries connected with GW170817 certainly represent a breakthrough in the field, but a lot remains to be understood concerning both this event and BNS mergers in general. Part of

[2]Under the assumption that GW190425 was also a BNS merger, the updated rate would be $R = 250$–$2810\,\mathrm{Gpc^{-3}\,yr^{-1}}$ (Abbott et al., 2020).

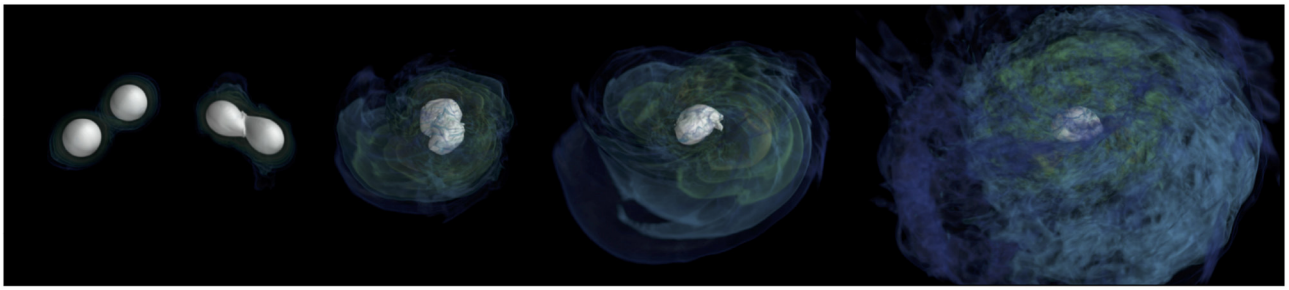

FIGURE 1 | Example of BNS merger simulation in GRMHD (from the models presented in Ciolfi et al., 2017). The temporal sequence shows the bulk of the NS(s) in white together with color-coded isodensity surfaces.

our ignorance can be ascribed to current observational limits. For instance, much better constraints on the NS EOS will become available with the considerably higher sensitivity of third-generation GW detectors (Punturo et al., 2010; Abbott et al., 2017a), allowing also for confident detection of the post-merger GW signal, while the merger rate, the formation scenarios of BNS systems, and the GW-based Hubble constant determination will improve greatly with the increasing number of detections. On the other hand, there are many aspects for which the information encoded in the observed signals (in particular in the EM counterparts) cannot be fully exploited because of the present limitations of theoretical models. This situation urgently calls for further development on the theory side, particularly in the context of BNS merger simulation in general relativity, which represents the leading approach to elucidating the physical mechanisms at work when two NSs merge.

In the following, we discuss recent results of BNS merger simulations and the associated limitations, focusing on interpretation of the August 2017 event. In particular, we consider the two most important EM counterparts of this event: (i) the SGRB and its multiwavelength afterglows, and (ii) the kilonova transient.

SGRB Central Engines and GRB 170817A

Understanding the launching mechanism of an SGRB jet from a BNS merger and the nature of the remnant object acting as central engine is among the main motivations for the development of numerical relativity simulations of such mergers (e.g., Rezzolla et al., 2011; Kiuchi et al., 2014; Kawamura et al., 2016; Ruiz et al., 2016; Ciolfi et al., 2017, 2019). The great progress made in this type of simulation, especially over the past decade, has allowed us to draw important conclusions, even though the final solution of the SGRB puzzle is still ahead of us.

According to the most discussed scenario, an SGRB jet would be launched by a spinning BH surrounded by a massive ($\sim 0.1\,M_{\odot}$) accretion disk, which is a likely outcome of a BNS merger. Recent simulations (Just et al., 2016; Perego et al., 2017b) have shown that a jet powered by neutrino-antineutrino annihilation would not be powerful enough to explain the phenomenology of SGRBs, reinforcing the idea that SGRB jets should instead be magnetically driven. Various GRMHD simulations (e.g., Rezzolla et al., 2011; Kiuchi et al., 2014; Kawamura et al., 2016; Ruiz et al., 2016) have explored the latter possibility, confirming the formation of a low-density funnel along the BH spin axis and finding indications of an emerging helical magnetic field structure that is favorable for accelerating an outflow. In addition, simulations reported in Ruiz et al. (2016) were the first to show the actual production of a magnetically dominated mildly relativistic outflow, and the authors argued that such an outflow could in principle reach terminal Lorentz factors compatible with an SGRB jet. While the results obtained so far do not provide the ultimate answer, current simulations suggest that the accreting BH scenario is a promising one (see e.g., Ciolfi, 2018, 2020b for a more detailed discussion).

The alternative scenario in which the central engine is a massive NS remnant has also been investigated via GRMHD BNS merger simulations, although a systematic study commenced only recently (Ciolfi et al., 2017, 2019; Ciolfi, 2020a). In this case, the higher level of baryon pollution along the spin axis could hamper the formation of an incipient jet. The longest (to date) simulations of this kind, recently presented in Ciolfi (2020a), showed for the first time that the NS differential rotation can still build up a helical magnetic field structure capable of accelerating a collimated outflow (see **Figure 2**), although such an outcome is not ubiquitous[3]. In addition, for the case under consideration, the properties of the collimated outflow (and in particular the very low terminal Lorentz factor) were found to be largely incompatible with an SGRB jet (Ciolfi, 2020a). This result reveals serious difficulties in powering an SGRB that might apply to massive NS remnants in general, thus pointing in favor of the alternative BH central engine. In order to confirm the above conclusion, however, a greater variety of physical conditions needs to be explored (e.g., by including neutrino radiation).

For the GRB 170817A event, neither the observations nor the current theoretical models can confidently exclude either one of the two scenarios. Nevertheless, BNS merger simulations have already provided valuable hints in favor of the accreting BH scenario (Ruiz et al., 2016; Ciolfi, 2020a), and the continuous

[3]Note that a collimated outflow was also reported in studies where an *ad-hoc* dipolar field was superimposed by hand on a differentially rotating NS remnant (e.g., Shibata et al., 2011; Siegel et al., 2014; Mösta et al., 2020).

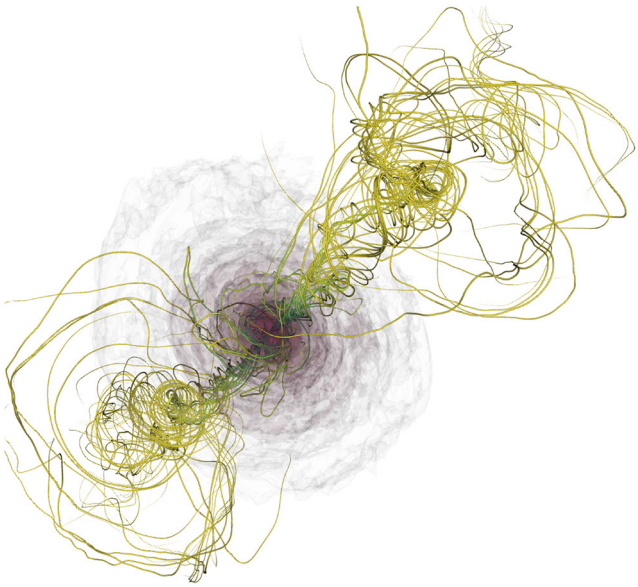

FIGURE 2 | Collimated helical magnetic field structure emerging along the spin axis of a long-lived BNS merger remnant (from a simulation presented in Ciolfi, 2020a). Several semi-transparent isodensity surfaces are also shown for the highest rest-mass density region (with density increasing from gray to red).

improvement of numerical codes and the degree of realism of their physical descriptions could soon lead to a definitive answer.

Another important limiting factor for the interpretation of GRB 170817A is the considerable gap between the relatively small time scales and spatial scales probed by GRMHD merger simulations (up to order ~ 100 ms and ~ 1000 km) and those relevant for the propagation of an incipient jet through the baryon-polluted environment surrounding the merger site ($\gtrsim 1$ s and $\gtrsim 10^5$ km). The ultimate angular structure and energetics of the escaping jet, which are directly related to the prompt and afterglow SGRB emission, are therefore very hard to associate with specific properties of the merging system and a specific launching mechanism. One of the most important challenges to be addressed in the near future is therefore to obtain a self-consistent model that is able to describe the full evolution from the pre-merger stage up to the final escaping jet.

Merger Ejecta and the Kilonova Transient AT 2017gfo

During and after a BNS merger, a relatively large amount of material (up to $\sim 0.1\ M_\odot$) can be ejected, either via dynamical mechanisms associated with the merger process (tidally driven and shock-driven ejecta) or via baryon-loaded winds launched by the (meta)stable massive NS remnant and/or by the accretion disk around the newly formed BH (if any). Depending on the thermodynamical history and composition (in particular the electron fraction Y_e) of each fluid element within the ejecta, the r-process nucleosynthesis takes place and produces a certain amount of heavy elements (i.e., heavier than iron). Later on, the radioactive decay of these elements powers the thermal transient commonly referred to as a kilonova (e.g., Metzger, 2019 and references therein).

For a given ejecta component, the peak luminosity, peak time, and peak frequency (or temperature) of the corresponding kilonova are mainly determined by the ejecta mass, velocity, and opacity (e.g., Grossman et al., 2014). While the mass and velocity depend on the mass ejection mechanism, the opacity is directly related to the nucleosynthesis yields. In particular, high electron fractions ($Y_e \gtrsim 0.25$) typically produce elements up to atomic mass numbers $A \lesssim 140$, maintaining a relatively low opacity of ~ 0.1–$1\ \mathrm{cm}^2/\mathrm{g}$, whereas more neutron-rich ejecta ($Y_e \lesssim 0.25$) allow the production of elements up to $A > 140$ (including the group of lanthanides), which leads to much higher opacities of $\sim 10\ \mathrm{cm}^2/\mathrm{g}$ (e.g., Kasen et al., 2013; Tanaka and Hotokezaka, 2013).

When applied to the kilonova of August 2017, the above picture reveals that the observed transient (AT 2017gfo) was generated by at least two distinct ejecta components (e.g., Kasen et al., 2017)[4], one having mass ≈ 1.5–$2.5 \times 10^{-2}\ M_\odot$, velocity ≈ 0.2–$0.3\ c$, and a relatively low opacity of $\approx 0.5\ \mathrm{cm}^2/\mathrm{g}$, leading to a "blue" kilonova peaking at ~ 1 day after merger, and the other having mass ≈ 4–$6 \times 10^{-2}\ M_\odot$, velocity $\approx 0.1\ c$, and a much higher opacity of $\sim 10\ \mathrm{cm}^2/\mathrm{g}$, leading to a "red" kilonova emerging on a time scale of ~ 1 week. One of the current challenges is to identify the mass ejection mechanisms responsible for these components. In such a quest, numerical relativity simulations of BNS mergers play a pivotal role.

The "red" part of the 2017 kilonova is perhaps the easier of the two to account for. The very large mass and low velocity would exclude dynamical mass ejection and point to a baryon-loaded wind. In particular, the mass expelled by the accretion disk around the BH (i.e., after the collapse of the NS remnant) appears to match the requirements, including a relatively high opacity, or equivalently a low electron fraction, for at least part of the material (e.g., Siegel and Metzger, 2018).

The origin of the "blue" kilonova is more debatable. The ejecta mass is rather high, but then so is the velocity ($v \gtrsim 0.2\ c$). The former still raises doubts over a dynamical ejection, while the latter represents a potential problem for post-merger baryon-loaded winds. The magnetically driven wind from the (meta)stable NS remnant offers a viable solution (Ciolfi and Kalinani, 2020), thanks to the enhanced mass ejection and the simultaneous acceleration due to the magnetic field (as previously suggested, e.g., in Metzger et al., 2018). In this case, neutrino irradiation would also be fundamental for raising the Y_e of the material, limiting the r-process nucleosynthesis, and thus maintaining a low opacity (Metzger et al., 2018). We stress, however, that other viable scenarios exist (e.g., Kawaguchi et al., 2018; Nedora et al., 2019).

Current kilonova models are still affected by several uncertainties around the microphysical parameters, the radiation transport (which is treated with strong approximations), and the mass ejection mechanisms. Nonetheless, we are witnessing rapid theoretical and numerical progress that will keep guiding us toward a more solid interpretation of the observational data.

[4]Three-component models were also proposed (e.g., Perego et al., 2017a).

CONCLUDING REMARKS

The growing interest in BNS mergers over the past few decades has recently been boosted by the multimessenger observation of the August 2017 event, GW170817. Among numerous breakthrough results, this BNS merger has provided fundamental confirmations of theoretical predictions, in particular the association with SGRBs, which was already supported by indirect evidence but still unproven, and the production of heavy r-process elements and the related kilonova transients. This success on the theory side certainly strengthens motivation for the development of models and numerical simulations. At the same time, the case of GW170817 has shown that present and near-future observations are likely to contain much more information than we are currently capable of exploiting, making further advancements in our ability to interpret the data more urgent than ever.

AUTHOR CONTRIBUTIONS

The author confirms being the sole contributor of this work and has approved it for publication.

REFERENCES

Abbott, B. P., Abbott, R., Abbott, T. D., Abernathy, M. R., Ackley, K., Adams, C., et al. (2017a). Exploring the sensitivity of next generation gravitational wave detectors. *Class. Quant. Gravity* 34:044001. doi: 10.1088/1361-6382/aa51f4

Abbott, B. P., Abbott, R., Abbott, T. D., Abraham, S., Acernese, F., Ackley, K., et al. (2020). GW190425: observation of a compact binary coalescence with total mass $\sim 3.4\ M_{\odot}$. *Astrophys. J. Lett.* 892:L3. doi: 10.3847/2041-8213/ab75f5

Abbott, B. P., Abbott, R., Abbott, T. D., Acernese, F., Ackley, K., Adams, C., et al. (2017b). A gravitational-wave standard siren measurement of the Hubble constant. *Nature* 551, 85–88. doi: 10.1038/nature24471

Abbott, B. P., Abbott, R., Abbott, T. D., Acernese, F., Ackley, K., Adams, C., et al. (2017c). Gravitational waves and gamma-rays from a binary neutron star merger: GW170817 and GRB 170817A. *Astrophys. J. Lett.* 848:L13. doi: 10.3847/2041-8213/aa920c

Abbott, B. P., Abbott, R., Abbott, T. D., Acernese, F., Ackley, K., Adams, C., et al. (2017d). GW170817: observation of gravitational waves from a binary neutron star inspiral. *Phys. Rev. Lett.* 119:161101. doi: 10.1103/PhysRevLett.119.161101

Abbott, B. P., Abbott, R., Abbott, T. D., Acernese, F., Ackley, K., Adams, C., et al. (2017e). Multi-messenger observations of a binary neutron star merger. *Astrophys. J. Lett.* 848:L12. doi: 10.3847/2041-8213/aa91c9

Abbott, B. P., Abbott, R., Abbott, T. D., Acernese, F., Ackley, K., Adams, C., et al. (2019). Properties of the binary neutron star merger GW170817. *Phys. Rev. X* 9:011001. doi: 10.1103/PhysRevX.9.011001

Alexander, K. D., Berger, E., Fong, W., Williams, P. K. G., Guidorzi, C., Margutti, R., et al. (2017). The electromagnetic counterpart of the binary neutron star merger LIGO/Virgo GW170817. VI. Radio constraints on a relativistic jet and predictions for late-time emission from the kilonova ejecta. *Astrophys. J. Lett.* 848:L21. doi: 10.3847/2041-8213/aa905d

Alexander, K. D., Margutti, R., Blanchard, P. K., Fong, W., Berger, E., Hajela, A., et al. (2018). A decline in the X-ray through radio emission from GW170817 continues to support an off-axis structured jet. *Astrophys. J. Lett.* 863:L18. doi: 10.3847/2041-8213/aad637

Arcavi, I., Hosseinzadeh, G., Howell, D. A., McCully, C., Poznanski, D., Kasen, D., et al. (2017). Optical emission from a kilonova following a gravitational-wave-detected neutron-star merger. *Nature* 551, 64–66. doi: 10.1038/nature24291

Baiotti, L., and Rezzolla, L. (2017). Binary neutron star mergers: a review of Einstein's richest laboratory. *Rep. Prog. Phys.* 80:096901. doi: 10.1088/1361-6633/aa67bb

Barthelmy, S. D., Chincarini, G., Burrows, D. N., Gehrels, N., Covino, S., Moretti, A., et al. (2005). An origin for short γ-ray bursts unassociated with current star formation. *Nature* 438, 994–996. doi: 10.1038/nature04392

Berger, E. (2014). Short-duration gamma-ray bursts. *Ann. Rev. Astron. Astrophys.* 52, 43–105. doi: 10.1146/annurev-astro-081913-035926

Ciolfi, R. (2018). Short gamma-ray burst central engines. *Int. J. Mod. Phys. D* 27:1842004. doi: 10.1142/S021827181842004X

Ciolfi, R. (2020a). Collimated outflows from long-lived binary neutron star merger remnants. *Mon. Not. R. Astron. Soc. Lett.* 495, L66–L70. doi: 10.1093/mnrasl/slaa062

Ciolfi, R. (2020b). The key role of magnetic fields in binary neutron star mergers. *arXiv* 2003.07572.

Ciolfi, R., and Kalinani, J. V. (2020). Magnetically driven baryon winds from binary neutron star merger remnants and the blue kilonova of August 2017. *arXiv* 2004.11298.

Ciolfi, R., Kastaun, W., Giacomazzo, B., Endrizzi, A., Siegel, D. M., and Perna, R. (2017). General relativistic magnetohydrodynamic simulations of binary neutron star mergers forming a long-lived neutron star. *Phys. Rev. D* 95:063016. doi: 10.1103/PhysRevD.95.063016

Ciolfi, R., Kastaun, W., Kalinani, J. V., and Giacomazzo, B. (2019). First 100 ms of a long-lived magnetized neutron star formed in a binary neutron star merger. *Phys. Rev. D* 100:023005. doi: 10.1103/PhysRevD.100.023005

Coulter, D. A., Foley, R. J., Kilpatrick, C. D., Drout, M. R., Piro, A. L., Shappee, B. J., et al. (2017). Swope Supernova Survey 2017a (SSS17a), the optical counterpart to a gravitational wave source. *Science* 358, 1556–1558. doi: 10.1126/science.aap9811

Eichler, D., Livio, M., Piran, T., and Schramm, D. N. (1989). Nucleosynthesis, neutrino bursts and gamma-rays from coalescing neutron stars. *Nature* 340, 126–128. doi: 10.1038/340126a0

Faber, J. A., and Rasio, F. A. (2012). Binary neutron star mergers. *Liv. Rev. Rel.* 15:8. doi: 10.12942/lrr-2012-8

Fox, D. B., Frail, D. A., Price, P. A., Kulkarni, S. R., Berger, E., Piran, T., et al. (2005). The afterglow of GRB050709 and the nature of the short-hard gamma-ray bursts. *Nature* 437, 845–850. doi: 10.1038/nature04189

Gehrels, N., Sarazin, C. L., O'Brien, P. T., Zhang, B., Barbier, L., Barthelmy, S. D., et al. (2005). A short γ-ray burst apparently associated with an elliptical galaxy at redshift z = 0.225. *Nature* 437, 851–854. doi: 10.1038/nature04142

Ghirlanda, G., Salafia, O. S., Paragi, Z., Giroletti, M., Yang, J., Marcote, B., et al. (2019). Compact radio emission indicates a structured jet was produced by a binary neutron star merger. *Science* 363, 968–971. doi: 10.1126/science.aau8815

Goldstein, A., Veres, P., Burns, E., Briggs, M. S., Hamburg, R., Kocevski, D., et al. (2017). An ordinary short gamma-ray burst with extraordinary implications: fermi-GBM detection of GRB 170817A. *Astrophys. J. Lett.* 848:L14. doi: 10.3847/2041-8213/aa8f41

Grossman, D., Korobkin, O., Rosswog, S., and Piran, T. (2014). The long-term evolution of neutron star merger remnants–II. Radioactively powered transients. *Mon. Not. R. Astron. Soc.* 439, 757–770. doi: 10.1093/mnras/stt2503

Hallinan, G., Corsi, A., Mooley, K. P., Hotokezaka, K., Nakar, E., Kasliwal, M. M., et al. (2017). A radio counterpart to a neutron star merger. *Science* 358, 1579–1583. doi: 10.1126/science.aap9855

Just, O., Obergaulinger, M., Janka, H.-T., Bauswein, A., and Schwarz, N. (2016). Neutron-star merger ejecta as obstacles to neutrino-powered jets of gamma-ray bursts. *Astrophys. J. Lett.* 816:L30. doi: 10.3847/2041-8205/816/2/L30

Kasen, D., Badnell, N. R., and Barnes, J. (2013). Opacities and spectra of the R-process ejecta from neutron star mergers. *Astrophys. J.* 774:25. doi: 10.1088/0004-637X/774/1/25

Kasen, D., Metzger, B., Barnes, J., Quataert, E., and Ramirez-Ruiz, E. (2017). Origin of the heavy elements in binary neutron-star mergers from a gravitational-wave event. *Nature* 551, 80–84. doi: 10.1038/nature24453

Kastaun, W., and Ohme, F. (2019). Finite tidal effects in GW170817: Observational evidence or model assumptions? *Phys. Rev. D* 100:103023. doi: 10.1103/PhysRevD.100.103023

Kawaguchi, K., Shibata, M., and Tanaka, M. (2018). Radiative transfer simulation for the optical and near-infrared electromagnetic counterparts to GW170817. *Astrophys. J. Lett.* 865:L21. doi: 10.3847/2041-8213/aade02

Kawamura, T., Giacomazzo, B., Kastaun, W., Ciolfi, R., Endrizzi, A., Baiotti, L., et al. (2016). Binary neutron star mergers and short gamma-ray bursts: effects of magnetic field orientation, equation of state, and mass ratio. *Phys. Rev. D* 94:064012. doi: 10.1103/PhysRevD.94.064012

Kiuchi, K., Kyutoku, K., Sekiguchi, Y., Shibata, M., and Wada, T. (2014). High resolution numerical relativity simulations for the merger of binary magnetized neutron stars. *Phys. Rev. D* 90:041502. doi: 10.1103/PhysRevD.90.041502

Kumar, P., and Zhang, B. (2015). The physics of gamma-ray bursts and relativistic jets. *Phys. Rep.* 561, 1–109. doi: 10.1016/j.physrep.2014.09.008

Lazzati, D., Perna, R., Morsony, B. J., Lopez-Camara, D., Cantiello, M., Ciolfi, R., et al. (2018). Late time afterglow observations reveal a collimated relativistic jet in the ejecta of the binary neutron star merger GW170817. *Phys. Rev. Lett.* 120:241103. doi: 10.1103/PhysRevLett.120.241103

Li, L.-X., and Paczyński, B. (1998). Transient events from neutron star mergers. *Astrophys. J.* 507, L59–L62. doi: 10.1086/311680

Lyman, J. D., Lamb, G. P., Levan, A. J., Mandel, I., Tanvir, N. R., Kobayashi, S., et al. (2018). The optical afterglow of the short gamma-ray burst associated with GW170817. *Nat. Astron.* 2, 751–754. doi: 10.1038/s41550-018-0511-3

Margutti, R., Berger, E., Fong, W., Guidorzi, C., Alexander, K. D., Metzger, B. D., et al. (2017). The electromagnetic counterpart of the binary neutron star merger LIGO/Virgo GW170817. V. Rising X-ray emission from an off-axis jet. *Astrophys. J. Lett.* 848:L20. doi: 10.3847/2041-8213/aa9057

Metzger, B. D. (2019). Kilonovae. *Liv. Rev. Rel.* 23:1. doi: 10.1007/s41114-019-0024-0

Metzger, B. D., Martínez-Pinedo, G., Darbha, S., Quataert, E., Arcones, A., Kasen, D., et al. (2010). Electromagnetic counterparts of compact object mergers powered by the radioactive decay of r-process nuclei. *Mon. Not. R. Astron. Soc.* 406, 2650–2662. doi: 10.1111/j.1365-2966.2010.16864.x

Metzger, B. D., Thompson, T. A., and Quataert, E. (2018). A magnetar origin for the kilonova ejecta in GW170817. *Astrophys. J. Lett.* 856:101. doi: 10.3847/1538-4357/aab095

Mooley, K. P., Deller, A. T., Gottlieb, O., Nakar, E., Hallinan, G., Bourke, S., et al. (2018a). Superluminal motion of a relativistic jet in the neutron-star merger GW170817. *Nature* 561, 355–359. doi: 10.1038/s41586-018-0486-3

Mooley, K. P., Nakar, E., Hotokezaka, K., Hallinan, G., Corsi, A., Frail, D. A., et al. (2018b). A mildly relativistic wide-angle outflow in the neutron-star merger event GW170817. *Nature* 554, 207–210. doi: 10.1038/nature25452

Mösta, P., Radice, D., Haas, R., Schnetter, E., and Bernuzzi, S. (2020). A magnetar engine for short GRBs and kilonovae. *arXiv* 2003.06043.

Narayan, R., Paczynski, B., and Piran, T. (1992). Gamma-ray bursts as the death throes of massive binary stars. *Astrophys. J. Lett.* 395, L83–L86. doi: 10.1086/186493

Nedora, V., Bernuzzi, S., Radice, D., Perego, A., Endrizzi, A., and Ortiz, N. (2019). Spiral-wave wind for the blue kilonova. *Astrophys. J. Lett.* 886:L30. doi: 10.3847/2041-8213/ab5794

Paczynski, B. (1986). Gamma-ray bursters at cosmological distances. *Astrophys. J. Lett.* 308, L43–L46. doi: 10.1086/184740

Perego, A., Radice, D., and Bernuzzi, S. (2017a). AT 2017gfo: an anisotropic and three-component kilonova counterpart of GW170817. *Astrophys. J. Lett.* 850:L37. doi: 10.3847/2041-8213/aa9ab9

Perego, A., Yasin, H., and Arcones, A. (2017b). Neutrino pair annihilation above merger remnants: implications of a long-lived massive neutron star. *J. Phys. G Nucl. Phys.* 44:084007. doi: 10.1088/1361-6471/aa7bdc

Pian, E., D'Avanzo, P., Benetti, S., Branchesi, M., Brocato, E., Campana, S., et al. (2017). Spectroscopic identification of r-process nucleosynthesis in a double neutron-star merger. *Nature* 551, 67–70. doi: 10.1038/nature24298

Piran, T. (2004). The physics of gamma-ray bursts. *Rev. Mod. Phys.* 76, 1143–1210. doi: 10.1103/RevModPhys.76.1143

Punturo, M., Abernathy, M., Acernese, F., Allen, B., Andersson, N., Arun, K., et al. (2010). The Einstein telescope: a third-generation gravitational wave observatory. *Class. Quant. Gravity* 27:194002. doi: 10.1088/0264-9381/27/19/194002

Rezzolla, L., Giacomazzo, B., Baiotti, L., Granot, J., Kouveliotou, C., and Aloy, M. A. (2011). The missing link: merging neutron stars naturally produce jet-like structures and can power short Gamma-Ray Bursts. *Astrophys. J. Lett.* 732:L6. doi: 10.1088/2041-8205/732/1/L6

Rosswog, S. (2005). Mergers of neutron star-black hole binaries with small mass ratios: nucleosynthesis, gamma-ray bursts, and electromagnetic transients. *Astrophys. J.* 634, 1202–1213. doi: 10.1086/497062

Ruiz, M., Lang, R. N., Paschalidis, V., and Shapiro, S. L. (2016). Binary neutron star mergers: a jet engine for short gamma-ray bursts. *Astrophys. J. Lett.* 824:L6. doi: 10.3847/2041-8205/824/1/L6

Savchenko, V., Ferrigno, C., Kuulkers, E., Bazzano, A., Bozzo, E., Brandt, S., et al. (2017). INTEGRAL detection of the first prompt gamma-ray signal coincident with the gravitational-wave event GW170817. *Astrophys. J. Lett.* 848:L15. doi: 10.3847/2041-8213/aa8f94

Shibata, M., Suwa, Y., Kiuchi, K., and Ioka, K. (2011). Afterglow of a binary neutron star merger. *Astrophys. J. Lett.* 734:L36. doi: 10.1088/2041-8205/734/2/L36

Shibata, M., and Taniguchi, K. (2011). Coalescence of black hole-neutron star binaries. *Liv. Rev. Rel.* 14:6. doi: 10.12942/lrr-2011-6

Siegel, D. M., Ciolfi, R., and Rezzolla, L. (2014). Magnetically driven winds from differentially rotating neutron stars and X-ray afterglows of short gamma-ray bursts. *Astrophys. J. Lett.* 785:L6. doi: 10.1088/2041-8205/785/1/L6

Siegel, D. M., and Metzger, B. D. (2018). Three-dimensional GRMHD simulations of neutrino-cooled accretion disks from neutron star mergers. *Astrophys. J.* 858:52. doi: 10.3847/1538-4357/aabaec

Smartt, S. J., Chen, T. W., Jerkstrand, A., Coughlin, M., Kankare, E., Sim, S. A., et al. (2017). A kilonova as the electromagnetic counterpart to a gravitational-wave source. *Nature* 551, 75–79. doi: 10.1038/nature24303

Tanaka, M., and Hotokezaka, K. (2013). Radiative transfer simulations of neutron star merger ejecta. *Astrophys. J.* 775:113. doi: 10.1088/0004-637X/775/2/113

Troja, E., Piro, L., van Eerten, H., Wollaeger, R. T., Im, M., Fox, O. D., et al. (2017). The X-ray counterpart to the gravitational-wave event GW170817. *Nature* 551, 71–74. doi: 10.1038/nature24290

Conflict of Interest: The author declares that the research was conducted in the absence of any commercial or financial relationships that could be construed as a potential conflict of interest.

frontiers in Astronomy and Space Sciences

MINI REVIEW
published: 28 July 2020
doi: 10.3389/fspas.2020.00046

A Brief Overview of Black Hole-Neutron Star Mergers

*Francois Foucart**

Department of Physics & Astronomy, University of New Hampshire, Durham, NH, United States

Of the three main types of binaries detectable through ground-based gravitational wave observations, black hole-neutron star (BHNS) mergers remain the most elusive. While candidates BHNS exist in the triggers released during the third observing run of the Advanced LIGO/Virgo collaboration, no detection has been confirmed so far. As for binary neutron star systems, BHNS binaries allow us to explore a wide range of physical processes, including the neutron star equation of state, nucleosynthesis, stellar evolution, high-energy astrophysics, and the expansion of the Universe. Here, we review some of the main features of BHNS systems: the distinction between disrupting and non-disrupting binaries, the types of outflows that BHNS mergers can produce, and the information that can be extracted from the observation of their gravitational wave and electromagnetic signals. We also emphasize that for the most likely binary parameters, BHNS mergers seem less likely to power electromagnetic signals than binary neutron star systems. Finally, we discuss some of the issues that still limit our ability to model and interpret electromagnetic signals from BHNS binaries.

Keywords: black holes, neutron stars, gravitational waves, kilonovae, gamma-ray bursts, numerical relativity

OPEN ACCESS

Edited by:
Rosalba Perna,
Stony Brook University, United States

Reviewed by:
Vyacheslav Ivanovich Dokuchaev,
Institute for Nuclear Research (RAS), Russia
Kenta Hotokezaka,
The University of Tokyo, Japan

***Correspondence:**
Francois Foucart
francois.foucart@unh.edu

Specialty section:
This article was submitted to Cosmology, a section of the journal Frontiers in Astronomy and Space Sciences

Received: *18 February 2020*
Accepted: *18 June 2020*
Published: *28 July 2020*

Citation:
Foucart F (2020) A Brief Overview of Black Hole-Neutron Star Mergers. Front. Astron. Space Sci. 7:46. doi: 10.3389/fspas.2020.00046

1. INTRODUCTION

The first observation by the LIGO-Virgo collaboration (LVC) of gravitational waves (GWs) coming from merging black holes (Abbott et al., 2016, GW150914) and neutron stars (Abbott et al., 2017c, GW170817) made GW astrophysics a reality. Since then, the LVC has confirmed an additional 9 binary black holes (BBH) (Abbott et al., 2019), with dozens of other systems announced in public alerts[1]. BBH mergers were also discovered by an independent search pipeline used on publicly available LVC data (Venumadhav et al., 2019). Most recently, an event that may have been a second binary neutron star (BNS) merger was reported by the LVC (Abbott et al., 2020, GW190425)[2].

BNS and black hole-neutron star (BHNS) systems play an especially interesting role in this new field of astrophysics. By observing neutron star mergers, we gather information about the equation of state of neutron stars (Flanagan and Hinderer, 2008; Abbott et al., 2018), about the origin of heavy elements produced through r-process nucleosynthesis (Freiburghaus et al., 1999; Drout et al., 2017; Pian et al., 2017), and about the expansion rate of the Universe (Abbott et al., 2017b; Hotokezaka et al., 2019). Neutron star mergers also power at least a subset of short gamma-ray bursts (SGRBs) (Abbott et al., 2017a), as well as UV/optical/infrared *kilonovae* (Li and Paczynski, 1998; Roberts et al., 2011; Chornock et al., 2017; Coulter et al., 2017; Cowperthwaite et al., 2017; Evans et al., 2017; Nicholl et al., 2017; Soares-Santos et al., 2017; Villar et al., 2017), and

[1]Public alerts from the LVC are available online at https://gracedb.ligo.org/.
[2]GW190425 has observed masses that could also plausibly be explained as a very low mass BHNS merger, if $\sim (2-3)M_{\odot}$ black holes exist.

radio emission from ultra-relativistic jets and mildly relativistic outflows (Nakar and Piran, 2011; Hotokezaka et al., 2016; Mooley et al., 2018). The event rates of BNS and BHNS mergers remain however very uncertain (Abadie et al., 2010; Belczynski et al., 2016; Abbott et al., 2020). Only two potential BNS mergers have been officially confirmed so far, and no BHNS mergers, even though a number of candidates can be found within the LVC's public alerts.

The evolution of BHNS binaries can be divided into three main phases: a millions-of-years long inspiral during which the two objects slowly lose energy and angular momentum to GW emission; a merger phase lasting about 1 ms and resulting in either the tidal disruption of the neutron star (see **Figure 1**) or its plunge into the black hole; and, for disrupting systems only, a seconds-long post-merger phase during which more matter is ejected or accreted onto the black hole. These three phases happen on widely different timescales, and involve different physical processes and observable signals. In this manuscript, we will review each stage of a BHNS's evolution in turn, and discuss important properties of the associated GW and electromagnetic (EM) signals.

BHNS systems cover a high-dimensional and largely unconstrained parameter space. Our priors for the properties of black holes and neutron stars in BHNS binaries come from their observation in other types of binary systems or from theoretical considerations, and are accordingly quite uncertain. While most neutron stars observed in BNS systems have masses in the $[1.2-1.6]\,M_\odot$ range (Özel et al., 2012), more massive neutron stars exist, up to at least $\sim 2M_\odot$ (Demorest et al., 2010; Antoniadis et al., 2013). Most galactic black holes have masses of $[5-15]\,M_\odot$ (Özel et al., 2010), but black holes observed through GWs are often more massive (Abbott et al., 2019). Whether black holes can be formed within the "mass gap" between the most massive neutron stars and $\sim 5M_\odot$ also remains an important open question. The magnitude and orientation of black hole spins are unknown, and while most BHNS binaries are expected to have negligible eccentricities (Peters and Mathews, 1963), eccentric BHNS binaries cannot entirely be ruled out and have evolutions very distinct from circular binaries (Stephens et al., 2011). Obtaining reliable models for the observable signals powered by BHNS binaries across this vast parameter space can be difficult, yet the dependence of these signals in the properties of BHNS binaries is what allows us to extract valuable information from observations. In this review, we mostly consider circular binaries, leaving as free parameters the masses $M_{\rm NS,BH}$ of the compact objects, their dimensionless spins $\vec{\chi}_{\rm NS,BH}$, and the equation of state of dense nuclear matter, which sets the radius $R_{\rm NS}$ of a given neutron star.

2. BINARY INSPIRAL

From an observational point of view, the millions of years of GW driven inspiral that eventually result in the merger of a BHNS binary constitute an extended dark age between the supernova

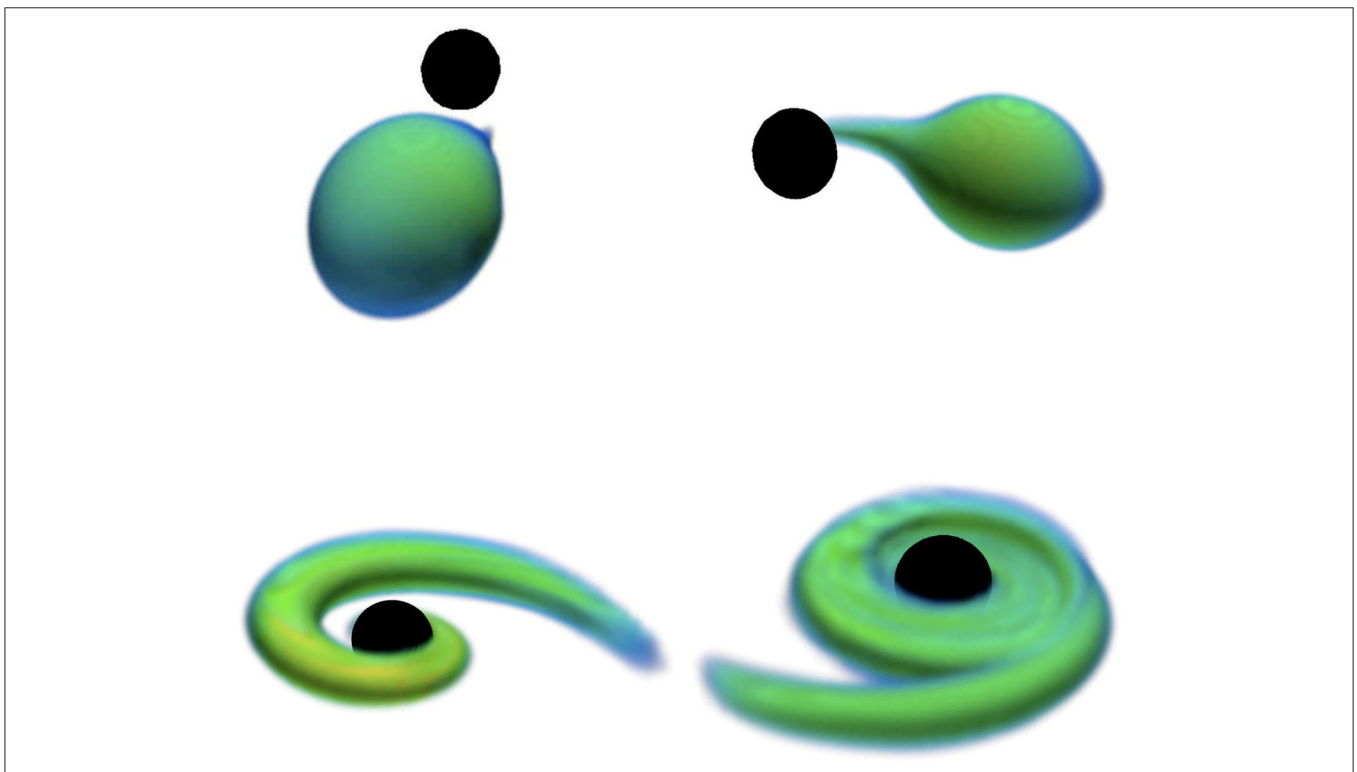

FIGURE 1 | Time evolution of a disrupting BHNS binary, including: onset of mass accretion (top left), unstable mass transfer (top right), evolution into a long tidal tail (bottom left), and circularization into an accretion disk (bottom right).

explosion that created the neutron star and the bright GW and EM emissions that accompany the merger. Ground-based GW detectors, such as LIGO and Virgo only become sensitive to BHNS binaries seconds to minutes before merger. Most of our efforts thus focus on understanding the very end of the inspiral. To first order, the GW-driven inspiral of BHNS binaries proceeds as for black holes of the same masses and spins. GW detectors are mostly sensitive to the chirp mass

$$M_c = \frac{(M_{\rm NS}M_{\rm BH})^{3/5}}{(M_{\rm BH}+M_{\rm NS})^{1/5}} \quad (1)$$

of a system, while individual mass measurements suffer from large statistical errors for all but the brightest events. As for BNS systems, the main observable effect of the finite size of neutron stars before merger is the acceleration of the GW-driven inspiral due to tides (Flanagan and Hinderer, 2008): large neutron stars merge earlier than more compact stars. GW detectors are primarily sensitive to the resulting change in the phase of the GW signal. To first order, that change is linear in the dimensionless tidal deformability parameter (Hinderer et al., 2010), defined for BHNS systems as

$$\tilde{\Lambda} = \frac{32}{39}\frac{M_{\rm NS}^4(M_{\rm NS}+12M_{\rm BH})}{(M_{\rm NS}+M_{\rm BH})^5}\frac{k_2}{C_{\rm NS}^5} \quad (2)$$

with $C_{\rm NS} = M_{\rm NS}G/(R_{\rm NS}c^2)$ the compaction of the neutron star, and k_2 its dimensionless $l = 2$ Love number. Both k_2 and $R_{\rm NS}$ depend on the equation of state of nuclear matter inside the neutron star. Unfortunately, $\tilde{\Lambda}$ becomes very small when $M_{\rm BH} \gg M_{\rm NS}$. As a result, finite size effects in BHNS mergers are expected to be detectable only for close-by events involving low-mass black holes (Lackey et al., 2014). The usefulness of BHNS binaries for the determination of the neutron star equation of state largely depends on the event rate of BHNS mergers that involve low-mass black holes. The existence of black holes within the supposed "mass gap" would be particularly convenient in that respect. For reference, recent results from the LVC (Abbott et al., 2018), NICER (Miller et al., 2019; Riley et al., 2019), and joint analysis of both datasets (Landry et al., 2020; Raaijmakers et al., 2020) find $R_{\rm NS} \sim (10.5-14.5)$ km, with variations due to the chosen astrophysical data, equation of state model and maximum NS mass.

Additionally, *it can be difficult to unequivocally determine that a given GW signal is powered by a BHNS merger*. In the absence of an EM signal, our main method to determine the nature of merging compact objects is to use their inferred masses, and to assume that any object below a fixed threshold mass is a neutron star. This clearly introduces an untested astrophysical prior in the interpretation of the data. It can also be difficult to determine whether a system is a high mass ratio BHNS system or a more symmetric BBH system with the same chirp mass (Hannam et al., 2013)[3]. Furthermore, if black holes are commonly formed with large spins misaligned with the orbital angular momentum of the binary, BHNS binaries may experience significant orbital precession. As the GW templates currently used by detection pipelines do not take orbital precession into account, this could lead to the loss of a significant fraction (∼30%) of BHNS systems (Harry et al., 2014), with an observational bias toward the detection of non-processing systems. Analysis of the observed population of BHNS binaries thus require careful consideration of observational biases and of the probabilistic nature of the characterization of a signal as a BHNS system.

Finally, we note that the availability of reliable GW templates is crucial to the analysis of merger events. In that respect, significant progress have been made in recent years on precessing waveform models (Schmidt et al., 2012; Hannam et al., 2014; Pan et al., 2014; Smith et al., 2016; Khan et al., 2019; Varma et al., 2019), which may be of particular importance for BHNS systems, and on the inclusion of tidal effects in waveform models (Lackey et al., 2014; Bernuzzi et al., 2015; Hinderer et al., 2016; Dietrich et al., 2017; Nagar et al., 2018). Recent high-accuracy numerical simulations of BHNS inspirals (Foucart et al., 2019) show reasonable agreement between tidal models and simulations, except for rapidly spinning neutron stars. It should however be noted that state-of-the art simulations still have numerical errors at the level of ∼10–20% of the phase difference between BBH and BHNS waveforms, which puts a limit on how far waveform models can be tested in practice.

3. MERGER DYNAMICS

The merger of a BHNS binary follows one out of two potential pathways: either the neutron star is disrupted by the tidal field of the black hole, leading to mass ejection and the formation of an accretion torus around the black hole; or the neutron star plunges into the black hole whole. Qualitatively, the physical processes leading to these two potential outcomes are well-understood (Lattimer and Schramm, 1976). As the binary spirals in, the neutron star first reaches either the radius of the innermost stable circular orbit (ISCO) of the black hole $R_{\rm ISCO}$, or the *disruption radius* $R_{\rm dis}$. Roughly speaking, disruption happens if $R_{\rm dis} \gtrsim R_{\rm ISCO}$, i.e., if the neutron star is tidally disrupted outside of the ISCO. This division between disrupting and non-disrupting systems creates two classes of events with very distinct observational properties.

Qualitatively, if the neutron star is treated as a test mass and the black hole spin is aligned with the orbital angular momentum of the binary, the ISCO radius scales as $R_{\rm ISCO} = f(\chi_{\rm BH})GM_{\rm BH}/c^2$, with f a function ranging from 1 to 9 and decreasing for increasing (prograde) spins (Bardeen et al., 1972). For large mass ratios and in Newtonian physics, the disruption radius scales as $R_{\rm dis} \sim k(M_{\rm BH}/M_{\rm NS})^{1/3}R_{\rm NS}$, with k a numerical constant with a mild dependence on the equation of state and the black hole spin (Fishbone, 1973; Wiggins and Lai, 2000). From these simple scalings, we deduce that disruption will be favored for (a) low-mass black holes; (b) prograde black hole spins; and (c) large neutron star radii.

[3] If we allow for primordial black holes within the same mass range as neutron stars, low-mass BHNS mergers can also mimic BNS systems, even if we observe an EM counterpart (Hinderer et al., 2019).

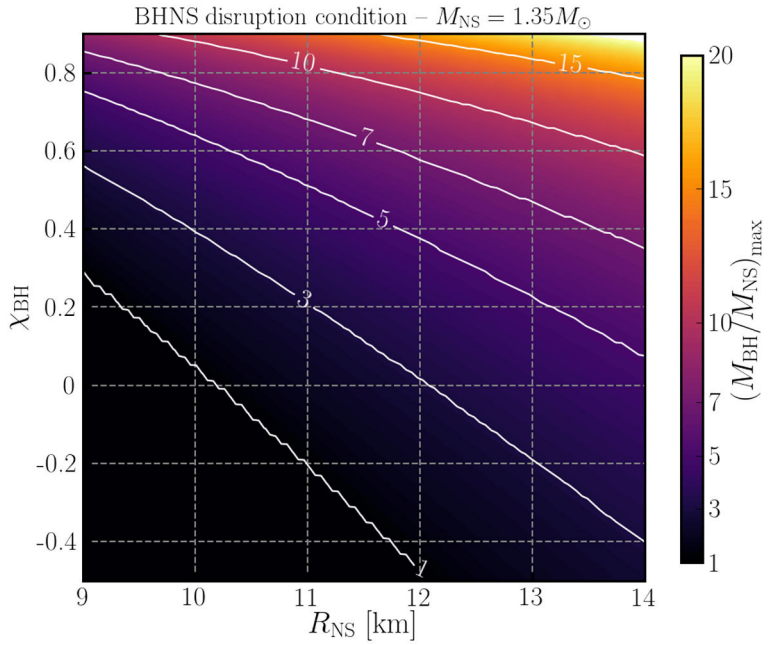

FIGURE 2 | Maximum value of the mass ratio $M_{\rm BH}/M_{\rm NS}$ for which a BHNS system will disrupt as a function of the neutron star radius $R_{\rm NS}$ and aligned component of the dimensionless black hole spin $\chi_{\rm BH}$, assuming $M_{\rm NS} = 1.35 M_\odot$ (Foucart et al., 2018). Results for other $M_{\rm NS}$ can be obtained by looking at the disruption condition at constant $C_{\rm NS} = GM_{\rm NS}/(R_{\rm NS}c^2)$.

A more quantitative understanding requires general relativistic simulations (Duez et al., 2008; Etienne et al., 2009; Chawla et al., 2010; Kyutoku et al., 2010; Foucart et al., 2012; Kawaguchi et al., 2015). Simulations tell us that for quasi-circular binaries, *mass transfer is always unstable*. We can also *predict which systems disrupt* (see **Figure 2**), and for disrupting systems *how much mass remains outside of the black hole after disruption* (Pannarale et al., 2011; Foucart, 2012; Foucart et al., 2018)—typically a few tenths of a solar mass. While these predictions were first made for systems with aligned black hole spins, simulations also show that for misaligned black hole spins, simply using in fitting formulae the aligned component of the black hole spin or replacing the ISCO radius by the radius of the innermost stable spherical orbit (ISSO) provides reasonably accurate predictions (Foucart et al., 2013b; Stone et al., 2013; Kawaguchi et al., 2015). Overall, *the outcome of a BHNS merger can be predicted with reasonable accuracy as a function of just three dimensionless parameters*: the symmetric mass ratio $\eta = M_{\rm NS}M_{\rm BH}/(M_{\rm NS}+M_{\rm BH})^2$, the aligned component of the dimensionless black hole spin $\chi_\parallel$, and the neutron star compaction $C_{\rm NS}$ (Foucart et al., 2018). However, these models do not apply to systems with large eccentricities: partial disruption of the neutron star is then possible (Stephens et al., 2011), and we do not have reliable predictions for the outcome of the merger in the larger-dimensional parameter space of eccentric BHNS systems. There have also been too few simulations to robustly characterize binaries with rapidly rotating neutron stars.

For non-disrupting BHNS systems, the merger ends the interesting part of the evolution. The GW signal is practically identical to a BBH system with the same component masses and spins (Foucart et al., 2013a; Lackey et al., 2014), there is neither mass ejection nor accretion disk, and we do not expect detectable post-merger EM signals. In the rest of this review, we will thus focus on the more interesting disrupting BHNS systems. However, *disrupting systems may very well be a small minority of the observed BHNS binaries*. Even a relatively low mass black hole ($M_{\rm BH} \sim 7M_\odot$) requires a moderate-to-high black hole spin $\chi_\parallel \gtrsim (0.2-0.7)$ to disrupt neutron stars with equations of state compatible with GW170817. The BBH systems detected so far have black holes of high mass and/or low spin (Abbott et al., 2019; Venumadhav et al., 2019) that would be highly unlikely to disrupt neutron stars—though the rapidly spinning BH candidate reported in Zackay et al. (2019) provides some hope for the existence of disrupting BHNS binaries. While we should be ready for a population of disrupting BHNS mergers, we should acknowledge that *the idea that most BHNS mergers undergo tidal disruption is currently disfavored*.

Disrupting BHNS systems provide us with a wealth of additional information. First, the GW signal is cut off when disruption occurs, at a frequency $f_{\rm cut} \sim (1-1.5)$ kHz that depends on the equation of state of the neutron star. The inclusion of that cut-off frequency in waveform models (Lackey et al., 2014; Pannarale et al., 2015) can help constrain the equation of state of neutron stars, complementing the information provided by the tidal dephasing (Lackey et al., 2012; Lackey et al., 2014). Second, a disrupting BHNS binary typically ejects a few percents of a solar mass of material. The ejection of neutron-rich matter at mildly relativistic speeds is extremely important

to the study of BHNS and BNS mergers: as the ejecta expands into the surrounding interstellar medium, it undergoes r-process nucleosynthesis, forming many of the heavy elements observed today on Earth. The outcome of the r-process is not, however, unique: more neutron-rich ejecta (approximately, with $<\sim$25% protons) forms heavier r-process elements than more neutron-poor ejecta (Wanajo et al., 2014; Lippuner and Roberts, 2015). This matters if we wish to understand nucleosynthesis in the Universe, but also to understand the properties of the observable optical/infrared kilonovae powered by radioactive decays in the ejecta. If heavier r-process elements are produced, the opacity of the ejecta increases, causing the kilonova to be dimmer, of longer duration, and shifted from the optical to the infrared (Kasen et al., 2013). Kilonova signals also contain information about the mass, velocity, composition, and geometry of the ejecta (Barnes and Kasen, 2013; Kawaguchi et al., 2016). Thus, *if we can connect the ejecta properties to the parameters of the binary, we can use kilonovae observations to complement and cross-check GW observations of BHNS systems*. In BHNS system, the merger ejecta, or *dynamical ejecta*, has fairly well-constrained properties. It is cold, very neutron-rich ($\sim$ 5% protons), and moves at an average velocity $v \sim (0.1-0.3)c$. It is also quite different from the dynamical ejecta of BNS mergers: there is more mass ejection in disrupting BHNS binaries, the ejecta is very asymmetric, and there is no neutron poor component to the ejecta that may power an optical kilonova. Fits to the result of numerical simulations have provided us with relatively robust predictions for its mass (Kawaguchi et al., 2016) and asymptotic velocity (Kawaguchi et al., 2016; Foucart et al., 2017) that can be used to develop kilonovae models. While higher accuracy predictions for the properties of the dynamical ejecta would certainly be useful in the long term, this phase of the evolution is quite well-understood when compared to the formation and evolution of post-merger remnants.

4. POST-MERGER REMNANTS

In our description of the evolution of BHNS binaries, we have so far only considered the effects of general relativity (GWs, ISCO, …), of ideal hydrodynamics (tides and tidal disruption), and of the nuclear equation of state of cold dense matter in neutrinoless beta-equilibrium. During inspiral and merger, this is generally sufficient to capture the most important observable features of BHNS binaries. This changes dramatically after merger: as bound matter from the disrupted neutron star begins to circularize, mostly through hydrodynamical shocks and interactions between the tidal tail and the forming accretion disk, magnetic fields and neutrinos start to play an important role. Magnetic fields and turbulent eddies will grow due to the Kelvin-Helmholtz instability at the disk-tail boundary, heating the disk and driving outflows (Kiuchi et al., 2015), while neutrinos cool the denser regions of the disk and heat its corona (Lee et al., 2009; Deaton et al., 2013; Janiuk et al., 2013; Foucart et al., 2015). Neutrino absorption in the corona can drive a disk wind (Dessart et al., 2009) and, more importantly, preferential absorption of electron neutrinos over electron antineutrinos leads to an increase in the ratio of protons to neutrons in the outflows (Foucart et al., 2015). At later times the growth of the magnetorotational instability leads to an increase in the strength of the magnetic field, angular momentum transport and heating in the disk, accretion of matter onto the black hole, and the production of mildly relativistic outflows for multiple seconds after the merger (Fernández and Metzger, 2013; Siegel and Metzger, 2017; Fernández et al., 2019). Finally, depending on the large-scale structure of the magnetic field after merger, continuous or more intermittent relativistic jets may be produced $\sim$0.1–1 s after merger (Paschalidis et al., 2015; Siegel and Metzger, 2017; Ruiz et al., 2018; Christie et al., 2019), potentially leading to the production of a SGRB.

Numerical simulations and theoretical models have made important strides in the study of post-merger remnants over the last decade, yet this remains by far the most uncertain part of the evolution. A first problem is that only one magnetohydrodynamics simulation has used sufficient resolution to capture the growth of the Kelvin-Helmholtz instability at the disk-tail boundary (Kiuchi et al., 2015), and it did not include any treatment of the neutrinos. In the absence of cooling, it predicted massive outflows from the forming disk (50% of the disk mass, an amount comparable to the dynamical ejecta). Lower-resolution simulations including neutrino cooling did not observe significant outflows at this stage (Deaton et al., 2013; Foucart et al., 2015), but lacked the heating provided by the Kelvin-Helmholtz instability. The physical answer lies somewhere in between these two extremes, leaving a large uncertainty regarding the mass of hot, mildly relativistic matter that may be ejected during the circularization of the accretion disk. This is particularly problematic because these early post-merger outflows could be the main source of optical kilonovae in BHNS systems.

A second important source of uncertainty is the large scale structure of the magnetic field after merger. Merger simulations have produced jets when a strong dipolar magnetic field was initialized outside of the neutron star before merger (Paschalidis et al., 2015; Ruiz et al., 2018), but no simulation has resolved the growth of a large-scale magnetic field from realistic initial field strengths. On the other hand, simulations of post-merger remnants show that the large scale structure of the magnetic field has a significant impact on the jet power and the ejected mass (Christie et al., 2019). This leaves us with important open questions regarding the connection between SGRB properties and the pre-merger characteristics of a BHNS binary, as well as regarding the mechanism for the production of relativistic jets, e.g., whether a strong magnetic field outside of the neutron star leads to the production of a jet $\sim$100 ms after merger (Paschalidis et al., 2015; Ruiz et al., 2018), or a dynamo mechanism within the disk creates a jet later on Christie et al. (2019).

One reliable constant in post-merger studies of BHNS systems is that a large fraction $\sim$(15–50)% of the bound matter remaining around the black hole after the disruption of a neutron star is ejected in mildly relativistic outflows. There is, however, a wide range of outflow mechanisms. We observe early outflows ($\lesssim$1 s post-merger) due to turbulent heating at the disk-tail interface (Kiuchi et al., 2015) and in the inner regions of the disk (Siegel and Metzger, 2017; Fernández et al., 2019), as well

as delayed outflows due to viscous heating and recombination of alpha-particles in the disk (Fernández and Metzger, 2013; Christie et al., 2019; Fernández et al., 2019). The former have highly uncertain masses, velocities and compositions, in part due to uncertain initial conditions in the post-merger remnant, and in part due to missing physics in the simulations (particularly neutrino radiation transport). The latter are better understood: they are relatively slow ($v \lesssim 0.05c$), and formed of ∼20–30% protons.

As post-merger outflows in BHNS mergers have a total mass roughly similar to that of the dynamical ejecta, they have a large impact on the properties of BHNS-powered kilonovae. Uncertainties in their mass (by a factor of 2–3), velocity, and composition (neutron rich/neutron poor) are the main source of error in the construction of theoretical models of BHNS outflows today. A better understanding of the post-merger winds, along with better nuclear models and improved understanding of the heating rate of merger outflows (Barnes et al., 2016), are critical to the production of reliable kilonova models for BHNS binaries. Currently, models either ignore the post-merger ejecta (Kawaguchi et al., 2016), take only some of the post-merger outflows into account (Barbieri et al., 2020), or suffer from large uncertainties due to our lack of understanding of the post-merger ejecta (Andreoni et al., 2019; Coughlin et al., 2019).

Finally, let us comment briefly on our understanding of BHNS binaries as engines for SGRBs. Relativistic jets have now been produced in simulations of BHNS merger (Paschalidis et al., 2015; Ruiz et al., 2018)[4] and/or of their post-merger remnant disks (Siegel and Metzger, 2017; Christie et al., 2019). We also know that the properties of the jet depend on the large scale structure of the post-merger magnetic field. However, connecting that large scale structure to the pre-merger properties of the system remains an important unsolved problem. It is unclear whether observations or simulations will first constrain the magnetic field structure of the remnant of a BHNS merger. At the moment, the most reliable information that comes from the joint observation of a SGRB and GW signal from a BHNS binary is that the neutron star was disrupted.

5. DISCUSSION

With the advent of GW astronomy, the study of BHNS mergers is undergoing a rapid transformation. More efforts are now being directed toward the modeling and interpretation of multi-messenger observations of binary mergers. It has also become clear that the study of BHNS systems suffers from significant complications when compared with BNS systems: statistical uncertainties in the individual masses of the merging compact objects make it difficult to unequivocally characterize a GW event as a BHNS binary, and many BHNS binaries likely involve high-mass and/or low-spin black holes for which the neutron star plunges whole into the black hole, preventing the emission of detectable post-merger EM signals.

To make optimal use of the available observational data, reliable models of the GW and EM signals powered by BHNS binaries are required. On the GW side, a number of models including finite-size effects for BHNS and/or BNS systems have been developed (Lackey et al., 2014; Bernuzzi et al., 2015; Hinderer et al., 2016; Dietrich et al., 2017; Nagar et al., 2018). Before merger, these models agree with numerical simulations of BHNS binaries within current numerical errors, except in the most extreme cases tested so far (Foucart et al., 2019). Models for the impact on the GW signal of the disruption of the neutron star have more room to improve: they remain only order-of-magnitude accurate, and typically limited in their coverage of the BHNS parameter space (Lackey et al., 2014; Pannarale et al., 2015).

On the EM side, a first model combining information from SGRBs and kilonovae was recently developed by Barbieri et al. (2020), adding to a previously developed model for the kilonova signals powered by the dynamical ejecta of BHNS mergers (Kawaguchi et al., 2016). Existing models remain however limited by our lack of understanding of post-merger outflows, as well as by nuclear physics and radiation transport uncertainties (Barnes et al., 2016). In particular, the large scale structure of magnetic fields within and outside of the post-merger accretion disk is not, at this point, well-constrained by merger simulations, despite its large impact on post-merger outflows and on the properties of SGRBs (Christie et al., 2019). To make optimal use of upcoming multi-messenger observations (or even non-detections), it is thus important to develop improved kilonova and SGRB models, and properly characterize model uncertainties.

[4] "Jets" here are outflow regions with large Poynting flux, that cannot reach Lorentz factor of more than a few due to the limits of existing merger simulations.

AUTHOR CONTRIBUTIONS

The author confirms being the sole contributor of this work and has approved it for publication.

FUNDING

FF gratefully acknowledges support from the NSF through grant PHY-1806278, from NASA through grant 80NSSC18K0565, and from the DOE through grant DE-SC0020435.

REFERENCES

Abadie, J., Abbott, B. P., Abbott, R., Abernathy, M., Accadia, T., Acernese, F., et al. (2010). Predictions for the rates of compact binary coalescences observable by ground-based gravitational-wave detectors. *Class. Quantum Grav.* 27:173001. doi: 10.1088/0264-9381/27/11/114007

Abbott, B. P., Abbott, R., Abbott, T. D., Abernathy, M. R., Acernese, F., Ackley, K., et al. (2016). GW150914: first results from the search for binary black hole coalescence with advanced LIGO. *Phys. Rev. D* 93:122003. doi: 10.1103/PhysRevD.93.122003

Abbott, B. P., Abbott, R., Abbott, T. D., Abraham, S., Acernese, F., Ackley, K., et al. (2019). GWTC-1: a gravitational-wave transient catalog of compact binary

mergers observed by LIGO and virgo during the first and second observing runs. *Phys. Rev. X* 9:031040. doi: 10.1103/PhysRevX.9.031040

Abbott, B. P., Abbott, R., Abbott, T. D., Abraham, S., Acernese, F., Ackley, K., et al. (2020). GW190425: observation of a compact binary coalescence with total mass $\sim 3.4 M_{\odot}$. *Astrophys. J. Lett.* (2020) 892:L3. doi: 10.3847/2041-8213/ab75f5

Abbott, B. P., Abbott, R., Abbott, T. D., Acernese, F., Ackley, K., Adams, C., et al. (2017a). Gravitational waves and gamma-rays from a binary neutron star merger: GW170817 and GRB 170817A. *Astrophys. J. Lett.* 848:L13. doi: 10.3847/2041-8213/aa920c

Abbott, B. P., Abbott, R., Abbott, T. D., Acernese, F., Ackley, K., Adams, C., et al. (2017b). A gravitational-wave standard siren measurement of the Hubble constant. *Nature* 551, 85–88. doi: 10.1038/nature24471

Abbott, B. P., Abbott, R., Abbott, T. D., Acernese, F., Ackley, K., Adams, C., et al. (2017c). GW170817: observation of gravitational waves from a binary neutron star inspiral. *Phys. Rev. Lett.* 119:161101. doi: 10.1103/PhysRevLett.119.161101

Abbott, B. P., Abbott, R., Abbott, T. D., Acernese, F., Ackley, K., Adams, C., et al. (2018). GW170817: measurements of neutron star radii and equation of state. *Phys. Rev. Lett.* 121:161101. doi: 10.1103/PhysRevLett.121.161101

Andreoni, I., Goldstein, D. A., Kasliwal, M. M., Nugent, P. E., Zhou, R., Newman, J. A., et al. (2019). GROWTH on S190814bv: deep synoptic limits on the optical/near-infrared counterpart to a neutron star-black hole merger. *Astrophys. J.* 890:131. doi: 10.3847/1538-4357/ab6a1b

Antoniadis, J., Freire, P. C. C., Wex, N., Tauris, T. M., Lynch, R. S., van Kerkwijk, M. H., et al. (2013). A massive pulsar in a compact relativistic binary. *Science* 340:6131. doi: 10.1126/science.1233232

Barbieri, C., Salafia, O. S., Perego, A., Colpi, M., and Ghirlanda, G. (2020). Electromagnetic counterparts of black hole-neutron star mergers: dependence on the neutron star properties. *Eur. Phys. J. A* 56:8. doi: 10.1140/epja/s10050-019-00013-x

Bardeen, J. M., Press, W. H., and Teukolsky, S. A. (1972). Rotating black holes: locally nonrotating frames, energy extraction, and scalar synchrotron radiation. *Astrophys. J.* 178:347. doi: 10.1086/151796

Barnes, J., and Kasen, D. (2013). Effect of a high opacity on the light curves of radioactively powered transients from compact object mergers. *Astrophys. J.* 775:18. doi: 10.1088/0004-637X/775/1/18

Barnes, J., Kasen, D., Wu, M.-R., and Mart'inez-Pinedo, G. (2016). Radioactivity and thermalization in the ejecta of compact object mergers and their impact on kilonova light curves. *Astrophys. J.* 829:110. doi: 10.3847/0004-637X/829/2/110

Belczynski, K., Repetto, S., Holz, D. E., O'Shaughnessy, R., Bulik, T., Berti, E., et al. (2016). Compact binary merger rates: comparison with LIGO/Virgo upper limits. *Astrophys. J.* 819:108. doi: 10.3847/0004-637X/819/2/108

Bernuzzi, S., Nagar, A., Dietrich, T., and Damour, T. (2015). Modeling the dynamics of tidally interacting binary neutron stars up to the merger. *Phys. Rev. Lett.* 114:161103. doi: 10.1103/PhysRevLett.114.161103

Chawla, S., Anderson, M., Besselman, M., Lehner, L., Liebling, S. L., Motl, P. M., et al. (2010). Mergers of magnetized neutron stars with spinning black holes: disruption, accretion and fallback. *Phys. Rev. Lett.* 105:111101. doi: 10.1103/PhysRevLett.105.111101

Chornock, R., Berger, E., Kasen, D., Cowperthwaite, P. S., Nicholl, M., Villar, V. A., et al. (2017). The electromagnetic counterpart of the binary neutron star merger LIGO/Virgo GW170817. IV. Detection of near-infrared signatures of R-process nucleosynthesis with Gemini-South. *Astrophys. J. Lett.* 848:L19. doi: 10.3847/2041-8213/aa905c

Christie, I. M., Lalakos, A., Tchekhovskoy, A., Fernández, R., Foucart, F., Quataert, E., et al. (2019). The role of magnetic field geometry in the evolution of neutron star merger accretion discs. *Mon. Not. R. Astron. Soc.* 490, 4811–4825. doi: 10.1093/mnras/stz2552

Coughlin, M. W., Dietrich, T., Antier, S., Bulla, M., Foucart, F., Hotokezaka, K., et al. (2019). Implications of the search for optical counterparts during the first six months of the advanced LIGO's and Advanced Virgo's third observing run: possible limits on the ejecta mass and binary properties. *Mon. Not. R. Astron. Soc.* 492, 863–876. doi: 10.1093/mnras/stz3457

Coulter, D. A., Foley, R. J., Kilpatrick, C. D., Drout, M. R., Piro, A. L., Shappee, B. J., et al. (2017). Swope Supernova Survey 2017a (SSS17a), the optical counterpart to a gravitational wave source. *Science* 358, 1556–1558. doi: 10.1126/science.aap9811

Cowperthwaite, P. S., Berger, E., Villar, V. A., Metzger, B. D., Nicholl, M., Chornock, R., et al. (2017). The electromagnetic counterpart of the binary neutron star merger LIGO/Virgo GW170817. II. UV, optical, and near-infrared light curves and comparison to kilonova models. *Astrophys. J.* 848:L17. doi: 10.3847/2041-8213/aa8fc7

Deaton, M. B., Duez, M. D., Foucart, F., O'Connor, E., Ott, C. D., Kidder, L. E., et al. (2013). Black hole-neutron star mergers with a hot nuclear equation of state: outflow and neutrino-cooled disk for a low-mass, high-spin case. *Astrophys. J.* 776:47. doi: 10.1088/0004-637X/776/1/47

Demorest, P., Pennucci, T., Ransom, S., Roberts, M., and Hessels, J. (2010). Shapiro delay measurement of a two solar mass neutron star. *Nature* 467, 1081–1083. doi: 10.1038/nature09466

Dessart, L., Ott, C. D., Burrows, A., Rosswog, S., and Livne, E. (2009). Neutrino signatures and the neutrino-driven wind in binary neutron star mergers. *Astrophys. J.* 690, 1681–1705. doi: 10.1088/0004-637X/690/2/1681

Dietrich, T., Bernuzzi, S., and Tichy, W. (2017). Closed-form tidal approximants for binary neutron star gravitational waveforms constructed from high-resolution numerical relativity simulations. *Phys. Rev. D* 96:121501. doi: 10.1103/PhysRevD.96.121501

Drout, M. R., Piro, A. L., Shappee, B. J., Kilpatrick, C. D., Simon, J. D., Contreras, C., et al. (2017). Light curves of the neutron star merger GW170817/SSS17a: implications for R-process nucleosynthesis. *Science* 358, 1570–1574. doi: 10.1126/science.aaq0049

Duez, M. D., Foucart, F., Kidder, L. E., Pfeiffer, H. P., Scheel, M. A., and Teukolsky, S. A. (2008). Evolving black hole-neutron star binaries in general relativity using pseudospectral and finite difference methods. *Phys. Rev. D* 78:104015. doi: 10.1103/PhysRevD.78.104015

Etienne, Z. B., Liu, Y. T., Shapiro, S. L., and Baumgarte, T. W. (2009). Relativistic simulations of black hole-neutron star mergers: effects of black-hole spin. *Phys. Rev. D* 79:044024. doi: 10.1103/PhysRevD.79.044024

Evans, P. A., Cenko, S. B., Kennea, J. A., Emery, S. W. K., Kuin, N. P. M., Korobkin, O., et al. (2017). Swift and NuSTAR observations of GW170817: detection of a blue kilonova. *Science* 358, 1565–1570. doi: 10.1126/science.aap9580

Fernández, R., and Metzger, B. D. (2013). Delayed outflows from black hole accretion tori following neutron star binary coalescence. *Mon. Not. R. Astron. Soc.* 435, 502–517. doi: 10.1093/mnras/stt1312

Fernández, R., Tchekhovskoy, A., Quataert, E., Foucart, F., and Kasen, D. (2019). Long-term GRMHD simulations of neutron star merger accretion discs: implications for electromagnetic counterparts. *Mon. Not. R. Astron. Soc.* 482, 3373–3393. doi: 10.1093/mnras/sty2932

Fishbone, L. G. (1973). The relativistic Roche problem. I. Equilibrium theory for a body in equatorial, circular orbit around a Kerr black hole. *Astrophys. J.* 185, 43–68. doi: 10.1086/152395

Flanagan, É. É., and Hinderer, T. (2008). Constraining neutron-star tidal Love numbers with gravitational-wave detectors. *Phys. Rev. D* 77:021502. doi: 10.1103/PhysRevD.77.021502

Foucart, F. (2012). Black-hole-neutron-star mergers: disk mass predictions. *Phys. Rev. D* 86:124007. doi: 10.1103/PhysRevD.86.124007

Foucart, F., Buchman, L., Duez, M. D., Grudich, M., Kidder, L. E., MacDonald, I., et al. (2013a). First direct comparison of nondisrupting neutron star-black hole and binary black hole merger simulations. *Phys. Rev. D* 88:064017. doi: 10.1103/PhysRevD.88.064017

Foucart, F., Deaton, M. B., Duez, M. D., Kidder, L. E., MacDonald, I., Ott, C. D., et al. (2013b). Black hole-neutron star mergers at realistic mass ratios: equation of state and spin orientation effects. *Phys. Rev. D* 87:084006. doi: 10.1103/PhysRevD.87.084006

Foucart, F., Desai, D., Brege, W., Duez, M. D., Kasen, D., Hemberger, D. A., et al. (2017). Dynamical ejecta from precessing neutron star-black hole mergers with a hot, nuclear-theory based equation of state. *Class. Quant. Grav.* 34:044002. doi: 10.1088/1361-6382/aa573b

Foucart, F., Duez, M. D., Hinderer, T., Caro, J., Williamson, A. R., Boyle, M., et al. (2019). Gravitational waveforms from spectral Einstein code simulations: neutron star-neutron star and low-mass black hole-neutron star binaries. *Phys. Rev. D* 99:044008. doi: 10.1103/PhysRevD.99.044008

Foucart, F., Duez, M. D., Kidder, L. E., Scheel, M. A., Szilágyi, B., and Teukolsky, S. A. (2012). Black hole-neutron star mergers for $10 M_{\odot}$ black holes. *Phys. Rev. D* 85:044015. doi: 10.1103/PhysRevD.85.044015

Foucart, F., Hinderer, T., and Nissanke, S. (2018). Remnant baryon mass in neutron star-black hole mergers: predictions for binary neutron star mimickers and rapidly spinning black holes. *Phys. Rev. D* 98:081501. doi: 10.1103/PhysRevD.98.081501

Foucart, F., O'Connor, E., Roberts, L., Duez, M. D., Haas, R., Kidder, L. E., et al. (2015). Post-merger evolution of a neutron star-black hole binary with neutrino transport. *Phys. Rev. D* 91:124021. doi: 10.1103/PhysRevD.91.124021

Freiburghaus, C., Rosswog, S., and Thielemann, F.-K. (1999). R-process in neutron star mergers. *Astrophys. J. Lett.* 525, L121–L124. doi: 10.1086/312343

Hannam, M., Brown, D. A., Fairhurst, S., Fryer, C. L., and Harry, I. W. (2013). When can gravitational-wave observations distinguish between black holes and neutron stars? *Astrophys. J. Lett.* 766:L14. doi: 10.1088/2041-8205/766/1/L14

Hannam, M., Schmidt, P., Bohé, A., Haegel, L., Husa, S., Ohme, F., et al. (2014). A simple model of complete precessing black-hole-binary gravitational waveforms. *Phys. Rev. Lett.* 113:151101. doi: 10.1103/PhysRevLett.113.151101

Harry, I. W., Nitz, A. H., Brown, D. A., Lundgren, A. P., Ochsner, E., and Keppel, D. (2014). Investigating the effect of precession on searches for neutron-star-black-hole binaries with advanced LIGO. *Phys. Rev. D* 89:024010. doi: 10.1103/PhysRevD.89.024010

Hinderer, T., Lackey, B. D., Lang, R. N., and Read, J. S. (2010). Tidal deformability of neutron stars with realistic equations of state and their gravitational wave signatures in binary inspiral. *Phys. Rev. D* 81:123016. doi: 10.1103/PhysRevD.81.123016

Hinderer, T., Nissanke, S., Foucart, F., Hotokezaka, K., Vincent, T., Kasliwal, M., et al. (2019). Distinguishing the nature of comparable-mass neutron star binary systems with multimessenger observations: GW170817 case study. *Phys. Rev. D* 100:06321. doi: 10.1103/PhysRevD.100.063021

Hinderer, T., Taracchini, A., Foucart, F., Buonanno, A., Steinhoff, J., Duez, M., et al. (2016). Effects of neutron-star dynamic tides on gravitational waveforms within the effective-one-body approach. *Phys. Rev. Lett.* 116:181101. doi: 10.1103/PhysRevLett.116.181101

Hotokezaka, K., Nakar, E., Gottlieb, O., Nissanke, S., Masuda, K., Hallinan, G., et al. (2019). A Hubble constant measurement from superluminal motion of the jet in GW170817. *Nat. Astron.* 3, 940–944. doi: 10.1038/s41550-019-0820-1

Hotokezaka, K., Nissanke, S., Hallinan, G., Lazio, T. J. W., Nakar, E., and Piran, T. (2016). Radio counterparts of compact binary mergers detectable in gravitational waves: a simulation for an optimized survey. *Astrophys. J.* 831:190. doi: 10.3847/0004-637X/831/2/190

Janiuk, A., Mioduszewski, P., and Moscibrodzka, M. (2013). Accretion and outflow from a magnetized, neutrino cooled torus around the gamma ray burst central engine. *Astrophys. J.* 776:105. doi: 10.1088/0004-637X/776/2/105

Kasen, D., Badnell, N. R., and Barnes, J. (2013). Opacities and spectra of the R-process ejecta from neutron star mergers. *Astrophys. J.* 774:25. doi: 10.1088/0004-637X/774/1/25

Kawaguchi, K., Kyutoku, K., Nakano, H., Okawa, H., Shibata, M., and Taniguchi, K. (2015). Black hole-neutron star binary merger: dependence on black hole spin orientation and equation of state. *Phys. Rev. D* 92:024014. doi: 10.1103/PhysRevD.92.024014

Kawaguchi, K., Kyutoku, K., Shibata, M., and Tanaka, M. (2016). Models of kilonova/macronova emission from black hole–neutron star mergers. *Astrophys. J.* 825:52. doi: 10.3847/0004-637X/825/1/52

Khan, S., Chatziioannou, K., Hannam, M., and Ohme, F. (2019). Phenomenological model for the gravitational-wave signal from precessing binary black holes with two-spin effects. *Phys. Rev. D* 100:024059. doi: 10.1103/PhysRevD.100.024059

Kiuchi, K., Sekiguchi, Y., Kyutoku, K., Shibata, M., Taniguchi, K., and Wada, T. (2015). High resolution magnetohydrodynamic simulation of black hole-neutron star merger: Mass ejection and short gamma ray bursts. *Phys. Rev. D* 92:064034. doi: 10.1103/PhysRevD.92.064034

Kyutoku, K., Shibata, M., and Taniguchi, K. (2010). Gravitational waves from nonspinning black hole-neutron star binaries: dependence on equations of state. *Phys. Rev. D* 82:044049. doi: 10.1103/PhysRevD.82.044049

Lackey, B. D., Kyutoku, K., Shibata, M., Brady, P. R., and Friedman, J. L. (2012). Extracting equation of state parameters from black hole-neutron star mergers: Nonspinning black holes. *Phys. Rev. D* 85:044061. doi: 10.1103/PhysRevD.85.044061

Lackey, B. D., Kyutoku, K., Shibata, M., Brady, P. R., and Friedman, J. L. (2014). Extracting equation of state parameters from black hole-neutron star mergers: aligned-spin black holes and a preliminary waveform model. *Phys. Rev. D* 89:043009. doi: 10.1103/PhysRevD.89.043009

Landry, P., Essick, R., and Chatziioannou, K. (2020). Nonparametric constraints on neutron star matter with existing and upcoming gravitational wave and pulsar observations. *Phys. Rev. D* 101:123007. doi: 10.1103/PhysRevD.101.123007

Lattimer, J. M., and Schramm, D. N. (1976). The tidal disruption of neutron stars by black holes in close binaries. *Astrophys. J.* 210, 549–567. doi: 10.1086/154860

Lee, W. H., Ramirez-Ruiz, E., and Diego-Lopez-Camara (2009). Phase transitions and He-synthesis driven winds in neutrino cooled accretion disks: prospects for late flares in short gamma-ray bursts. *Astrophys. J.* 699, L93–L96. doi: 10.1088/0004-637X/699/2/L93

Li, L.-X., and Paczynski, B. (1998). Transient events from neutron star mergers. *Astrophys. J.* 507:L59. doi: 10.1086/311680

Lippuner, J., and Roberts, L. F. (2015). R-process lanthanide production and heating rates in kilonovae. *Astrophys. J.* 815:82. doi: 10.1088/0004-637X/815/2/82

Miller, M., Lamb, F. K., Dittmann, A. J., Bogdanov, S., Arzoumanian, Z., Gendreau, K. C., et al. (2019). PSR J0030+0451 mass and radius from *NICER* data and implications for the properties of neutron star matter. *Astrophys. J. Lett.* 887:L24. doi: 10.3847/2041-8213/ab50c5

Mooley, K. P., Deller, A. T., Gottlieb, O., Nakar, E., Hallinan, G., Bourke, S., et al. (2018). Superluminal motion of a relativistic jet in the neutron-star merger GW170817. *Nature* 561, 355–359. doi: 10.1038/s41586-018-0486-3

Nagar, A., Bernuzzi, S., Del Pozzo, W., Riemenschneider, G., Akcay, S., Carullo, G., et al. (2018). Time-domain effective-one-body gravitational waveforms for coalescing compact binaries with nonprecessing spins, tides and self-spin effects. *Phys. Rev. D* 98:104052. doi: 10.1103/PhysRevD.98.104052

Nakar, E., and Piran, T. (2011). Radio remnants of compact binary mergers–the electromagnetic signal that will follow the gravitational waves. *Nature* 478, 82–84. doi: 10.1038/nature10365

Nicholl, M., Berger, E., Kasen, D., Metzger, B. D., Elias, J., Briceño, C., et al. (2017). The electromagnetic counterpart of the binary neutron star merger LIGO/Virgo GW170817. III. Optical and UV spectra of a blue kilonova from fast polar ejecta. *Astrophys. J. Lett.* 848:L18. doi: 10.3847/2041-8213/aa9029

Özel, F., Psaltis, D., Narayan, R., and McClintock, J. E. (2010). The black hole mass distribution in the galaxy. *Astrophys. J.* 725:1918. doi: 10.1088/0004-637X/725/2/1918

Özel, F., Psaltis, D., Narayan, R., and Santos Villarreal, A. (2012). On the mass distribution and birth masses of neutron stars. *Astrophys. J.* 757:55. doi: 10.1088/0004-637X/757/1/55

Pan, Y., Buonanno, A., Taracchini, A., Kidder, L. E., Mroué, A. H., Pfeiffer, H. P., et al. (2014). Inspiral-merger-ringdown waveforms of spinning, precessing black-hole binaries in the effective-one-body formalism. *Phys. Rev. D* 89:084006. doi: 10.1103/PhysRevD.89.084006

Pannarale, F., Berti, E., Kyutoku, K., Lackey, B. D., and Shibata, M. (2015). Aligned spin neutron star-black hole mergers: a gravitational waveform amplitude model. *Phys. Rev. D* 92:084050. doi: 10.1103/PhysRevD.92.084050

Pannarale, F., Tonita, A., and Rezzolla, L. (2011). Black hole-neutron star mergers and short GRBs: a relativistic toy model to estimate the mass of the torus. *Astrophys. J.* 727:95. doi: 10.1088/0004-637X/727/2/95

Paschalidis, V., Ruiz, M., and Shapiro, S. L. (2015). Relativistic simulations of black hole-neutron star coalescence: the jet emerges. *Astrophys. J.* 806:L14. doi: 10.1088/2041-8205/806/1/L14

Peters, P. C., and Mathews, J. (1963). Gravitational radiation from point masses in a Keplerian orbit. *Phys. Rev.* 131:435. doi: 10.1103/PhysRev.131.435

Pian, E., D'Avanzo, P., Benetti, S., Branchesi, M., Brocato, E., Campana, S., et al. (2017). Spectroscopic identification of r-process nucleosynthesis in a double neutron-star merger. *Nature* 551, 67–70. doi: 10.1038/nature24298

Raaijmakers, G., Greif, S. K., Riley, T. E., Hinderer, T., Hebeler, K., Schwenk, A., et al. (2020). Constraining the dense matter equation of state with joint analysis of NICER and LIGO/Virgo measurements. *Astrophys. J. Lett.* 893:L21. doi: 10.3847/2041-8213/ab822f

Riley, T. E., Watts, A. L., Bogdanov, S., Ray, P. S., Ludlam, R. M., Guillot, S., et al. (2019). A *NICER* view of PSR J0030+0451: millisecond pulsar parameter estimation. *Astrophys. J. Lett.* 887:L21. doi: 10.3847/2041-8213/ab481c

Roberts, L. F., Kasen, D., Lee, W. H., and Ramirez-Ruiz, E. (2011). Electromagnetic transients powered by nuclear decay in the tidal tails of coalescing compact binaries. *Astrophys. J. Lett.* 736:L21. doi: 10.1088/2041-8205/736/1/L21

Ruiz, M., Shapiro, S. L., and Tsokaros, A. (2018). Jet launching from binary black hole-neutron star mergers: dependence on black hole spin, binary mass ratio and magnetic field orientation. *Phys. Rev. D* 98:123017. doi: 10.1103/PhysRevD.98.123017

Schmidt, P., Hannam, M., and Husa, S. (2012). Towards models of gravitational waveforms from generic binaries: a simple approximate mapping between precessing and non-precessing inspiral signals. *Phys. Rev. D* 86:104063. doi: 10.1103/PhysRevD.86.104063

Siegel, D. M., and Metzger, B. D. (2017). Three-dimensional general-relativistic magnetohydrodynamic simulations of remnant accretion disks from neutron star mergers: outflows and *r*-process nucleosynthesis. *Phys. Rev. Lett.* 119:231102. doi: 10.1103/PhysRevLett.119.231102

Smith, R., Field, S. E., Blackburn, K., Haster, C.-J., Pürrer, M., Raymond, V., et al. (2016). Fast and accurate inference on gravitational waves from precessing compact binaries. *Phys. Rev. D* 94:044031. doi: 10.1103/PhysRevD.94.044031

Soares-Santos, M., Holz, D. E., Annis, J., Chornock, R., Herner, K., Berger, E., et al. (2017). The electromagnetic counterpart of the binary neutron star merger LIGO/Virgo GW170817. I. Discovery of the optical counterpart using the dark energy camera. *Astrophys. J. Lett.* 848:L16. doi: 10.3847/2041-8213/aa9055

Stephens, B. C., East, W. E., and Pretorius, F. (2011). Eccentric black hole-neutron star mergers. *Astrophys. J.* 737:L5. doi: 10.1088/2041-8205/737/1/L5

Stone, N., Loeb, A., and Berger, E. (2013). Pulsations in short gamma ray bursts from black hole-neutron star mergers. *Phys. Rev. D* 87, 084053. doi: 10.1103/PhysRevD.87.084053

Varma, V., Field, S. E., Scheel, M. A., Blackman, J., Gerosa, D., Stein, L. C., et al. (2019). Surrogate models for precessing binary black hole simulations with unequal masses. *Phys. Rev. Res.* 1:033015. doi: 10.1103/PhysRevResearch.1.033015

Venumadhav, T., Zackay, B., Roulet, J., Dai, L., and Zaldarriaga, M. (2019). New binary black hole mergers in the second observing run of advanced LIGO and advanced Virgo. *Phys. Rev. D* 101:083030. doi: 10.1103/PhysRevD.101.083030

Villar, V. A., Guillochon, J., Berger, E., Metzger, B. D., Cowperthwaite, P. S., Nicholl, M., et al. (2017). The combined ultraviolet, optical, and near-infrared light curves of the kilonova associated with the binary neutron star merger GW170817: unified data set, analytic models, and physical implications. *Astrophys. J.* 851:L21. doi: 10.3847/2041-8213/aa9c84

Wanajo, S., Sekiguchi, Y., Nishimura, N., Kiuchi, K., Kyutoku, K., and Shibata, M. (2014). Production of all the R-process nuclides in the dynamical ejecta of neutron star mergers. *Astrophys. J. Lett.* 789:L39. doi: 10.1088/2041-8205/789/2/L39

Wiggins, P., and Lai, D. (2000). Tidal interaction between a fluid star and a Kerr black hole: relativistic Roche-Riemann model. *Astrophys. J.* 532:530. doi: 10.1086/308565

Zackay, B., Venumadhav, T., Dai, L., Roulet, J., and Zaldarriaga, M. (2019). Highly spinning and aligned binary black hole merger in the advanced LIGO first observing run. *Phys. Rev. D* 100:023007. doi: 10.1103/PhysRevD.100.023007

Conflict of Interest: The author declares that the research was conducted in the absence of any commercial or financial relationships that could be construed as a potential conflict of interest.

frontiers in Astronomy and Space Sciences

MINI REVIEW
published: 16 June 2020
doi: 10.3389/fspas.2020.00028

Gravitational Waves From Binary Black Hole Mergers: Modeling and Observations

*Patricia Schmidt**

School of Physics and Astronomy and Institute for Gravitational Wave Astronomy, University of Birmingham, Birmingham, United Kingdom

Only a few years after the first detection of gravitational waves from coalescing stellar-mass black holes, the field of gravitational-wave astronomy is now firmly established after the detection of several more. These discoveries have opened up a new window onto the universe, which allows us to probe gravity and astrophysics in some of the most extreme environments in the universe. The detection and, in particular, the subsequent inference of the binaries' properties rely heavily on theoretical models of the signals. In this review, we first discuss the techniques used to model the gravitational-wave signals from coalescing black holes, before we summarize the observations made to date. We conclude with a brief outlook onto the prospects for binary black hole observations in the future.

Keywords: gravitational waves, compact binaries, black holes, modeling, observations

OPEN ACCESS

Edited by:
Bruno Giacomazzo, University of Milano-Bicocca, Italy

Reviewed by:
Christian Corda, International School of University Studies for Research and Education, Italy
Sachiko Kuroyanagi, Nagoya University, Japan

***Correspondence:**
Patricia Schmidt
P.Schmidt@bham.ac.uk

Specialty section:
This article was submitted to Cosmology, a section of the journal Frontiers in Astronomy and Space Sciences

Received: *19 February 2020*
Accepted: *08 May 2020*
Published: *16 June 2020*

Citation:
Schmidt P (2020) Gravitational Waves From Binary Black Hole Mergers: Modeling and Observations. Front. Astron. Space Sci. 7:28. doi: 10.3389/fspas.2020.00028

1. INTRODUCTION

The first detection of gravitational waves (GWs) from the coalescence of two stellar-mass black holes (BHs) in 2015 by the Advanced LIGO GW-detectors (Abbott et al., 2016d) marked the beginning of a new area: GW astronomy. Since then, more than ten binary black hole (BBH) mergers have been identified (Abbott et al., 2019c, 2020; Nitz et al., 2019a; Venumadhav et al., 2019a). First predicted in the 1910s by Einstein's General Theory of Relativity (GR) (Einstein, 1915, 1918), the hunt for these perturbations of spacetime itself spanned many decades and was ultimately enabled by tremendous technological and theoretical advances.

Stellar mass BBHs with a total mass between one and a few hundred solar masses, are prime GW sources for the currently operating ground-based interferometric GW detectors Advanced LIGO (Aasi et al., 2015) and Virgo (Acernese et al., 2015) as well the Japanese detector KAGRA (Akutsu et al., 2019), set to join the global GW detector network shortly. These detectors are sensitive to GWs with frequencies between 10 Hz to a few kHz. In order to detect GWs in lower frequency bands, such as from the collisions of supermassive black holes in the centers of galaxies, the Earth's seismic wall needs to be overcome, which will be achieved with space-based GW missions expected to commence operation in the next decade.

The observation of GWs from inspiralling BBHs provides us with a unique means to study black holes, allowing us to perform precision tests of GR in the high-curvature, strong-field regime and shedding light on the astrophysical origin and nature of entire populations of black holes.

Gravitational waves from BBHs carry characteristic information about the astrophysical properties of the BHs, such as their masses and spins. These properties can be inferred via Bayesian inference (Bayes, 1764) by using highly accurate general-relativistic waveform models, which describe the last stages of the gravitationally-driven BBH evolution: the inspiral, the merger and the ringdown of the remnant black hole. This allows us to constrain the mass and spin distributions of stellar-mass black holes, which has implications for their possible formation history, and put constraints on the rate of such merger events in the universe.

In this review, we will first summarize the current avenues of modeling GWs from binary black holes (section 2), then discuss the current status of observations (section 3), before concluding with a very brief outlook onto the future of BBH GW astronomy in section 4.

2. MODELING BINARY BLACK HOLES

Compact binaries, such as two black holes, on quasi-spherical orbits, lose orbital energy due to the emission of GWs, which causes their orbital separation to shrink until the two black holes plunge, merge and, in General Relativity, form a Kerr black hole. Intrinsically, a BBH is characterized by seven parameters: the mass ratio, $q = m_1/m_2 \geq 1$, where $m_1 \geq m_2$, and the two (dimensionless) spin angular momenta $\vec{\chi}_1$ and $\vec{\chi}_2$. We note that the total mass $M = m_1 + m_2$ of the binary is not relevant intrinsically but determines the GW frequency in physical units and is therefore relevant for detection. Moreover, for astrophysical black holes one commonly assumes charge neutrality.

Two black holes in orbit undergo a purely gravitationally-driven evolution, which is characterized by three distinct stages: the inspiral, the merger and the ringdown of the remnant black holes. The emission of gravitational radiation causes the orbital separation to shrink. If the spin angular momenta of the two black holes are (anti-)parallel to the orbital angular momentum of the binary motion, the orbital motion is confined to a two-dimensional plane whose orientation is fixed in time. In this case, the emitted GW signal is the characteristic *chirp* signal, a wave with monotonically increasing amplitude and frequency until the merger is reached. An example of such a waveform is shown in **Figure 1**. The largest amount of radiation is emitted along the direction of the orbital angular momentum (O'Shaughnessy et al., 2011; Schmidt et al., 2011), and the signal is well-described by the dominant (quadrupole) harmonic, h_{22}.

Any misalignment between the spins and the orbital angular momentum, however, induces relativistic precession effects, which cause the orbital plane to change its spatial orientation as the binary evolves (Apostolatos et al., 1994; Kidder, 1995). This more complex dynamics is directly reflected into the emitted GW signal, which, depending on the relative orientation w.r.t. the observer, can show strong amplitude and phase modulations (Apostolatos et al., 1994; Kidder, 1995; Schmidt et al., 2012). Further, due to the time-dependent orientation of the binary, the quadrupole approximation may no longer be sufficient to describe the radiation and higher-order harmonic modes need to be taken into account.

Due to the lack of analytic solutions of the general relativistic two-body problem, the dynamics and the corresponding GW signal must be approximated using a variety of analytic and numerical techniques. During the inspiral stage, where the orbital separation between two black holes is much larger than their extent, the BHs can be treated as point particles and their motion as well as the GW signal can be described using the post-Newtonian (PN) formalism. At small separations, however, the PN approximation is no longer valid and the Einstein field equations must be solved numerically to obtain the late-time dynamics and GW signal. In GW data analysis applications, such as matched-filter searches (Allen et al., 2012; Usman et al., 2016; Messick et al., 2017; Nitz et al., 2017; Venumadhav et al., 2019b) and Bayesian inference (Veitch et al., 2015; Zackay et al., 2018; Biwer et al., 2019), semi-analytic models with a continuous dependence on the binary parameters are most commonly used. This requires the smooth connection between PN and numerical relativity results. We briefly summarize the main modeling strategies below.

2.1. Post-Newtonian Theory

The post-Newtonian (PN) formalism is an approximation to GR valid in the slow-motion, weak-field regime (see Blanchet, 2014 and references therein for an extensive review). It is well-suited for describing the motion of compact binaries and their GW emission in the inspiral regime. In PN theory, relativistic corrections to the Newtonian solution are incorporated systematically order-by-order in the expansion parameter $\epsilon = v^2/c^2$, where v is the orbital velocity and c the speed of light. The PN formalism starts to break down when the orbital velocity of the black holes becomes comparable to the speed of light, i.e., $v \sim c$. At this point, one requires numerical solutions to the Einstein field equations.

2.2. Numerical Relativity

Solving the general relativistic two-body problem in its full generality was considered the holy grail of numerical relativity (NR) for many decades. It is only possible since the breakthroughs in 2005 (Pretorius, 2005; Campanelli et al., 2006b; Baker et al., 2007) to simulate two merging black holes and obtain the GW signal emitted in the highly dynamical, non-linear merger regime. Since the initial breakthroughs, the simulations of BBHs have become a standard tool in GW astrophysics, with ever improving accuracy and also aided by faster compute cores. To date thousands of NR simulations across the BBH parameter space have been performed (Mroue et al., 2013; Husa et al., 2016; Jani et al., 2016; Boyle et al., 2019; Healy et al., 2019), but the sampling is still very sparse mainly due to the high computational cost. Moreover, large mass ratio ($q \geq 20$) and high spin magnitudes ($|\vec{\chi}_i| \geq 0.9$) pose particularly challenging problems that are yet to be overcome.

Since the initial breakthrough in 2005, significant progress has been made: While the first successful simulations were those of equal-mass non-spinning BBHs spanning only the last few orbits, today simulations of aligned-spin as well as precessing quasi-circular binaries, eccentric-orbit binaries (Sperhake et al., 2008; Gold and Brügmann, 2013; Lewis et al., 2017; Hinder et al., 2018; Huerta et al., 2019; Ramos-Buades et al., 2020), and even

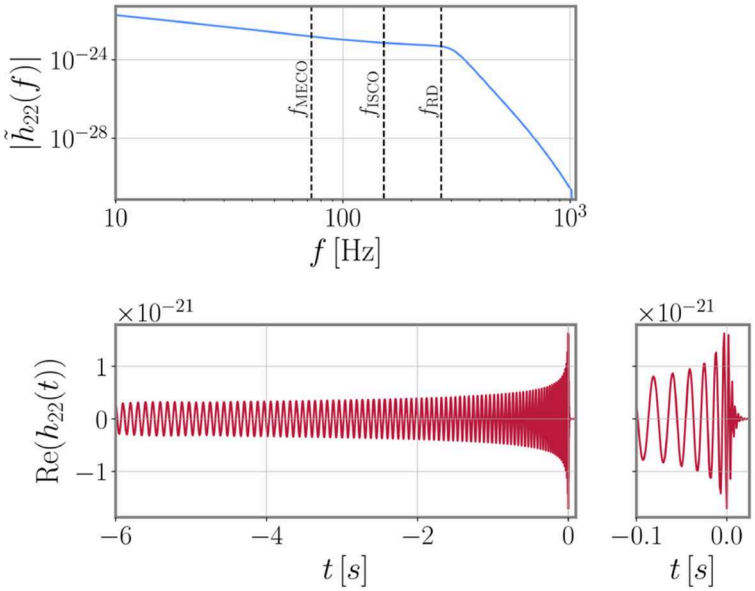

FIGURE 1 | The gravitational waveform of a non-spinning $30 + 30 M_\odot$ binary black hole at a distance of 400 Mpc generated from the phenomenological waveform model IMRPhenomX (Pratten et al., 2020b). The top panel shows the frequency-domain GW strain starting at 10 Hz when viewed face-on. The vertical dashed lines indicate three characteristic frequencies: the frequency of the innermost stable circular orbit ($f_{\rm ISCO}$), the minimal energy circular orbit ($f_{\rm MECO}$) and the ringdown frequency ($f_{\rm RD}$). The bottom panel shows the corresponding time-domain GW, where the smaller right panel shows a close-up of the last few inspiral cycles, the merger, and ringdown waveform.

evolutions that are long enough to reach into the early-inspiral regime (Szilágyi et al., 2015) are performed. Today, several codes based on different numerical techniques and formulations are capable of stably evolving BBHs and extracting their GW signal (Campanelli et al., 2006a; Scheel et al., 2006; Sperhake, 2007; Vaishnav et al., 2007; Brügmann et al., 2008; Loffler et al., 2012; Babiuc-Hamilton et al., 2019).

Numerical relativity does not only provide the waveform through merger but also for the ringdown. The quasi-normal mode spectrum emitted during this last stage of the binary evolution is analytically described by black hole perturbation theory (Teukolsky, 1973; Kokkotas and Schmidt, 1999). While the analytic prescription provides the mode frequencies and mode damping times (Berti et al., 2006), it does not provide the amplitude of the waves. Numerical relativity simulations, on the other hand, provide this crucial information, which, in combination, allows for the construction of parameter space fits (Kamaretsos et al., 2012; London et al., 2014).

The merger-ringdown waveforms obtained from NR are a key ingredient in the construction and verification of accurate waveform models used in GW data analysis. These applications, however, often require a continuous sampling across the parameter space, hence semi-analytic models or interpolants are paramount. In current analyses, waveforms from three families are most commonly employed: effective-one-body waveforms, phenomenological waveforms, and NR surrogates. While the first two paradigms model the complete inspiral-merger-ringdown (IMR) signal, NR-based surrogates are commonly restricted to a few GW cycles before the merger, the merger, and the ringdown.

2.3. Effective-One-Body

The effective-one-body (EOB) formalism combines information from the test particle limit as well PN results to obtain a complete description of the two-body dynamics as well as the IMR GW signal (Buonanno and Damour, 1999, 2000). It is based on a Hamiltonian map of the conservative dynamics of the two bodies to an effective one-body prescription, where a test particle with the reduced mass μ of the two-body system moves in an effective Kerr background spacetime characterized by the total mass M, the symmetric mass ratio η and the total spin $\vec{S}$:

$$H = M\sqrt{1 + 2\eta\left(\frac{H_{\rm eff}}{\mu} - 1\right)}. \quad (1)$$

The EOB prescription requires that the test particle limit reduces to the motion of a particle in a Kerr spacetime and that the EOB Hamiltonian reduces to the PN Hamiltonian in the weak-field, slow-motion limit. While the Hamiltonian encapsulates the inspiral dynamics, one additionally requires a prescription for the calculation of the GWs and the radiation reaction forces as well as a smooth transition to the ringdown of a perturbed black hole. The radiative degrees of freedom are described by factorized waveforms, which include a calibration to NR simulations. We note that the EOB formalism is inherently time-domain and requires solving a system of coupled ordinary differential equations, which makes the waveform generation rather costly.

The EOB waveform family includes highly accurate quadrupolar models for non-spinning and aligned-spin binaries (Bohé et al., 2017; Nagar et al., 2018), NR-calibrated

extensions to higher-order harmonics (Cotesta et al., 2018; Nagar et al., 2020a,b), and extensions to precessing BBH (Pan et al., 2014; Ossokine et al., 2020). Recently, extensions to include eccentric motion have been presented (Cao and Han, 2017; Hinderer and Babak, 2017).

2.4. Phenomenological Waveforms

The phenomenological framework takes a different approach: The focus here is exclusively on modeling the IMR GW signal itself without providing equations of motions for the BH dynamics (Ajith et al., 2007). The aim is to provide a fast-to-evaluate, closed-form expression of the GW signal in the frequency domain by splitting the signal into an amplitude and a phase, assuming the following schematic form:

$$\tilde{h}(f;\vec{\lambda},\vec{\theta}) = \tilde{A}(f;\vec{\lambda})e^{i\tilde{\Psi}(f;\vec{\theta})}, \tag{2}$$

where $\vec{\lambda}$ are (phenomenological) parameters in the amplitude and $\vec{\theta}$ in the phase respectively.

The amplitude and phase are modeled separately, where each part is subdivided into three regions: the inspiral ($f_{\rm GW} \leq f_{\rm MECO}$, where MECO denotes the minimum-energy circular orbit), an intermediate region and the ringdown. The inspiral is modeled based on analytic PN information augmented with an artificial extension (pseudo PN terms), which are calibrated to analytic, e.g., EOB, results. The intermediate region, which governs the merger phase, is modeled as a polynomial, while the ringdown is well-described by a deformed Lorentzian. These latter two regions are calibrated to NR information. For further details see (Santamaría et al., 2010; Khan et al., 2016; Pratten et al., 2020b).

Phenomenological waveform model are constructed in the frequency domain, which makes them computationally fast to evaluate and hence particularly attractive for data analysis applications. We emphasize, however, that the validity range of *any* NR-calibrated waveform model depends strongly on the calibration region, which, due to the lack of NR simulations for $q \geq 10$, is limited. The most recent waveform family, PhenomX (Garcia-Quiros et al., 2020; Pratten et al., 2020b), also includes extreme mass-ratio information which allows for a smooth evaluation up to $q \simeq 1{,}000$ (Harms et al., 2016), although the accuracy of waveforms between $19 \leq q \leq 1{,}000$ cannot be assessed. The current Phenom waveform families include aligned-spin models with and without higher-order modes as well as precessing ones (Hannam et al., 2014; Khan et al., 2019; Pratten et al., 2020a). An example of the IMR waveform of an equal-mass non-spinning BBH in the both the frequency and the time domain is shown in **Figure 1**.

2.5. Numerical Relativity Surrogates

In recent years it has become possible to produce thousands of NR simulations for restricted parameter ranges. These relatively short waveforms can then directly be used to construct an NR-based interpolant, i.e., a surrogate model, across a (limited) volume of the binary parameter space (Field et al., 2014; Blackman et al., 2017; Varma et al., 2019a,b). Such NR-based surrogates are considered the most accurate merger models but due to their restrictions in length and parameter space coverage, their usage is currently limited.

2.6. Gravitational Self-Force

While moderate to high mass ratio NR simulations remain a challenge, and therefore limit the accuracy of NR-calibrated waveform models in this regime, in the extreme mass ratio limit ($q \geq 10^4$) and possibly even the intermediate mass ratio regime ($q \sim 100$), a perturbative approach, often referred to as gravitational self-force (GSF), can be used to obtain an accurate approximation (see Poisson et al., 2011; Barack and Pound, 2019 for detailed reviews). Recent progress has seen the first second-order calculations (Pound et al., 2020), which will be crucial in order to fulfill the waveform accuracy requirements for future ground- and space-based GW observations of intermediate and extreme mass ratio binary black holes (Berry et al., 2019).

3. OBSERVATIONS OF BINARY BLACK HOLES

The first observation of GWs from a coalescing BBH by the Advanced LIGO – Virgo detector network, GW150914, in September 2015, marked the beginning of the GW discovery era. The LIGO Scientific and Virgo Collaborations have since announced a total of eleven confident detections of GWs from merging BBHs (Abbott et al., 2019c): GW150914 (Abbott et al., 2016d), GW151012 (Abbott et al., 2016b), GW151226 (Abbott et al., 2016c), GW170104 (Abbott et al., 2017a), GW170608 (Abbott et al., 2017b), GW170729, GW170809 (Abbott et al., 2019c), GW170814 (Abbott et al., 2017c), GW170818, GW170823 (Abbott et al., 2019c), and most recently GW190412 (Abbott et al., 2020). Moreover, several tens of BBH candidates have been identified in the currently ongoing third observing run (LIGO Scientific, Virgo Collaboration). Independent analyses of the publicly available GW strain data (LIGO Scientific Collaboration, Virgo Collaboration, 2018) have claimed the detection of additional eight binary black hole events (Nitz et al., 2019a; Venumadhav et al., 2019a; Zackay et al., 2019): Nitz et al. (2019a) reported GW170121, GW170304, GW170727, and GW151205; Venumadhav et al. (2019a) and Zackay et al. (2019) also reported GW170121, GW170304, GW170727 as well as GW151216, GW170202, GW170403 and GW170425. These observations allow us to put GR to the test in the strong-field regime (Abbott et al., 2016e, 2019d; Yunes et al., 2016), probe the astrophysics of black holes in previously unexplored mass regimes and shed light on the possible formation scenarios of black holes (Abbott et al., 2016a, 2019b).

The majority of GW events was identified via matched filtering (Sathyaprakash and Dhurandhar, 1991; Allen et al., 2012), the optimal method to extract GW signals from compact binary coalescences from noise, by comparing GR-based waveform models (see section 2) to the data. Very high-mass short-duration signals have also been identified by unmodeled searches (Klimenko et al., 2016), i.e, searches that do not rely on waveforms models but rather look for generic features.

The black hole binaries observed through GWs to date span a wide range of total masses from just under $20\,M_\odot$ for GW170608 (Abbott et al., 2017b), to more than $100\,M_\odot$ for GW151205 (Nitz et al., 2019a)[1] at the 90% credible level as shown in **Figure 2**. In particular, the heavier black holes have masses not previously seen in x-ray binaries (Corral-Santana et al., 2016), and they raise interesting questions regarding their possible formation process and history such as secondary mergers (Gerosa and Berti, 2017). So far, no black holes in either the lower mass gap between observed neutron star and BH masses (Özel et al., 2010; Farr et al., 2011), and the upper mass gap due to pair instability supernovae (Woosley, 2016; Marchant et al., 2018), have been identified. Further, most BBH observations are consistent with equal mass or marginally unequal mass binaries (Abbott et al., 2019c; Nitz et al., 2019a; Venumadhav et al., 2019a) but recently, the first BBH with an asymmetric mass ratio ($q \sim 0.28$) has been reported (Abbott et al., 2020).

Placing precise constraints on the spins of the black holes is more difficult with the best measured spin parameter being $\chi_{\rm eff}$, a mass-weighted linear combination of the dimensionless spin components along the orbital angular momentum direction $\hat{L}$ (Racine, 2008; Ajith et al., 2011),

$$\chi_{\rm eff} = \frac{(m_1\vec{\chi}_1 + m_2\vec{\chi}_2)\cdot\hat{L}}{m_1 + m_2}. \tag{3}$$

The majority of observations is consistent with $\chi_{\rm eff} = 0$ at the 90% credible level as shown in **Figure 2**, with the exceptions of: GW151226 (Abbott et al., 2016c), GW170729 (Abbott et al., 2019c), GW190412 (Abbott et al., 2020), GW151216, and GW170403 (Venumadhav et al., 2019b; Zackay et al., 2019). It should be noted, however, that the latter two events were analyzed under different spin prior assumptions. A recent re-analysis suggests that the $\chi_{\rm eff}$-values reported in Venumadhav et al. (2019b) and Zackay et al. (2019) for those two events may not be robust (Huang et al., 2018).

The individual black hole spin magnitudes are more difficult to constrain due to the strong dependence of the GW phase on $\chi_{\rm eff}$. However, a few observations find a net positive spin in the binary, implying that at least one of the two BHs must have a positive, non-zero spin angular momentum. Misalignment between the orbital angular momentum and the black holes spins induces relativistic precession, which is directly reflect into the GW signal (Apostolatos et al., 1994; Kidder, 1995). The observation of such precessional signatures is considered to be of key importance for distinguishing different BBH formation channels (Mandel and O'Shaughnessy, 2010; Rodriguez et al., 2016; Stevenson et al., 2017): BBHs formed in the field are expected to have predominantly aligned spins (Kalogera, 2000), while BBHs formed dynamically in dense environments are expected to have a more isotropic spin distribution (Rodriguez et al., 2016). In the GW observations made to date, spin misalignment remains unconstrained but it is anticipated that future observations will yield the first concrete measurements of precession.

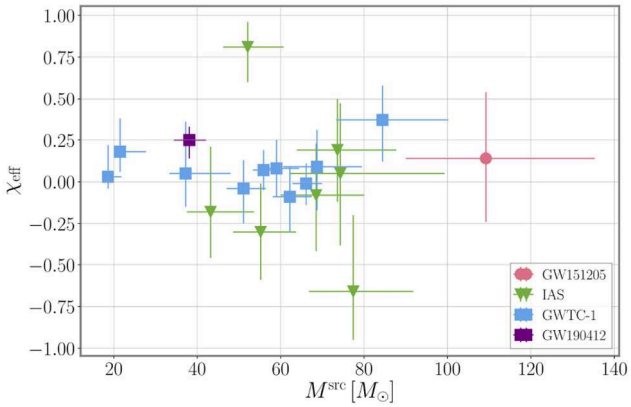

FIGURE 2 | Inferred total source-frame masses and effective inspiral spin of BBH observations. The error bars indicate the 90% credible interval of the 1D posterior probability. Blue square markers: Ten BBH events from GWTC-1 (Abbott et al., 2019c); purple square marker: GW190412 (Abbott et al., 2020); green triangular markers: events from Zackay et al. (2019) and Venumadhav et al. (2019a); red round marker: event GW151205 from Nitz et al. (2019a). Posterior samples were obtained from LIGO Scientific Collaboration, Virgo Collaboration (2018), Nitz et al. (2019b), Venumadhav et al. (2019c), and Abbott et al. (2020). The conversion from detector-frame to source-frame masses assumes a flat ΛCDM cosmology (Ade et al., 2016).

Gravitational waves from merging black holes are a unique probe of GR in the strong-field high-curvature regime, and hence these observations can be used to test their consistency with the predictions from GR (Berti et al., 2015). Due to the absence of complete IMR waveforms derived in alternative theories of gravity[2], we cannot directly test the validity of GR by comparison against these other theories but can perform a variety of consistency tests. One possibility is to introduce *ad hoc* parameterized modifications to the GR waveforms, representing either modifications in the strong-field regime or the wave propagation (Yunes and Pretorius, 2009; Mirshekari et al., 2012; Agathos et al., 2014; Berti et al., 2018b; Abbott et al., 2019d). One can then determine to which degree the inferred values of these modifications agree with the values predicted by GR. For binaries where the complete IMR signal is observed, one can further test the consistency of the inferred final mass and spin of the remnant black hole with the parameters inferred from the low- and high-frequency regimes of the signal (Hughes and Menou, 2005; Ghosh et al., 2016a,b). A detector network with non co-aligned detectors allows us to investigate the presence of additional polarization states as predicted in some alternative metric theories of gravity (Eardley et al., 1973; Corda, 2009).

[1]We note that this event is considered marginal. The most significant high-mass BBH discovered to date is GW170729 (Abbott et al., 2019c).

[2]Although recent progress has been made in simulating BBH mergers in alternative theories of gravity (Okounkova et al., 2019; Witek et al., 2019) and there is also ongoing effort in deriving inspiral waveforms (Sennett et al., 2016), which allow for concrete tests of alternative predictions beyond all-violations encompassing parameterized tests.

Current observations show significant preference for purely tensor polarizations over purely scalar or vector polarizations respectively (Abbott et al., 2017c, 2019d). To date, all tests of GR using BBHs yield results that are consistent with GR. For current observations, the limits on deviations from GR are dominated by the statistical uncertainty due to the detector noise. Improved detector sensitivities will allow for these constraints to tighten but the impact of systematic modeling errors, such as the neglect of eccentricity (Moore and Yunes, 2020), must be carefully taken into account (Berti et al., 2015).

4. OUTLOOK

The observation of GWs from coalescing black holes has opened a new window onto the electromagnetically dark universe. The observations to date have already revealed the existence of black holes in previously unexplored mass regimes and have allowed us to perform the first tests of GR in a novel regime. The next generation of ground-based facilities will be significantly more sensitive than current detectors (Punturo et al., 2010; Reitze et al., 2019), allowing for even tighter measurements of black hole masses and spins, and probing the existence of stellar mass black holes throughout the history of the universe. Moreover, future observations will enable us to perform black hole spectroscopy by measuring individual quasi-normal modes (Berti et al., 2006, 2018a), probe the Kerr nature of astrophysical black holes and constrain parameterized deviations from GR in the strong-field regime to unrivaled precision (Sathyaprakash et al., 2012). Recent progress has been made calculating gravitational waveforms in alternative theories of gravity, which will allow for concrete tests of predictions beyond all-violations encompassing parameterized tests as are performed at the moment.

The detection of hundreds of BBH will allow for the cross-correlations between the GW signals and galaxy catalogs will allow for an independent, precise measurement of Hubble constant H_0 (Abbott et al., 2019a), which can help shed light on the current tensions between early-time and late-time cosmological probes (Verde et al., 2019).

Furthermore, observing the mergers of BBHs throughout the history of the universe will allow us to probe fundamental physics at a range of energy scales (Barack et al., 2019; Barausse et al., 2020). Intermediate mass black holes, in particular, have the potential to provide us with important evidences as to what the nature of dark matter may be (Eda et al., 2015; Bertone et al., 2019).

Planned space-based missions such as LISA will see a fraction of stellar mass BBHs that will later be detected by ground-based observatories while they are still in the early inspiral stage, enabling multi-band GW astronomy and providing early-warnings to both GW and electromagnetic observatories (Sesana, 2016). This will allow us to pin-point telescopes and detect any coincident electromagnetic emission.

Gravitational-wave science has already delivered key insights into the nature and astrophysics of black holes and future observations will continue to nurture and improve our understanding of these fundamental objects in the universe.

AUTHOR CONTRIBUTIONS

PS has written this review article on her own to the best of her knowledge, she has produced all figures herself from publicly available data and codes. The references are extensive but they are by no means exhaustive.

FUNDING

PS acknowledges Dutch Research Council (NWO) Veni Grant No. 680-47-460.

REFERENCES

Aasi, J., Abbott, B. P., Abbott, R., Abbott, T., Abernathy, M. R., Ackley, K. et al. (2015). Advanced LIGO. *Class. Quant. Grav*. 32:074001.

Abbott, B. P., Abbott, R., Abbott, T. D., Abernathy, M. R., Acernese, F., Ackley, K., et al. (2016a). Astrophysical implications of the Binary Black-Hole Merger GW150914. *Astrophys. J. Lett*. 818:L22. doi: 10.3847/2041-8205/818/2/L22

Abbott, B. P., Abbott, R., Abbott, T. D., Abernathy, M. R., Acernese, F., Ackley, K., et al. (2016b). Binary Black Hole Mergers in the first Advanced LIGO observing run. *Phys. Rev. X* 6:041015. doi: 10.1103/PhysRevX.6.041015

Abbott, B. P., Abbott, R., Abbott, T. D., Abernathy, M. R., Acernese, F., Ackley, K., et al. (2016c). GW151226: observation of gravitational waves from a 22-solar-mass binary black hole coalescence. *Phys. Rev. Lett*. 116:241103. doi: 10.1103/PhysRevLett.116.241103

Abbott, B. P., Abbott, R., Abbott, T. D., Abernathy, M. R., Acernese, F., Ackley, K., et al. (2016d). Observation of gravitational waves from a binary black hole merger. *Phys. Rev. Lett*. 116:061102. doi: 10.1103/PhysRevLett.116.061102

Abbott, B. P., Abbott, R., Abbott, T. D., Abernathy, M. R., Acernese, F., Ackley, K., et al. (2016e). Tests of general relativity with GW150914. *Phys. Rev. Lett*. 116:221101. doi: 10.1103/PhysRevLett.116.221101

Abbott, B. P., Abbott, R., Abbott, T. D., Abernathy, M. R., Acernese, F., Ackley, K., et al. (2017a). GW170104: observation of a 50-solar-mass binary black hole coalescence at redshift 0.2. *Phys. Rev. Lett*. 118:221101. doi: 10.1103/PhysRevLett.118.221101

Abbott, B. P., Abbott, R., Abbott, T. D., Abernathy, M. R., Acernese, F., Ackley, K., et al. (2017b). GW170608: observation of a 19-solar-mass binary black hole coalescence. *Astrophys. J*. 851:L35. doi: 10.3847/2041-8213/aa9f0c

Abbott, B. P., Abbott, R., Abbott, T. D., Abernathy, M. R., Acernese, F., Ackley, K., et al. (2017c). GW170814: A three-detector observation of gravitational waves from a binary black hole coalescence. *Phys. Rev. Lett*. 119:141101. doi: 10.1103/PhysRevLett.119.141101

Abbott, B. P., Abbott, R., Abbott, T. D., Abernathy, M. R., Acernese, F., Ackley, K., et al. (2019b). Binary black hole population properties inferred from the first and second observing runs of advanced LIGO and advanced Virgo. *Astrophys. J*. 882:L24. doi: 10.3847/2041-8213/ab3800

Abbott, B. P., Abbott, R., Abbott, T. D., Abernathy, M. R., Acernese, F., Ackley, K., et al. (2019c). GWTC-1: a gravitational-wave transient catalog of compact binary mergers observed by LIGO and Virgo during the first and second observing runs. *Phys. Rev. X* 9:031040. doi: 10.1103/PhysRevX.9.031040

Abbott, B. P., Abbott, R., Abbott, T. D., Abernathy, M. R., Acernese, F., Ackley, K., et al. (2019d). Tests of general relativity with the binary black hole signals from the LIGO-Virgo catalog GWTC-1. *Phys. Rev*. D100:104036. doi: 10.1103/PhysRevD.100.062006

Abbott, B. P., Abbott, R., Abbott, T. D., Abraham, S., Acernese, F., Ackley, K., et al. (2019a). A gravitational-wave measurement of the Hubble constant following

the second observing run of Advanced LIGO and Virgo. *arXiv [Preprint]. arXiv:1908.06060*.

Abbott, R., Abbott, T. D., Abraham, S., Acernese, F., Ackley, K., Adams, C., et al. (2020). GW190412: observation of a binary-black-hole coalescence with asymmetric masses. *arXiv [Preprint]. arXiv:2004.08342*.

Acernese, F., Agathos, M., Agatsuma, K., Aisa, D., Allemandou, N., Allocca, A., et al. (2015). Advanced Virgo: a second-generation interferometric gravitational wave detector. *Class. Quant. Grav.* 32:024001. doi: 10.1088/0264-9381/32/2/024001

Ade, P. A. R., Aghanim, N., Arnaud, M., Ashdown, M., Aumont, J., Baccigalupi, C., et al. (2016). Planck 2015 results. XIII. Cosmological parameters. *Astron. Astrophys.* 594:A13. doi: 10.1051/0004-6361/201525830

Agathos, M., Del Pozzo, W., Li, T. G. F., Van Den Broeck, C., Veitch, J., and Vitale, S. (2014). TIGER: a data analysis pipeline for testing the strong-field dynamics of general relativity with gravitational wave signals from coalescing compact binaries. *Phys. Rev. D* 89:082001. doi: 10.1103/PhysRevD.89.082001

Ajith, P., Babak, S., Chen, Y., Hewitson, M., Krishnan, B., Whelan, J. L., et al. (2007). Phenomenological template family for black-hole coalescence waveforms. *Classic. Quant. Grav.* 24, S689-S700. doi: 10.1088/0264-9381/24/19/S31

Ajith, P., Hannam, M., Husa, S., Chen, Y., Brügmann, B., Dorband, N., et al. (2011). Inspiral-merger-ringdown waveforms for black-hole binaries with non-precessing spins. *Phys. Rev. Lett.* 106:241101. doi: 10.1103/PhysRevLett.106.241101

Akutsu, T., Ando, M., Arai, K., Arai, Y., Araki, S., Araya, A., et al. (2019). KAGRA: 2.5 generation interferometric gravitational wave detector. *Nat. Astron.* 3, 35–40. doi: 10.1038/s41550-018-0658-y

Allen, B., Anderson, W. G., Brady, P. R., Brown, D. A., and Creighton, J. D. E. (2012). FINDCHIRP: an algorithm for detection of gravitational waves from inspiraling compact binaries. *Phys. Rev. D* 85:122006. doi: 10.1103/PhysRevD.85.122006

Apostolatos, T. A., Cutler, C., Sussman, G. J., and Thorne, K. S. (1994). Spin induced orbital precession and its modulation of the gravitational wave forms from merging binaries. *Phys. Rev. D* 49, 6274–6297. doi: 10.1103/PhysRevD.49.6274

Babiuc-Hamilton, M., Brandt, S. R., Diener, P., Elley, M., Etienne, Z., Ficarra, G. et al. (2019). *The Einstein Toolkit. To Find Out More*. Available online at: http://einsteintoolkit.org

Baker, J. G., van Meter, J. R., McWilliams, S. T., Centrella, J., and Kelly, B. J. (2007). Consistency of post-Newtonian waveforms with numerical relativity. *Phys. Rev. Lett.* 99:181101. doi: 10.1103/PhysRevLett.99.181101

Barack, L., Cardoso, V., Nissanke, S., Sotiriou, T. P., Askar, A., Belczynski, C., et al. (2019). Black holes, gravitational waves and fundamental physics: a roadmap. *Class. Quant. Grav.* 36:143001. doi: 10.1088/1361-6382/ab0587

Barack, L., and Pound, A. (2019). Self-force and radiation reaction in general relativity. *Rept. Prog. Phys.* 82:016904. doi: 10.1088/1361-6633/aae552

Barausse, E., Berti, E., Hertog, T., Hughes, S. A., Jetzer, P., Pani, P., et al. (2020). Prospects for fundamental physics with LISA. *arXiv [Preprint]. arXiv:2001.09793*.

Bayes, R. T. (1764). An essay toward solving a problem in the doctrine of chances. *Philos. Trans. R. Soc. Lond.* 53, 370–418. doi: 10.1098/rstl.1763.0053

Berry, C. P. L., Hughes, S. A., Sopuerta, C. F., Chua, A. J. K., Heffernan, A., Holley-Bockelmann, K., et al. (2019). The unique potential of extreme mass-ratio inspirals for gravitational-wave astronomy. *arXiv [Preprint]. arXiv:1903.03686*.

Berti, E., Barausse, E., Cardoso, V., Gualtieri, L., Pani, P., Sperhake, U., et al. (2015). Testing general relativity with present and future astrophysical observations. *Classic. Quant. Grav.* 32:243001. doi: 10.1088/0264-9381/32/24/243001

Berti, E., Cardoso, V., and Will, C. M. (2006). On gravitational-wave spectroscopy of massive black holes with the space interferometer LISA. *Phys. Rev. D* 73:064030. doi: 10.1103/PhysRevD.73.064030

Berti, E., Yagi, K., Yang, H., and Yunes, N. (2018a). Extreme gravity tests with gravitational waves from compact binary coalescences: (II) ringdown. *Gen. Rel. Grav.* 50:49. doi: 10.1007/s10714-018-2372-6

Berti, E., Yagi, K., and Yunes, N. (2018b). Extreme gravity tests with gravitational waves from compact binary coalescences: (I) inspiral-merger. *Gen. Rel. Grav.* 50:46. doi: 10.1007/s10714-018-2362-8

Bertone, G., Croon, D., Amin, M. A., Boddy, K. K., Kavanagh, B. J., Mack, K. J., et al. (2019). Gravitational wave probes of dark matter: challenges and opportunities. *arXiv [Preprint]. arXiv:1907.10610*.

Biwer, C. M., Capano, C. D., De, S., Cabero, M., Brown, D. A., Nitz, A. H., et al. (2019). PyCBC inference: a Python-based parameter estimation toolkit for compact binary coalescence signals. *Publ. Astron. Soc. Pac.* 131:024503. doi: 10.1088/1538-3873/aaef0b

Blackman, J., Field, S. E., Scheel, M. A., Galley, C. R., Ott, C. D., Boyle, M., et al. (2017). Numerical relativity waveform surrogate model for generically precessing binary black hole mergers. *Phys. Rev. D* 96:024058. doi: 10.1103/PhysRevD.96.024058

Blanchet, L. (2014). Gravitational radiation from post-Newtonian sources and inspiralling compact binaries. *Living Rev. Relativ.* 17:2. doi: 10.12942/lrr-2014-2

Bohé, A., Shao, L., Taracchini, A., Buonanno, A., Babak, S., Harry, I. W., et al. (2017). An improved effective-one-body model of spinning, nonprecessing binary black holes for the era of gravitational-wave astrophysics with advanced detectors. *Phys. Rev. D* 95:044028. doi: 10.1103/PhysRevD.95.044028

Boyle, M., Hemberger, D., Iozzo, D. A. B., Lovelace, G., Ossokine, S., Pfeiffer, H. P., et al. (2019). The SXS Collaboration catalog of binary black hole simulations. *Class. Quant. Grav.* 36:195006. doi: 10.1088/1361-6382/ab34e2

Brügmann, B., González, J. A., Hannam, M., Husa, S., Sperhake, U., and Tichy, W. (2008). Calibration of moving puncture simulations. *Phys. Rev. D* 77:024027. doi: 10.1103/PhysRevD.77.024027

Buonanno, A., and Damour, T. (1999). Effective one-body approach to general relativistic two-body dynamics. *Phys. Rev. D* 59:084006. doi: 10.1103/PhysRevD.59.084006

Buonanno, A., and Damour, T. (2000). Transition from inspiral to plunge in binary black hole coalescences. *Phys. Rev. D* 62:064015. doi: 10.1103/PhysRevD.62.064015

Campanelli, M., Lousto, C. O., Marronetti, P., and Zlochower, Y. (2006a). Accurate evolutions of orbiting black-hole binaries without excision. *Phys. Rev. Lett.* 96:111101. doi: 10.1103/PhysRevLett.96.111101

Campanelli, M., Lousto, C. O., and Zlochower, Y. (2006b). Spinning-black-hole binaries: the orbital hang up. *Phys. Rev. D* 74:041501. doi: 10.1103/PhysRevD.74.041501

Cao, Z., and Han, W.-B. (2017). Waveform model for an eccentric binary black hole based on the effective-one-body-numerical-relativity formalism. *Phys. Rev. D* 96:044028. doi: 10.1103/PhysRevD.96.044028

Corda, C. (2009). Interferometric detection of gravitational waves: the definitive test for General Relativity. *Int. J. Mod. Phys. D* 18, 2275–2282. doi: 10.1142/S0218271809015904

Corral-Santana, J. M., Casares, J., Munoz-Darias, T., Bauer, F. E., Martinez-Pais, I. G., and Russell, D. M. (2016). BlackCAT: a catalogue of stellar-mass black holes in X-ray transients. *Astron. Astrophys.* 587:A61. doi: 10.1051/0004-6361/201527130

Cotesta, R., Buonanno, A., Bohe, A., Taracchini, A., Hinder, I., and Ossokine, S. (2018). Enriching the symphony of gravitational waves from binary black holes by tuning higher harmonics. *Phys. Rev. D* 98:084028. doi: 10.1103/PhysRevD.98.084028

Eardley, D. M., Lee, D. L., and Lightman, A. P. (1973). Gravitational-wave observations as a tool for testing relativistic gravity. *Phys. Rev. D* 8, 3308–3321. doi: 10.1103/PhysRevD.8.3308

Eda, K., Itoh, Y., Kuroyanagi, S., and Silk, J. (2015). Gravitational waves as a probe of dark matter minispikes. *Phys. Rev. D* 91:044045. doi: 10.1103/PhysRevD.91.044045

Einstein, A. (1915). On the general theory of relativity. *Sitzungsber. Preuss. Akad. Wiss. Berlin* 1915, 778–786.

Einstein, A. (1918). On gravitational waves. *Sitzungsber. Preuss. Akad. Wiss. Berlin* 1918, 154–167.

Farr, W. M., Kremer, K., Lyutikov, M., and Kalogera, V. (2011). Spin tilts in the double pulsar reveal supernova spin angular-momentum production. *Astrophys. J.* 742:81. doi: 10.1088/0004-637X/742/2/81

Field, S. E., Galley, C. R., Hesthaven, J. S., Kaye, J., and Tiglio, M. (2014). Fast prediction and evaluation of gravitational waveforms using surrogate models. *Phys. Rev. X* 4:031006. doi: 10.1103/PhysRevX.4.031006

Garcia-Quiros, C., Colleoni, M., Husa, S., Estelles, H., Pratten, G., Ramos-Buades, A., et al. (2020). IMRPhenomXHM: A multi-mode frequency-domain model for the gravitational wave signal from non-precessing black-hole binaries.

Gerosa, D., and Berti, E. (2017). Are merging black holes born from stellar collapse or previous mergers? *Phys. Rev. D* 95:124046. doi: 10.1103/PhysRevD.95.124046

Ghosh, A., Del Pozzo, W., and Ajith, P. (2016a). Estimating parameters of binary black holes from gravitational-wave observations of their inspiral, merger and ringdown. *Phys. Rev. D* 94:104070. doi: 10.1103/PhysRevD.94.104070

Ghosh, A., Ghosh, A., Johnson-Mcdaniel, N. K., Mishra, C. K., Ajith, P., Del Pozzo, W., et al. (2016b). Testing general relativity using golden black-hole binaries. *Phys. Rev. D* 94:021101. doi: 10.1103/PhysRevD.94.021101

Gold, R., and Brügmann, B. (2013). Eccentric black hole mergers and zoom-whirl behavior from elliptic inspirals to hyperbolic encounters. *Phys. Rev. D* 88:064051. doi: 10.1103/PhysRevD.88.064051

Hannam, M., Schmidt, P., Bohé, A., Haegel, L., Husa, S., Ohme, F., et al. (2014). Simple model of complete precessing black-hole-binary gravitational waveforms. *Phys. Rev. Lett.* 113:151101. doi: 10.1103/PhysRevLett.113.151101

Harms, E., Lukes-Gerakopoulos, G., Bernuzzi, S., and Nagar, A. (2016). Asymptotic gravitational wave fluxes from a spinning particle in circular equatorial orbits around a rotating black hole. *Phys. Rev. D* 93:044015. doi: 10.1103/PhysRevD.93.044015

Healy, J., Lousto, C. O., Lange, J., O'Shaughnessy, R., Zlochower, Y., and Campanelli, M. (2019). Second RIT binary black hole simulations catalog and its application to gravitational waves parameter estimation. *Phys. Rev. D* 100:024021. doi: 10.1103/PhysRevD.100.024021

Hinder, I., Kidder, L. E., and Pfeiffer, H. P. (2018). Eccentric binary black hole inspiral-merger-ringdown gravitational waveform model from numerical relativity and post-Newtonian theory. *Phys. Rev. D* 98:044015. doi: 10.1103/PhysRevD.98.044015

Hinderer, T., and Babak, S. (2017). Foundations of an effective-one-body model for coalescing binaries on eccentric orbits. *Phys. Rev. D* 96:104048. doi: 10.1103/PhysRevD.96.104048

Huang, Y., Middleton, H., Ng, K. K. Y., Vitale, S., and Veitch, J. (2018). Characterization of low-significance gravitational-wave compact binary sources. *Phys. Rev. D* 98:123021. doi: 10.1103/PhysRevD.98.123021

Huerta, E.A., Haas, R., Habib, S., Gupta, A., Rebei, A., Chavva, V., et al. (2019). Physics of eccentric binary black hole mergers: a numerical relativity perspective. *Phys. Rev. D* 100:064003. doi: 10.1103/PhysRevD.100.064003

Hughes, S. A., and Menou, K. (2005). Golden binaries for LISA: robust probes of strong-field gravity. *Astrophys. J.* 623, 689–699. doi: 10.1086/428826

Husa, S., Khan, S., Hannam, M., Pürrer, M., Ohme, F., Forteza, X. J., et al. (2016). Frequency-domain gravitational waves from nonprecessing black-hole binaries. I. New numerical waveforms and anatomy of the signal. *Phys. Rev. D* 93:044006. doi: 10.1103/PhysRevD.93.044006

Jani, K., Healy, J., Clark, J. A., London, L., Laguna, P., and Shoemaker, D. (2016). Georgia tech catalog of gravitational waveforms. *Class. Quant. Grav.* 33:204001. doi: 10.1088/0264-9381/33/20/204001

Kalogera, V. (2000). Spin orbit misalignment in close binaries with two compact objects. *Astrophys. J.* 541, 319–328. doi: 10.1086/309400

Kamaretsos, I., Hannam, M., Husa, S., and Sathyaprakash, B. S. (2012). Black-hole hair loss: learning about binary progenitors from ringdown signals. *Phys. Rev. D* 85:024018. doi: 10.1103/PhysRevD.85.024018

Khan, S., Chatziioannou, K., Hannam, M., and Ohme, F. (2019). Phenomenological model for the gravitational-wave signal from precessing binary black holes with two-spin effects. *Phys. Rev. D* 100:024059. doi: 10.1103/PhysRevD.100.024059

Khan, S., Husa, S., Hannam, M., Ohme, F., Pürrer, M., Jiménez Forteza, X., et al. (2016). Frequency-domain gravitational waves from nonprecessing black-hole binaries. II. A phenomenological model for the advanced detector era. *Phys. Rev. D* 93:044007. doi: 10.1103/PhysRevD.93.044007

Kidder, L. E. (1995). Coalescing binary systems of compact objects to postNewtonian 5/2 order. 5. Spin effects. *Phys. Rev.* D52:821–847. doi: 10.1103/PhysRevD.52.821

Klimenko, S., Vedovato, G., Drago, M., Salemi, F., Tiwari, V., Prodi, G. A., et al. (2016). Method for detection and reconstruction of gravitational wave transients with networks of advanced detectors. *Phys. Rev. D* 93:042004. doi: 10.1103/PhysRevD.93.042004

Kokkotas, K. D., and Schmidt, B. G. (1999). Quasinormal modes of stars and black holes. *Living Rev. Relat.* 2:2. doi: 10.12942/lrr-1999-2

Lewis, A. G. M., Zimmerman, A., and Pfeiffer, H. P. (2017). Fundamental frequencies and resonances from eccentric and precessing binary black hole inspirals. *Class. Quant. Grav.* 34:124001. doi: 10.1088/1361-6382/aa66f4

LIGO Scientific Collaboration, Virgo Collaboration (2018). *GWTC-1*. doi: 10.7935/82H3-HH23

LIGO Scientific, Virgo Collaboration. GraceDB. Available online at: https://gracedb.ligo.org/superevents/public/O3/

Loffler, F., Faber, J., Bentivegna, E., Bode, T., Diener, P., Haas, R., et al. (2012). The Einstein Toolkit: a community computational infrastructure for relativistic astrophysics. *Class. Quant. Grav.* 29:115001. doi: 10.1088/0264-9381/29/11/115001

London, L., Shoemaker, D., and Healy, J. (2014). Modeling ringdown: beyond the fundamental quasinormal modes. *Phys. Rev. D* 90(12):124032. doi: 10.1103/PhysRevD.90.124032

Mandel, I., and O'Shaughnessy, R. (2010). Compact binary coalescences in the band of ground-based gravitational-wave detectors. *Classic. Quant. Grav.* 27:114007. doi: 10.1088/0264-9381/27/11/114007

Marchant, P., Renzo, M., Farmer, R., Pappas, K. M. W., Taam, R. E., de Mink, S., et al. (2018). Pulsational pair-instability supernovae in very close binaries. *Astrophys. J.* 882:36. doi: 10.3847/1538-4357/ab3426

Messick, C., Blackburn, K., Brady, Brockill, P., Cannon, K., Cariou, R., et al. (2017). Analysis framework for the prompt discovery of compact binary mergers in gravitational-wave data. *Phys. Rev. D* 95:042001. doi: 10.1103/PhysRevD.95.042001

Mirshekari, S., Yunes, N., and Will, C. M. (2012). Constraining generic lorentz violation and the speed of the graviton with gravitational waves. *Phys. Rev. D* 85:024041. doi: 10.1103/PhysRevD.85.024041

Moore, B., and Yunes, N. (2020). Constraining gravity with eccentric gravitational waves: projected upper bounds and model selection. *arXiv [Preprint]*. doi: 10.1088/1361-6382/ab8bb6

Mroue, A. H., Scheel, M. A., Szilagyi, B., Pfeiffer, H. P., Boyle, M., Hemberger, D. A., et al. (2013). Catalog of 174 binary black hole simulations for gravitational wave astronomy. *Phys. Rev. Lett.* 111:241104. doi: 10.1103/PhysRevLett.111.241104

Nagar, A., Bernuzzi, S., Del Pozzo, W., Riemenschneider, G., Akcay, S., Carullo, G., et al. (2018). Time-domain effective-one-body gravitational waveforms for coalescing compact binaries with nonprecessing spins, tides and self-spin effects. *Phys. Rev. D* 98:104052. doi: 10.1103/PhysRevD.98.104052

Nagar, A., Pratten, G., Riemenschneider, G., and Gamba, R. (2020a). Multipolar effective one body model for nonspinning black hole binaries. *Phys. Rev. D* 101:024041. doi: 10.1103/PhysRevD.101.024041

Nagar, A., Riemenschneider, G., Pratten, G., Rettegno, P., and Messina, F. (2020b). A multipolar effective one body waveform model for spin-aligned black hole binaries. *arXiv [Preprint]. arXiv:2001.09082*.

Nitz, A. H., Dent, T., Davies, G. S., Kumar, S., Capano, C. D., Harry, I., et al. (2019a). 2-OGC: open gravitational-wave catalog of binary mergers from analysis of public Advanced LIGO and Virgo data. *arXiv [Preprint]. arXiv:1910.05331*. doi: 10.3847/1538-4357/ab733f

Nitz, A. H., Dent, T., Davies, G. S., Kumar, S., Capano, C. D., Harry, I., et al. (2019b). *Posterior Samples*. Available online at: https://github.com/gwastro/2-ogc/

Nitz, A. H., Harry, I. W., Willis, J. L., Biwer, C. M., Brown, D. A., Pekowsky, L. P., et al. (2017). PyCBC Software. *GitHub Repository*. doi: 10.5281/zenodo.344823

Okounkova, M., Stein, L. C., Moxon, J., Scheel, M. A., and Teukolsky, S. A. (2019). Numerical relativity simulation of GW150914 beyond general relativity. *arXiv [Preprint]. arXiv:1911.02588*. doi: 10.1103/PhysRevD.101.104016

O'Shaughnessy, R., Vaishnav, B., Healy, J., Meeks, Z., and Shoemaker, D. (2011). Efficient asymptotic frame selection for binary black hole spacetimes using asymptotic radiation. *Phys. Rev. D* 84:124002. doi: 10.1103/PhysRevD.84.124002

Ossokine, S., Buonanno, A., Marsat, S., Cotesta, R., Babak, S., Dietrich, T., et al. (2020). Multipolar effective-one-body waveforms for precessing binary black holes: construction and validation. *arXiv [Preprint]. arXiv:2004.09442*.

Özel, F., Psaltis, D., Narayan, R., and McClintock, J. E. (2010). The black hole mass distribution in the galaxy. *Astrophys. J.* 725, 1918–1927. doi: 10.1088/0004-637X/725/2/1918

Pan, Y., Buonanno, A., Taracchini, A., Kidder, L. E., Mroué, A. H., Pfeiffer, H. P., et al. (2014). Inspiral-merger-ringdown waveforms of spinning,

precessing black-hole binaries in the effective-one-body formalism. *Phys. Rev. D* 89:084006. doi: 10.1103/PhysRevD.89.084006

Poisson, E., Pound, A., and Vega, I. (2011). The Motion of point particles in curved spacetime. *Living Rev. Relat.* 14:7. doi: 10.12942/lrr-2011-7

Pound, A., Wardell, B., Warburton, N., and Miller, J. (2020). Second-order self-force calculation of the gravitational binding energy in compact binaries. *Phys. Rev. Lett.* 124:021101. doi: 10.1103/PhysRevLett.124.021101

Pratten, G., García-Quirós, C., Colleoni, M., Ramos-Buades, A., Estellés, H., Mateu-Lucena, M., et al. (2020a). Let's twist again: computationally efficient models for the dominant and sub-dominant harmonic modes of precessing binary black holes. *arXiv [Preprint]*. a*rXiv:2004.06503*.

Pratten, G., Husa, S., Garcia-Quiros, C., Colleoni, M., Ramos-Buades, A., Estelles, H., et al. (2020b). Setting the cornerstone for the IMRPhenomX family of models for gravitational waves from compact binaries: the dominant harmonic for non-precessing quasi-circular black holes. *arXiv [preprint]. arXiv:2001.11412*. Available online at: https://dcc.ligo.org/LIGO-P2000018

Pretorius, F. (2005). Evolution of binary black hole spacetimes. *Phys. Rev. Lett.* 95:121101. doi: 10.1103/PhysRevLett.95.121101

Punturo, M., Abernathy, M., Acernese, F., Allen, B., Andersson, N., Arun, K., et al. (2010). The Einstein telescope: a third-generation gravitational wave observatory. *Classic. Quant. Grav.* 27:194002. doi: 10.1088/0264-9381/27/19/194002

Racine, É. (2008). Analysis of spin precession in binary black hole systems including quadrupole-monopole interaction. *Phys. Rev. D* 78:044021. doi: 10.1103/PhysRevD.78.044021

Ramos-Buades, A., Husa, S., Pratten, G., Estellés, H., García-Quirós, C., Mateu-Lucena, M., et al. (2020). First survey of spinning eccentric black hole mergers: Numerical relativity simulations, hybrid waveforms, and parameter estimation. *Phys. Rev. D* 101:083015. doi: 10.1103/PhysRevD.101.083015

Reitze, D., Adhikari, R. X., Ballmer, S., Barish, B., Barsotti, L., Billingsley,G., et al. (2019). Cosmic Explorer: the U.S. contribution to gravitational-wave astronomy beyond LIGO. *Bull. Am. Astron. Soc.* 51:035.

Rodriguez, C. L., Zevin, M., Pankow, C., Kalogera, V., and Rasio, F. A. (2016). Illuminating black hole binary formation channels with spins in advanced LIGO. *Astrophys. J. Lett.* 83:L2. doi: 10.3847/2041-8205/832/1/L2

Santamaría, L., Ohme, F., Ajith, P., Brugmann, B., Dorband, N., Hannam, M., et al. (2010). Matching post-Newtonian and numerical relativity waveforms: systematic errors and a new phenomenological model for non-precessing black hole binaries. *Phys. Rev. D* 82:064016. doi: 10.1103/PhysRevD.82.064016

Sathyaprakash, B., Abernathy, M., Acernese, F., Ajith, P., Allen, B., Amaro-Seoane, P., et al. (2012). Scientific objectives of Einstein telescope. *Classic. Quant. Grav.* 29:124013. doi: 10.1088/0264-9381/30/7/079501

Sathyaprakash, B. S., and Dhurandhar, S. V. (1991). Choice of filters for the detection of gravitational waves from coalescing binaries. *Phys. Rev. D* 44, 3819–3834. doi: 10.1103/PhysRevD.44.3819

Scheel, M. A., Pfeiffer, H. P., Lindblom, L., Kidder, L. E., Rinne, O., and Teukolsky, S. A. (2006). Solving Einstein's equations with dual coordinate frames. *Phys. Rev. D* 74:104006. doi: 10.1103/PhysRevD.74.104006

Schmidt, P., Hannam, M., and Husa, S. (2012). Towards models of gravitational waveforms from generic binaries: a simple approximate mapping between precessing and non-precessing inspiral signals. *Phys. Rev. D* 86:104063. doi: 10.1103/PhysRevD.86.104063

Schmidt, P., Hannam, M., Husa, S., and Ajith, P. (2011). Tracking the precession of compact binaries from their gravitational-wave signal. *Phys. Rev. D* 84:024046. doi: 10.1103/PhysRevD.84.024046

Sennett, N., Marsat, S., and Buonanno, A. (2016). Gravitational waveforms in scalar-tensor gravity at 2PN relative order. *Phys. Rev. D* 94:084003. doi: 10.1103/PhysRevD.94.084003

Sesana, A. (2016). Prospects for multiband gravitational-wave astronomy after GW150914. *Phys. Rev. Lett.* 116:231102. doi: 10.1103/PhysRevLett.116.231102

Sperhake, U. (2007). Binary black-hole evolutions of excision and puncture data. *Phys. Rev. D* 76:104015. doi: 10.1103/PhysRevD.76.104015

Sperhake, U., Berti, E., Cardoso, V., González, J. A., Brügmann, B., and Ansorg, M. (2008). Eccentric binary black-hole mergers: the transition from inspiral to plunge in general relativity. *Phys. Rev. D* 78:064069. doi: 10.1103/PhysRevD.78.064069

Stevenson, S., Berry, C. P., and Mandel, I. (2017). Hierarchical analysis of gravitational-wave measurements of binary black hole spin-orbit misalignments. *Mon. Not. R. Astron. Soc.* 471, 2801–2811. doi: 10.1093/mnras/stx1764

Szilágyi, B., Blackman, J., Buonanno, A., Taracchini, A., Pfeiffer, H. P., Scheel, M. A., et al. (2015). Approaching the post-newtonian regime with numerical relativity: a compact-object binary simulation spanning 350 gravitational-wave cycles. *Phys. Rev. Lett.* 115:031102. doi: 10.1103/PhysRevLett.115.031102

Teukolsky, S. A. (1973). Perturbations of a rotating black hole. 1. Fundamental equations for gravitational electromagnetic and neutrino field perturbations. *Astrophys. J.* 185, 635–647. doi: 10.1086/152444

Usman, S. A., Nitz, A. H., Harry, I. W., Biwer, C. W., Brown, D. A., Cabero, M., et al. (2016). The PyCBC search for gravitational waves from compact binary coalescence. *Classic. Quant. Grav.* 33:215004. doi: 10.1088/0264-9381/33/21/215004

Vaishnav, B., Hinder, I., Herrmann, F., and Shoemaker, D. (2007). Matched filtering of numerical relativity templates of spinning binary black holes. *Phys. Rev. D* 76:084020. doi: 10.1103/PhysRevD.76.084020

Varma, V., Field, S. E., Scheel, M. A., Blackman, J., Gerosa, D., Stein, L. C., et al. (2019a). Surrogate models for precessing binary black hole simulations with unequal masses. *Phys. Rev. Res.* 1:033015. doi: 10.1103/PhysRevResearch.1.033015

Varma, V., Field, S. E., Scheel, M. A., Blackman, J., Kidder, L. E., and Pfeiffer, H. P. (2019b). Surrogate model of hybridized numerical relativity binary black hole waveforms. *Phys. Rev. D* 99:064045. doi: 10.1103/PhysRevD.99.064045

Veitch, J., Raymond, V., Blackburn, K., and Smith, R. (2015). Parameter estimation for compact binaries with ground-based gravitational-wave observations using the LALInference software library. *Phys. Rev. D* 91:042003. doi: 10.1103/PhysRevD.91.042003

Venumadhav, T., Zackay, B., Roulet, J., Dai, L., and Zaldarriaga, M. (2019a). New binary black hole mergers in the second observing run of advanced LIGO and advanced Virgo. *Phys. Rev. D* 101:083030. doi: 10.1103/PhysRevD.101.083030

Venumadhav, T., Zackay, B., Roulet, J., Dai, L., and Zaldarriaga, M. (2019b). New search pipeline for compact binary mergers: Results for binary black holes in the first observing run of Advanced LIGO. *Phys. Rev. D* 100:023011. doi: 10.1103/PhysRevD.100.023011

Venumadhav, T., Zackay, B., Roulet, J., Dai, L., and Zaldarriaga, M. (2019c). *O2 Samples*. Available online at: https://github.com/jroulet/O2_samples

Verde, L., Treu, T., and Riess, A. G. (2019). Tensions between the early and the late universe. *arXiv [Preprint]*. doi: 10.1038/s41550-019-0902-0

Witek, H., Gualtieri, L., Pani, P., and Sotiriou, T. P. (2019). Black holes and binary mergers in scalar Gauss-Bonnet gravity: scalar field dynamics. *Phys. Rev. D* 99:064035. doi: 10.1103/PhysRevD.99.064035

Woosley, S. E. (2016). The progenitor of Gw150914. *Astrophys. J. Lett.* 824:L10. doi: 10.3847/2041-8205/824/1/L10

Yunes, N., and Pretorius, F. (2009). Fundamental theoretical bias in gravitational wave astrophysics and the parameterized post-Einsteinian framework. *Phys. Rev. D* 80:122003. doi: 10.1103/PhysRevD.80.122003

Yunes, N., Yagi, K., and Pretorius, F. (2016). Theoretical physics implications of the binary black-hole mergers GW150914 and GW151226. *Phys. Rev. D* 94:084002. doi: 10.1103/PhysRevD.94.084002

Zackay, B., Dai, L., and Venumadhav, T. (2018). Relative binning and fast likelihood evaluation for gravitational wave parameter estimation. *arXiv [Preprint]. arXiv:1806.08792.*

Zackay, B., Venumadhav, T., Dai, L., Roulet, J., and Zaldarriaga, M. (2019). Highly spinning and aligned binary black hole merger in the Advanced LIGO first observing run. *Phys. Rev. D* 100:023007. doi: 10.1103/PhysRevD.100.023007

Conflict of Interest: The author declares that the research was conducted in the absence of any commercial or financial relationships that could be construed as a potential conflict of interest.

frontiers in Astronomy and Space Sciences

MINI REVIEW
published: 09 November 2020
doi: 10.3389/fspas.2020.578849

Short Duration Gamma-Ray Bursts and Their Outflows in Light of GW170817

Davide Lazzati *

Department of Physics, Oregon State University, Corvallis, OR, United States

The detection of GW170817, it's extensive multi-wavelength follow-up campaign, and the large amount of theoretical development and interpretation that followed, have resulted in a significant step forward in the understanding of the binary neutron star merger phenomenon as a whole. One of its aspects is seeing the merger as a progenitor of short gamma-ray bursts (SGRB), which will be the subject of this review. On the one hand, GW170817 observations have confirmed some theoretical expectations, exemplified by the confirmation that binary neutron star mergers are the progenitors of SGRBs. In addition, the multimessenger nature of GW170817 has allowed for gathering of unprecedented data, such as the trigger time of the merger, the delay with which the gamma-ray photons were detected, and the brightening afterglow of an off-axis event. All together, the incomparable richness of the data from GW170817 has allowed us to paint a fairly detailed picture of at least one SGRB. I will detail what we learned, what new questions have arisen, and the perspectives for answering them when a sample of GW170817-comparable events have been studied.

Keywords: gamma-ray bursts, relativistic astrophysics, hydrodynamics, gravitational waves, binary mergers, transient sources

OPEN ACCESS

Edited by:
Bruno Giacomazzo, University of Milano-Bicocca, Italy

Reviewed by:
Maria Dainotti, Jagiellonian University, Poland
Herman J. Mosquera Cuesta, Departamento Administrativo Nacional de Ciencia, Tecnologia e Innovacion, Colciencias, Colombia

***Correspondence:**
Davide Lazzati
davide.lazzati@oregonstate.edu

Specialty section:
This article was submitted to Cosmology, a section of the journal Frontiers in Astronomy and Space Sciences

Received: *01 July 2020*
Accepted: *11 September 2020*
Published: *09 November 2020*

Citation:
Lazzati D (2020) Short Duration Gamma-Ray Bursts and Their Outflows in Light of GW170817. Front. Astron. Space Sci. 7:578849. doi: 10.3389/fspas.2020.578849

1 INTRODUCTION

Gamma-ray bursts (GRBs) are some of the most energetic explosions in the present day Universe, characterized by the release of large amounts of energy, within a few milliseconds to tens of seconds, resulting in the acceleration of relativistic outflows and the release of high-energy photons (Fishman and Meegan, 1995; Piran, 1999; Mészáros, 2002; Gehrels et al., 2009; Kumar and Zhang, 2015). They can be divided in at least two classes, based on the duration of their prompt phase, in which their emission is concentrated in the hard X-ray and gamma-ray bands and is characterized by fast variability (Kouveliotou et al., 1993). Long duration GRBs last 2 s or more, while short duration GRBs (SGRBs) last between a few milliseconds and 2 s. Alternative classifications have also been introduced, considering, e.g., short GRBs with extended emission (Norris and Bonnell, 2006; Dainotti et al., 2010; Norris et al., 2010; Barkov and Pozanenko, 2011; Dainotti et al., 2017), or attempting a more physical classification based on inferred progenitor properties (Lü et al., 2010; Bromberg et al., 2013).

In the last two and a half decades, the study of GRBs has concentrated on long duration GRBs, and a general consensus has grown around a model in which these events are associated with the collapse of the core of massive stars (Woosley and Bloom, 2006). While the collapse of most massive stars would ignite a core-collapse supernova, those that are fastly spinning and metal poor could also trigger a long duration GRB, powered by a compact central engine (Woosley, 1993;

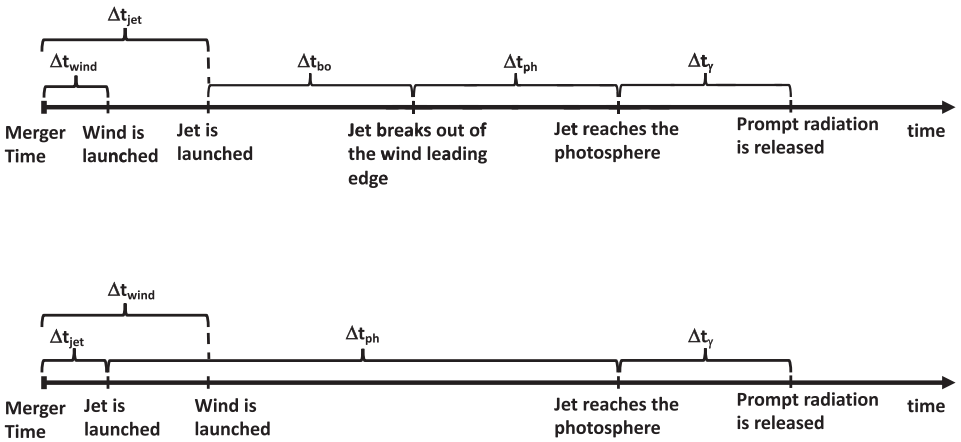

FIGURE 1 | The two possible timelines with all the phases that may contribute to the detected delay $\Delta t_{GW-\gamma}$. Due to the presence of a structured outflow, GW170817 most likely followed the top timeline. The relative contribution of the various phases is a matter of debate, but consensus is growing around $\Delta t_{wind} < \Delta t_{jet} \ll 1$ s, $\Delta t_{bo} \ll 1$ s, $\Delta t_{\gamma} \sim 0$, and $\Delta t_{ph} \sim \Delta t_{GW-\Gamma}$. The meaning of all the symbols is explained in Section 2

Woosley and Heger, 2006; Yoon et al., 2006). Whether the central engine is a fastly spinning, highly magnetized neutron star (NS) (Bucciantini et al., 2008; Bucciantini et al., 2009; Metzger et al., 2011) or an accreting black hole (BH) (Woosley, 1993; Lee et al., 2000; Lei et al., 2013) is the matter of open debate.

The interest on SGRBs had increased in the last decade, initially as a consequence of the launch of the Fermi satellite, which had a higher efficiency for detecting and localizing them compared to its predecessors (Meegan et al., 2009). More recently, the theoretical expectation that SGRBs had to be associated with the merger of binary NS systems (or, perhaps, system made by a BH and a NS) (Belczynski et al., 2006; Lee and Ramirez-Ruiz, 2007; Fong and Berger, 2013; Giacomazzo et al., 2013; Ruiz et al., 2016; Ciolfi, 2018) has made them the expected and highly anticipated high-frequency counterparts of gravitational wave sources (Nakar et al., 2006; Kiuchi et al., 2010; Schutz, 2011). Such expectations were supported by energetic and temporal arguments. Powering a GRB requires a large amount of energy, comparable to the rest mass of a stellar object converted to energy. In addition, said energy needs to be released in a matter of a fraction of a second, at least for SGRBs. Naked compact objects (NS and BH) are the only available candidates that can offer the required energy within a region of less than a light second. However, isolated NS and BH are unlikely progenitors, since some catastrophic event needs to take place to cause the sudden release of a large fraction of their total energy. Binary mergers are therefore a natural candidate, when at least one of the two members is a NS, since a binary BH system would merge in a bigger BH that would swallow all the matter and energy, instead of ejecting them as a relativistic outflow.[1]

All these expectations were confirmed by the detection of GW170817 (Abbott et al., 2017a) and its associated GRB GRB170817A (Abbott et al., 2017b; Goldstein et al., 2017; Savchenko et al., 2017; Zhang et al., 2018), afterglow, and kilonova (KN) (Abbott et al., 2017c; Abdalla et al., 2017; Alexander et al., 2017; Arcavi et al., 2017; Coulter et al., 2017; Cowperthwaite et al., 2017; Evans et al., 2017; Haggard et al., 2017; Hallinan et al., 2017; Kasen et al., 2017; Kim et al., 2017; Margutti et al., 2017; Pian et al., 2017; Siebert et al., 2017; Smartt et al., 2017; Soares-Santos et al., 2017; Tanvir et al., 2017; Troja et al., 2017; Valenti et al., 2017; D'Avanzo et al., 2018; Margutti et al., 2018; Mooley et al., 2018a; Mooley et al., 2018c; Lyman et al., 2018; Resmi et al., 2018; Villar et al., 2018; Ghirlanda et al., 2019; Lamb et al., 2019a). In this contribution I will review the key observations of GW170817 as a SGRB (also known as GRB170817A), the questions that were answered, and the new ones that were spurred, and briefly discuss what more insight is expected from the detection of more systems akin to GW170817 in future GW observing runs.

2 BEFORE THE PROMPT EMISSION

In this **Section 1** will review the physics of the SGRB outflow before the prompt emission phase begins, as it happened in GW170817. First of all, there is little doubt that the GW signal of GW170817 came from a binary compact merger, and that the masses of the two compact objects are compatible with being NS (Abbott et al., 2017a; Abbott et al., 2017b; Abbott et al., 2017c). The GW signal by itself does not allow to distinguish between NSs and BHs, but the richness of the electromagnetic signal that followed requires the presence of baryonic matter, and therefore at least one of the two components of the binary had to be a NS. Most likely they were both NSs (Coughlin and Dietrich, 2019).

2.1 The Time Delay

Besides the identification of the progenitor, a very important piece of information that GW170817 provided is the merger time,

[1]Some have suggested, however, that even binary BH mergers could produce a weak electromagnetic transient, under certain conditions (Perna et al., 2016; Liu et al. 2016; Zhang, 2016).

which allowed for the measuring of the time delay between the GWs and the gamma-ray signals. This delay, which we indicate as $\Delta t_{GW-\gamma}$ can be due to several reasons, as detailed below and shown in **Figure 1** (Granot et al., 2017; Lin et al., 2018; Zhang, 2019; Lazzati et al., 2020; Lucca and Sagunski 2020).

- Engine Delay—While the time of the merger is the earliest time at which the jet from the central engine can be produced, there is the possibility of some delay (Cook et al., 1994; Lasota et al., 1996; Vietri and Stella, 1998; Ciolfi and Siegel, 2015). Such delay is difficult to predict theoretically but can be likely due either to the need of a transition in the engine itself or to the need of amplifying the magnetic field to a value large enough to launch a jet. The former can be quite long, up to years, and usually invokes a metastable, fastly spinning NS that collapses into a BH when its rotation period is increased by either internal or external torques. We indicate this delay time as Δt_{eng}.
- Wind Delay—Owing to the detection of a KN and an off-axis SGRB from a structured outflow, we know that GW170817 ejected a non-relativistic wind. There can be a delay in launching such a wind as well, and we indicate it as Δt_{wind}. It should be noted, however, that this delay can in principle be negative since the NS surfaces are tidally shredded in the last few orbits before the merger.
- Breakout delay—If the wind is ejected before the jet, then the jet has to propagate through the wind. The propagation happens at sub-relativistic speed, causing a delay of the head of the jet with respect to the GW signal that travels at the speed of light (Matzner, 2003; Morsony et al., 2007; Bromberg et al., 2011; Lazzati and Perna, 2019). We indicate the time it takes for the jet head to cross the wind as Δt_{bo}. The jet-wind interaction also causes the development of a cocoon (Ramirez-Ruiz et al., 2002), confined by the surrounding wind. This leads to the development of a structured outflow that maintains a bright core but develops wide, energetic wings at large polar angles (Lazzati et al., 2017a; Lazzati et al., 2017b).
- Photospheric delay—After the outflow has broken out of the leading edge of the wind, it needs to propagate out to the photospheric radius. At this point the jet becomes transparent and the necessary conditions for the release of the prompt gamma-ray radiation are met. We indicate the delay due to the propagation from the break out radius to the photospheric radius as Δt_{ph}.
- Dissipation delay—While at the photospheric radius the prompt emission can be radiated, it does not mean it is. In some models, such as the popular internal shock synchrotron model, the outflow needs to propagate out to the internal shock radius before the bulk energy of the flow is dissipated and turned into radiation. We indicate this additional delay as Δt_{γ}.

For the first time, a measurement of the sum of all these possible delays was available for GW170817 (Abbott et al., 2017b). The prompt gamma-ray radiation was detected with a delay $\Delta t_{GW-\gamma} \simeq 1.75$ s. Several attempts have been made to constrain the various individual contributions, but a general consensus has not been achieved (Shoemaker and Murase, 2018; Gill et al., 2019b; Beniamini et al., 2020a; Hamidani et al., 2020). A few robust inferences can however be made (Lazzati et al., 2020). Overall, the measured delay was fairly small, since GW170817 ejected a significant amount of energy toward the observer but its Lorentz factor could be at most moderate ($\Gamma < 7$) (Beniamini et al., 2020b). These combine to a large photospheric radius and a photospheric delay

$$\Delta t_{ph} \sim \frac{R_{ph}}{c\Gamma^2} = 1.4 \frac{R_{ph}}{2 \times 10^{12}\ \mathrm{cm}} \left(\frac{7}{\Gamma}\right)^2 \mathrm{s} \quad (1)$$

The photospheric delay therefore had to contribute to a sizable part of the delay, since any other non-photospheric emission mechanism would require a longer delay (this allows to use the above equation to put a Lower limit on Γ (Beniamini 2020a). The wind delay, if there was any, had to be smaller than the jet delay, so that the jet-wind interaction could generate a structured outflow, as requested for modeling the afterglow emission. For the same reason, the jet delay itself could be fairly small but could not be null. Finally, the breakout and dissipation delays had to be small in order to accommodate the large expected photospheric delay. Note, however, that the prompt emission spectrum had a non-thermal shape, a property that is not expected form a simple photospheric emission model (see **Section 3** for a more thorough discussion).

2.2 The Shaping of the Outflow

GW170817 was also the first GRB for which evidence of a structured outflow could be unequivocally determined. The structure of the outflow could be intrinsic, as the jet itself could have been launched with a non-uniform polar structure (Aloy et al., 2005; Kathirgamaraju et al., 2019). However, the relatively large energetics of GW170817 in gamma-rays and the shape of its afterglow lightcurve (see **Section 4**) suggest a wide structure, most likely brought about by the jet interaction with the wind from the merger (Lazzati and Perna, 2019; Salafia et al., 2020).

A typical SGRB jet with isotropic equivalent energy $E_{iso} = 10^{53}$ erg and asymptotic Lorentz factor $\eta = 100$ has a baryon rest mass $M_0 = E_{iso}/\eta c^2 \sim 10^{-4} M_{\odot}$. If it encounters a wind mass $M_{wind} \geq M_0/\eta \sim 10^{-6} M_{\odot}$ it is shocked and the velocity of propagation of its head is slowed until the working surface of the jet head is in causal contact, allowing for the wind material and the shocked jet material to move to the side instead of accumulating in front of the jet and thereby slowing it down (Matzner, 2003; Morsony et al., 2007; Bromberg et al., 2011; Lazzati and Perna, 2019). As a consequence, a high-pressure cocoon inflates around the jet, composed by partially mixed jet and wind material. As the jet breaks out of the wind leading edge, the cocoon loses the confining effect of the wind material and is released. Since it has large pressure, it accelerates creating a broad structure around the jet with decreasing energy and Lorentz factor for increasing polar angle. This process therefore turns a collimated jet into a structured outflow. It requires a small wind mass that is well below the expected amount of baryons ejected in a binary NS merger. The cocoon structure can be studied analytically, by enforcing pressure balance between the jet, cocoon, and wind material at their respective contact surfaces, or through numerical simulations. Despite its importance for

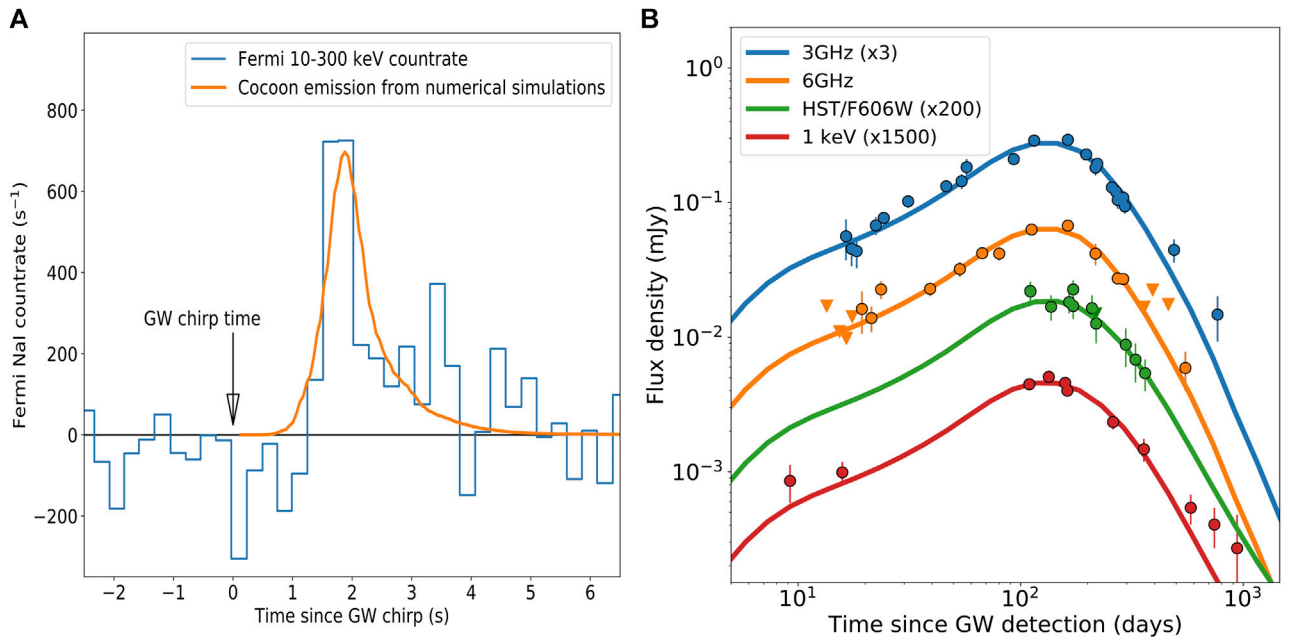

FIGURE 2 | Left panel (A): the prompt emission of GW170817. The blue step-line shows the Fermi data (Goldstein et al., 2017), while the orange solid line is the prediction from a theoretical simulation that assumes a structured outflow from the jet-wind interaction (Lazzati et al., 2017b). The radiation is assumed to be released at the photosphere. **Right panel (B)**: Afterglow of GW170817. Symbols with error-bars show observations in the radio, optical, and X-ray bands. Solid lines show the best fit result for an afterglow model with a structured outflow and an observer located at $\theta_o = 35°$ from the line of sight. Additional data at different radio frequencies were used to constrain the model, but only two radio bands are shown for clarity. Adapted from Makhathini et al. (2020).

predicting burst/merger observability and understanding the structure and composition of the merger wind and jet, the polar profile of the outflow is highly debated. Analytic functions ranging from Gaussian, power-law, and exponential have been tested, and even numerical simulations do not provide an unequivocal answer (Murguia-Berthier et al., 2014; Nagakura et al., 2014; Lazzati et al., 2017b; Murguia-Berthier et al., 2017a; Murguia-Berthier et al., 2017b; Duffell et al., 2018; Granot et al., 2018a; Wu and MacFadyen, 2018; Xie et al., 2018; Geng et al., 2019; Gill et al., 2019a; Kathirgamaraju et al., 2019; Hamidani et al., 2020; Hamidani and Ioka, 2020; Murguia-Berthier et al., 2020; Takahashi and Ioka 2020a; Takahashi and Ioka 2020b).

3 THE PROMPT EMISSION

Approximately 1.75 s after the GW chirp, a gamma–ray pulse was observed by both the Fermi and INTEGRAL satellites from a position compatible with the direction from which the GWs arrived (Goldstein et al., 2017; Savchenko et al., 2017). The pulse was made by an initial spike of about half a second followed by a broader, less intense tail, for an overall duration of ~ 2 s. Two characteristics make this gamma-ray pulse different from the population of previously observed SGRBs: it is markedly less energetic than an average cosmological SGRB and, given its energetics, it has a very high peak frequency (Fong et al., 2015). As a matter of fact, the detection itself was surprising because the chance of having a SGRB jet pointing along the line of sight for the first GW-selected binary merger was expected to be small (Metzger and Berger, 2012; Ghirlanda et al., 2016). That is because the amplitude of the GWs depend only mildly on the orientation of the binary, while the intensity of the radiation from a narrow, relativistic jet drops quickly for any line of sight outside the jet itself. Such an expectation was based, however, on the properties of a narrow jet and not on the possibility that the jet-wind interaction would cause a structured outflow to form. Predictions from models with structured outflows had indeed shown that, for moderately large off-axis angles, a detectable signal would be expected from a GW-detected merger (Lazzati et al., 2017a; Lazzati et al., 2017b). A similar effect might be responsible for X-ray flashes, when a long duration GRB is seen off-axis (Yamazaki 2020, Yamazaki 2003).

The structured outflow model was successful at predicting that a SGRB would be detectable even at large off-axis angles (Lazzati et al., 2017a; Lazzati et al., 2017b). It correctly predicted the off-axis burst energetics and its duration. It could also successfully explain the detected delay between the GWs and the γ-rays. A comparison between the Fermi data and the bolometric photospheric emission (Lazzati et al., 2017b) is shown in the left panel of **Figure 2**. The one aspect of GW170817 that cannot be accounted for by the simple photospheric cocoon emission is the γ-ray spectrum of the prompt emission. At least in first approximation, the photosphere of an off-axis structured outflow is expected to produce a thermal pulse with temperature (Lazzati et al., 2017a; Lazzati et al., 2017b)

$$T_{\rm obs} \simeq \left(\frac{L\Gamma^2}{4\pi\sigma R_{\rm ph}^2}\right)^{\frac{1}{4}} = 10^7 \left(\frac{L}{10^{47}{\rm erg}}\right)^{\frac{1}{4}} \left(\frac{\Gamma}{100}\right)^{\frac{1}{2}} \left(\frac{10^{12}{\rm cm}}{R_{\rm ph}}\right)^{\frac{1}{2}} {\rm K} \quad (2)$$

which would produce a spectrum peaked at a few KeV, in severe tension with the observed peak frequency at ~ 150 keV (Goldstein et al., 2017). This is due to the fact that the cocoon, which energized the outflow at large off axis, is not expected to be radially structured, and therefore no significant dissipation is expected to occur around the photospheric radius, differently from the photospheres of long GRBs (Lazzati et al., 2009; Parsotan et al., 2018). One possible explanation is that the prompt radiation was due to an external shock (Veres et al., 2018). However, given the low Lorentz factor and low interstellar medium densities expected in the surroundings of GW170817, the timing of the prompt emission, less than 2 s after the launching of the jet, is difficult to explain. Alternatively, the prompt emission could be due to the breakout of the cocoon from the leading edge of the wind (Kasliwal et al., 2017; Bromberg et al., 2018; Gottlieb et al., 2018; Nakar et al., 2018). The shock breakout model can explain the energetics and spectrum of the prompt emission (Nakar and Sari, 2012) but requires a finely tuned setup in which the wind is very fast, so that it can reach a large enough radius at the breakout time. The origin of the prompt emission spectrum is therefore not been explained in a completely satisfactory way, yet (Kisaka et al., 2018; Meng et al., 2018; Pozanenko et al., 2018; Ioka and Nakamura, 2019; Matsumoto et al., 2019). The observation of more SGRBs from GW-detected mergers will offer further observational constraints to shed light on this remaining riddle.

4 THE AFTERGLOW

The afterglow of GW170817 had its own share of unique features. To begin with, it was not detected for more then a week, until it was bright enough to be seen first in X-rays (Margutti et al., 2017; Troja et al., 2017) and, at around the two weeks mark, in radio waves (Hallinan et al., 2017; Troja et al., 2017). The detection of the afterglow at optical wavelengths had to wait for the dimming of the associated KN, and was performed only around day 110 with the Hubble Space Telescope (Lyman et al., 2018). Such late appearance of an afterglow is unprecedented, since the typical behavior is that the afterglow peaks very early, minutes to hours after the burst, and only dims with time afterward (van Paradijs et al., 2000; Nousek et al., 2006). A second unique feature of the afterglow of GW170817 was that, even after it was detected, it sustained a slow brightening at all wavelengths (Margutti et al., 2017; Mooley et al., 2018c; Ruan et al., 2018; Troja et al., 2019b), eventually peaking ~ 150 days after the GW detection and dropping in luminosity steeply afterwords (Dobie et al., 2018; Makhathini et al., 2020) (see the right panel of **Figure 2**).

The outflow from GW170817 along the direction toward Earth was under-energetic by a factor 10,000 to 100,000 times with respect to a typical SGRB (Fong et al., 2017). An outstanding question was therefore whether GW170817 had a misaligned, SGRB-like jet pointing in a different direction or not (Lazzati et al., 2018; Mooley et al., 2018a; Salafia et al., 2018). If it did, then the identification of the SGRB progenitors with binary NS mergers would be secured. If did not, then what GW10817 was associated with would be a new class of dim, possibly isotropic, γ-ray transients. Unfortunately, telling whether a misaligned relativistic jet is present is not easy, since all the radiation is relativistically beamed away from the line of sight. The slow but steady brightening was shown to be consistent with the presence of a jet, its energy contribution along the line of sight growing with the deceleration of the external shock (Xiao et al., 2017; De Colle et al., 2018; Finstad et al., 2018; Granot et al., 2018b; Lamb and Kobayashi, 2018; Lazzati et al., 2018; Nakar et al., 2018; Fraija et al., 2019a; Fraija et al., 2019b; Beniamini et al., 2020b; Oganesyan et al., 2020). However, a radially stratified spherical outflow could reproduce the observations as well, albeit at the price of adding a never observed before component to the models (Li et al., 2018; Mooley et al., 2018c; Nakar et al., 2018; Nakar and Piran, 2018; Salafia et al., 2018). Some evidence in favor of a jet was provided by the steep post-peak decay at all wavelengths (Alexander et al., 2018; Jin et al., 2018; Lamb et al., 2018; Mooley et al., 2018b; Nynka et al., 2018; Fong et al., 2019; Hajela et al., 2019). In addition, it was soon realized that either a relatively large linear polarization (Gill and Granot, 2018) or a small but detectable proper motion of the radio transient could potentially give the final clue. Both observations were carried out. Polarization turned out to be small (Corsi et al., 2018), and only an upper limit of 12 per cent was obtained, still consistent with either explanation. Long baseline radio interferometry turned out to be the key. In one experiment, a small but significant proper motion was detected (Mooley et al., 2018a), while in a second experiment the radio source was confirmed to be point-like (Ghirlanda et al., 2019). Both these characteristics are incompatible with a spherical expansion. In the future, the detection of the counter-jet emission might give additional evidence (Yamazaki 2018).

To date, despite the very high quality of the available data, the unique afterglow of GW170817 can be modeled successfully with the good old external shock synchrotron model (Mészáros and Rees, 1997; Sari et al., 1998), with the only required addition of considering off-axis observers (Granot et al., 2002) and allowing for some structure in the polar direction (Lazzati et al., 2017b; Lazzati et al., 2018). The type of polar stratification is not univocally constrained, since Gaussian, power-law, and exponential profile seem all to give an adequate fit to the data (Lazzati et al., 2018; Troja et al., 2018a; Xie et al., 2018; Ghirlanda et al., 2019). Numerical simulations are also ambiguous, different codes yielding different polar structures, including the three mentioned above (Murguia-Berthier et al., 2014; Nagakura et al., 2014; Lazzati et al., 2017b; Murguia-Berthier et al., 2017a; Murguia-Berthier et al., 2017b; Duffell et al., 2018; Granot et al., 2018a; Wu and MacFadyen, 2018; Xie et al., 2018; Geng et al., 2019; Gill et al., 2019b; Kathirgamaraju et al., 2019; Hamidani et al., 2020). Constraints can be obtained from the lack of a large populations of cosmological off-axis bursts (Beniamini 2019). More observations and further theoretical work are needed to pin down this important aspect that has implications not only on the detectability of bursts but also on the nature of the inner engine and the composition of the ejected jet and wind.

5 SUMMARY, DISCUSSION, AND A LOOK AT THE FUTURE

GW170817 was a rich event, a cornerstone detection in our understanding of SGRBs. It confirmed that binary NS mergers are the progenitor of at least some short bursts, it showed us that the top-hat jet model is woefully inadequate for describing the relativistic outflows of SGRBs (and possibly long duration GRBs as well) and it gave us, for the first time ever, a measure of the trigger time and of the delay between the launching of the jet and the detection of the prompt emission radiation.

We now know that the burst associated with GW170817 was a fairly canonical SGRB (Salafia et al., 2019), with a powerful relativistic jet that, after interacting with the merger wind, turned into a structured outflow (Lazzati et al., 2017b; Lazzati et al., 2018). Our line of sight lied somewhere between 15° and 35° away from the jet axis, the lower value obtained by high resolution radio imaging (Mooley et al., 2018c; Ghirlanda et al., 2019), while the larger value being favored by multi-band afterglow modeling and ejecta considerations (Lazzati et al., 2018; Mandel, 2018; Zou et al., 2018). The prompt emission was powered by an energetic cocoon inflated by the interaction of the jet with the merger wind. The gamma-ray radiation was likely released at or near the photosphere, either by a shock breakout (Nakar and Sari, 2012; Kasliwal et al., 2017; Gottlieb et al., 2018) or by other non-thermal mechanisms (Savchenko et al., 2017; Veres et al., 2018). The external shock developed later than usual due to the lower than customary Lorentz factor of the outflow along the line of sight and the afterglow was unusual, characterized by an initial increase in luminosity that lasted for a few months before peaking and beginning a steep declining phase. This behavior is understood to be due to the structure of the outflow, characterized by a polar stratification with a steep decline as a function of angle in both the energy per unit solid angle and the Lorentz factor.

Despite the large amount of observational evidence that allowed us to paint a detailed picture of the dynamic of the relativistic ejecta of GW170817 and their electromagnetic signatures, some questions remain open. First, we do not know the nature of the compact object that launched the relativistic jet. It could have been either a meta-stable NS or a BH, and consensus in this respect hasn't been reached (Piro et al., 2019; Metzger et al., 2018; Pooley et al., 2018; Abedi and Afshordi, 2019). A related mystery is the origin of the observed 1.75 s delay between the GW and the prompt emission. As discussed in **Section 2.1** the delay is the sum of many components and it is unclear which dominates, or if several of them have comparable magnitude. Since the photospheric delay is strongly dependent on the viewing angle, observation of several SGRBs from a diverse set of angles will help better understand the origin of the delay. Still unclear is also the physics of the dissipation that powered the prompt emission and the prompt emission mechanism itself. Shock breakouts, internal dissipation such as internal shocks, and even external shocks have been proposed (see **Section 3**).

Finally, we still do not know how typical GW170817 was. The fact that most likely it originated from a binary NS merger does not exclude the possibility that some—if not most—SGRB are made in NS-BH mergers. It might even be that GW170817 itself was a NS-BH merger (Coughlin and Dietrich, 2019; Kyutoku et al., 2020). Re-analysis of several past bursts have yielded some support the presence of kilonovae in their light curves (Troja et al., 2018b; Beniamini et al., 2019; Lamb et al., 2019b; Troja et al., 2019a) or similarities in their prompt emission (Burns 2018, von Kienlin 2019), showing that GW170817 was not unique. However, there might be cases in which the jet is not successful in breaking out of the wind leading edge, and a weaker transient would be produced (Kasliwal et al., 2017; Mooley et al., 2018c; Salafia et al., 2018). Future GW detections with the power of multimessenger observations will allow to better understand the connection between binary NS mergers, binary NS-BH mergers, and SGRBs.

AUTHOR CONTRIBUTIONS

DL has written this review article on his own to the best of his knowledge, he has produced all figures himself from publicly available data and codes. The references are extensive but they are by no means exhaustive.

FUNDING

DL acknowledges support from NASA grants 80NSSC18K1729 (Fermi) and NNX17AK42G (ATP), Chandra grant TM9-20002X, and NSF grant AST-1907955.

REFERENCES

Abbott, B. P., Abbott, R., Abbott, T. D., Acernese, F., Ackley, K., Adams, C., et al. (2017a). GW170817: Observation of gravitational waves from a binary neutron star inspiral. *Phys. Rev. Lett.* 119, 161101. doi:10.1103/PhysRevLett.119.161101

Abbott, B. P., Abbott, R., Abbott, T. D., Acernese, F., Ackley, K., Adams, C., et al. (2017b). Gravitational waves and gamma-rays from a binary neutron star merger: GW170817 and GRB 170817A. *Astrophys. J.* 848, L13. doi:10.3847/2041-8213/aa920c

Abbott, B. P., Abbott, R., Abbott, T. D., Acernese, F., Ackley, K., Adams, C., et al. (2017c). Multi-messenger observations of a binary neutron star merger. *Astrophys. J.* 848, L12. doi:10.3847/2041-8213/aa91c9

Abdalla, H., Abramowski, A., Aharonian, F., Ait Benkhali, F., Angüner, E. O., Arakawa, M., et al. (2017). TeV gamma-ray observations of the binary neutron star merger GW170817 with H.E.S.S. *Astrophys. J. Lett.* 850, L22. doi:10.3847/2041-8213/aa97d2

Abedi, J., andAfshordi, N. (2019). Echoes from the abyss: a highly spinning black hole remnant for the binary neutron star merger GW170817. *J. Cosmol. Astropart. Phys.* 2019, 010. doi:10.1088/1475-7516/2019/11/010

Alexander, K. D., Berger, E., Fong, W., Williams, P. K. G., Guidorzi, C., Margutti, R., et al. (2017). The electromagnetic counterpart of the binary neutron star merger LIGO/virgo GW170817. VI. Radio constraints on a relativistic jet and predictions for late-time emission from the kilonova ejecta. *Astrophys. J.* 848, L21. doi:10.3847/2041-8213/aa905d

Alexander, K. D., Margutti, R., Blanchard, P. K., Fong, W., Berger, E., Hajela, A., et al. (2018). A decline in the X-ray through radio emission from GW170817

continues to support an off-axis structured jet. *Astrophys. J.* 863, L18. doi:10.3847/2041-8213/aad637

Aloy, M. A., Janka, H.-T., andMüller, E. (2005). Relativistic outflows from remnants of compact object mergers and their viability for short gamma-ray bursts. *Astron. Astrophys.* 436, 273–311. doi:10.1051/0004-6361:20041865

Arcavi, I., Hosseinzadeh, G., Howell, D. A., McCully, C., Poznanski, D., Kasen, D., et al. (2017). Optical emission from a kilonova following a gravitational-wave-detected neutron-star merger. *Nature* 551, 64–66. doi:10.1038/nature24291

Barkov, M. V., andPozanenko, A. S. (2011). Model of the extended emission of short gamma-ray bursts. *Mon. Not. R. Astron. Soc.* 417, 2161–2165. doi:10.1111/j.1365-2966.2011.19398.x

Belczynski, K., Perna, R., Bulik, T., Kalogera, V., Ivanova, N., andLamb, D. Q. (2006). A study of compact object mergers as short gamma-ray burst progenitors. *Astrophys. J.* 648, 1110–1116. doi:10.1086/505169

Beniamini, P., Duran, R. B., Petropoulou, M., andGiannios, D. (2020a). Ready, set, launch: time interval between a binary neutron star merger and short gamma-ray burst jet formation. *Astrophys. J.* 895, L33. doi:10.3847/2041-8213/ab9223

Beniamini, P., Granot, J., andGill, R. (2020b). Afterglow light curves from misaligned structured jets. *Mon. Not. R. Astron. Soc.* 493, 3521–3534. doi:10.1093/mnras/staa538

Beniamini, P., andNakar, E. (2019). Observational constraints on the structure of gamma-ray burst jets. mnras 482 (4), 5430–5440. doi:10.1093/mnras/sty3110.

Beniamini, P., Petropoulou, M., Barniol Duran, R., andGiannios, D. (2019). A lesson from GW170817: most neutron star mergers result in tightly collimated successful GRB jets. *Mon. Not. R. Astron. Soc.* 483, 840–851. doi:10.1093/mnras/sty3093

Bromberg, O., Nakar, E., Piran, T., andSari, R. E. (2011). The propagation of relativistic jets in external media. *Astrophys. J.* 740, 100. doi:10.1088/0004-637X/740/2/100

Bromberg, O., Nakar, E., Piran, T., andSari, R. E. (2013). Short versus long and collapsars versus non-collapsars: a quantitative classification of gamma-ray bursts. *Astrophys. J.* 764, 179. doi:10.1088/0004-637X/764/2/179

Bromberg, O., Tchekhovskoy, A., Gottlieb, O., Nakar, E., andPiran, T. (2018). The γ-rays that accompanied GW170817 and the observational signature of a magnetic jet breaking out of NS merger ejecta. *Mon. Not. R. Astron. Soc.* 475, 2971–2977. doi:10.1093/mnras/stx3316

Bucciantini, N., Quataert, E., Arons, J., Metzger, B. D., andThompson, T. A. (2008). Relativistic jets and long-duration gamma-ray bursts from the birth of magnetars. *Mon. Not. R. Astron. Soc. Lett.* 383, L25–L29. doi:10.1111/j.1745-3933.2007.00403.x

Bucciantini, N., Quataert, E., Metzger, B. D., Thompson, T. A., Arons, J., andDel Zanna, L. (2009). Magnetized relativistic jets and long-duration GRBs from magnetar spin-down during core-collapse supernovae. *Mon. Not. R. Astron. Soc.* 396, 2038–2050. doi:10.1111/j.1365-2966.2009.14940.x

Burns, E., Veres, P., Connaughton, V., Racusin, J., Briggs, M.-S., and Christensen, N. (2018). Fermi GBM observations of GRB 150101B: a second nearby event with a short hard spike and a soft tail. *apjl* 863 (2), L34. doi:10.3847/2041-8213/aad813.

Ciolfi, R. (2018). Short gamma-ray burst central engines. *Int. J. Mod. Phys.* 27, 1842004. doi:10.1142/S021827181842004X

Ciolfi, R., andSiegel, D. M. (2015). Short gamma-ray bursts in the "time-reversal" scenario. *Astrophys. J.* 798, L36. doi:10.1088/2041-8205/798/2/L36

Cook, G. B., Shapiro, S. L., andTeukolsky, S. A. (1994). Rapidly rotating polytropes in general relativity. *Astrophys. J.* 422, 227–242. doi:10.1086/173721

Corsi, A., Hallinan, G. W., Lazzati, D., Mooley, K. P., Murphy, E. J., Frail, D. A., et al. (2018). An upper limit on the linear polarization fraction of the GW170817 radio continuum. *Astrophys. J.* 861, L10. doi:10.3847/2041-8213/aacdfd

Coughlin, M. W., andDietrich, T. (2019). Can a black hole-neutron star merger explain GW170817, AT2017gfo, and GRB170817A? *Phys. Rev. D* 100, 043011. doi:10.1103/PhysRevD.100.043011

Coulter, D. A., Foley, R. J., Kilpatrick, C. D., Drout, M. R., Piro, A. L., Shappee, B. J., et al. (2017). Swope Supernova Survey 2017a (SSS17a), the optical counterpart to a gravitational wave source. *Science* 358, 1556–1558. doi:10.1126/science.aap9811

Cowperthwaite, P. S., Berger, E., Villar, V. A., Metzger, B. D., Nicholl, M., Chornock, R., et al. (2017). The electromagnetic counterpart of the binary neutron star merger LIGO/virgo GW170817. II. UV, optical, and near-infrared light curves and comparison to kilonova models. *Astrophys. J.* 848, L17. doi:10.3847/2041-8213/aa8fc7

Dainotti, M. G., Hernandez, X., Postnikov, S., Nagataki, S., O'brien, P., Willingale, R., et al. (2017). A study of the gamma-ray burst fundamental plane. *Astrophys. J.* 848, 88. doi:10.3847/1538-4357/aa8a6b

Dainotti, M. G., Willingale, R., Capozziello, S., Cardone, V. F., andOstrowski, M . (2010). Discovery of a tight correlation for gamma-ray burst afterglows with "canonical" light curves. *Astrophys. J.* 722, L215–L219. doi:10.1088/2041-8205/722/2/L215

D'Avanzo, P., Campana, S., Salafia, O. S., Ghirland, A. G., Ghisellini, G., Melandri, A., et al. (2018). The evolution of the X-ray afterglow emission of GW 170817/GRB 170817A in XMM-Newton observations. *Astron. Astrophys.* 613, L1. doi:10.1051/0004-6361/201832664

De Colle, F., Kumar, P., andAguilera-Dena, D. R. (2018). Radio emission from the cocoon of a GRB jet: implications for relativistic supernovae and off-axis GRB emission. *Astrophys. J.* 863, 1. doi:10.3847/1538-4357/aad04d

Dobie, D., Kaplan, D. L., Murphy, T., Lenc, E., Mooley, K. P., Lynch, C., et al. (2018). A turnover in the radio light curve of GW170817. *Astrophys. J.* 858, L15. doi:10.3847/2041-8213/aac105

Duffell, P. C., Quataert, E., Kasen, D., andKlion, H. (2018). Jet dynamics in compact object mergers: GW170817 likely had a successful jet. *Astrophys. J.* 866, 1. doi:10.3847/1538-4357/aae084

Evans, P. A., Cenko, S. B., Kennea, J. A., Emery, S. W. K., Kuin, N. P. M., Korobkin, O., et al. (2017). SwiftandNuSTARobservations of GW170817: detection of a blue kilonova. *Science* 358, 1565–1570. doi:10.1126/science.aap9580

Finstad, D., De, S., Brown, D. A., Berger, E., andBiwer, C. M. (2018). Measuring the viewing angle of GW170817 with electromagnetic and gravitational waves. *Astrophys. J.* 860, L2. doi:10.3847/2041-8213/aac6c1

Fishman, G. J., andMeegan, C. A. (1995). Gamma-ray bursts. *Annu. Rev. Astron. Astrophys.* 33, 415–458. doi:10.1146/annurev.aa.33.090195.002215

Fong, W., Blanchard, P. K., Alexander, K. D., Strader, J., Margutti, R., Hajela, A., et al. (2019). The optical afterglow of GW170817: an off-axis structured jet and deep constraints on a globular cluster origin. *Astrophys. J.* 883, L1. doi:10.3847/2041-8213/ab3d9e

Fong, W., Berger, E., Blanchard, P. K., Margutti, R., Cowperthwaite, P. S., Chornock, R., et al. (2017). The electromagnetic counterpart of the binary neutron star merger LIGO/virgo GW170817. VIII. A comparison to cosmological short-duration gamma-ray bursts. *Astrophys. J.* 848, L23. doi:10.3847/2041-8213/aa9018

Fong, W., andBerger, E. (2013). The locations of short gamma-ray bursts as evidence for compact object binary progenitors. *Astrophys. J.* 776, 18. doi:10.1088/0004-637X/776/1/18

Fong, W., Berger, E., Margutti, R., andZauderer, B. A. (2015). A decade of short-duration gamma-ray burst broadband Afterglows: energetics, circumburst densities, and jet opening angles. *Astrophys. J.* 815, 102. doi:10.1088/0004-637X/815/2/102

Fraija, N., Colle, F. D., Veres, P., Dichiara, S., Duran, R. B., Galvan-Gamez, A., et al. (2019a). The short GRB 170817A: modeling the off-axis emission and implications on the ejecta magnetization. *Astrophys. J.* 871, 123. doi:10.3847/1538-4357/aaf564

Fraija, N., Pedreira, A. C. C. D. E. S., andVeres, P. (2019b). Light curves of a shock-breakout material and a relativistic off-axis jet from a binary neutron star system. *Astrophys. J.* 871, 200. doi:10.3847/1538-4357/aaf80e

Gehrels, N., Ramirez-Ruiz, E., andFox, D. B. (2009). Gamma-ray bursts in theSwiftEra. *Annu. Rev. Astron. Astrophys.* 47, 567–617. doi:10.1146/annurev.astro.46.060407.145147

Geng, J. J., Zhang, B., Kölligan, A., Kuiper, R., andHuang, Y. F. (2019). Propagation of a short GRB jet in the ejecta: jet launching delay time, jet structure, and GW170817/GRB 170817A. *Astrophys. J.* 877, L40. doi:10.3847/2041-8213/ab224b

Ghirlanda, G., Salafia, O. S., Paragi, Z., Giroletti, M., Yang, J., Marcote, B., et al. (2019). Compact radio emission indicates a structured jet was produced by a binary neutron star merger. *Science* 363, 968–971. doi:10.1126/science.aau8815

Ghirlanda, G., Salafia, O. S., Pescalli, A., Ghisellini, G., Salvaterra, R., Chassande–Mottin, E., et al. (2016). Short gamma-ray bursts at the dawn of the gravitational wave era. *Astron. Astrophys.* 594, A84. doi:10.1051/0004-6361/201628993

Giacomazzo, B., Perna, R., Rezzolla, L., Troja, E., andLazzati, D. (2013). Compact binary progenitors of short gamma-ray bursts. *Astrophys. J.* 762, L18. doi:10.1088/2041-8205/762/2/L18

Gill, R., andGranot, J. (2018). Afterglow imaging and polarization of misaligned structured GRB jets and cocoons: breaking the degeneracy in GRB 170817A. *Mon. Not. R. Astron. Soc.* 478, 4128–4141. doi:10.1093/mnras/sty1214

Gill, R., Granot, J., De Colle, F., andUrrutia, G. (2019a). Numerical simulations of an initially top-hat jet and the afterglow of GW170817/GRB170817A. *Astrophys. J.* 883, 15. doi:10.3847/1538-4357/ab3577

Gill, R., Nathanail, A., andRezzolla, L. (2019b). When did the remnant of GW170817 collapse to a black hole? *Astrophys. J.* 876, 139. doi:10.3847/1538-4357/ab16da

Goldstein, A., Veres, P., Burns, E., Briggs, M. S., Hamburg, R., Kocevski, D., et al. (2017). An ordinary short gamma-ray burst with extraordinary implications: Fermi -GBM detection of GRB 170817A. *Astrophys. J.* 848, L14. doi:10.3847/2041-8213/aa8f41

Gottlieb, O., Nakar, E., Piran, T., andHotokezaka, K. (2018). A cocoon shock breakout as the origin of the γ-ray emission in GW170817. *Mon. Not. R. Astron. Soc.* 479, 588–600. doi:10.1093/mnras/sty1462

Granot, J., De Colle, F., andRamirez-Ruiz, E. (2018a). Off-axis afterglow light curves and images from 2D hydrodynamic simulations of double-sided GRB jets in a stratified external medium. *Mon. Not. R. Astron. Soc.* 481, 2711–2720. doi:10.1093/mnras/sty2454

Granot, J., Gill, R., Guetta, D., andDe Colle, F. (2018b). Off-axis emission of short GRB jets from double neutron star mergers and GRB 170817A. *Mon. Not. R. Astron. Soc.* 481, 1597–1608. doi:10.1093/mnras/sty2308

Granot, J., Guetta, D., andGill, R. (2017). Lessons from the short GRB 170817A: the first gravitational-wave detection of a binary neutron star merger. *Astrophys. J.* 850, L24. doi:10.3847/2041-8213/aa991d

Granot, J., Panaitescu, A., Kumar, P., andWoosley, S. E. (2002). Off-axis afterglow emission from jetted gamma-ray bursts. *Astrophys. J.* 570, L61–L64. doi:10.1086/340991

Haggard, D., Nynka, M., Ruan, J. J., Kalogera, V., Cenko, S. B., Evans, P., et al. (2017). A deep Chandra X-ray study of neutron star coalescence GW170817. *Astrophys. J.* 848, L25. doi:10.3847/2041-8213/aa8ede

Hajela, A., Margutti, R., Alexander, K. D., Kathirgamaraju, A., Baldeschi, A., Guidorzi, C., et al. (2019). Two years of nonthermal emission from the binary neutron star merger GW170817: rapid fading of the jet afterglow and first constraints on the kilonova fastest ejecta. *Astrophys. J.* 886, L17. doi:10.3847/2041-8213/ab5226

Hallinan, G., Corsi, A., Mooley, K. P., Hotokezaka, K., Nakar, E., Kasliwal, M. M., et al. (2017). A radio counterpart to a neutron star merger. *Science* 358, 1579–1583. doi:10.1126/science.aap9855

Hamidani, H., andIoka, K. (2020). Jet propagation in expanding medium for gamma-ray bursts. *arXiv e-prints*.

Hamidani, H., Kiuchi, K., andIoka, K. (2020). Jet propagation in neutron star mergers and GW170817. *Mon. Not. R. Astron. Soc.* 491, 3192–3216. doi:10.1093/mnras/stz3231

Ioka, K., andNakamura, T. (2019). Spectral puzzle of the off-axis gamma-ray burst in GW170817. *Mon. Not. R. Astron. Soc.* 487, 4884–4889. doi:10.1093/mnras/stz1650

Jin, Z.-P., Li, X., Wang, H., Wang, Y.-Z., He, H.-N., Yuan, Q., et al. (2018). Short GRBs: opening angles, local neutron star merger rate, and off-axis events for GRB/GW association. *Astrophys. J.* 857, 128. doi:10.3847/1538-4357/aab76d

Kasen, D., Metzger, B., Barnes, J., Quataert, E., andRamirez-Ruiz, E. (2017). Origin of the heavy elements in binary neutron-star mergers from a gravitational-wave event. *Nature* 551, 80–84. doi:10.1038/nature24453

Kasliwal, M. M., Nakar, E., Singer, L. P., Kaplan, D. L., Cook, D. O., Van Sistine, A., et al. (2017). Illuminating gravitational waves: a concordant picture of photons from a neutron star merger. *Science* 358, 1559–1565. doi:10.1126/science.aap9455

Kathirgamaraju, A., Tchekhovskoy, A., Giannios, D., andBarniol Duran, R. (2019). EM counterparts of structured jets from 3D GRMHD simulations. *Mon. Not. R. Astron. Soc.* 484, L98–L103. doi:10.1093/mnrasl/slz012

Kim, S., Schulze, S., Resmi, L., González-López, J., Higgins, A. B., Ishwara-Chandra, C. H., et al. (2017). ALMA and GMRT constraints on the off-axis gamma-ray burst 170817A from the binary neutron star merger GW170817. *Astrophys. J.* 850, L21. doi:10.3847/2041-8213/aa970b

Kisaka, S., Ioka, K., Kashiyama, K., andNakamura, T. (2018). Scattered short gamma-ray bursts as electromagnetic counterparts to gravitational waves and implications of GW170817 and GRB 170817A. *Astrophys. J.* 867, 39. doi:10.3847/1538-4357/aae30a

Kiuchi, K., Sekiguchi, Y., Shibata, M., andTaniguchi, K. (2010). Exploring binary-neutron-star-merger scenario of short-gamma-ray bursts by gravitational-wave observation. *Phys. Rev. Lett.* 104, 141101. doi:10.1103/PhysRevLett.104.141101

Kouveliotou, C., Meegan, C. A., Fishman, G. J., Bhat, N. P., Briggs, M. S., Koshut, T. M., et al. (1993). Identification of two classes of gamma-ray bursts. *Astrophys. J.* 413, L101. doi:10.1086/186969

Kumar, P., andZhang, B. (2015). The physics of gamma-ray bursts and relativistic jets. *Phys. Rep.* 561, 1–109. doi:10.1016/j.physrep.2014.09.008

Kyutoku, K., Fujibayashi, S., Hayashi, K., Kawaguchi, K., Kiuchi, K., Shibata, M., et al. (2020). On the possibility of GW190425 being a black hole-neutron star binary merger. *Astrophys. J.* 890, L4. doi:10.3847/2041-8213/ab6e70

Lamb, G. P., andKobayashi, S. (2018). GRB 170817A as a jet counterpart to gravitational wave triggerGW 170817. *Mon. Not. R. Astron. Soc.* 478, 733–740. doi:10.1093/mnras/sty1108

Lamb, G. P., Lyman, J. D., Levan, A. J., Tanvir, N. R., Kangas, T., Fruchter, A. S., et al. (2019a). The optical afterglow of GW170817 at one year post-merger. *Astrophys. J.* 870, L15. doi:10.3847/2041-8213/aaf96b

Lamb, G. P., Mandel, I., andResmi, L. (2018). Late-time evolution of afterglows from off-axis neutron star mergers. *Mon. Not. R. Astron. Soc.* 481, 2581–2589. doi:10.1093/mnras/sty2196

Lamb, G. P., Tanvir, N. R., Levan, A. J., Postigo, A. D. U., Kawaguchi, K., Corsi, A., et al. (2019b). Short GRB 160821B: a reverse shock, a refreshed shock, and a well-sampled kilonova. *Astrophys. J.* 883, 48. doi:10.3847/1538-4357/ab38bb

Lasota, J.-P., Haensel, P., andAbramowicz, M. A. (1996). Fast rotation of neutron stars. *Astrophys. J.* 456, 300. doi:10.1086/176650

Lazzati, D., Ciolfi, R., andPerna, R. (2020). Intrinsic properties of the engine and jet that powered the short gamma-ray burst associated with GW170817. *Astrophys. J.* 898, 1–59. doi:10.3847/1538-4357/ab9a44

Lazzati, D., Deich, A., Morsony, B. J., andWorkman, J. C. (2017a). Off-axis emission of short γ-ray bursts and the detectability of electromagnetic counterparts of gravitational-wave-detected binary mergers. *Mon. Not. R. Astron. Soc.* 471, 1652–1661. doi:10.1093/mnras/stx1683

Lazzati, D., López-Cámara, D., Cantiello, M., Morsony, B. J., Perna, R., andWorkman, J. C. (2017b). Off-axis prompt X-ray transients from the cocoon of short gamma-ray bursts. *Astrophys. J.* 848, L6. doi:10.3847/2041-8213/aa8f3d

Lazzati, D., Morsony, B. J., andBegelman, M. C. (2009). Very high efficiency photospheric emission in long-duration γ-ray bursts. *Astrophys. J.* 700, L47–L50. doi:10.1088/0004-637X/700/1/L47

Lazzati, D., andPerna, R. (2019). Jet-cocoon outflows from neutron star mergers: structure, light curves, and fundamental physics. *Astrophys. J.* 881, 89. doi:10.3847/1538-4357/ab2e06

Lazzati, D., Perna, R., Morsony, B. J., Lopez-Camara, D., Cantiello, M., Ciolfi, R., et al. (2018). Late time afterglow observations reveal a collimated relativistic jet in the ejecta of the binary neutron star merger GW170817. *Phys. Rev. Lett.* 120, 241103. doi:10.1103/PhysRevLett.120.241103

Lee, H. K., Wijers, R. A. M. J., andBrown, G. E. (2000). The Blandford-Znajek process as a central engine for a gamma-ray burst. *Phys. Rep.* 325, 83–114. doi:10.1016/S0370-1573(99)00084-8

Lee, W. H., andRamirz-Ruiz, E. (2007). The progenitors of short gamma-ray bursts. *New J. Phys.* 9, 17. doi:10.1088/1367-2630/9/1/017

Lei, W.-H., Zhang, B., andLiang, E.-W. (2013). Hyperaccreting black hole as gamma-ray burst central engine. I. Baryon loading in gamma-ray burst jets. *Astrophys. J.* 765, 125. doi:10.1088/0004-637X/765/2/125

Li, B., Li, L.-B., Huang, Y.-F., Geng, J.-J., Yu, Y.-B., andSong, L.-M. (2018). Continued brightening of the afterglow of GW170817/GRB 170817A as being due to a delayed energy injection. *Astrophys. J.* 859, L3. doi:10.3847/2041-8213/aac2c5

Lin, D.-B., Liu, T., Lin, J., Wang, X.-G., Gu, W.-M., andLiang, E.-W. (2018). First electromagnetic pulse associated with a gravitational-wave event: profile, duration, and delay. *Astrophys. J.* 856, 90. doi:10.3847/1538-4357/aab3d7

Liu, T., Romero, G. E., Liu, M.-L., andLi, A. (2016). Fast radio bursts and their gamma-ray or radio afterglows as kerr-newman black hole binaries. . *apj* 826 (1), 82.. doi:10.3847/0004-637X/826/1/82.

Lü, H.-J., Liang, E.-W., Zhang, B.-B., andZhang, B. (2010). A new classification method for gamma-ray bursts. *Astrophys. J.* 725, 1965–1970. doi:10.1088/0004-637X/725/2/1965

Lucca, M., and Sagunski, L. (2020). The lifetime of binary neutron star merger remnants. *J. High Energy Astrophys.* 27, 33–37. doi:10.1016/j.jheap.2020.04.003.

Lyman, J. D., Lamb, G. P., Levan, A. J., Mandel, I., Tanvir, N. R., Kobayashi, S., et al. (2018). The optical afterglow of the short gamma-ray burst associated with GW170817. *Nat. Astron.* 2, 751–754. doi:10.1038/s41550-018-0511-3

Makhathini, S., Mooley, K. P., Brightman, M., Hotokezaka, K., Nayana, A., Intema, H. T., et al. (2020). The Panchromatic Afterglow of GW170817: the full uniform dataset, modeling, comparison with previous results and implications. arXiv e-prints arXiv:2006.02382.

Mandel, I. (2018). The orbit of GW170817 was inclined by less than 28o to the line of sight. *Astrophys. J.* 853, L12. doi:10.3847/2041-8213/aaa6c1

Margutti, R., Alexander, K. D., Xie, X., Sironi, L., Metzger, B. D., Kathirgamaraju, A., et al. (2018). The binary neutron star event LIGO/virgo GW170817 160 Days after merger: synchrotron emission across the electromagnetic spectrum. *Astrophys. J.* 856, L18. doi:10.3847/2041-8213/aab2ad

Margutti, R., Berger, E., Fong, W., Guidorzi, C., Alexander, K. D., Metzger, B. D., et al. (2017). The electromagnetic counterpart of the binary neutron star merger LIGO/virgo GW170817. V. Rising X-ray emission from an off-axis jet. *Astrophys. J.* 848, L20. doi:10.3847/2041-8213/aa9057

Matsumoto, T., Nakar, E., andPiran, T. (2019). Constraints on the emitting region of the gamma-rays observed in GW170817. *Mon. Not. R. Astron. Soc.* 483, 1247–1255. doi:10.1093/mnras/sty3200

Matzner, C. D. (2003). Supernova hosts for gamma-ray burst jets: dynamical constraints. *Mon. Not. R. Astron. Soc.* 345, 575–589. doi:10.1046/j.1365-8711.2003.06969.x

Meegan, C., Lichti, G., Bhat, P. N., Bissaldi, E., Briggs, M. S., Connaughton, V., et al. (2009). Thefermigamma-ray burst monitor. *Astrophys. J.* 702, 791–804. doi:10.1088/0004-637X/702/1/791

Meng, Y.-Z., Geng, J.-J., Zhang, B.-B., Wei, J.-J., Xiao, D., Liu, L.-D., et al. (2018). The origin of the prompt emission for short GRB 170817A: photosphere emission or synchrotron emission? *Astrophys. J.* 860, 72. doi:10.3847/1538-4357/aac2d9

Mészáros, P. (2002). Theories of gamma-ray bursts. *Annu. Rev. Astron. Astrophys.* 40, 137–169. doi:10.1146/annurev.astro.40.060401.093821

Mészáros, P., andRees, M. J. (1997). Optical and long-wavelength afterglow from gamma-ray bursts. *Astrophys. J.* 476, 232–237. doi:10.1086/303625

Metzger, B. D., andBerger, E. (2012). What is the most promising electromagnetic counterpart of a neutron star binary merger? *Astrophys. J.* 746, 48. doi:10.1088/0004-637X/746/1/48

Metzger, B. D., Giannios, D., Thompson, T. A., Bucciantini, N., andQuataert, E. (2011). The protomagnetar model for gamma-ray bursts. *Mon. Not. R. Astron. Soc.* 413, 2031–2056. doi:10.1111/j.1365-2966.2011.18280.x

Metzger, B. D., Thompson, T. A., andQuataert, E. (2018). A magnetar origin for the kilonova ejecta in GW170817. *Astrophys. J.* 856, 101. doi:10.3847/1538-4357/aab095

Mooley, K. P., Deller, A. T., Gottlieb, O., Nakar, E., Hallinan, G., Bourke, S., et al. (2018a). Superluminal motion of a relativistic jet in the neutron-star merger GW170817. *Nature* 561, 355–359. doi:10.1038/s41586-018-0486-3

Mooley, K. P., Frail, D. A., Dobie, D., Lenc, E., Corsi, A., De, K., et al. (2018b). A strong jet signature in the late-time light curve of GW170817. *Astrophys. J.* 868, L11. doi:10.3847/2041-8213/aaeda7

Mooley, K. P., Nakar, E., Hotokezaka, K., Hallinan, G., Corsi, A., Frail, D. A., et al. (2018c). A mildly relativistic wide-angle outflow in the neutron-star merger event GW170817. *Nature* 554, 207–210. doi:10.1038/nature25452

Morsony, B. J., Lazzati, D., andBegelman, M. C. (2007). Temporal and angular properties of gamma-ray burst jets emerging from massive stars. *Astrophys. J.* 665, 569–598. doi:10.1086/519483

Murguia-Berthier, A., Montes, G., Ramirez-Ruiz, E., De Colle, F., andLee, W. H. (2014). Necessary conditions for short gamma-ray burst production in binary neutron star mergers. *Astrophys. J.* 788, L8. doi:10.1088/2041-8205/788/1/L8

Murguia-Berthier, A., Ramirez-Ruiz, E., De Colle, F., Janiuk, A., Rosswog, S., andLee, W. H. (2020). The fate of the merger remnant in GW170817 and its imprint on the jet structure. *arXiv e-prints*.

Murguia-Berthier, A., Ramirez-Ruiz, E., Kilpatrick, C. D., Foley, R. J., Kasen, D., Lee, W. H., et al. (2017a). A neutron star binary merger model for GW170817/GRB 170817A/SSS17a. *Astrophys. J.* 848, L34. doi:10.3847/2041-8213/aa91b3

Murguia-Berthier, A., Ramirez-Ruiz, E., Montes, G., De Colle, F., Rezzolla, L., Rosswog, S., et al. (2017b). The properties of short gamma-ray burst jets triggered by neutron star mergers. *Astrophys. J.* 835, L34. doi:10.3847/2041-8213/aa5b9e

Nagakura, H., Hotokezaka, K., Sekiguchi, Y., Shibata, M., andIoka, K. (2014). Jet collimation in the ejecta of double neutron star mergers: a new canonical picture of short gamma-ray bursts. *Astrophys. J.* 784, L28. doi:10.1088/2041-8205/784/2/L28

Nakar, E., Gal-Yam, A., andFox, D. B. (2006). The local rate and the progenitor lifetimes of short-hard gamma-ray bursts: synthesis and predictions for the laser interferometer gravitational-wave observatory. *Astrophys. J.* 650, 281–290. doi:10.1086/505855

Nakar, E., Gottlieb, O., Piran, T., Kasliwal, M. M., andHallinan, G. (2018). From γ to radio: the electromagnetic counterpart of GW170817. *Astrophys. J.* 867, 18. doi:10.3847/1538-4357/aae205

Nakar, E., andPiran, T. (2018). Implications of the radio and X-ray emission that followed GW170817. *Mon. Not. R. Astron. Soc.* 478, 407–415. doi:10.1093/mnras/sty952

Nakar, E., andSari, R. E. (2012). Relativistic shock breakouts-a variety of gamma-ray flares: from low-luminosity gamma-ray bursts to type ia supernovae. *Astrophys. J.* 747, 88. doi:10.1088/0004-637X/747/2/88

Norris, J. P., andBonnell, J. T. (2006). Short gamma-ray bursts with extended emission. *Astrophys. J.* 643, 266–275. doi:10.1086/502796

Norris, J. P., Gehrels, N., andScargle, J. D. (2010). Threshold for extended emission in short gamma-ray bursts. *Astrophys. J.* 717, 411–419. doi:10.1088/0004-637X/717/1/411

Nousek, J. A., Kouveliotou, C., Grupe, D., Page, K. L., Granot, J., Ramirez-Ruiz, E., et al. (2006). Evidence for a canonical gamma-ray burst afterglow light curve in theSwiftXRT data. *Astrophys. J.* 642, 389–400. doi:10.1086/500724

Nynka, M., Ruan, J. J., Haggard, D., andEvans, P. A. (2018). Fading of the X-ray afterglow of neutron star merger GW170817/GRB 170817A at 260 days. *Astrophys. J.* 862, L19. doi:10.3847/2041-8213/aad32d

Oganesyan, G., Ascenzi, S., Branchesi, M., Salafia, O. S., Dall'Osso, S., andGhirlanda, G. (2020). Structured jets and X-ray plateaus in gamma-ray burst phenomena. *Astrophys. J.* 893, 88. doi:10.3847/1538-4357/ab8221

Parsotan, T., López-Cámara, D., andLazzati, D. (2018). Photospheric emission from variable engine gamma-ray burst simulations. *Astrophys. J.* 869, 103. doi:10.3847/1538-4357/aaeed1

Perna, R., Lazzati, D., andGiacomazzo, B. (2016). Short gamma-ray bursts from the merger of two black holes. *Astrophys. J.* 821, L18. doi:10.3847/2041-8205/821/1/L18

Pian, E., D'Avanzo, P., Benetti, S., Branchesi, M., Brocato, E., Campana, S., et al. (2017). Spectroscopic identification of r-process nucleosynthesis in a double neutron-star merger. *Nature* 551, 67–70. doi:10.1038/nature24298

Piran, T. (1999). Gamma-ray bursts and the fireball model. *Phys. Rep.* 314, 575–667. doi:10.1016/S0370-1573(98)00127-6

Piro, L., Troja, E., Zhang, B., Ryan, G., van Eerten, H., Ricci, R., et al. (2019). A long-lived neutron star merger remnant in GW170817: constraints and clues from X-ray observations. *Mon. Not. R. Astron. Soc.* 483, 1912–1921. doi:10.1093/mnras/sty3047

Pooley, D., Kumar, P., Wheeler, J. C., andGrossan, B. (2018). GW170817 most likely made a black hole. *Astrophys. J.* 859, L23. doi:10.3847/2041-8213/aac3d6

Pozanenko, A. S., Barkov, M. V., Minaev, P. Y., Volnova, A. A., Mazaeva, E. D., Moskvitin, A. S., et al. (2018). GRB 170817A associated with GW170817: multi-frequency observations and modeling of prompt gamma-ray emission. *Astrophys. J.* 852, L30. doi:10.3847/2041-8213/aaa2f6

Ramirez-Ruiz, E., Celotti, A., andRees, M. J. (2002). Events in the life of a cocoon surrounding a light, collapsar jet. *Mon. Not. R. Astron. Soc.* 337, 1349–1356. doi:10.1046/j.1365-8711.2002.05995.x

Resmi, L., Schulze, S., Ishwara-Chandra, C. H., Misra, K., Buchner, J., Pasquale, M. D., et al. (2018). Low-frequency view of GW170817/GRB 170817A with the giant metrewave radio telescope. *Astrophys. J.* 867, 57. doi:10.3847/1538-4357/aae1a6

Ruan, J. J., Nynka, M., Haggard, D., Kalogera, V., andEvans, P. (2018). Brightening X-ray emission from GW170817/GRB 170817A: further evidence for an outflow. *Astrophys. J.* 853, L4. doi:10.3847/2041-8213/aaa4f3

Ruiz, M., Lang, R. N., Paschalidis, V., andShapiro, S. L. (2016). Binary neutron star mergers: a jet engine for short gamma-ray bursts. *Astrophys. J.* 824, L6. doi:10.3847/2041-8205/824/1/L6

Salafia, O. S., Barbieri, C., Ascenzi, S., andToffano, M. (2020). Gamma-ray burst jet propagation, development of angular structure, and the luminosity function. *Astron. Astrophys.* 636, A105. doi:10.1051/0004-6361/201936335

Salafia, O. S., Ghirlanda, G., Ascenzi, S., andGhisellini, G. (2019). On-axis view of GRB 170817A. *Astron. Astrophys.* 628, A18. doi:10.1051/0004-6361/201935831

Salafia, O. S., Ghisellini, G., Ghirlanda, G., andColpi, M. (2018). Interpreting GRB170817A as a giant flare from a jet-less double neutron star merger. *Astron. Astrophys.* 619, A18. doi:10.1051/0004-6361/201732259

Sari, R. E., Piran, T., andNarayan, R. (1998). Spectra and light curves of gamma-ray burst afterglows. *Astrophys. J.* 497, L17–L20. doi:10.1086/311269

Savchenko, V., Ferrigno, C., Kuulkers, E., Bazzano, A., Bozzo, E., Brandt, S., et al. (2017). INTEGRAL detection of the first prompt gamma-ray signal coincident with the gravitational-wave event GW170817. *Astrophys. J.* 848, L15. doi:10.3847/2041-8213/aa8f94

Schutz, B. F. (2011). Networks of gravitational wave detectors and three figures of merit. *Class. Quantum Gravity.* 28, 125023. doi:10.1088/0264-9381/28/12/125023

Shoemaker, I. M., andMurase, K. (2018). Constraints from the time lag between gravitational waves and gamma rays: implications of GW170817 and GRB 170817A. *Phys. Rev. D* 97, 083013. doi:10.1103/PhysRevD.97.083013

Siebert, M. R., Foley, R. J., Drout, M. R., Kilpatrick, C. D., Shappee, B. J., Coulter, D. A., et al. (2017). The unprecedented properties of the first electromagnetic counterpart to a gravitational-wave source. *Astrophys. J.* 848, L26. doi:10.3847/2041-8213/aa905e

Smartt, S. J., Chen, T. W., Jerkstrand, A., Coughlin, M., Kankare, E., Sim, S. A., et al. (2017). A kilonova as the electromagnetic counterpart to a gravitational-wave source. *Nature* 551, 75–79. doi:10.1038/nature24303

Soares-Santos, M., Holz, D. E., Annis, J., Chornock, R., Herner, K., Berger, E., et al. (2017). The electromagnetic counterpart of the binary neutron star merger LIGO/virgo GW170817. I. Discovery of the optical counterpart using the dark energy camera. *Astrophys. J.* 848, L16. doi:10.3847/2041-8213/aa9059

Tanvir, N. R., Levan, A. J., González-Fernández, C., Korobkin, O., Mandel, I., Rosswog, S., et al. (2017). The emergence of a lanthanide-rich kilonova following the merger of two neutron stars. *Astrophys. J.* 848, L27. doi:10.3847/2041-8213/aa90b6

Takahashi, K., andIoka, K. (2020a). Diverse jet structures consistent with the off-axis afterglow of GRB 170817A. *arXiv e-prints*.

Takahashi, K., andIoka, K. (2020b). Inverse reconstruction of jet structure from off-axis gamma-ray burst afterglows. *mnras*. 497 (1), 1217–1235. doi:10.1093/mnras/staa1984.

Troja, E., Castro-Tirado, A. J., González, J. B., Hu, Y., Ryan, G. S., Cenko, S. B., et al. (2019a). The afterglow and kilonova of the short GRB 160821B. *Mon. Not. R. Astron. Soc.* 489, 2104–2116. doi:10.1093/mnras/stz2255

Troja, E., Piro, L., Ryan, G., van Eerten, H., Ricci, R., Wieringa, M. H., et al. (2018a). The outflow structure of GW170817 from late-time broad-band observations. *Mon. Not. R. Astron. Soc.* 478, L18–L23. doi:10.1093/mnrasl/sly061

Troja, E., Piro, L., van Eerten, H., Wollaeger, R. T., Im, M., Fox, O. D., et al. (2017). The X-ray counterpart to the gravitational-wave event GW170817. *Nature* 551, 71–74. doi:10.1038/nature24290

Troja, E., Ryan, G., Piro, L., van Eerten, H., Cenko, S. B., Yoon, Y., et al. (2018b). A luminous blue kilonova and an off-axis jet from a compact binary merger at z = 0.1341. *Nat. Commun.* 9, 4089. doi:10.1038/s41467-018-06558-7

Troja, E., van Eerten, H., Ryan, G., Ricci, R., Burgess, J. M., Wieringa, M. H., et al. (2019b). A year in the life of GW170817: the rise and fall of a structured jet from a binary neutron star merger. *Mon. Not. R. Astron. Soc.* 489, 1919–1926. doi:10.1093/mnras/stz2248

Valenti, S., Sand, D. J., Yang, S., Cappellaro, E., Tartaglia, L., Corsi, A., et al. (2017). The discovery of the electromagnetic counterpart of GW170817: kilonova at 2017gfo/DLT17ck. *Astrophys. J.* 848, L24. doi:10.3847/2041-8213/aa8edf

van Paradijs, J., Kouveliotou, C., andWijers, R. A. M. J. (2000). Gamma-ray burst afterglows. *Annu. Rev. Astron. Astrophys.* 38, 379–425. doi:10.1146/annurev.astro.38.1.379

Veres, P., Mészáros, P., Goldstein, A., Fraija, N., Connaughton, V., Burns, E., et al. (2018). Gamma-ray burst models in light of the GRB 170817A - GW170817 connection. arXiv e-prints arXiv:1802.07328.

Vietri, M., andStella, L. (1998). A gamma-ray burst model with small baryon contamination. *Astrophys. J.* 507, L45–L48. doi:10.1086/311674

Villar, V. A., Cowperthwaite, P. S., Berger, E., Blanchard, P. K., Gomez, S., Alexander, K. D., et al. (2018). Spitzer Space telescope infrared observations of the binary neutron star merger GW170817. *Astrophys. J.* 862, L11. doi:10.3847/2041-8213/aad281

von Kienlin, A., Veres, P., Roberts, O.-J., Hamburg, R., Bissaldi, E. et al. (2019). Fermi-GBM GRBs with Characteristics Similar to GRB 170817A. *apj* 876 (1), 89. doi:10.3847/1538-4357/ab10d8.

Woosley, S. E. (1993). Gamma-ray bursts from stellar mass accretion disks around black holes. *Astrophys. J.* 405, 273. doi:10.1086/172359

Woosley, S. E., andBloom, J. S. (2006). The supernova-gamma-ray burst connection. *Annu. Rev. Astron. Astrophys.* 44, 507–556. doi:10.1146/annurev.astro.43.072103.150558

Woosley, S. E., andHeger, A. (2006). The progenitor stars of gamma-ray bursts. *Astrophys. J.* 637, 914–921. doi:10.1086/498500

Wu, Y., andMacFadyen, A. (2018). Constraining the outflow structure of the binary neutron star merger event GW170817/GRB170817A with a Markov chain Monte Carlo analysis. *Astrophys. J.* 869, 55. doi:10.3847/1538-4357/aae9de

Xiao, D., Liu, L.-D., Dai, Z.-G., andWu, X.-F. (2017). Afterglows and kilonovae associated with nearby low-luminosity short-duration gamma-ray bursts: application to GW170817/GRB 170817A. *Astrophys. J.* 850, L41. doi:10.3847/2041-8213/aa9b2b

Xie, X., Zrake, J., andMacFadyen, A. (2018). Numerical simulations of the jet dynamics and synchrotron radiation of binary neutron star merger event GW170817/GRB 170817A. *Astrophys. J.* 863, 58. doi:10.3847/1538-4357/aacf9c

Yamazaki, R., Ioka, K., andNakamura, T. (2018). Prompt emission from the counter jet of a short gamma-ray burst. Prog. *Theor. Exp. Phys*. 2018 (3), 033E01 doi:10.1093/ptep/pty012.

Yamazaki, R., Ioka, K., andNakamura, T. (2020). X-ray flashes from off-axis gamma-ray bursts. *apjl* 571 (1), L31–L35. doi:10.1086/341225.

Yamazaki, R., Yonetoku, D., andNakamura, T. (2003). An off-axis jet model for GRB 980425 and low-energy gamma-ray bursts. *apjl* 594 (2), L79–L82. doi:10.1086/378736.

Yoon, S.-C., Langer, N., andNorman, C. (2006). Single star progenitors of long gamma-ray bursts. *Astron. Astrophys.* 460, 199–208. doi:10.1051/0004-6361:20065912

Zhang, B. (2016). Mergers of charged black holes: gravitational-wave events, short gamma-ray bursts, and fast radio bursts. *Astrophys. J.* 827, L31. doi:10.3847/2041-8205/827/2/L31

Zhang, B. (2019). The delay time of gravitational wave–gamma-ray burst associations. *Front. Phys.* 14, 64402. doi:10.1007/s11467-019-0913-4

Zhang, B.-B., Zhang, B., Sun, H., Lei, W.-H., Gao, H., Li, Y., et al. (2018). A peculiar low-luminosity short gamma-ray burst from a double neutron star merger progenitor. *Nat. Commun.* 9, 447. doi:10.1038/s41467-018-02847-3

Zou, Y.-C., Wang, F.-F., Moharana, R., Liao, B., Chen, W., Wu, Q., et al. (2018). Determining the Lorentz factor and viewing angle of GRB 170817A. *Astrophys. J.* 852 L1. doi:10.3847/2041-8213/aaa123

Conflict of Interest: The authors declare that the research was conducted in the absence of any commercial or financial relationships that could be construed as a potential conflict of interest.

frontiers in Physics

REVIEW
published: 28 October 2020
doi: 10.3389/fphy.2020.00355

The Physics of Kilonovae

*Jennifer Barnes**

Department of Physics and Columbia Astrophysics Laboratory, Columbia University, New York, NY, United States

The science returns of gravitational wave astronomy will be maximized if electromagnetic counterparts to gravitational-wave sources can be identified. Kilonovae are promising counterparts to compact binary mergers, both because their long timescales and approximately isotropic emission make them relatively easy to observe, and because they offer astronomers a unique opportunity to probe astrophysical heavy-element nucleosynthesis and merger-driven mass ejection. In the following, I review progress in theoretical modeling that underpinned advances in our understanding of kilonovae leading up the first detection of a neutron star merger, GW170817. I then review the important lessons from this event and discuss the challenges and opportunities that await us in the future.

Keywords: gravitational wave astronomy, kilonovae, kilonovae: TNS 2017 gfo, DLT17ck, SSS17a, r-process nucleosynthesis, neutron star binaries

OPEN ACCESS

Edited by:
Rosalba Perna,
Stony Brook University, United States

Reviewed by:
Anthony Piro,
Carnegie Observatories (CIS), United States
Sayantan Choudhury,
Max Planck Institute for Gravitational Physics (AEI), Germany

***Correspondence:**
Jennifer Barnes
jlb2331@columbia.edu

Specialty section:
This article was submitted to Cosmology, a section of the journal Frontiers in Physics

Received: *20 March 2020*
Accepted: *27 July 2020*
Published: *28 October 2020*

Citation:
Barnes J (2020) The Physics of Kilonovae. Front. Phys. 8:355. doi: 10.3389/fphy.2020.00355

1. INTRODUCTION

Multi-messenger astronomy refers to the revolutionary possibility of combining electromagnetic (EM) and gravitational-wave (GW) observations to gain new insight into astrophysical phenomena. In the current era of ground-based gravitational-wave detectors, the mergers of compact objects—black holes (BHs) and neutron stars (NSs)—are the systems most accessible to multi-messenger astronomy, and their routine observation promises to teach us more about stellar binary evolution, dynamics in the strong gravity regime, the production and evolution of astrophysical jets, the NS equation of state (EOS), and the origin of the heavy elements. Among mergers' EM counterparts, "kilonovae," radioactively-powered, quasi-isotropic transients that shine at optical and infrared wavelengths and evolve on timescales of days to weeks, are unique in their ability to shed light on merger-driven mass ejection and nucleosynthesis.

2. BACKGROUND ON *R*-PROCESS TRANSIENTS

The idea that compact object mergers produce radioactively-powered EM emission in addition to gravitational wave signals is rooted in the realization [1–3] that mergers could synthesize unstable nuclei whose decays would power an electromagnetic transient [4].

More specifically, the partial disruption of a NS in a NS^2 or NSBH merger produces a neutron-rich outflow capable of assembling a broad range of heavy, unstable nuclei via rapid neutron capture, or the *r*-process. As first outlined by [5] and [6], the *r*-process occurs in explosive environments featuring a high flux of free neutrons, which allows successive captures of free neutrons onto light seed nuclei on timescales shorter than typical β-decay lifetimes. This drives the composition of the gas toward heavy, neutron-rich regions of the chart of the nuclides, in many cases close to the neutron drip line. When neutron capture ceases, the newly-born nuclei decay toward stability, producing an abundance pattern with characteristic peaks around mass numbers $A = 82, 130, 196$. The stable and long-lived daughters account for about half of the elements in the Periodic Table more massive than Iron.

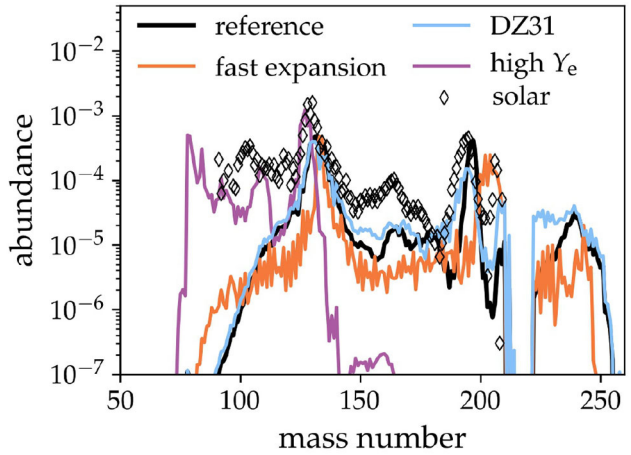

FIGURE 1 | The impact of nuclear physics and astrophysical uncertainties on predicted *r*-process abundances. The reference case (black curve) was calculated using the FRDM mass model [15] for a low-entropy, neutron-rich gas. Every other curve differs from the reference case in only one way. The **orange** curve shows the impact of decreasing the expansion time, while the purple curve demonstrates the much stronger effect of raising Y_e. The influence of the choice of nuclear mass model is illustrated by the **light blue** curve. **Scaled solar *r*-process abundances from [16] are plotted as black diamonds.** This figure was adapted from Figure 1 of [17] with permission from J. Barnes.

The complexity of *r*-process nucleosynthesis allows for variation in the final abundance pattern. While a lack of relevant experimental data (e.g., nuclear masses and neutron-capture cross sections) for many nuclei involved in the *r*-process present a challenge for theoretical *r*-process simulations [7, 8], even if nuclear physics uncertainties were eliminated, abundance yields would still be sensitive to conditions when nucleosynthesis begins. Traditionally [9, e.g.], gasses with the potential to undergo an *r*-process have been parametrized in terms of three variables: expansion timescale ($\tau_{\rm exp}$), entropy per baryon ($s_{\rm B}$), and initial electron fraction (Y_e), which is defined as the number of protons per baryon and quantifies the relative number of free neutrons available to build up heavy nuclei.

The final abundance pattern depends on the interplay of all these factors [e.g., [10]]. However, for conditions expected for compact object mergers (i.e., neutron-rich, low-entropy gasses), abundances appear from simulations to be particularly sensitive to Y_e, with $Y_e \approx 0.25$ emerging as a threshold above which the *r*-process fails to burn nuclei beyond the second *r*-peak [11, 12]. Such a truncated *r*-process is termed a "light" *r*-process, as opposed to the "heavy" *r*-process, which takes place under very neutron-rich conditions and synthesizes stable and semi-stable nuclei up to $A \sim 260$. In a merger, the NS material that forms the expanding gas is very neutron rich [13], and will remain so unless weak-current interactions are strong enough to push the composition toward a more moderate Y_e [14]. The potential for *r*-process variability is illustrated in **Figure 1**.

The role of *r*-process nucleosynthesis and decay in generating EM signals associated with compact object mergers was first discussed by [4], who derived the earliest theoretical model of *r*-process-powered transient emission. Since this groundbreaking work, the community has undertaken increasingly detailed studies of all the major parameters governing the nature of *r*-process transients, from the energy supplied by the *r*-process, to the ejected mass, to the optical properties of *r*-process atoms and ions.

3. KEY PARAMETERS

While detailed computational models are required to fully explain the evolution of radioactive astrophysical transients, the basic character of these systems are functions of a few physical parameters whose relationships to the emission can be understood from basic physical principles.

In simple (semi-)analytic models [à la, [18]], a transient's luminosity peaks when the expansion time t equals the timescale for photons to diffuse through the ejecta, $t_{\rm diff} \propto (M_{\rm ej}\kappa/v)^{1/2}$, where $M_{\rm ej}$ and $v_{\rm ej}$ are the mass and characteristic velocity of the ejecta, respectively, and κ is its effective opacity. The luminosity at peak is roughly equivalent to the instantaneous rate at which radioactive decay is heating the ejecta. This correspondence reappears on the tail of the light curve, when the ejecta is mostly transparent and the luminosity directly reflects radioactive heating. Consideration of the above reveals that the energy released (per unit mass) in the radioactive decays of *r*-process nuclei is a crucial determinant of kilonova emission, as are the mass, velocity, and opacity of merger-driven outflows. The effects of these parameters on kilonovae's bolometric light curves **are** presented in **Figure 2**.

3.1. *R*-Process Heating and Radioactivity

The dominant decay channel for unstable *r*-process nuclei is β-decay [$(Z,N) \rightarrow (Z{+}1,N{-}1)$; 20], which emits high-energy β-particles, neutrinos, and γ-rays. In most realizations of the *r*-process, select nuclei will also undergo α-decay ($(Z,N) \rightarrow (Z{-}2,N{-}2)$) and fission, releasing energy in the form of more massive α-particles and fission fragments. [17, 21–23]. These suprathermal particles and photons transfer heat the ejecta as they interact with it, and the thermal photons produced by the heated gas diffuse outward to form the light curve. The emerging luminosity, as well as the relationship between luminosity and ejected mass, depend both on the rate at which the *r*-process produces energy and the efficiency with which that energy is converted to thermal photons.

When [4] constructed the first kilonova models, they treated the overall normalization of energy from *r*-process decay as a free parameter proportional to the rest mass energy of the ejected material. In other words, the sum of all the energy released from radioactivity was taken to equal $fM_{\rm ej}c^2$, with f allowed to vary. Despite this simplification, their model of the *r*-process uncovered what turned out to be a robust feature of *r*-process radioactivity. By assuming the lifetimes τ of decaying nuclei were evenly distributed logarithmically and ignoring the correlation between τ and decay energy, Li et al. [4] calculated that *r*-process decay should release energy like $\dot{E}_{\rm rad} \propto 1/t$. More rigorous calculations using full *r*-process nuclear reaction networks [20,

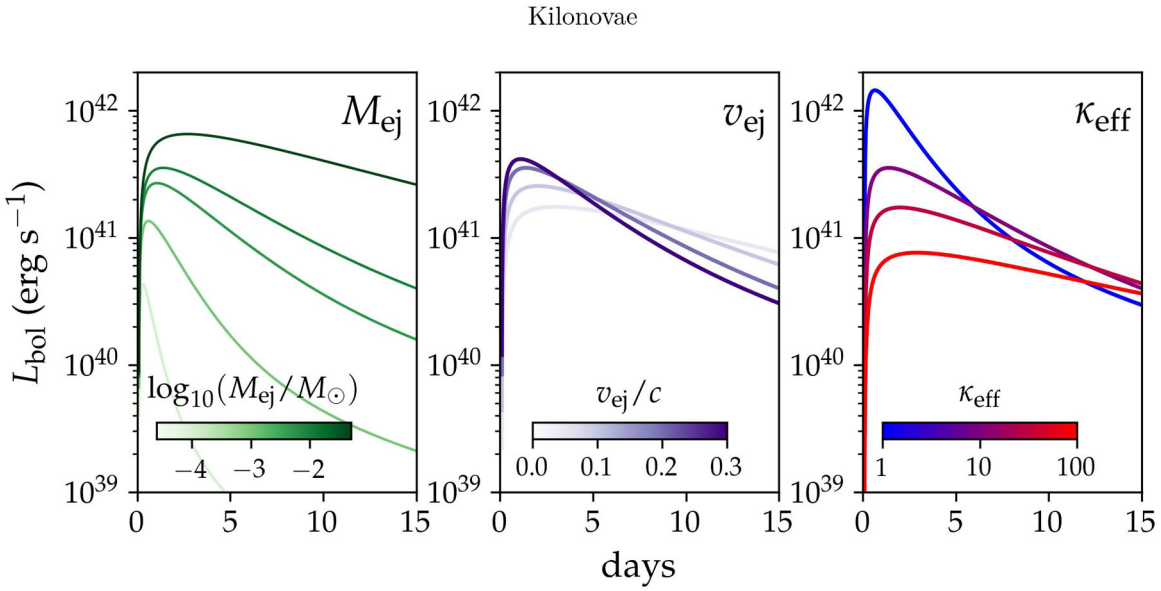

FIGURE 2 | Toy-model bolometric kilonova light curves, similar to those of [19], illustrating the effects of ejecta mass **(left)**, velocity **(middle)**, opacity **(right)** on emission. *R*-process heating has been approximated as a simple power law with $\zeta = 1.3$. In the middle and right panels, $M_{\rm ej}$ is set to $0.01M_\odot$. The value of $\kappa_{\rm eff}$ is 10 cm^2 g^{-1} in the left and middle panels, and $v_{\rm ej}$ is $0.2c$ in the left and right panels. Thermalization has been estimated from the numerical results of [17].

24, 25] as well as more robust analytic treatments [26] modified this picture, finding that, when heating is dominated by the β-decays of a broad ensemble of nuclei, the energy production is well-approximated by a steeper power-law, $\dot{E}_{\rm rad} \propto t^{-\zeta}$ with $\zeta = 1.2 - 1.4$.

However, while power-law heating is a useful model, uncertainties in *r*-process calculations resulting from unmeasured quantities, as well as the sensitivity of the *r*-process to its astrophysical environment, leave room for variability in nucleosynthesis and decay, and therefore $\dot{E}_{\rm rad}$. In particular, the behavior of $\dot{E}_{\rm rad}$ is likely to deviate from a power-law if α-decay or fission becomes dominant over β-decay, or if only a small number of nuclei are contributing to the heating [22, 23, 27].

More detailed nuclear calculations also revealed the absolute scale of the energy released by *r*-process decay, allowing [20] to predict that the peak luminosity of transients from NS^2 mergers would be about a thousand time brighter than a classical nova, motivating the term "kilonova."

Metzger et al. [20] was also the first to estimate the fraction of the energy from *r*-process decay able to effectively heat the gas (the "thermalization fraction"). More detailed numerical work on thermalization was carried out by [17], who found that thermalization increased for denser ejecta configurations, lower-energy decay spectra, and radioactivity profiles that favored α-decay or fission relative to β-decay. These themes were revisted in [28]. Later analytic work [27, 29], showed that thermalization also depends on how the decay spectrum and $\dot{E}_{\rm rad}$ evolve with time. The potential variation in *r*-process heating [see e.g., [23]], and the sensitivity of the thermalization efficiency to that variation, suggest that further detailed numerical studies may be useful for understanding the true allowed range of kilonova heating and luminosity.

3.2. Mass Ejection

There are three main channels through which merging compact objects ejecta mass [see reviews by [30, 31]]. All produce an outflow neutron rich enough to support at least a light *r*-process.

High-velocity *tidally shredded* outflows are produced during the final stages of inspiral when a NS is disrupted by the differential gravitational field of its binary companion. While the quantity of ejected mass depends on the NS EOS (less compact EOSs are more easily shredded) as well as the mass ratio of the binary and the spins of the component stars [32–35], it is generally expected to be small [$\sim 10^{-4} M_\odot$; [36, 37]] for a NS^2 merger, though it can be substantially larger ($\sim 0.1 M_\odot$) for a NSBH merger provided the NS disrupts outside the innermost stable circular orbit [38, 39]. Tidal shredding produces a cold, low-entropy outflow with an abundance of free neutrons. It is therefore expected to undergo a robust *r*-process with nucleosynthesis beyond the third peak [e.g., [13]].

In contrast, *dynamically squeezed* matter is subject to enough weak interactions to inhibit the synthesis of the heaviest elements. Dynamical squeezing occurs when merging NSs finally collide [36, 37, 40]. The violence of the collision expels material from the contact interface via shocks, which accelerate the resulting outflow to high velocities and heat it to high temperatures, allowing the production of thermal electron/positron pairs and neutrinos. Absorption of these particles then raises the $Y_{\rm e}$ of the gas [41, 42].

The mass of this component increases with NS compactness [36], since NSs with smaller radii make contact at a smaller separation, and therefore a higher velocity, leading to more energetic collisions capable of unbinding more matter (this trend holds only up to a point; mass ejection is minimal if the colliding NSs are compact enough to collapse promptly to a BH [43], though mass asymmetry can offset this effect [37]).

Some simulations [36, 44] suggest that, in certain cases, this outflow will feature a high-velocity, low-mass ($\sim 10^{-5} M_\odot$) tail of material whose rapid expansion hinders neutron capture, resulting in a composition dominated by lighter nuceli and leftover free neutrons [21]. Under such conditions, the free-neutron decay could power a short-lived transient peaking on timescales close to the free-neutron half life [45].

The most robust mass ejection channel may be ***winds from accretion disks*** surrounding the mergers' central remnants (CRs). In NSBH mergers, the disk is formed from disrupted NS matter that remains gravitationally bound. For NS^2 mergers, the primary source of disk material is a NS CR, which pushes material off its surface as it transitions from differential to solid-body rotation [46] (The prompt collapse of a CR therefore inhibits disk formation for NS^2 mergers.) Disk material is unbound through some combination of viscous heating [47], magnetic turbulence [48], α-recombination [49], and ν-absorption [50, 51].

The effect of weak interactions on the disk composition is uncertain, and likely depends strongly on the CR. While a central NS would be strong source of neutrinos [e.g., [52]], a central BH would not be; in the latter case, weak interactions in the disk would be limited to those driven by thermal neutrinos and positrons produced by the disk itself [53]. Many studies [48, 54, 55] have found that, for a BH CR, the accretion disk regulates its composition to a low Y_e, though the exact distribution of Y_e appears to be sensitive to the neutrino transport method adopted [e.g., [56]].

As with other mass ejection methods, the mass of the disk (and therefore the disk wind) depends on the binary parameters and NS EOS [e.g., [40]]. Less compact NS EOSs produce more massive disks, and therefore more massive disk outflows. The EOS also affects the composition (at least for NS^2 mergers) by controlling the fate of the CR, and the exposure of the disk to neutrino irradiation [57–59].

3.3. Opacity

The distinct compositions burned in the various outflows generated in NS^2 and NSBH mergers have major effects on kilonova emission because the composition of the gas determines the opacity of the ejecta, which in turn influences the light curve and the spectral energy distribution (SED).

As the gas expands, it cools to temperatures ($\sim$few $\times 10^3$ K) that support low levels of ionization. Under these conditions, the dominant source of opacity is bound-bound ("line") opacity [60]. In the bound-bound regime, the absorption of photons by atoms results not in ionization, but in the excitation of its bound electrons to a higher-energy configuration. While the probability that any *particular* absorption will occur is a function of the many-body quantum mechanics governing the absorbing atom, the effective *continuum* opacity depends on the number of opportunities for a photon of a given energy to suffer an absorption—i.e., on the density of moderate to strong lines in wavelength space.

Determining bound-bound opacity is particularly challenging for *r*-process compositions, since there is limited experimental data on energy levels and absorption probabilities for many of the species burned by the *r*-process. Nevertheless, general trends can be deduced from simple heuristics. First, the more unique species are present in a composition, the greater the number of lines, and the higher the opacity. Second, and more significantly, the presence of atomic species with a high degree of complexity (i.e., with a greater number of distinct electronic configurations) will increase opacity.

Atomic complexity is a function of the size of an atom's valence electron shell. A valence shell that accommodates a larger number of electrons allows for more distinct electronic configurations; each configuration has a slightly different energy, so the net effect is a greater number of energy levels, more transitions between energy levels, and a higher opacity [see e.g., [61]]. This picture has been borne out both by available experimental data [62] and by atomic structure calculations, with groups using different atomic structure modeling codes all finding a striking increase in opacity as valence shell size increases [61, 63, 64].

The relationship between atomic complexity and opacity has profound implications for kilonovae. Lanthanides and actinides are the most complex elements in the Periodic Table. These species have a high number of closely spaced energy levels, resulting in an abundance of low-energy bound-bound transitions and a high opacity that extends out into the near infrared (NIR). While lanthanides and actinides are easily synthesized by the heavy *r*-process, they are produced in negligible quantities in a light *r*-process event [11, 12]. The opacity of the kilonova ejecta—and the color of its emission—therefore depend sensitively on the nucleosynthesis that took place in its ejecta.

As first explained in [65], the high opacity of a lanthanide-rich (heavy *r*-process) ejecta delays and dims the light curve peak, while the extreme density of lines at optical wavelengths pushes the emission redward, causing the spectrum to peak in the NIR [see also [62]]. Of course, not all outflows from compact object mergers will undergo a heavy *r*-process. Light *r*-process compositions, will have a lower opacity. The emission associated with these outflows will have a faster rise; a sharper, brighter light-curve peak; and an SED concentrated at blue/optical wavelengths, similar to the original predictions of [20].

Kilonova emission may be due to a combination of signals from multiple outflows characterized by different histories of nucleosynthesis: a "red" component associated with a lanthanide-rich outflow, and a "blue" component from a composition that failed to burn lanthanides [58, 65]. The outcome of the *r*-process is closely tied to the manner of mass ejection and, in the case of disk winds, the nature or lifetime of the CR. The presence or relative prominence of red or blue kilonova components can therefore reveal the mass ejection mechanisms at play, and even shine an (indirect) light on the NS EOS.

4. LESSONS FROM GW170817

The theory outlined above was established before a compact object merger was definitively detected, but was corroborated by the first such detection. On August 17, 2017, the LIGO*-Virgo network picked up a signal consistent with the inspiral of a merging neutron star binary [66]. A spatially-coincident short-gamma ray burst was observed contemporaneously [67–69], increasing confidence in the signal and triggering a worldwide search by observational astronomers for a radioactive counterpart, which was soon identified in a galaxy a mere 40 Mpc distant [70–77]. These observations yielded a wealth of data which, in combination with theory, crystallized into a fairly coherent picture of the post-merger system.

The bolometric light-curve evolution was consistent with an approximately power-law injection of energy, as expected from the decay of a large ensemble of *r*-process nuclei [78]. The transient's broadband evolution showed signs of two distinct components, with the blue and optical bands rising to an early peak and declining swiftly thereafter, while emission in the redder bands evolved on a much longer (∼2 week) timescale [e.g., [70, 72, 72, 78, 79]]. The disparate behavior at red and blue wavelengths was interpreted by most groups [72, 80–82] to require two separate outflows [but see [83]]: a lanthanide-poor one driving the early blue component, and a lanthanide-rich one powering the extended red and NIR emission.

Since long-lived red emission is difficult to explain without invoking the uniquely high opacity of the lanthanides and actinides produced in abundance by the heavy *r*-process [84, 85], the broadband light curves confirmed that GW170817 had indeed triggered *r*-process nucleosynthesis, and that its optical counterpart was in fact a kilonova.

The identification of kilonova spectral features with particular *r*-process ions would further corroborate this conclusion, and early work on GW170817 demonstrated the promise of such an approach. For example, [86] linked one feature of the kilonova spectrum to singly-ionized Strontium, thus claiming the first detection of an individual *r*-process element in an electromagnetic transient. Future studies of kilonova spectra will increase confidence in such identifications and improve our ability to constrain compositions from spectral analysis.

In the meantime, kilonova spectra encode information critical for a rigorous reconstruction of the outflow(s) that produced their electromagnetic emission. The spectrum of the GW170817 kilonova was originally dominated by a smooth blue blackbody [73, 87–89], which was replaced after a few days by pseudo-blackbody peaking in the NIR and exhibiting broad absorption features [74, 90]. While the dramatic shift from blue to redder wavelengths is consistent with the kilonova's broadband evolution, the spectrum provided additional information on the velocities of the outflows associated with each component of the emission. The lack of features in the blue spectrum suggested velocities high enough to smooth out any absorption lines, $v_{\rm ej} \sim 0.3c$ [e.g., [73, 80]]. In contrast, the broad absorption troughs in the red spectrum indicate a slower outflow with $v_{\rm ej} \sim 0.1c$.

The combination of spectral and photometric data suggested that the merger launched a high-velocity, lanthanide-poor outflow in addition to a lower-velocity outflow rich in lanthanides. Some authors [e.g., [80, 85, 87]] have attributed the "blue" component to shock-heated, dynamically "squeezed" ejecta. However, the mass required to explain the luminosity ($M_{\rm blue} \approx 0.01 M_\odot$) is higher than predicted by numerical relativity simulations [36, 37, 41, 91], motivating others to consider alternate scenarios [92, 93].

The kilonova's red component has been somewhat more securely associated with a wind unbound from the accretion disk surrounding the CR. The mass ($M_{\rm red} \approx 0.04 M_\odot$ and velocity inferred for this component are consistent with expectations from simulations [48, 55], and the conditions in the disk are thought to be favorable for heavy *r*-process nucleosynthesis as long as the CR collapses instantly to a BH or survives for only a limited time as a hyper- or supramassive NS [although see [56] for an illustration of the how the treatment of neutrino transport in disks can alter the predicted nucleosynthetis].

5. OPEN QUESTIONS AND A LOOK TO THE FUTURE

GW170817 allowed the astronomy community to make inroads on some of most pressing questions multimessenger astronomy promises to help untangle. First, it demonstrated a long-theorized [94–99] association between short gamma-ray bursts and compact object mergers. Second, it allowed the derivation of the first multi-messenger constraints on the NS EOS [e.g. [100, 101]]. It also allowed an entirely original and independent calculation of the Hubble Constant H_0 [102, 103]. Finally, it conclusively identified mergers as an astrophysical site of *r*-process nucleosynthesis [70, 72, 80, 90, among many others]. However, the mysteries surrounding mergers and post-merger phenomena are far from resolved.

One major remaining question is related to the source of the blue kilonova component. While the emission seems to be powered by radioactivity, the NS EOS required to produce such a massive outflow via dynamical squeezing is seemingly too compact to *simultaneously* explain the similarly high mass of the red disk wind component. (Recall that disk wind represents a fraction of the total disk mass, and that less compact EOS's favor heavier accretion disks.) Further observations of kilonovae, especially at early times, will be instrumental in revealing the nature of the blue component and providing additional tools for evaluating the NS EOS [104].

A second question is the role of mergers in astrophysical *r*-process production. GW170817 proved that NS^2 mergers are *a* site of the *r*-process nucleosynthesis, and simple estimates suggest that the entire *r*-process content of the Universe may originate in compact object mergers [80, 105]. However, these arguments hinge on the (still very uncertain) merger rates and average *r*-process mass per event, not to mention the largely unconstrained contribution from NSBH mergers.

In addition to these uncertainties, there are concerns about whether mergers can explain *r*-process enrichment everywhere it is observed [106]. For example, *r*-process-enriched extremely metal poor stars seem to require an early-Universe source of the

r-process, while mergers typically occur at a delay of hundreds of millions or even billions of years relative to star formation [e.g., 107]. Likewise, it is difficult to explain enrichment in ultra-faint dwarf galaxies [108] with mergers, given that the velocities pre-merger binaries acquire when their component stars go supernova generally exceed the low escape velocities of these low-mass galaxies [109]. A variety of alternative *r*-process sites have been proposed [110–113]; however, a complete census of merging systems will clarify rates and ejected mass, and illuminate the role of mergers in burning the heaviest elements.

Additional observations will also unveil the full diversity of merging systems and kilonovae (this is an especially enticing prospect given how distinct the second NS^2 merger, GW190425, was from the first [114]). Neutron star-black hole (NSBH) mergers, which have not yet been observed, should provide an additional source of heterogeneity, as they are expected to produce ejecta that is more massive [32], more neutron-rich [115], and less isotropic [39] than a typical NS^2 merger. There is also likely to be substantial diversity *among* kilonovae from NSBH mergers, since mass ejection is sensitive to parameters such as mass ratio and component star spin [e.g., [116]]. Observations of NSBH mergers and their kilonovae are therefore crucial for documenting the full range of compact objects mergers' radioactively powered EM emission.

We can hope, in the next several years, to better constrain merger rates, and to understand how merging systems are distributed by total binary mass, mass ratio, and binary type (NS^2 v. NSBH). We can map out the relationship between binary and kilonova parameters, a map that will become increasingly accurate as parallel advances and theory and nuclear physics experiment (e.g., the Facility for Rare Isotopes Beams; [117]) allow us to more confidently infer ejected mass from observations. We can determine how common various components are (and we can hope to observe as-yet unseen components, like tidal tails or neutron precursors) and assess whether the net enrichment from these components is consistent observed stellar *r*-process abundances (and variations in those abundances). Ideally, we will develop the tools to measure or constrain abundance yields from the spectra of individual merger events. Our deeper understanding of kilonovae will allow us to confidently progress on the questions—*r*-process origins, NS EOS, H_0—that multi-messenger astronomy is uniquely well-poised to address.

AUTHOR CONTRIBUTIONS

The author confirms being the sole contributor of this work and has approved it for publication.

FUNDING

JB was supported by the National Aeronautics and Space Administration (NASA) through the Einstein Fellowship Program, grant number PF7-180162.

REFERENCES

1. Lattimer JM, Schramm DN. Black-hole-neutron-star collisions. *Astrophys J*. (1974) 192:L145–7. doi: 10.1086/181612
2. Lattimer JM, Schramm DN. The tidal disruption of neutron stars by black holes in close binaries. *Astrophys J*. (1976) 210:549–67. doi: 10.1086/154860
3. Symbalisty E, Schramm DN. Neutron star collisions and the r-process. *Astrophys Lett*. (1982) 22:143.
4. Li LX, Paczyński B. Transient events from neutron star mergers. *Astrophys J Lett*. (1998) 507:L59–62. doi: 10.1086/311680
5. Burbidge EM, Burbidge GR, Fowler WA, Hoyle F. Synthesis of the elements in stars. *Rev Modern Phys*. (1957) 29:547–650. doi: 10.1103/RevModPhys.29.547
6. Cameron AGW. On the origin of the heavy elements. *Astrophys J*. (1957) 62:9–10. doi: 10.1086/107435
7. Mendoza-Temis J, Vargas CE, Bagatella-Flores N. r-process nucleosynthesis calculations in neutron-star mergers (NSM): main nuclear physics requirements. In: Morriset C, Delgado-Inglada G, García-Rojas J, editors. *Cosmic Feast of the Elements*. Puebla: Universidad Nacional Autónoma de México (2017). p. 22.
8. Cowan JJ, Sneden C, Lawler JE, Aprahamian A, Wiescher M, Langanke K, et al. Making the heaviest elements in the universe: a review of the rapid neutron capture process. *arXiv preprint arXiv:1901.01410*.
9. Qian YZ, Woosley SE. Nucleosynthesis in neutrino-driven winds. I. The physical conditions. *Astrophys J*. (1996) 471:331. doi: 10.1086/177973
10. Qian YZ. The origin of the heavy elements: recent progress in the understanding of the r-process [review article]. *Prog Particle Nuclear Phys*. (2003) 50:153–99. doi: 10.1016/S0146-6410(02)00178-3
11. Wanajo S, Sekiguchi Y, Nishimura N, Kiuchi K, Kyutoku K, Shibata M. Production of all the r-process nuclides in the dynamical ejecta of neutron star mergers. *Astrophys J*. (2014). 789:L39. doi: 10.1088/2041-8205/789/2/L39
12. Lippuner J, Roberts LF. r-process lanthanide production and heating rates in kilonovae. *Astrophys J*. (2015) 815:82. doi: 10.1088/0004-637X/815/2/82
13. Meyer BS. Decompression of initially cold neutron star matter: a mechanism for the r-process? *Astrophys J*. (1989) 343:254. doi: 10.1086/167702
14. Meyer BS, McLaughlin GC, Fuller GM. Neutrino capture and r-process nucleosynthesis. *Phys Rev C*. (1998) 58:3696–710. doi: 10.1103/PhysRevC.58.3696
15. Möller P, Nix JR, Myers WD, Swiatecki WJ. Nuclear ground-state masses and deformations. *Atom Data Nucl Data Tabl*. (1995) 59:185–381. doi: 10.1006/adnd.1995.1002
16. Arnould M, Goriely S, Takahashi K. The r-process of stellar nucleosynthesis: astrophysics and nuclear physics achievements and mysteries. *Phys Rep*. (2007) 450:97–213. doi: 10.1016/j.physrep.2007.06.002
17. Barnes J, Kasen D, Wu MR, Martinez-Pinedo G. Radioactivity and thermalization in the ejecta of compact object mergers and their impact on kilonova light curves. *Astrophys J*. (2016) 829:110. doi: 10.3847/0004-637X/829/2/110
18. Arnett WD. Type I supernovae. I - Analytic solutions for the early part of the light curve. *Astrophys J*. (1982) 253:785–97. doi: 10.1086/159681
19. Metzger BD. Kilonovae. *Living Rev Relat*. (2019) 23:1. doi: 10.1007/s41114-019-0024-0
20. Metzger BD, Martinez-Pinedo G, Darbha S, Quataert E, Arcones A, Kasen D, et al. Electromagnetic counterparts of compact object mergers powered by the radioactive decay of r-process nuclei. *Mnthly Notices R Astron Soc*. (2010) 406:2650–62. doi: 10.1111/j.1365-2966.2010.16864.x
21. Mendoza-Temis JdJ, Wu MR, Langanke K, Martinez-Pinedo G, Bauswein A, Janka HT. Nuclear robustness of the r process in neutron-star mergers. *Phys Rev C*. (2015) 92:055805. doi: 10.1103/PhysRevC.92.055805
22. Zhu Y, Wollaeger RT, Vassh N, Surman R, Sprouse TM, Mumpower MR, et al. Californium-254 and kilonova light curves. *Astrophys J Lett*. (2018) 863:L23. doi: 10.3847/2041-8213/aad5de

23. Wu MR, Barnes J, Martinez-Pinedo G, Metzger BD. Fingerprints of heavy-element nucleosynthesis in the late-time lightcurves of kilonovae. *Phys Rev Lett*. (2019) 122:062701. doi: 10.1103/PhysRevLett.122.062701
24. Roberts LF, Kasen D, Lee WH, Ramirez-Ruiz E. Electromagnetic transients powered by nuclear decay in the tidal tails of coalescing compact binaries. *Astrophys J Lett*. (2011) 736:L21. doi: 10.1088/2041-8205/736/1/L21
25. Korobkin O, Rosswog S, Arcones A, Winteler C. On the astrophysical robustness of the neutron star merger r-process. *Mnthly Notices R Astron Soc*. (2012) 426:1940–9. doi: 10.1111/j.1365-2966.2012.21859.x
26. Hotokezaka K, Sari R, Piran T. Analytic heating rate of neutron star merger ejecta derived from Fermi's theory of beta decay. *Mnthly Notices R Astron Soc*. (2017) 468:91–6. doi: 10.1093/mnras/stx411
27. Kasen D, Barnes J. Radioactive heating and late time kilonova light curves. *Astrophys J*. (2019) 876:128. doi: 10.3847/1538-4357/ab06c2
28. Hotokezaka K, Nakar E. Radioactive heating rate of r-process elements and macronova light curve. *arXiv preprint arXiv:1909.02581*. doi: 10.3847/1538-4357/ab6a98
29. Waxman E, Ofek EO, Kushnir D. Late-time kilonova light curves and implications to GW170817. *Astrophys J*. (2019) 878:93. doi: 10.3847/1538-4357/ab1f71
30. Fernández R, Metzger BD. Electromagnetic signatures of neutron star mergers in the advanced LIGO era. *Annu Rev Nuclear Particle Sci*. (2016) 66:23–45. doi: 10.1146/annurev-nucl-102115-044819
31. Shibata M, Hotokezaka K. Merger and mass ejection of neutron star binaries. *Annu Rev Nuclear Particle Sci*. (2019) 69:41–64. doi: 10.1146/annurev-nucl-101918-023625
32. Kyutoku K, Ioka K, Shibata M. Anisotropic mass ejection from black hole-neutron star binaries: Diversity of electromagnetic counterparts. *Phys Rev D*. (2013) 88:041503. doi: 10.1103/PhysRevD.88.041503
33. Kawaguchi K, Kyutoku K, Nakano H, Okawa H, Shibata M, Taniguchi K. Black hole-neutron star binary merger: Dependence on black hole spin orientation and equation of state. *Phys Rev D*. (2015) 92:024014. doi: 10.1103/PhysRevD.92.024014
34. Lehner L, Liebling SL, Palenzuela C, Caballero OL, O'Connor E, Anderson M, et al. Unequal mass binary neutron star mergers and multimessenger signals. *Classic Quant Gravity*. (2016) 33:184002. doi: 10.1088/0264-9381/33/18/184002
35. Dietrich T, Bernuzzi S, Ujevic M, Tichy W. Gravitational waves and mass ejecta from binary neutron star mergers: effect of the stars' rotation. *Phys Rev D*. (2017) 95:044045. doi: 10.1103/PhysRevD.95.044045
36. Bauswein A, Goriely S, Janka HT. Systematics of dynamical mass ejection, nucleosynthesis, and radioactively powered electromagnetic signals from neutron-star mergers. *Astrophys J*. (2013) 773:78. doi: 10.1088/0004-637X/773/1/78
37. Hotokezaka K, Kiuchi K, Kyutoku K, Okawa H, Sekiguchi Yi, Shibata M, et al. Mass ejection from the merger of binary neutron stars. *Phys Rev D*. (2013) 87:024001. doi: 10.1103/PhysRevD.87.024001
38. East WE, Pretorius F, Stephens BC. Eccentric black hole-neutron star mergers: effects of black hole spin and equation of state. *Phys Rev D*. (2012) 85:124009. doi: 10.1103/PhysRevD.85.124009
39. Kyutoku K, Ioka K, Okawa H, Shibata M, Taniguchi K. Dynamical mass ejection from black hole-neutron star binaries. *Phys Rev D*. (2015) 92:044028. doi: 10.1103/PhysRevD.92.044028
40. Oechslin R, Janka HT, Marek A. Relativistic neutron star merger simulations with non-zero temperature equations of state. I. Variation of binary parameters and equation of state. *Astron Astrophys*. (2007) 467:395–409. doi: 10.1051/0004-6361:20066682
41. Sekiguchi Y, Kiuchi K, Kyutoku K, Shibata M. Dynamical mass ejection from binary neutron star mergers: Radiation-hydrodynamics study in general relativity. *Phys Rev D*. (2015). 91:064059. doi: 10.1103/PhysRevD.91.064059
42. Radice D, Galeazzi F, Lippuner J, Roberts LF, Ott CD, Rezzolla L. Dynamical mass ejection from binary neutron star mergers. *Mnthly Notices R Astron Soc*. (2016) 460:3255–71. doi: 10.1093/mnras/stw1227
43. Bauswein A, Baumgarte TW, Janka HT. Prompt merger collapse and the maximum mass of neutron stars. *Phys Rev Lett*. (2013) 111:131101. doi: 10.1103/PhysRevLett.111.131101
44. Kyutoku K, Ioka K, Shibata M. Ultrarelativistic electromagnetic counterpart to binary neutron star mergers. *Mnthly Notices R Astron Soc*. (2014) 437:L6–10. doi: 10.1093/mnrasl/slt128
45. Metzger BD, Bauswein A, Goriely S, Kasen D. Neutron-powered precursors of kilonovae. *Mnthly Notices R Astron Soc*. (2015) 446:1115–20. doi: 10.1093/mnras/stu2225
46. Oechslin R, Janka HT. Torus formation in neutron star mergers and well-localized short gamma-ray bursts. *Mnthly Notices R Astron Soc*. (2006) 368:1489–99. doi: 10.1111/j.1365-2966.2006.10238.x
47. Metzger BD, Piro AL, Quataert E. Time-dependent models of accretion discs formed from compact object mergers. *Mnthly Notices R Astron Soc*. (2008) 390:781–97. doi: 10.1111/j.1365-2966.2008.13789.x
48. Siegel DM, Metzger BD. Three-dimensional GRMHD simulations of neutrino-cooled accretion disks from neutron star mergers. *Astrophys J*. (2018) 858:52. doi: 10.3847/1538-4357/aabaec
49. Fernández R, Metzger BD. Delayed outflows from black hole accretion tori following neutron star binary coalescence. *Mnthly Notices R Astron Soc*. (2013) 435:502–17. doi: 10.1093/mnras/stt1312
50. Surman R, McLaughlin GC, Hix WR. Nucleosynthesis in the outflow from gamma-ray burst accretion disks. *Astrophys J*. (2006) 643:1057–64. doi: 10.1086/501116
51. Metzger BD, Thompson TA, Quataert E. On the conditions for neutron-rich gamma-ray burst outflows. *Astrophys J*. (2008) 676:1130–50. doi: 10.1086/526418
52. Dessart L, Ott CD, Burrows A, Rosswog S, Livne E. Neutrino signatures and the neutrino-driven wind in binary neutron star mergers. *Astrophys J*. (2009) 690:1681–705. doi: 10.1088/0004-637X/690/2/1681
53. Popham R, Woosley SE, Fryer C. Hyperaccreting black holes and gamma-ray bursts. *Astrophys J*. (1999) 518:356–74. doi: 10.1086/307259
54. Just O, Bauswein A, Ardevol Pulpillo R, Goriely S, Janka HT. Comprehensive nucleosynthesis analysis for ejecta of compact binary mergers. *Mnthly Notices R Astron Soc*. (2015) 448:541–67. doi: 10.1093/mnras/stv009
55. Fernández R, Tchekhovskoy A, Quataert E, Foucart F, Kasen D. Long-term GRMHD simulations of neutron star merger accretion discs: implications for electromagnetic counterparts. *Mnthly Notices R Astron Soc*. (2019) 482:3373–93. doi: 10.1093/mnras/sty2932
56. Miller JM, Ryan BR, Dolence JC, Burrows A, Fontes CJ, Fryer CL, et al. Full transport model of GW170817-like disk produces a blue kilonova. *Phys Rev D*. (2019) 100:023008. doi: 10.1103/PhysRevD.100.023008
57. Metzger BD, Fernández R. Red or blue? A potential kilonova imprint of the delay until black hole formation following a neutron star merger. *Mnthly Notices R Astron Soc*. (2014) 441:3444–53. doi: 10.1093/mnras/stu802
58. Kasen D, Fernández R, Metzger BD. Kilonova light curves from the disc wind outflows of compact object mergers. *Mnthly Notices R Astron Soc*. (2015) 450:1777–86. doi: 10.1093/mnras/stv721
59. Lippuner J, Fernández R, Roberts LF, Foucart F, Kasen D, Metzger BD, et al. Signatures of hypermassive neutron star lifetimes on r-process nucleosynthesis in the disc ejecta from neutron star mergers. *Mnthly Notices R Astron Soc*. (2017) 472:904–18. doi: 10.1093/mnras/stx1987
60. Pinto PA, Eastman RG. The physics of type IA supernova light curves. II. Opacity and Diffusion. *Astrophys J*. (2000) 530:757–76. doi: 10.1086/308380
61. Kasen D, Badnell NR, Barnes J. Opacities and spectra of the r-process ejecta from neutron star mergers. *Astrophys J*. (2013) 774:25. doi: 10.1088/0004-637X/774/1/25
62. Tanaka M, Hotokezaka K. Radiative transfer simulations of neutron star merger ejecta. *Astrophys J*. (2013) 775:113. doi: 10.1088/0004-637X/775/2/113
63. Tanaka M, Kato D, Gaigalas G, Kawaguchi K. Systematic opacity calculations for kilonovae. *arXiv preprint arXiv:1906.08914*. doi: 10.1093/mnras/staa1576
64. Fontes CJ, Fryer CL, Hungerford AL, Wollaeger RT, Korobkin O. A line-binned treatment of opacities for the spectra and light curves from neutron star mergers. *Mnthly Notices R Astron Soc*. (2020) 493:4143–171. doi: 10.1093/mnras/staa485

65. Barnes J, Kasen D. Effect of a high opacity on the light curves of radioactively powered transients from compact object mergers. *Astrophys J*. (2013) 775:18. doi: 10.1088/0004-637X/775/1/18
66. Abbott BP, Abbott R, Abbott TD, Acernese F, Ackley K, Adams C, et al. GW170817: observation of gravitational waves from a binary neutron star inspiral. *Phys Rev Lett*. (2017) 119:161101. doi: 10.1103/PhysRevLett.119.161101
67. Goldstein A, Veres P, Burns E, Briggs MS, Hamburg R, Kocevski D, et al. An ordinary short gamma-ray burst with extraordinary implications: fermi-GBM detection of GRB 170817A. *Astrophys J Lett*. (2017) 848:L14. doi: 10.3847/2041-8213/aa8f41
68. Savchenko V, Ferrigno C, Kuulkers E, Bazzano A, Bozzo E, Brandt S, et al. INTEGRAL Detection of the First Prompt Gamma-Ray Signal Coincident with the Gravitational-wave Event GW170817. *Astrophys J Lett*. (2017) 848:L15. doi: 10.3847/2041-8213/aa8f94
69. Abbott BP, Abbott R, Abbott TD, Acernese F, Ackley K, Adams C, et al. Gravitational waves and gamma-rays from a binary neutron star merger: GW170817 and GRB 170817A. *Astrophys J Lett*. (2017) 848:L13. doi: 10.3847/2041-8213/aa920c
70. Arcavi I, Hosseinzadeh G, Howell DA, McCully C, Poznanski D, Kasen D, et al. Optical emission from a kilonova following a gravitational-wave-detected neutron-star merger. *Nature*. (2017) 551:64–6. doi: 10.1038/nature24291
71. Coulter DA, Foley RJ, Kilpatrick CD, Drout MR, Piro AL, Shappee BJ, et al. Swope Supernova Survey (2017a). (SSS17a), the optical counterpart to a gravitational wave source. *Science*. (2017). 358:1556–8. doi: 10.1126/science.aap9811
72. Drout MR, Piro AL, Shappee BJ, Kilpatrick CD, Simon JD, Contreras C, et al. Light curves of the neutron star merger GW170817/SSS17a: implications for r-process nucleosynthesis. *Science*. (2017) 358:1570–74. doi: 10.1126/science.aaq0049
73. Shappee BJ, Simon JD, Drout MR, Piro AL, Morrell N, Prieto JL, et al. Early spectra of the gravitational wave source GW170817: evolution of a neutron star merger. *Science*. (2017) 358:1574–8. doi: 10.1126/science.aaq0186
74. Smartt SJ, Chen TW, Jerkstrand A, Coughlin M, Kankare E, Sim SA, et al. A kilonova as the electromagnetic counterpart to a gravitational-wave source. *Nature*. (2017) 551:75–9. doi: 10.1038/nature24303
75. Soares-Santos M, Holz DE, Annis J, Chornock R, Herner K, Berger E, et al. The electromagnetic counterpart of the binary neutron star merger LIGO/virgo GW170817. I. Discovery of the optical counterpart using the dark energy camera. *Astrophys J Lett*. (2017) 848:L16. doi: 10.3847/2041-8213/aa9059
76. Valenti S, Sand DJ, Yang S, Cappellaro E, Tartaglia L, Corsi A, et al. The discovery of the electromagnetic counterpart of GW170817: kilonova AT 2017gfo/DLT17ck. *Astrophys J Lett*. (2017) 848:L24. doi: 10.3847/2041-8213/aa8edf
77. Abbott BP, Abbott R, Abbott TD, Acernese F. Multi-messenger observations of a binary neutron star merger. *Astrophys J Lett*. (2017) 848:L12. doi: 10.3847/2041-8213/aa91c9
78. Cowperthwaite PS, Berger E, Villar VA, Metzger BD, Nicholl M, Chornock R, et al. The electromagnetic counterpart of the binary neutron star merger LIGO/virgo GW170817. II. UV, optical, and near-infrared light curves and comparison to kilonova models. *Astrophys J Lett*. (2017) 848:L17. doi: 10.3847/2041-8213/aa8fc7
79. Troja E, Piro L, van Eerten H, Wollaeger RT, Im M, Fox OD, et al. The X-ray counterpart to the gravitational-wave event GW170817. *Nature*. (2017) 551:71–4. doi: 10.1038/nature24290
80. Kasen D, Metzger B, Barnes J, Quataert E, Ramirez-Ruiz E. Origin of the heavy elements in binary neutron-star mergers from a gravitational-wave event. *Nature*. (2017) 551:80–4. doi: 10.1038/nature24453
81. Kasliwal MM, Nakar E, Singer LP, Kaplan DL, Cook DO, Van Sistine A, et al. Illuminating gravitational waves: A concordant picture of photons from a neutron star merger. *Science*. (2017) 358:1559–65. doi: 10.1126/science.aap9455
82. Tanaka M, Utsumi Y, Mazzali PA, Tominaga N, Yoshida M, Sekiguchi Y, et al. Kilonova from post-merger ejecta as an optical and near-Infrared counterpart of GW170817. *Publ Astron Soc Japan*. (2017) 69:102. doi: 10.1093/pasj/psx121
83. Waxman E, Ofek EO, Kushnir D, Gal-Yam A. Constraints on the ejecta of the GW170817 neutron star merger from its electromagnetic emission. *Mnthly Notices R Astron Soc*. (2018) 481:3423–41. doi: 10.1093/mnras/sty2441
84. Villar VA, Guillochon J, Berger E, Metzger BD, Cowperthwaite PS, Nicholl M, et al. The combined ultraviolet, optical, and near-infrared light curves of the kilonova associated with the binary neutron star merger GW170817: unified data set, analytic models, and physical implications. *Astrophys J Lett*. (2017) 851:L21. doi: 10.3847/2041-8213/aa9c84
85. Perego A, Radice D, Bernuzzi S. AT 2017gfo: an anisotropic and three-component kilonova counterpart of GW170817. *Astrophys J Lett*. (2017) 850:L37. doi: 10.3847/2041-8213/aa9ab9
86. Watson D, Hansen CJ, Selsing J, Koch A, Malesani DB, Andersen AC, et al. Identification of strontium in the merger of two neutron stars. *Nature*. (2019) 574:497–500. doi: 10.1038/s41586-019-1676-3
87. Nicholl M, Berger E, Kasen D, Metzger BD, Elias J, Briceño C, et al. The electromagnetic counterpart of the binary neutron star merger LIGO/virgo GW170817. III. Optical and UV spectra of a blue kilonova from fast polar ejecta. *Astrophys J Lett*. (2017) 848:L18. doi: 10.3847/2041-8213/aa9029
88. McCully C, Hiramatsu D, Howell DA, Hosseinzadeh G, Arcavi I, Kasen D, et al. The rapid reddening and featureless optical spectra of the optical counterpart of GW170817, AT 2017gfo, during the first four days. *Astrophys J Lett*. (2017) 848:L32. doi: 10.3847/2041-8213/aa9111
89. Evans PA, Cenko SB, Kennea JA, Emery SWK, Kuin NPM, Korobkin O, et al. Swift and NuSTAR observations of GW170817: detection of a blue kilonova. *Science*. (2017) 358:1565–70. doi: 10.1126/science.358.6370.1551-i
90. Chornock R, Berger E, Kasen D, Cowperthwaite PS, Nicholl M, Villar VA, et al. The electromagnetic counterpart of the binary neutron star merger LIGO/virgo GW170817. IV. Detection of near-infrared signatures of r-process nucleosynthesis with gemini-south. *Astrophys J Lett*. (2017) 848:L19. doi: 10.3847/2041-8213/aa905c
91. Radice D, Perego A, Hotokezaka K, Fromm SA, Bernuzzi S, Roberts LF. Binary neutron star mergers: mass ejection, electromagnetic counterparts, and nucleosynthesis. *Astrophys J*. (2018) 869:130. doi: 10.3847/1538-4357/aaf054
92. Metzger BD, Thompson TA, Quataert E. A magnetar origin for the kilonova ejecta in GW170817. *Astrophys J*. (2018) 856:101. doi: 10.3847/1538-4357/aab095
93. Piro AL, Kollmeier JA. Evidence for cocoon emission from the early light curve of SSS17a. *Astrophys J*. (2018) 855:103. doi: 10.3847/1538-4357/aaaab3
94. Paczynski B. Gamma-ray bursters at cosmological distances. *Astrophys J Lett*. (1986) 308:L43–6. doi: 10.1086/184740
95. Narayan R, Paczynski B, Piran T. Gamma-ray bursts as the death throes of massive binary stars. *Astrophys J Lett*. (1992) 395:L83–6. doi: 10.1086/186493
96. Eichler D, Livio M, Piran T, Schramm DN. Nucleosynthesis, neutrino bursts and gamma-rays from coalescing neutron stars. *Nature*. (1989) 340:126–8. doi: 10.1038/340126a0
97. Piran T. The physics of gamma-ray bursts. *Rev Modern Phys*. (2004) 76:1143–210. doi: 10.1103/RevModPhys.76.1143
98. Lee WH, Ramirez-Ruiz E. The progenitors of short gamma-ray bursts. *N J Phys*. (2007) 9:17. doi: 10.1088/1367-2630/9/1/017
99. Kumar P, Zhang B. The physics of gamma-ray bursts & relativistic jets. *Phys Rep*. (2015) 561:1–109. doi: 10.1016/j.physrep.2014.09.008
100. Margalit B, Metzger BD. Constraining the maximum mass of neutron stars from multi-messenger observations of GW170817. *Astrophys J Lett*. (2017) 850:L19. doi: 10.3847/2041-8213/aa991c
101. Radice D, Perego A, Zappa F, Bernuzzi S. GW170817: joint constraint on the neutron star equation of state from multimessenger observations. *Astrophys J Lett*. (2018) 852:L29. doi: 10.3847/2041-8213/aaa402
102. Abbott BP, Abbott R, Abbott TD, Acernese F, Ackley K, Adams C, et al. A gravitational-wave standard siren measurement of the Hubble constant. *Nature*. (2017) 551:85–8. doi: 10.1038/nature24471
103. The LIGO Scientific Collaboration, the Virgo Collaboration, Abbott BP, Abbott R, Abbott TD, Abraham S, et al. A gravitational-wave measurement of the Hubble constant following the second observing run of Advanced LIGO and Virgo. *arXiv preprint arXiv:1908.06060*. Available online at: https://ui.adsabs.harvard.edu/abs/2017Natur.551...85A/exportcitation

104. Arcavi I. The first hours of the GW170817 kilonova and the importance of early optical and ultraviolet observations for constraining emission models. *Astrophys J Lett*. (2018) 855:L23. doi: 10.3847/2041-8213/aab267
105. Côté B, Fryer CL, Belczynski K, Korobkin O, Chruślińska M, Vassh N, et al. The origin of r-process elements in the milky way. *Astrophys J*. (2018) 855:99. doi: 10.3847/1538-4357/aaad67
106. Côté B, Eichler M, Arcones A, Hansen CJ, Simonetti P, Frebel A, et al. Neutron star mergers might not be the only source of r-process elements in the milky way. *Astrophys J*. (2019) 875:106. doi: 10.3847/1538-4357/ab10db
107. Safarzadeh M, Sarmento R, Scannapieco E. On neutron star mergers as the source of r-process-enhanced metal-poor stars in the milky way. *Astrophys J*. (2019) 876:28. doi: 10.3847/1538-4357/ab1341
108. Ji AP, Frebel A, Chiti A, Simon JD. R-process enrichment from a single event in an ancient dwarf galaxy. *Nature*. (2016) 531:610–3. doi: 10.1038/nature17425
109. Bonetti M, Perego A, Dotti M, Cescutti G. Neutron star binary orbits in their host potential: effect on early r-process enrichment. *Mnthly Notices R Astron Soc*. (2019) 490:296–311. doi: 10.1093/mnras/stz2554
110. Mösta P, Roberts LF, Halevi G, Ott CD, Lippuner J, Haas R, et al. r-process nucleosynthesis from three-dimensional magnetorotational core-collapse supernovae. *Astrophys J*. (2018) 864:171. doi: 10.3847/1538-4357/aad6ec
111. Halevi G, Mösta P. r-process nucleosynthesis from three-dimensional jet-driven core-collapse supernovae with magnetic misalignments. *Mnthly Notices R Astron Soc*. (2018) 477:2366–2375. doi: 10.1093/mnras/sty797
112. Siegel DM, Barnes J, Metzger BD. Collapsars as a major source of r-process elements. *Nature*. (2019) 569:241–4. doi: 10.1038/s41586-019-1136-0
113. Fischer T, Wu MR, Wehmeyer B, Bastian NUF, Martinez-Pinedo G, Thielemann FK. Core-collapse supernova explosions driven by the hadron-quark phase transition as rare *r* process site. *arXiv preprint arXiv:2003.00972*. doi: 10.3847/1538-4357/ab86b0
114. The LIGO Scientific Collaboration, the Virgo Collaboration, Abbott BP, Abbott R, Abbott TD, Abraham S, et al. GW190425: observation of a compact binary coalescence with total mass $\sim 3.4M - \odot$. *arXiv preprint arXiv:2001.01761*. Available online at: https://ui.adsabs.harvard.edu/abs/2017Natur.551...85A/exportcitation
115. Roberts LF, Lippuner J, Duez MD, Faber JA, Foucart F, Lombardi JC, et al. The influence of neutrinos on r-process nucleosynthesis in the ejecta of black hole–neutron star mergers. *Mnthly Notices R Astron Soc*. (2017) 464:3907–19. doi: 10.1093/mnras/stw2622
116. Foucart F, Hinderer T, and Nissanke S. Remnant baryon mass in neutron star-black hole mergers: Predictions for binary neutron star mimickers and rapidly spinning black holes. *Phys Rev D*. (2018) 98:081501. doi: 10.1103/PhysRevD.98.081501
117. Horowitz CJ, Arcones A, Côté B, Dillmann I, Nazarewicz W, Roederer IU, et al. r-process nucleosynthesis: connecting rare-isotope beam facilities with the cosmos. *J Phys G Nuclear Phys*. (2019) 46:083001. doi: 10.1088/1361-6471/ab0849

Conflict of Interest: The author declares that the research was conducted in the absence of any commercial or financial relationships that could be construed as a potential conflict of interest.

frontiers in Astronomy and Space Sciences

MINI REVIEW
published: 09 July 2020
doi: 10.3389/fspas.2020.00038

Binary Black Hole Mergers: Formation and Populations

Michela Mapelli [1,2,3]*

[1] Physics and Astronomy Department Galileo Galilei, University of Padova, Padova, Italy, [2] INFN–Padova, Padova, Italy, [3] INAF–Osservatorio Astronomico di Padova, Padova, Italy

We review the main physical processes that lead to the formation of stellar binary black holes (BBHs) and to their merger. BBHs can form from the isolated evolution of massive binary stars. The physics of core-collapse supernovae and the process of common envelope are two of the main sources of uncertainty about this formation channel. Alternatively, two black holes can form a binary by dynamical encounters in a dense star cluster. The dynamical formation channel leaves several imprints on the mass, spin and orbital properties of BBHs.

Keywords: stars: black holes, black hole physics, Galaxy: open clusters and associations: general, stars: kinematics and dynamics, gravitational waves

OPEN ACCESS

Edited by:
Rosalba Perna,
Stony Brook University, United States

Reviewed by:
Maxim Yurievich Khlopov,
UMR7164 Astroparticule et Cosmologie (APC), France
Ataru Tanikawa,
The University of Tokyo, Japan

***Correspondence:**
Michela Mapelli
michela.mapelli@unipd.it

Specialty section:
This article was submitted to Cosmology, a section of the journal Frontiers in Astronomy and Space Sciences

Received: *25 February 2020*
Accepted: *03 June 2020*
Published: *09 July 2020*

Citation:
Mapelli M (2020) Binary Black Hole Mergers: Formation and Populations. Front. Astron. Space Sci. 7:38. doi: 10.3389/fspas.2020.00038

1. BLACK HOLE FORMATION FROM SINGLE STARS: WHERE WE STAND NOW

About 4 years ago, the LIGO detectors obtained the first direct detection of gravitational waves, GW150914 (Abbott et al., 2016; Abbott et al., 2016a,b), associated with the merger of two black holes (BHs). This event marks the dawn of gravitational wave astronomy: we now know that binary black holes (BBHs) exist, can reach coalescence by gravitational wave emission, and are composed of BHs with mass ranging from few solar masses to ~ 50 M$_\odot$. Here, we review the main physical processes that lead to the formation of BBHs and to their merger. We restrict our attention to stellar-born BHs. As to primordial BHs, which might form from gravitational instabilities in the early Universe, we refer the reader to Carr et al. (2016) and Belotsky et al. (2019), and references therein. Before we start discussing binaries, we must briefly summarize the state-of-the-art knowledge about stellar-origin BHs: this is a necessary step to understand their pairing mechanisms.

Stellar-mass BHs are thought to be the final outcome of the evolution of a massive star (zero-age main sequence mass $m_{\rm ZAMS} \gtrsim 20$ M$_\odot$). Hence the mass of the BH should be affected by the two main processes that influence the evolution of a single star: (i) mass loss by stellar winds and (ii) the final collapse.

1.1. Stellar Winds

Hot ($> 10^4$ K) massive stars ($m_{\rm ZAMS} \gtrsim 30$ M$_\odot$) lose a non-negligible fraction of their mass by line-driven winds. This process depends on metallicity (Z): the mass-loss rate by stellar winds can be described as $\dot{m} \propto Z^\beta$, where Z is the absolute metallicity (see e.g., Vink et al., 2001 and references therein). The most recent models suggest that β is not constant, but depends at least on the luminosity of the star (Gräfener and Hamann, 2008; Vink et al., 2011; Chen et al., 2015): the closer the luminosity L_* is to the Eddington value $L_{\rm Edd}$, the higher the mass loss, basically canceling the dependence on metallicity when $L_* \gtrsim L_{\rm Edd}$.

In single stars, stellar winds uniquely determine the final mass of the star at the onset of collapse. If we consider a star with $m_{\rm ZAMS} = 90$ M$_\odot$ and metallicity $Z = 0.02$ (i.e., approximately solar), its final mass will be only $m_{\rm fin} \sim 30$ M$_\odot$; while the same star with $Z < 0.0002$ has $m_{\rm fin} \gtrsim 0.8\, m_{\rm ZAMS}$. The final mass of a star $m_{\rm fin}$ is the strongest upper limit to the mass of the BH.

1.2. Core-Collapse Supernovae

For example, Fryer (1999) and Fryer and Kalogera (2001) suggest that if the final mass of the star is $m_{\rm fin} \gtrsim 40$ M$_\odot$, the fate of the star is to collapse to a BH directly, without supernova, because the binding energy of the outer stellar layers is too big to be overcome by the explosion. Fryer et al. (2012) elaborate on these early results proposing that the mass of the compact object depends not only on $m_{\rm fin}$ but also on the final mass of the carbon-oxygen core. Alternatively, O'Connor and Ott (2011) proposed the role of the compactness parameter $\xi_M = \frac{M/{\rm M}_\odot}{R(\leq M)/1000\,{\rm km}}$: if the compactness is small (e.g., $\xi_{2.5} \leq 0.2-0.4$), the SN explosion is successful, otherwise we expect the star to collapse directly. All of these simplified models as well as more sophisticated ones (e.g., Ertl et al., 2016) point toward a similar direction: if the star ends its life with a large final mass, its carbon-oxygen core grows larger, its compactness is generally higher, and so on. Hence, we expect that metal-poor stars, which retain a larger fraction of their mass to the very end and develop larger cores, are more likely to collapse to BHs directly, producing larger BHs (e.g., Mapelli et al., 2009, 2010; Zampieri and Roberts, 2009; Belczynski et al., 2010). This simplified picture seems to agree with observations, but must be taken with several grains of salt: we need a vigorous step forward in core-collapse SN simulations and theoretical models, before we can draw robust conclusions (e.g., Burrows et al., 2018).

1.3. Pair Instability

Core-collapse SNe are not the only mechanism that can end the life of a massive star. When the helium core of a star grows to ≥ 60 M$_\odot$ and the central temperature reaches $\sim 10^9$ K, electron and positron pairs are produced at an efficient rate, leading to a softening of the equation of state. The star undergoes pair instability (PI, Ober et al., 1983; Bond et al., 1984; Heger et al., 2003; Woosley et al., 2007): oxygen, neon, and silicon are burned explosively and the entire star is disrupted leaving no remnant, unless its helium core is ≥ 130 M$_\odot$. In the latter case, the gravity of the outer layers is so big that the star collapses to a massive BH directly as an effect of PI (Heger et al., 2003). Smaller helium cores ($\sim 30-60$ M$_\odot$) are associated with a less dramatic manifestation of PI: the softened equation of state drives oscillations of the core (pulsational PI, Barkat et al., 1967; Woosley et al., 2007; Chen et al., 2014; Yoshida et al., 2016); during each oscillation the star sheds some mass till it finds a new equilibrium to a lower core mass, but leaves a BH smaller than expected without pulsational PI (Belczynski et al., 2016a; Spera and Mapelli, 2017; Woosley, 2017, 2019; Marchant et al., 2019; Stevenson et al., 2019; Renzo et al., 2020).

From the combination of PI, core-collapse SNe and stellar-wind mass loss prescriptions, we expect the mass spectrum of BHs to behave roughly as shown in **Figure 1**. In particular, PI is expected to carve a gap in the mass spectrum of BHs between $\sim 50(-10,+20)$ M$_\odot$ and $\approx 120-130$ M$_\odot$. The uncertainty on this mass gap is mainly connected with uncertainties nuclear reaction rates (Farmer et al., 2019), on the collapse of the residual hydrogen envelope and on the role of stellar rotation (Mapelli et al., 2020). Within this framework, we predict a reasonable mass range for stellar-origin BHs to be $\sim 3-65$ M$_\odot$ (assuming the most conservative value for the lower edge of pair-instability mass gap). If exotic metal-poor stars exist with mass $m_{\rm ZAMS} > 250$ M$_\odot$, these might directly collapse to intermediate-mass BHs (IMBHs) with mass > 100 M$_\odot$.

2. BINARY BH FORMATION IN ISOLATION

The scenario highlighted in the previous section assumes that the progenitor star is single. But gravitational waves have shown the existence of BBHs with a very short orbital separation: the initial separation of a BBH must be of the order of few ten solar radii for the BBH to merge within a Hubble time by gravitational-wave emission. This challenges our understanding of binary star evolution. A close binary star undergoes several physical processes during its life, which can completely change its final fate (see e.g., Eggleton, 2006). The most important processes include mass transfer and common envelope, tides and natal kicks (Hurley et al., 2002).

Mass transfer and common envelope are crucial in this regard. After main sequence, a massive star can develop a stellar radius as large as several thousand solar radii. Hence, if this star is member of a binary system and its orbital separation is of few hundred to few thousand solar radii, the binary system undergoes Roche lobe overflow and possibly common envelope (Ivanova et al., 2013). If common envelope occurs between a BH and a giant companion star, the BH and the core of the giant star orbit about each other surrounded by the giant's envelope: they feel a strong gas drag from the envelope and lose kinetic energy, inspiralling about each other. This transfers thermal energy to the envelope, which might trigger the ejection of the envelope. If the envelope is not ejected, the binary system merges prematurely giving birth to a single BH. In contrast, if the envelope is ejected, the final binary system is composed of the BH and the core of the giant. Because of the spiral-in, the final semi-major axis of the binary is just few solar radii, much smaller than the initial one. If the naked core collapses to a BH without receiving a strong natal kick, the system becomes a BBH with a short orbital period, able to merge within a Hubble time. Unfortunately, our understanding of common envelope is still poor (see Fragos et al., 2019 for a recent simulation) and this uncertainty heavily affects our knowledge of BBH demography. The left-hand panel of **Figure 2** is a schematic view of the isolated binary evolution channel through common envelope.

Several alternative scenarios to common envelope have been proposed (de Mink and Mandel, 2016; Mandel and de Mink, 2016; Marchant et al., 2016). For example, in the over-contact binary evolution, Marchant et al. (2016) show that, when two massive stars in a tight binary are fast rotators, they remain fully mixed as a result of their tidally induced high spin; in this case, the binary avoids premature merger even if it is overfilling its Roche lobe and might evolve into a tight BBH.

The isolated binary evolution scenario has several characteristic signatures. In the *common envelope* isolated binary evolution scenario, the *masses* of the two BHs span from ~ 3 M$_\odot$ up to ~ 45 M$_\odot$ (see e.g., Giacobbo and Mapelli, 2018) and the *mass ratios* are preferentially close to 1 (although all

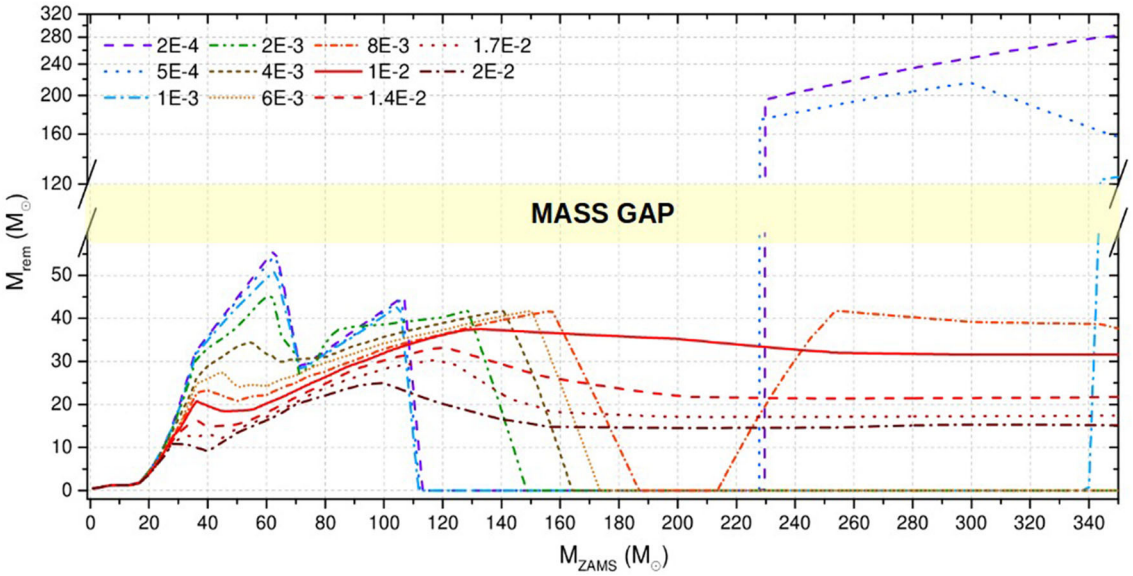

FIGURE 1 | Predicted compact object mass (M_{rem}) as a function of the zero-age main-sequence (ZAMS) mass of the progenitor star (M_{ZAMS}) for 11 different metallicities, ranging from $Z = 2 \times 10^{-4}$ to $Z = 2 \times 10^{-2}$, as shown in the legend. The yellow area highlights the pair-instability mass gap. These models are obtained with the SEVN population synthesis code (Spera et al., 2019), using PARSEC evolutionary tracks (Bressan et al., 2012) and the delayed model from Fryer et al. (2012). See Spera and Mapelli (2017) for details.

mass ratios $q = m_2/m_1 \gtrsim 0.1$ are possible, see e.g., Giacobbo and Mapelli, 2018). Most processes in binary evolution tend to produce aligned *spins* (e.g., Rodriguez et al., 2016), while the magnitude of the spin is basically unconstrained (but see Qin et al., 2018, 2019; Fuller and Ma, 2019 for some recent attempts to quantify spins). Mass transfer episodes and gravitational-wave decay are expected to efficiently damp *eccentricity*, so that almost all isolated binaries have near zero eccentricity in the LIGO-Virgo band. Finally, local merger rate densities span from a few to few thousand events $\mathrm{Gpc^{-3}\ yr^{-1}}$, depending on the details of common envelope and natal kicks (e.g., Dominik et al., 2013; Belczynski et al., 2016b; Mapelli et al., 2017; Giacobbo and Mapelli, 2018, 2020; Mapelli and Giacobbo, 2018; Neijssel et al., 2019; Santoliquido et al., 2020; Tang et al., 2020). The scenarios which include alternatives to common envelope predict an even stronger prevalence of systems with $q \sim 1$, a preferred mass range $\sim 25 - 60\ \mathrm{M_\odot}$ (Marchant et al., 2016), high and aligned spins, zero eccentricity in the LIGO-Virgo band, and long delay times ($\gtrsim$ 3 Gyr, de Mink and Mandel, 2016). Local merger rate densities are expected to be $\sim$ 10 $\mathrm{Gpc^{-3}\ yr^{-1}}$ (Mandel and de Mink, 2016), with large uncertainties.

3. BINARY BH FORMATION IN STAR CLUSTERS

Star clusters are among the densest places in the Universe. There is a plethora of star clusters, with their distinguishing features: (i) globular clusters (Gratton et al., 2019) are old ($\sim$ 12 Gyr) and massive systems ($\sim 10^{4-6}\ \mathrm{M_\odot}$), (ii) nuclear star clusters can be even more massive ($\sim 10^7\ \mathrm{M_\odot}$) and lie at the center of many galaxies, in some cases coexisting with the supersessive BH (Neumayer et al., 2020), (iii) open clusters and young star clusters (Portegies Zwart et al., 2010) are generally less massive (up to $\sim 10^5\ \mathrm{M_\odot}$) and short lived (less than a few Gyr), but are the main birthplace of massive stars in the local Universe (Lada and Lada, 2003).

The central density of star clusters is sufficiently high ($\gtrsim 10^3$ stars $\mathrm{pc^{-3}}$) and their typical velocity dispersion sufficiently low (from a few to a few tens of km $\mathrm{s^{-1}}$, possibly with the exception of nuclear star clusters) that their central two-body relaxation time (Spitzer, 1987) is shorter than their lifetime. This has one fascinating implication: the orbits of stars and binary stars in a star cluster are constantly perturbed by dynamical encounters with other cluster members. This process affects the formation and the evolution of binary BHs in multiple ways (e.g., Portegies Zwart and McMillan, 2000).

Dynamical Exchanges

Dynamical exchanges occur when a binary system interacts with a single stellar object and the latter replaces one of the members of the binary. We have known for a long time that massive objects are more likely to acquire companions by dynamical exchanges (Hills and Fullerton, 1980). Since BHs are among the most massive objects in a star cluster, they are very efficient in forming new binaries through exchanges (e.g., Ziosi et al., 2014).

During a three-body encounter, a binary star exchanges a fraction of its internal energy with the third body. If the binary is particularly tight (hard binary), such encounters tend to harden the binary star, i.e., to increase its binding energy by reducing its semi-major axis (*dynamical hardening*). In the case of a BBH,

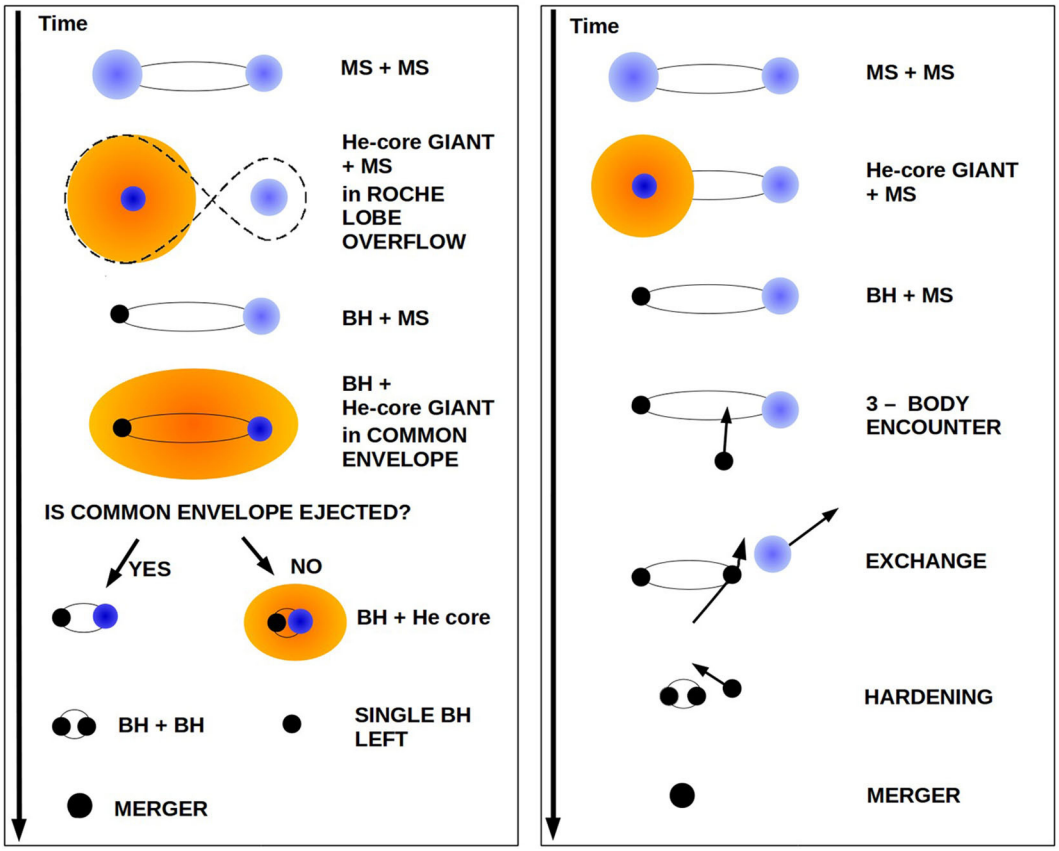

FIGURE 2 | Left: cartoon of isolated BBH formation through common envelope; **Right**: cartoon of dynamical BBH formation in star clusters.

this hardening might speed up the merger, because it drives the semi-major axis of the BBH in the regime where orbital decay by gravitational waves becomes efficient (see e.g., Figure 10 of Mapelli, 2018). On the other hand, the least massive BBHs can even be *ionized*, i.e., split by strong dynamical encounters with massive intruders.

Mergers of Massive Stars

Mergers of massive stars are common in dense young star clusters, because of the short dynamical friction timescale (Portegies Zwart et al., 2010). Under some assumptions, these mergers can lead to the formation of massive BHs ($m_{\rm BH} > 60$ $M_\odot$), with mass in the pair-instability gap (Di Carlo et al., 2019a). In star clusters, such massive BHs can acquire a companion by dynamical exchanges, leading to the formation of BBHs in the mass gap. A fast sequence of stellar mergers in the dense core of a young star cluster (also known as *runaway collision*, Portegies Zwart et al., 2004; Giersz et al., 2015) might even lead to the formation of intermediate-mass BHs (IMBHs), i.e., BHs with mass $m_{\rm BH} > 100$ $M_\odot$, especially at low metallicity (Mapelli, 2016).

The dynamical processes we briefly summarized above (and in the right-hand panel of **Figure 2**) leave a clear imprint on BBHs. First, dynamically formed BBHs extend to higher masses than isolated BBHs: they might even be in the pair-instability mass gap or in the IMBH regime (Di Carlo et al., 2019b; Rodriguez et al., 2019). Secondly, dynamical exchanges randomize the spin direction, leading to an isotropic distribution of BH spins. In contrast, isolated BBHs have a preference for aligned spins (Rodriguez et al., 2016; Gerosa et al., 2018). Third, dynamics can trigger the merger of BBHs with non-zero eccentricity even in the LIGO-Virgo band (Samsing et al., 2014; Rodriguez et al., 2018; Samsing, 2018; Zevin et al., 2019). These signatures provide an unique opportunity to differentiate among the isolated and the dynamical formation channel when the number of gravitational-wave detections will be of the order of a few hundreds (e.g., Zevin et al., 2017; Bouffanais et al., 2019).

AUTHOR CONTRIBUTIONS

MM collected the material and wrote the review.

FUNDING

MM acknowledges financial support from the European Research Council for the ERC Consolidator grant DEMOBLACK, under contract no. 770017.

REFERENCES

Abbott, B. P., Abbott, R., Abbott, T. D., Abernathy, M. R., Acernese, F., Ackley, K., et al. (2016). Observation of gravitational waves from a binary black hole merger. *Phys. Rev. Lett*. 116:061102. doi: 10.1103/PhysRevLett.116.061102

Abbott, B. P., Abbott, R., Abbott, T. D., Abernathy, M. R., Acernese, F., Ackley, K., et al. (2016a). Astrophysical implications of the binary black-hole merger GW150914. *Astrophys. J. Lett*. 818:L22. doi: 10.3847/2041-8205/818/2/L22

Abbott, B. P., Abbott, R., Abbott, T. D., Abernathy, M. R., Acernese, F., Ackley, K., et al. (2016b). Binary black hole mergers in the first advanced LIGO observing run. *Phys. Rev. X* 6:041015. doi: 10.1103/PhysRevX.6.041015

Barkat, Z., Rakavy, G., and Sack, N. (1967). Dynamics of supernova explosion resulting from pair formation. *Phys. Rev. Lett*. 18, 379–381. doi: 10.1103/PhysRevLett.18.379

Belczynski, K., Bulik, T., Fryer, C. L., Ruiter, A., Valsecchi, F., Vink, J. S., et al. (2010). On the maximum mass of stellar black holes. *Astrophys. J*. 714, 1217–1226. doi: 10.1088/0004-637X/714/2/1217

Belczynski, K., Heger, A., Gladysz, W., Ruiter, A. J., Woosley, S., Wiktorowicz, G., et al. (2016a). The effect of pair-instability mass loss on black-hole mergers. *Astron. Astrophys*. 594:A97. doi: 10.1051/0004-6361/201628980

Belczynski, K., Holz, D. E., Bulik, T., and O'Shaughnessy, R. (2016b). The first gravitational-wave source from the isolated evolution of two stars in the 40-100 solar mass range. *Nature* 534, 512–515. doi: 10.1038/nature18322

Belotsky, K. M., Dokuchaev, V. I., Eroshenko, Y. N., Esipova, E. A., Khlopov, M. Y., Khromykh, L. A., et al. (2019). Clusters of primordial black holes. *Eur. Phys. J. C* 79:246. doi: 10.1140/epjc/s10052-019-6741-4

Bond, J. R., Arnett, W. D., and Carr, B. J. (1984). The evolution and fate of very massive objects. *Astrophys. J*. 280, 825–847. doi: 10.1086/162057

Bouffanais, Y., Mapelli, M., Gerosa, D., Di Carlo, U. N., Giacobbo, N., Berti, E., et al. (2019). Constraining the fraction of binary black holes formed in isolation and young star clusters with gravitational-wave data. *Astrophys. J*. 886:25. doi: 10.3847/1538-4357/ab4a79

Bressan, A., Marigo, P., Girardi, L., Salasnich, B., Dal Cero, C., Rubele, S., et al. (2012). PARSEC: stellar tracks and isochrones with the PAdova and TRieste Stellar Evolution Code. *Mnthly. Notices R Astron. Soc*. 427, 127–145. doi: 10.1111/j.1365-2966.2012.21948.x

Burrows, A., Vartanyan, D., Dolence, J. C., Skinner, M. A., and Radice, D. (2018). Crucial physical dependencies of the core-collapse supernova mechanism. *Space Sci. Rev*. 214:33. doi: 10.1007/s11214-017-0450-9

Carr, B., Kühnel, F., and Sandstad, M. (2016). Primordial black holes as dark matter. *Phys. Rev. D* 94:083504. doi: 10.1103/PhysRevD.94.083504

Chen, K.-J., Woosley, S., Heger, A., Almgren, A., and Whalen, D. J. (2014). Two-dimensional simulations of pulsational pair-instability supernovae. *Astrophys. J*. 792:28. doi: 10.1088/0004-637X/792/1/28

Chen, Y., Bressan, A., Girardi, L., Marigo, P., Kong, X., and Lanza, A. (2015). PARSEC evolutionary tracks of massive stars up to 350 $M_{\odot}$ at metallicities $0.0001 \leq Z \leq 0.04$. *Mnthly. Notices R Astron. Soc*. 452, 1068–1080. doi: 10.1093/mnras/stv1281

de Mink, S. E., and Mandel, I. (2016). The chemically homogeneous evolutionary channel for binary black hole mergers: rates and properties of gravitational-wave events detectable by advanced LIGO. *Mnthly. Notices R Astron. Soc*. 460, 3545–3553. doi: 10.1093/mnras/stw1219

Di Carlo, U. N., Giacobbo, N., Mapelli, M., Pasquato, M., Spera, M., Wang, L., et al. (2019a). Merging black holes in young star clusters. *Mnthly. Notices R Astron. Soc*. 487, 2947–2960. doi: 10.1093/mnras/stz1453

Di Carlo, U. N., Mapelli, M., Bouffanais, Y., Giacobbo, N., Bressan, S., Spera, M., et al. (2019b). Binary black holes in the pair-instability mass gap. *arXiv [Preprint] arXiv:1911.01434*.

Dominik, M., Belczynski, K., Fryer, C., Holz, D. E., Berti, E., Bulik, T., et al. (2013). Double compact objects. II. Cosmological merger rates. *Astrophys. J*. 779:72. doi: 10.1088/0004-637X/779/1/72

Eggleton, P. (2006). Evolutionary processes in binary and multiple stars. doi: 10.1017/CBO9780511536205

Ertl, T., Janka, H. T., Woosley, S. E., Sukhbold, T., and Ugliano, M. (2016). A two-parameter criterion for classifying the explodability of massive stars by the neutrino-driven mechanism. *Astrophys. J*. 818:124. doi: 10.3847/0004-637X/818/2/124

Farmer, R., Renzo, M., de Mink, S. E., Marchant, P., and Justham, S. (2019). Mind the gap: the location of the lower edge of the pair-instability supernova black hole mass gap. *Astrophys. J*. 887:53. doi: 10.3847/1538-4357/ab518b

Fragos, T., Andrews, J. J., Ramirez-Ruiz, E., Meynet, G., Kalogera, V., Taam, R. E., et al. (2019). The complete evolution of a neutron-star binary through a common envelope phase using 1D hydrodynamic simulations. *Astrophys. J. Lett*. 883:L45. doi: 10.3847/2041-8213/ab40d1

Fryer, C. L. (1999). Mass limits for black hole formation. *Astrophys. J*. 522, 413–418. doi: 10.1086/307647

Fryer, C. L., Belczynski, K., Wiktorowicz, G., Dominik, M., Kalogera, V., and Holz, D. E. (2012). Compact remnant mass function: dependence on the explosion mechanism and metallicity. *Astrophys. J*. 749:91. doi: 10.1088/0004-637X/749/1/91

Fryer, C. L., and Kalogera, V. (2001). Theoretical Black Hole Mass Distributions. Astrophys. J. 554, 548–560. doi: 10.1086/321359

Fuller, J., and Ma, L. (2019). Most black holes are born very slowly rotating. *Astrophys. J. Lett*. 881:L1. doi: 10.3847/2041-8213/ab339b

Gerosa, D., Berti, E., O'Shaughnessy, R., Belczynski, K., Kesden, M., Wysocki, D., et al. (2018). Spin orientations of merging black holes formed from the evolution of stellar binaries. *Phys. Rev. D* 98:084036. doi: 10.1103/PhysRevD.98.084036

Giacobbo, N., and Mapelli, M. (2018). The progenitors of compact-object binaries: impact of metallicity, common envelope and natal kicks. *Mnthly. Notices R Astron. Soc*. 480, 2011–2030. doi: 10.1093/mnras/sty1999

Giacobbo, N., and Mapelli, M. (2020). Revising natal kick prescriptions in population synthesis simulations. *Astrophys. J*. 891:141. doi: 10.3847/1538-4357/ab7335

Giersz, M., Leigh, N., Hypki, A., Lützgendorf, N., and Askar, A. (2015). MOCCA code for star cluster simulations - IV. A new scenario for intermediate mass black hole formation in globular clusters. *Mnthly. Notices R Astron. Soc*. 454, 3150–3165. doi: 10.1093/mnras/stv2162

Gräfener, G., and Hamann, W.-R. (2008). Mass loss from late-type WN stars and its Z-dependence. Very massive stars approaching the Eddington limit. *Astron. Astrophys*. 482, 945–960. doi: 10.1051/0004-6361:20066176

Gratton, R., Bragaglia, A., Carretta, E., D'Orazi, V., Lucatello, S., and Sollima, A. (2019). What is a globular cluster? An observational perspective. *Astron. Astrophys. Rev*. 27:8. doi: 10.1007/s00159-019-0119-3

Heger, A., Fryer, C. L., Woosley, S. E., Langer, N., and Hartmann, D. H. (2003). How massive single stars end their life. *Astrophys. J*. 591, 288–300. doi: 10.1086/375341

Hills, J. G., and Fullerton, L. W. (1980). Computer simulations of close encounters between single stars and hard binaries. *Astrophys. J*. 85, 1281–1291. doi: 10.1086/112798

Hurley, J. R., Tout, C. A., and Pols, O. R. (2002). Evolution of binary stars and the effect of tides on binary populations. *Mnthly. Notices R Astron. Soc*. 329, 897–928. doi: 10.1046/j.1365-8711.2002.05038.x

Ivanova, N., Justham, S., Chen, X., De Marco, O., Fryer, C. L., Gaburov, E., et al. (2013). Common envelope evolution: where we stand and how we can move forward. *Astron. Astrophys. Rev*. 21:59. doi: 10.1007/s00159-013-0059-2

Lada, C. J., and Lada, E. A. (2003). Embedded clusters in molecular clouds. *Annu. Rev. Astron. Astrophys*. 41, 57–115. doi: 10.1146/annurev.astro.41.011802.094844

Mandel, I., and de Mink, S. E. (2016). Merging binary black holes formed through chemically homogeneous evolution in short-period stellar binaries. *Mnthly. Notices R Astron. Soc*. 458, 2634–2647. doi: 10.1093/mnras/stw379

Mapelli, M. (2016). Massive black hole binaries from runaway collisions: the impact of metallicity. *Mnthly. Notices R Astron. Soc*. 459, 3432–3446. doi: 10.1093/mnras/stw869

Mapelli, M. (2018). Astrophysics of stellar black holes. *arXiv [Preprint] arXiv:1809.09130*.

Mapelli, M., Colpi, M., and Zampieri, L. (2009). Low metallicity and ultra-luminous X-ray sources in the Cartwheel galaxy. *Mnthly. Notices R Astron. Soc*. 395, L71–L75. doi: 10.1111/j.1745-3933.2009.00645.x

Mapelli, M., and Giacobbo, N. (2018). The cosmic merger rate of neutron stars and black holes. *Mnthly. Notices R Astron. Soc*. 479, 4391–4398. doi: 10.1093/mnras/sty1613

Mapelli, M., Giacobbo, N., Ripamonti, E., and Spera, M. (2017). The cosmic merger rate of stellar black hole binaries from the Illustris simulation.

Mnthly. Notices R Astron. Soc. 472, 2422–2435. doi: 10.1093/mnras/stx2123

Mapelli, M., Ripamonti, E., Zampieri, L., Colpi, M., and Bressan, A. (2010). Ultra-luminous X-ray sources and remnants of massive metal-poor stars. *Mnthly. Notices R Astron. Soc.* 408, 234–253. doi: 10.1111/j.1365-2966.2010.17048.x

Mapelli, M., Spera, M., Montanari, E., Limongi, M., Chieffi, A., Giacobbo, N., et al. (2020). Impact of the rotation and compactness of progenitors on the mass of black holes. *Astrophys. J.* 888:76. doi: 10.3847/1538-4357/ab584d

Marchant, P., Langer, N., Podsiadlowski, P., Tauris, T. M., and Moriya, T. J. (2016). A new route towards merging massive black holes. *Astron. Astrophys.* 588:A50. doi: 10.1051/0004-6361/201628133

Marchant, P., Renzo, M., Farmer, R., Pappas, K. M. W., Taam, R. E., de Mink, S. E., et al. (2019). Pulsational pair-instability supernovae in very close binaries. *Astrophys. J.* 882:36. doi: 10.3847/1538-4357/ab3426

Neijssel, C. J., Vigna-Gómez, A., Stevenson, S., Barrett, J. W., Gaebel, S. M., Broekgaarden, F. S., et al. (2019). The effect of the metallicity-specific star formation history on double compact object mergers. *Mnthly. Notices R Astron. Soc.* 490, 3740–3759. doi: 10.1093/mnras/stz2840

Neumayer, N., Seth, A., and Boeker, T. (2020). Nuclear star clusters. *arXiv [Preprint] arXiv:2001.03626*.

Ober, W. W., El Eid, M. F., and Fricke, K. J. (1983). Evolution of massive pregalactic stars - part two - nucleosynthesis in pair creation supernovae and pregalactic enrichment. *Astron. Astrophys.* 119:61.

O'Connor, E., and Ott, C. D. (2011). Black hole formation in failing core-collapse supernovae. *Astrophys. J.* 730:70. doi: 10.1088/0004-637X/730/2/70

Portegies Zwart, S. F., Baumgardt, H., Hut, P., Makino, J., and McMillan, S. L. W. (2004). Formation of massive black holes through runaway collisions in dense young star clusters. *Nature* 428, 724–726. doi: 10.1038/nature02448

Portegies Zwart, S. F., and McMillan, S. L. W. (2000). Black hole mergers in the universe. *Astrophys. J. Lett.* 528:L17–L20. doi: 10.1086/312422

Portegies Zwart, S. F., McMillan, S. L. W., and Gieles, M. (2010). Young massive star clusters. *Annu. Rev. Astron. Astrophys.* 48, 431–493. doi: 10.1146/annurev-astro-081309-130834

Qin, Y., Fragos, T., Meynet, G., Andrews, J., Sørensen, M., and Song, H. F. (2018). The spin of the second-born black hole in coalescing binary black holes. *Astron. Astrophys.* 616:A28. doi: 10.1051/0004-6361/201832839

Qin, Y., Marchant, P., Fragos, T., Meynet, G., and Kalogera, V. (2019). On the Origin of Black Hole Spin in High-mass X-Ray Binaries. *Astrophys. J. Lett.* 870:L18. doi: 10.3847/2041-8213/aaf97b

Renzo, M., Farmer, R. J., Justham, S., de Mink, S. E., Götberg, Y., and Marchant, P. (2020). Sensitivity of the lower edge of the pair-instability black hole mass gap to the treatment of time-dependent convection. *Mnthly. Notices R Astron. Soc.* 493, 4333–4341. doi: 10.1093/mnras/staa549

Rodriguez, C. L., Amaro-Seoane, P., Chatterjee, S., and Rasio, F. A. (2018). Post-newtonian dynamics in dense star clusters: highly eccentric, highly spinning, and repeated binary black hole mergers. Phys. Rev. Lett.120:151101. doi: 10.1103/PhysRevLett.120.151101

Rodriguez, C. L., Zevin, M., Amaro-Seoane, P., Chatterjee, S., Kremer, K., Rasio, F. A., and Ye, C. S. (2019). Black holes: The next generation-repeated mergers in dense star clusters and their gravitational-wave properties. *Phys. Rev. D* 100:043027. doi: 10.1103/PhysRevD.100.043027

Rodriguez, C. L., Zevin, M., Pankow, C., Kalogera, V., and Rasio, F. A. (2016). Illuminating black hole binary formation channels with spins in advanced LIGO. *Astrophys. J. Lett.* 832:L2. doi: 10.3847/2041-8205/832/1/L2

Samsing, J. (2018). Eccentric black hole mergers forming in globular clusters. *Phys. Rev. D* 97:103014. doi: 10.1103/PhysRevD.97.103014

Samsing, J., MacLeod, M., and Ramirez-Ruiz, E. (2014). The formation of eccentric compact binary inspirals and the role of gravitational wave emission in binary-single stellar encounters. *Astrophys. J.* 784:71. doi: 10.1088/0004-637X/784/1/71

Santoliquido, F., Mapelli, M., Bouffanais, Y., Giacobbo, N., Di Carlo, U. N., Rastello, S., et al. (2020). The cosmic merger rate density evolution of compact binaries formed in young star clusters and in isolated binaries. *arXiv [Preprint] arXiv:2004.09533*.

Spera, M., and Mapelli, M. (2017). Very massive stars, pair-instability supernovae and intermediate-mass black holes with the sevn code. *Mnthly. Notices R Astron. Soc.* 470, 4739–4749. doi: 10.1093/mnras/stx1576

Spera, M., Mapelli, M., Giacobbo, N., Trani, A. A., Bressan, A., and Costa, G. (2019). Merging black hole binaries with the SEVN code. *Mnthly. Notices R Astron. Soc.* 485, 889–907. doi: 10.1093/mnras/stz359

Spitzer, L. (1987). Dynamical evolution of globular clusters. doi: 10.1515/9781400858736

Stevenson, S., Sampson, M., Powell, J., Vigna-Gómez, A., Neijssel, C. J., Szécsi, D., et al. (2019). The impact of pair-instability mass loss on the binary black hole mass distribution. *Astrophys. J.* 882:121. doi: 10.3847/1538-4357/ab3981

Tang, P. N., Eldridge, J. J., Stanway, E. R., and Bray, J. C. (2020). Dependence of gravitational wave transient rates on cosmic star formation and metallicity evolution history. *Mnthly. Notices R Astron. Soc.* 493, L6–L10. doi: 10.1093/mnrasl/slz183

Vink, J. S., de Koter, A., and Lamers, H. J. G. L. M. (2001). Mass-loss predictions for O and B stars as a function of metallicity. *Astron. Astrophys.* 369, 574–588. doi: 10.1051/0004-6361:20010127

Vink, J. S., Muijres, L. E., Anthonisse, B., de Koter, A., Gräfener, G., and Langer, N. (2011). Wind modelling of very massive stars up to 300 solar masses. *Astron. Astrophys.* 531:A132. doi: 10.1051/0004-6361/201116614

Woosley, S. E. (2017). Pulsational Pair-instability Supernovae. *Astrophys. J.* 836:244. doi: 10.3847/1538-4357/836/2/244

Woosley, S. E. (2019). The evolution of massive helium stars, including mass loss. *Astrophys. J.* 878:49. doi: 10.3847/1538-4357/ab1b41

Woosley, S. E., Blinnikov, S., and Heger, A. (2007). Pulsational pair instability as an explanation for the most luminous supernovae. *Nature* 450, 390–392. doi: 10.1038/nature06333

Yoshida, T., Umeda, H., Maeda, K., and Ishii, T. (2016). Mass ejection by pulsational pair instability in very massive stars and implications for luminous supernovae. *Mnthly. Notices R Astron. Soc.* 457, 351–361. doi: 10.1093/mnras/stv3002

Zampieri, L., and Roberts, T. P. (2009). Low-metallicity natal environments and black hole masses in ultraluminous X-ray sources. *Mnthly. Notices R Astron. Soc.* 400, 677–686. doi: 10.1111/j.1365-2966.2009.15509.x

Zevin, M., Pankow, C., Rodriguez, C. L., Sampson, L., Chase, E., Kalogera, V., et al. (2017). Constraining formation models of binary black holes with gravitational-wave observations. *Astrophys. J.* 846:82. doi: 10.3847/1538-4357/aa8408

Zevin, M., Samsing, J., Rodriguez, C., Haster, C.-J., and Ramirez-Ruiz, E. (2019). Eccentric black hole mergers in dense star clusters: the role of binary-binary encounters. *Astrophys. J.* 871:91. doi: 10.3847/1538-4357/aaf6ec

Ziosi, B. M., Mapelli, M., Branchesi, M., and Tormen, G. (2014). Dynamics of stellar black holes in young star clusters with different metallicities - II. Black hole-black hole binaries. *Mnthly. Notices R Astron. Soc.* 441, 3703–3717. doi: 10.1093/mnras/stu824

Conflict of Interest: The author declares that the research was conducted in the absence of any commercial or financial relationships that could be construed as a potential conflict of interest.

frontiers in Astronomy and Space Sciences

MINI REVIEW
published: 18 February 2021
doi: 10.3389/fspas.2021.601646

Black Hole Science With the Laser Interferometer Space Antenna

Alberto Sesana *

Department of Physics G. Occhialini, University of Milano - Bicocca, Piazza della Scienza 3, Milano, Italy

The author reviews the scientific potential of the Laser Interferometer Space Antenna (LISA), a space-borne gravitational wave (GW) observatory to be launched in the early 30s. Thanks to its sensitivity in the milli-Hz frequency range, LISA will reveal a variety of GW sources across the Universe, from our Solar neighborhood potentially all the way back to the Big Bang, promising to be a game changer in our understanding of astrophysics, cosmology, and fundamental physics. This review dives in the LISA Universe, with a specific focus on black hole science, including the formation and evolution of massive black holes in galaxy centers, the dynamics of dense nuclei and formation of extreme mass ratio inspirals, and the astrophysics of stellar-origin black hole binaries.

Keywords: gravitational waves, black hole physics, binary systems, cosmology, tests of gravity

OPEN ACCESS

Edited by:
Rosalba Perna,
Stony Brook University, United States

Reviewed by:
Cs Unnikrishnan,
Tata Institute of Fundamental Research, India
Maxim Yurievich Khlopov,
UMR7164 Astroparticule et Cosmologie, France

***Correspondence:**
Alberto Sesana
alberto.sesana@unimib.it

Specialty section:
This article was submitted to Cosmology, a section of the journal Frontiers in Astronomy and Space Sciences

Received: *01 September 2020*
Accepted: *14 January 2021*
Published: *18 February 2021*

Citation:
Sesana A (2021) Black Hole Science With the Laser Interferometer Space Antenna. Front. Astron. Space Sci. 8:601646. doi: 10.3389/fspas.2021.601646

1 INTRODUCTION

Despite the wealth of revolutionary results already delivered (Abbott et al., 2019), gravitational wave (GW) astronomy is still in its infancy. LIGO (Abbott et al., 2009) and Virgo (Acernese et al., 2015) are in fact only sensitive to binary systems of $\lesssim 100 M_\odot$ out to $z \approx 1$, leaving us still blind to the vast majority of GW sources in the Universe. This will profoundly change within the next 2 decades, when GW revelation instruments and techniques will access sources covering a much larger spectrum of masses (upto $10^{10} M_\odot$) essentially anywhere in the Universe. The 3G detectors Einstein Telescope (Punturo et al., 2010) and Cosmic Explorer (Reitze et al., 2019) will cover the Hz to kilo-Hz frequency range, populated by binaries of compact objects (CO) of different nature, out to high redshift. Neutron star binaries (NSBs) will be observed out to $z > 2$ at a rate of tens of thousands per year, and similar rates are expected for black hole binaries (BHBs) which will be observable out to $z \approx 20$ (Van Den Broeck, 2014). Interestingly, the extension of the sensitivity window down to few Hz will open up the uncharted land of intermediate mass black holes (Jani et al., 2019). At the opposite end of the frequency and source mass spectrum, radio millisecond pulsar data, collected and analyzed by pulsar timing array (PTA, Foster and Backer, 1990) collaborations (Desvignes et al., 2016; Arzoumanian et al., 2018; Kerr et al., 2020), are the gateway to the μ – Hz to nano-Hz frequency range. Here, the expectation is to detect a stochastic GW background (GWB) emerging from the incoherent superposition of signals from a cosmic population of massive black hole binaries (MBHBs), forming in the aftermath of galaxy mergers occurring along the assembly of cosmic structures (Sesana et al., 2008; Ravi et al., 2012). The international PTA (IPTA, Verbiest et al., 2016) is working in this direction and with the advent of the Square Kilometer Array (SKA, Dewdney et al., 2009), there is also the expectation to resolve the most massive inspiralling individual MBHBs in the Universe (Sesana et al., 2009; Kelley et al., 2018).

The bridging milli-Hz frequency window will be explored from space, thanks to the Laser Interferometer Space Antenna (LISA Amaro-Seoane et al., 2017), one of the next large missions of the European Space Agency with the participation of NASA, to be flown in the early 30s. Being sensitive to the milli-Hz frequency band, from ≈ 0.1 milli-Hz to 0.1Hz, LISA is ideally suited to

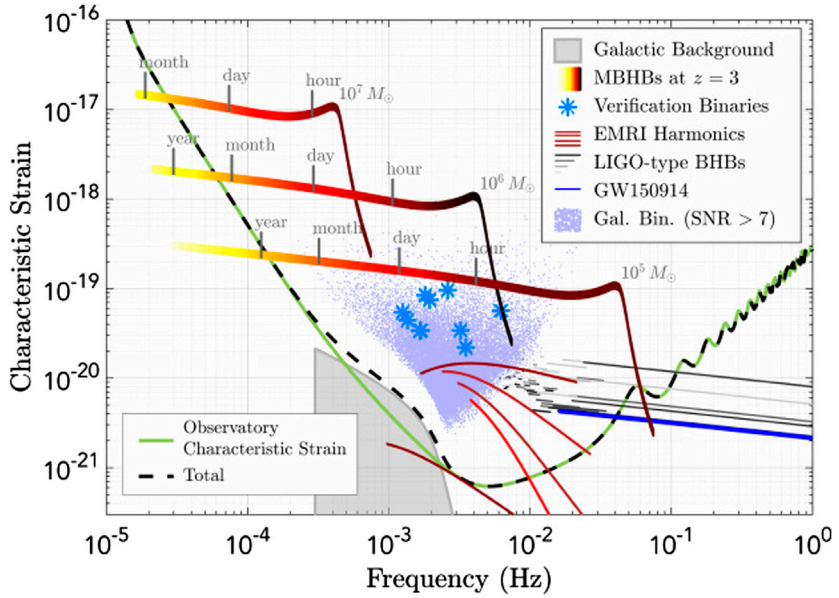

FIGURE 1 | The dimensionless "characteristic strain" of GW sources in the LISA frequency band. The nominal detector sensitivity is shown by the green line. Displayed are tracks of three equal MBHBs at $z = 3$ with total masses of $10^5, 10^6, 10^7 M_\odot$, the first five harmonics of an EMRI at $z = 1.2$ (red solid lines), a sample of stellar-mass BHBs (black solid lines), and several thousands of resolvable galactic binaries (blue dots). The subset of known "verification binaries" is shown with blue asterisks. The "confusion noise" arising from the millions of galactic binaries that cannot be resolved individually is shown by the gray shaded area (Amaro-Seoane et al., 2017).

probe GW sources across the mass and distance scales, from the Solar neighborhood to the Big Bang. Starting from our backyard, contrary to ground-based detectors and PTAs, LISA is expected to observe a bonanza of sources within the Milky Way (MW). Those include millions of galactic compact objects (COs), mostly double white dwarfs (DWDs), building up an unresolved confusion noise around 0.5–2 milli-Hz (Nelemans et al., 2001). Up to 20 k such DWDs will be individually resolvable (Nissanke et al., 2012), along with several tens of NSBs (Lau et al., 2020) and few BHBs (Seto, 2016; Sesana et al., 2020). Moreover, LISA has the unique potential to detect the presence of planets around nearby DWDs (Tamanini and Danielski, 2019) and perhaps dozens of brown dwarfs and substellar objects orbiting SgrA* (Freitag, 2003), known as X-MRI (Amaro-Seoane, 2019). LISA will detect many more BHBs outside the MW, being sensitive to the early inspiral of these systems centuries to weeks before they enter the ground-based detector sensitivity band, out to $z \approx 0.5$ Sesana (2016). COs inspiralling onto MBHBs, known as extreme mass ratio inspirals (EMRIs), can be detected out to $z \approx 2$ Babak et al. (2017), whereas coalescing massive black hole binaries MBHBs in the mass range $10^4 M_\odot < M < 10^7 M_\odot$ can be seen anywhere in the Universe Klein et al. (2016). Last but not least, the frequency range covered by LISA makes it sensitive to TeV energy scales, where a stochastic GWB might be produced in the early Universe by, e.g., first-order phase transitions or cosmic defects like strings and loops. A visual summary of selected LISA sources is depicted in **Figure 1**, from Amaro-Seoane et al. (2017). The observation of each class of sources will provide invaluable insights in astrophysics, cosmology, and fundamental physics, which is beyond what can be reasonably tackled within the few pages of this review. We therefore focus on a subset of sources, specifically MBHBs, EMRIs, and BHBs, highlighting their astrophysical potential in particular. The payouts of studying fundamental physics with low frequency GWs are extensively described in a dedicated LRR article Gair et al. (2013), whereas a comprehensive review of cosmological GWBs with much focus on LISA can be found in Caprini and Figueroa (2018).

2 MASSIVE BLACK HOLE BINARIES

MBHBs are expected to form in large number along the cosmic history (Volonteri et al., 2003). Pairing in the aftermath of galaxy mergers, they are tracers of structure formation in the Universe and can be seen by LISA out to $z > 20$, beyond the foreseeable capabilities of any electromagnetic (EM) observation. The poor knowledge of protogalaxy and black hole seed formation at high redshift is mirrored in the large uncertainties in detection rate predictions (e.g., Sesana et al., 2011; Barausse et al., 2020). Nonetheless, LISA is expected to observe between a few and a hundred MBHB coalescences per year. The unique potential of this observatory is shown in **Figure 2**, where LISA signal-to-noise ratio (S/N) contours for equal-mass, nonspinning binaries are superimposed to the differential distribution of mergers occurring in 4 years (the nominal mission lifetime) in the chirp mass-redshift plane, as predicted by four selected MBH evolution models (Bonetti et al., 2019).

In the case of high-mass seeds from direct collapse shown in the bottom panels of the figure (see Woods et al., 2018, for a recent review), LISA can see essentially every single merger occurring within the observable Universe. If instead seeds are

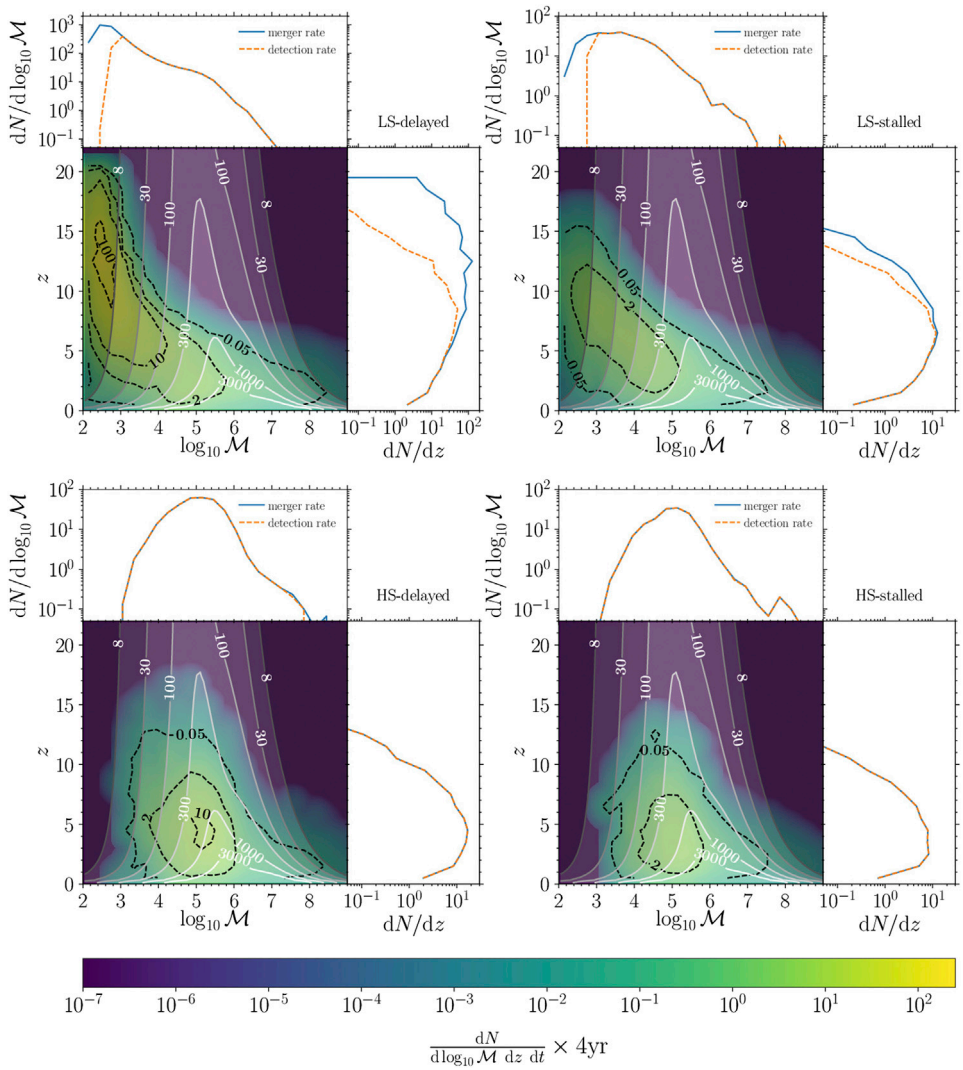

FIGURE 2 | LISA observational capabilities vs. predicted MBHB merger rates in the chirp mass-redshift plane. In each panel, gray shaded contours show the S/N of LISA observations for equal-mass, nonspinning binaries. The superimposed yellow-green color gradient with black dashed contours represents the differential number of mergers during the planned 4-year mission lifetime. From the upper-left panel, clockwise, we show four different astrophysical models: LS-delayed, LS-stalled, HS-stalled, and HS-delayed (Bonetti et al., 2019, for details). For each model, the upper and right-side panels show the merger rate (blue line) and detection rate (orange line) distributions marginalized over redshift and chirp mass, respectively (Bonetti et al., 2019).

produced as remnants of popIII stars (Madau and Rees, 2001), as in the top panels of the figure, LISA will miss the first round of mergers, but it will still probe the subsequent growth history of MBHs out to $z \approx 20$. In the latter case, an intriguing possibility is to complement LISA with ground-based 3G observations to fully reconstruct the cosmic history of those systems (see, e.g., Jani et al., 2019). In any case, LISA will provide a unique sample of up to several hundred MBHB coalescences: a potential revolution in physics and astronomy.

2.1 Extracting Information

MBHBs will generally enter the LISA band during their inspiral, completing thousands of cycles before merging within the detector's band. This will allow the accumulation of such high S/N that the main source of error in the parameter recovery, at least for the loudest sources, might come from inaccuracies in the available waveforms rather than from the intrinsic detector noise. In fact, currently available inspiral-merger-ringdown (IMR) waveforms (Bohé et al., 2017; Khan et al., 2018) are not even close to the needed level of accuracy. This is particularly critical for tests of GR with, e.g., ringdown spectroscopy (Berti et al., 2006; Gair et al., 2013), which relies on measuring tiny deviations from the higher multipoles of the ringdown radiation compared to GR expectations (Baibhav et al., 2018), especially to extract information from the higher multipoles of the radiation (Baibhav and Berti, 2019).

Nonetheless, waveforms employed so far include most of the relevant physics and can therefore provide a reliable estimate of

LISA's capabilities. As an example, Klein et al. (2016) carried out a comprehensive study based on spinning precessing post-Newtonian waveforms, corrected for the enhancement in S/N provided by adding merger and ringdown. They found that LISA can recover individual redshifted masses, i.e., $(1+z)M$, to better than 1% for loud sources at $z<5$. To get the intrinsic mass, however, one must know the redshift to the source, which is computed from the D_L measurement, by assuming a fiducial cosmology. At $z>1$, LISA will measure D_L to a few% accuracy, and weak lensing will affect the $D_L - z$ conversion adding another few% error (Shapiro et al., 2010). Considering both effects, LISA will provide an estimate of individual source frame masses within <10% relative accuracy for sources at $z<5$. Note that such precise measurements are today available only for MBHs in the local Universe, including SgrA* [Ghez et al. (2008), Gillessen et al. (2009), M87 Event Horizon Telescope Collaboration et al. (2019a), Event Horizon Telescope Collaboration et al. (2019b)], and few systems powering megamaser Miyoshi et al. (1995). The other relevant property of astrophysical MBHs is their spin magnitude and orientation, which are notoriously difficult to measure and are as of today estimated (with large uncertainties) only for ≈ 20 systems in the low-redshift Universe (see, e.g., Reynolds, 2014). Moving to the early epoch of structure formation, estimating parameters of systems at $z>10$ will be more challenging. In particular, the error on D_L tends to become much larger; nonetheless LISA can still place a 95% lower limit to the source redshift of $\approx 0.66z$ (Sesana, 2013).

2.2 MBH Cosmic History Reconstruction

Because of its excellent parameter estimation capabilities, LISA will deliver an unprecedented catalog of MBHB coalescences that will provide precious information about their formation and evolution along the cosmic history (Sesana et al., 2011). This is because the mass, redshift, and spin distribution of LISA events carry the imprint of the underlying physics driving their formation and evolution, including the origin, abundance, mass function, and redshift distribution of the first seeds; the detailed properties of the subsequent accretion processes driving their mass growth; the dynamical details of the pairing and hardening process of MBHBs forming in the aftermath of galaxy mergers, for example, the seeding mechanism as a direct impact on the number of observable sources. Astrophysical low (popIII) and high (direct collapse) mass seed scenarios have been extensively explored and result in very different number of mergers in the LISA band. Furthermore, the MBH seeding process can be connected to the production of primordial BHs in the early Universe (Khlopov, 2010; Clesse and García-Bellido, 2015), a scenario that can be tested by LISA as more quantitative predictions of merger rates become available. On the other hand, measured MBH spins are mainly determined by the geometry of the accretion flow, with prolonged accretion in a defined plane resulting in efficient MBH spin-ups (Thorne, 1974), in contrast to the spin-down caused by interaction with cold gas clouds incoming from random directions (King et al., 2005). Mergers also play a role in determining the magnitude and relative orientation of the MBH spins: in gas rich environment, interaction with a putative massive circumbinary disk (Perego et al., 2009) tends to align individual spins with the binary angular momentum, whereas spins of MBHBs merging in gas poor environment are expected to be randomly oriented (Bogdanović et al., 2007). Moreover, the redshift distribution of detected systems is strongly affected by the time required for the binary to complete its journey from kpc scales down to final coalescence, following the host galaxy merger (Bonetti et al., 2019; Barausse et al., 2020). One of the main challenges of future astrophysical modeling will be to make the best out of the LISA dataset to address the "inverse problem" of reconstructing the MBHB cosmic history from observations. In a proof-of-concept study, Sesana et al. (2011) showed that LISA can separate different seed models (popIII vs. direct collapse) and accretion geometries (coherent vs. chaotic), with only a handful of events.

2.3 EM Counterparts and Multimessenger Astronomy

Occurring at the very center of galaxy merger remnants, MBHBs form and evolve within a dense environment that might favor the presence of EM signals matching the inspiral and coalescence of the pair. As mentioned above, in gas rich environments, binaries are expected to be surrounded by a massive circumbinary disk. Gas can leak from the inner edge of the disc, feeding minidiscs around individual MBHs (Farris et al., 2014), resulting in a number of distinctive EM signals. For example, feeding of the minidiscs might be modulated over the period of the binary, eventually resulting in a periodicity of their emission (Tang et al., 2018); the cavity evacuated by the binary torques, removing a significant portion of the inner disc, will produce a distinctive shape of the UV continuum (Tanaka et al., 2012); streams can produce periodic nonthermal X-ray bursts upon impact onto the outer edge of the minidiscs (Roedig et al., 2014); finally, the inverse Compton upscatter of photons in the corona might produce distinctive double Kα lines (Sesana et al., 2012).The main challenge will be the detection and identification of all those putative features. Being an omnidirectional detector, LISA sky localization capabilities are mostly determined by the evolution of the antenna response function as it moves along its orbit around the Sun. For MBHBs this will allow localization of $z<2$ sources within $\Delta\Omega < 10\,(0.5)\,\mathrm{deg}^2$ weeks (hours) before coalescence (McWilliams et al., 2010; Mangiagli et al., 2020). This is a remarkable feat foe GW astronomy, allowing for searches with optical, radio, and X-ray wide-field instruments, such as LSST (LSST Science Collaboration et al., 2009), SKA, and Athena (McGee et al., 2020). After merger, the high S/N added at coalescence, LISA sky localization will improve to several arcminutes; deeper EM observations might then reveal a number of features related to the postmerger dynamics of the surrounding medium. These include the birth of a quasar as the gas in the circumbinary disc refills the cavity and is efficiently accreted (Milosavljević and Phinney, 2005), the launch of a relativistic jet (Palenzuela et al., 2010), or nonthermal emission from shocks prompted within the disk by the sudden change of the potential due to gravitational recoil (Rossi et al., 2010). Convincing identification of any such counterpart would be an

unprecedented milestone in accretion physics, opening up the study of interaction between gravity and matter in the time-dependent, strong field regime of a merging binary, as well as probing accretion onto MBHs of known masses and spins thus allowing, among other things, testing theoretical conjectures linking MBH spins to jet launching (Blandford and Znajek, 1977). Last but not least, joint EM and GW detections of MBHB will provide a unique class of standard sirens, extending up to $z > 5$ (Tamanini et al., 2016), thus probing the expansion history of the Universe in uncharted territory.

3 EXTREME MASS RATIO INSPIRALS

EMRIs are distinct from MBHBs both in their properties and their origin. As the name indicates, they are binaries involving objects of very different masses, generally a MBH interacting with a CO that can be a WD, NS, or stellar-mass BH. Consequently, their origin is not related to galaxy mergers or, more broadly, to the hierarchical structure formation paradigm but is rooted in the relativistic dynamics of dense nuclei. Sitting at galactic centers, in fact, MBHs are surrounded by a dense distribution of stars and COs. In such a dense environment, the central MBH can "capture" a stellar BH as a result of several dynamical processes, including different flavor of relaxation mechanisms deflecting BHs onto low angular momentum orbits or the tidal breakup of a compact binary close to the MBH. The captured BH will then inspiral onto the central MBH completing millions of orbits before eventually plunging into it (Amaro-Seoane, 2018). The detection of the resulting GW signal poses a major challenge for GW modelers, since it requires matching hundreds of thousands of cycles with accurate enough waveform templates (Barack and Cutler, 2004; Barack, 2009; Chua and Gair, 2015; Chua et al., 2017). But payouts are well worth the investment of theoretical and computational resources. Upon detection EMRIs will deliver unprecedented measurements of the system parameters, including the central MBH mass and spin to a precision of $< 10^{-4}$, a luminosity distance accuracy of a few percent, and sky localization within $\approx 1\mathrm{deg}^2$ (Barack and Cutler, 2004; Babak et al., 2017), making them formidable probes of MBH astrophysics, fundamental physics, and cosmology.

Capable of detecting EMRIs out to $z \approx 2$, LISA will detect from few to thousands of these systems per year (Babak et al., 2017). Very uncertain rates stem from poorly known underlying physics, meaning that EMRIs will provide a new wealth of information about the conditions of dense nuclei, in particular the mass function and occupation fractions of dormant MBHs in the mass range $10^5 M_\odot - 10^6 M_\odot$, difficult to probe by other means (Gair et al., 2010). Source abundance and individual EMRI parameters, such as eccentricity and orbital inclination, will help constrain their formation channel, shedding new light on extreme dynamics in dense nuclei (Amaro-Seoane, 2018). A fraction of EMRIs might also form and evolve within AGN discs (Levin, 2007). If this is the case, drag from the disc will leave distinctive signatures in the waveform, giving us access to the conditions of the plasma in the midplane of optically thick accretion discs, something that is beyond the reach of photon-based astronomy (Kocsis et al., 2011; Barausse et al., 2014). Exquisite parameter estimation accuracy makes EMRIs unique tools for probing space-time. For example, the central MBH quadrupole moment can be measured to a fractional precision of $< 10^{-4}$, allowing the detection of tiny deviation from Kerr geometry. Finally, although generally lacking EM counterparts, the excellent measurement of EMRIs distance and sky location will allow for effectively determining their redshift via statistical methods. Estimates suggest that H_0 could be measured to an accuracy of ≈1% with an ensemble of 20 EMRIs detected out to $z \approx 0.5$ (MacLeod and Hogan, 2008).

4 STELLAR-MASS BLACK HOLE BINARIES AND MULTIBAND DETECTIONS

Last but not least, LISA will observe stellar-mass BHBs still far from coalescence, before they enter the ground-based detector band. This was soon realized after the detection of GW150914, a system so massive and nearby that would have been observed by LISA with S/N ≈ 5 about five years before coalescence (Sesana, 2016). Subsequent studies have demonstrated that LISA can detect several tens of BHBs, up to hundreds of years before coalescence. A fraction of them will be caught in the last few years of inspiral and will cross all the way to the LIGO-Virgo band, paving the way to multiband GW astronomy (Kyutoku and Seto, 2016; Sesana, 2017; Gerosa et al., 2019). LISA will localize these multiband sources within $\approx 0.1\mathrm{deg}^2$, predicting their coalescence time with an error of <10s. We will therefore be in the unprecedented position of knowing exactly where and when a BHB is going to merge, a condition that will allow prepointing of EM facilities to search for possible counterparts coincident with the merger with a depth which is inconceivable with wide-field monitors (Sesana, 2016). Reconstructing the phase evolution of the system across 5 decades in frequency, and possibly fine-tuning the sensitivity of Earth-based detectors, will lead to improved tests of general relativity [Barausse et al. (2016), Carson and Yagi (2019), Berti et al. (2019), Chamberlain and Yunes (2017), Tso et al. (2018), Gnocchi et al. (2019)]. As an example, observations of the same source in the early and late inspiral will place unique constraints on additional emission multipoles (Barausse et al., 2016).

Even without multiband observations, detecting stellar-origin BHBs with LISA may have important astrophysical implications. Far from coalescence, LISA can measure the eccentricity (e) of these binaries as long as $e \gtrsim 10^{-3}$ at GW frequencies $f \sim 10^{-2}$ Hz (Nishizawa et al., 2016). Field binaries are expected to have small eccentricities at these frequencies (Kowalska et al., 2011); therefore these measurements can be used to discriminate between the dynamical and field formation channels (Breivik et al., 2016; Nishizawa et al., 2017; Samsing and D'Orazio, 2018). Combined with ground-based spin measurements, LISA eccentricity measurements can have an important role in our understanding of BHB formation. If the rate turns out to be large, specific stellar subpopulations could potentially be constrained (e.g., Gerosa et al., 2019). Cosmology will also benefit. Similar to EMRIs, the sky location and distance of at least a subset of these systems can be precise enough that we could use them as standard

candles, allowing for an independent statistical measurement of H_0 within a few percent accuracy (Kyutoku and Seto, 2017; Del Pozzo et al., 2018).

5 CONCLUSION

The future of GW astronomy is going to be loud. Building on the successes of LIGO and Virgo, the GW community is investing in a number of projects that will tremendously expand our knowledge of the dark side of the Universe. 3G ground-based detectors will observe hundreds of thousands CO mergers across the Universe and PTAs will unveil the most massive black hole binaries in the Universe. In this context, LISA will be one of our finest ears on the Universe. By surveying the milli-Hz frequency band, LISA will detect a variety of GW sources, across several decades in the mass scale, from the Solar neighborhood back to the formation of the first cosmic structure, promising an unprecedented revolution in our understanding of the Universe.

ACKNOWLEDGMENTS

The author is supported by the European Research Council (ERC) under the European Union's Horizon 2020 research and innovation program ERC-2018-COG under grant agreement No. 818691 (B Massive). The author is also indebted to Emanuele Berti for early contributions to this review.

AUTHOR CONTRIBUTIONS

The author confirms being the sole contributor of this work and has approved it for publication.

REFERENCES

Abbott, B. P., Abbott, R., Adhikari, R., Ajith, P., Allen, B., Allen, G., et al. (2009). LIGO: the laser interferometer gravitational-wave observatory. *Rept. Prog. Phys.* 72, 076901. doi:10.1088/0034-4885/72/7/076901

Abbott, B. P., Abbott, R., and Adhikari, R. e. a. (2019). GWTC-1: a gravitational-wave transient catalog of compact binary mergers observed by LIGO and Virgo during the first and second observing runs. *Phys. Rev. X* 9, 031040. doi:10.1103/PhysRevX.9.031040

LSST Science CollaborationAbell, P. A., Allison, J., Anderson, S. F., Andrew, J. R., Angel, J. R. P., et al. (2009). LSST science book.Version 2.0. e-prints: arXiv:0912.0201.

Acernese, F., Agathos, M., Agatsuma, K., Aisa, D., Allemandou, N., Allocca, A., et al. (2015). Advanced Virgo: a second-generation interferometric gravitational wave detector. *Class. Quantum Grav.* 32, 024001. doi:10.1088/0264-9381/32/2/024001

Event Horizon Telescope CollaborationAkiyama, K., Alberdi, A., Alef, W., Asada, K., Azulay, R., et al. (2019a). First M87 event Horizon telescope results. I. The shadow of the supermassive black hole. *Astrophys. J. Lett.* 875, L1. doi:10.3847/2041-8213/ab0ec7

Event Horizon Telescope CollaborationAkiyama, K., Alberdi, A., Alef, W., Asada, K., Azulay, R., et al. (2019b). First M87 event Horizon telescope results. VI. The shadow and mass of the central black hole. *Astrophys. J. Lett.* 875, L6. doi:10.3847/2041-8213/ab1141

Amaro-Seoane, P. (2018). Relativistic dynamics and extreme mass ratio inspirals. *Living Rev. Relat.* 21, 4. doi:10.1007/s41114-018-0013-8

Amaro-Seoane, P., Audley, H., Babak, S., Baker, J., Barausse, E., Bender, P., et al. (2017). Laser interferometer space antenna. e-prints: arXiv:1702.00786.

Amaro-Seoane, P. (2019). Extremely large mass-ratio inspirals. *Phys. Rev. D* 99, 123025. doi:10.1103/PhysRevD.99.123025

Arzoumanian, Z., Brazier, A., Burke-Spolaor, S., Chamberlin, S., Chatterjee, S., Christy, B., et al. (2018). The NANOGrav 11-year data set: high-precision timing of 45 millisecond pulsars. *ApJS* 235, 37. doi:10.3847/1538-4365/aab5b0

Babak, S., Gair, J., Sesana, A., Barausse, E., Sopuerta, C. F., Berry, C. P. L., et al. (2017). Science with the space-based interferometer LISA. V. Extreme mass-ratio inspirals. *Phys. Rev. D* 95, 103012. doi:10.1103/PhysRevD.95.103012

Baibhav, V., Berti, E., Cardoso, V., and Khanna, G. (2018). Black hole spectroscopy: systematic errors and ringdown energy estimates. *Phys. Rev. D* 97, 044048. doi:10.1103/PhysRevD.97.044048

Baibhav, V., and Berti, E. (2019). Multimode black hole spectroscopy. *Phys. Rev. D* 99, 024005. doi:10.1103/PhysRevD.99.024005

Barack, L., and Cutler, C. (2004). LISA capture sources: approximate waveforms, signal-to-noise ratios, and parameter estimation accuracy. *Phys. Rev. D* 69, 082005. doi:10.1103/PhysRevD.69.082005

Barack, L. (2009). Gravitational self-force in extreme mass-ratio inspirals. *Class. Quantum. Grav.* 26, 213001. doi:10.1088/0264-9381/26/21/213001

Barausse, E., Yunes, N., and Chamberlain, K. (2016). Theory-agnostic constraints on black-hole dipole radiation with multiband gravitational-wave astrophysics. *Phys. Rev. Lett.* 116, 241104. doi:10.1103/PhysRevLett.116.241104

Barausse, E., Cardoso, V., and Pani, P. (2014). Can environmental effects spoil precision gravitational-wave astrophysics? *Phys. Rev. D* 89, 104059. doi:10.1103/PhysRevD.89.104059

Barausse, E., Dvorkin, I., Tremmel, M., Volonteri, M., and Bonetti, M. (2020). Massive black hole merger rates: the effect of kpc separation wandering and supernova feedback. *Astrophys. J.* 904, 16. doi:10.3847/1538-4357/abba7f

Berti, E., Barausse, E., Cholis, I., Garcia-Bellido, J., Holley-Bockelmann, K., Hughes, S. A., et al. (2019). Tests of general relativity and fundamental physics with space-based gravitational wave detectors. *Bull. Am. Astron. Soc.* Vol. 51, 32.

Berti, E., Cardoso, V., and Will, C. M. (2006). Gravitational-wave spectroscopy of massive black holes with the space interferometer LISA. *Phys. Rev. D* 73, 064030. doi:10.1103/PhysRevD.73.064030

Blandford, R. D., and Znajek, R. L. (1977). Electromagnetic extraction of energy from Kerr black holes. *Mon. Notices Royal Astron. Soc.* 179, 433–456. doi:10.1093/mnras/179.3.433

Bogdanović, T., Reynolds, C. S., and Miller, M. C. (2007). Alignment of the spins of supermassive black holes prior to coalescence. *Astrophys. J. Lett.* 661, L147–L150. doi:10.1086/518769

Bohé, A., Shao, L., Taracchini, A., Buonanno, A., Babak, S., Harry, I. W., et al. (2017). Improved effective-one-body model of spinning, nonprecessing binary black holes for the era of gravitational-wave astrophysics with advanced detectors. *Phys. Rev. D* 95, 044028. doi:10.1103/PhysRevD.95.044028

Bonetti, M., Sesana, A., Haardt, F., Barausse, E., and Colpi, M. (2019). Post-Newtonian evolution of massive black hole triplets in galactic nuclei–IV. Implications for LISA. *Mon. Notices Royal Astron. Soc.* 486, 4044–4060. doi:10.1093/mnras/stz903

Breivik, K., Rodriguez, C. L., Larson, S. L., Kalogera, V., and Rasio, F. A. (2016). Distinguishing between formation channels for binary black holes with LISA. *Astrophys. J.* 830, L18. doi:10.3847/2041-8205/830/1/L18

Caprini, C., and Figueroa, D. G. (2018). Cosmological backgrounds of gravitational waves. *Class. Quantum Grav.* 35, 163001. doi:10.1088/1361-6382/aac608

Carson, Z., and Yagi, K. (2019). Multi-band gravitational wave tests of general relativity. *Class. Quantum Grav.* 37. doi:10.1088/1361-6382/ab5c9a

Chamberlain, K., and Yunes, N. (2017). Theoretical physics implications of gravitational wave observation with future detectors. *Phys. Rev. D* 96, 084039. doi:10.1103/PhysRevD.96.084039

Chua, A. J. K., and Gair, J. R. (2015). Improved analytic extreme-mass-ratio inspiral model for scoping out eLISA data analysis. *Class. Quantum Grav.* 32, 232002. doi:10.1088/0264-9381/32/23/232002

Chua, A. J. K., Moore, C. J., and Gair, J. R. (2017). Augmented kludge waveforms for detecting extreme-mass-ratio inspirals. *Phys. Rev. D* 96, 044005. doi:10.1103/PhysRevD.96.044005

Clesse, S., and García-Bellido, J. (2015). Massive primordial black holes from hybrid inflation as dark matter and the seeds of galaxies. *Phys. Rev. D* 92, 023524. doi:10.1103/PhysRevD.92.023524

Del Pozzo, W., Sesana, A., and Klein, A. (2018). Stellar binary black holes in the LISA band: a new class of standard sirens. *Mon. Notices Royal Astron. Soc.* 475, 3485–3492. doi:10.1093/mnras/sty057

Desvignes, G., Caballero, R. N., Lentati, L., Verbiest, J. P. W., Champion, D. J., Stappers, B. W., et al. (2016). High-precision timing of 42 millisecond pulsars with the European pulsar timing array. *Mon. Notices Royal Astron. Soc.* 458, 3341–3380. doi:10.1093/mnras/stw483

Dewdney, P. E., Hall, P. J., Schilizzi, R. T., and Lazio, T. J. L. W. (2009). The Square Kilometre array. *Proc. IEEE.* 97, 1482–1496. doi:10.1109/JPROC.2009.2021005

Farris, B. D., Duffell, P., MacFadyen, A. I., and Haiman, Z. (2014). Binary black hole accretion from a circumbinary disk: gas dynamics inside the central cavity. *Astrophys. J.* 783, 134. doi:10.1088/0004-637X/783/2/134

Foster, R. S., and Backer, D. C. (1990). Constructing a pulsar timing array. *Astrophys. J.* 361, 300. doi:10.1086/169195

Freitag, M. (2003). Gravitational waves from stars orbiting the Sagittarius A* black hole. *Astrphys. J. Lett.* 583, L21–L24. doi:10.1086/367813

Gair, J. R., Vallisneri, M., Larson, S. L., and Baker, J. G. (2013). Testing general relativity with low-frequency, space-based gravitational-wave detectors. *Living Rev. Relat.* 16, 7. doi:10.12942/lrr-2013-7

Gair, J. R., Tang, C., and Volonteri, M. (2010). LISA extreme-mass-ratio inspiral events as probes of the black hole mass function. *Phys. Rev. D* 81, 104014. doi:10.1103/PhysRevD.81.104014

Gerosa, D., Ma, S., Wong, K. W. K., Berti, E., O'Shaughnessy, R., Chen, Y., et al. (2019). Multiband gravitational-wave event rates and stellar physics. *Phys. Rev. D* 99, 103004. doi:10.1103/PhysRevD.99.103004

Ghez, A. M., Salim, S., Weinberg, N. N., Lu, J. R., Do, T., Dunn, J. K., et al. (2008). Measuring distance and properties of the Milky Way's central supermassive black hole with stellar orbits. *Astrophys. J.* 689, 1044–1062. doi:10.1086/592738

Gillessen, S., Eisenhauer, F., Trippe, S., Alexander, T., Genzel, R., Martins, F., et al. (2009). Monitoring stellar orbits around the massive black hole in the galactic center. *Astrophys. J.* 692, 1075–1109. doi:10.1088/0004-637X/692/2/1075

Gnocchi, G., Maselli, A., Abdelsalhin, T., Giacobbo, N., and Mapelli, M. (2019). Bounding alternative theories of gravity with multi-band GW observations. *Phys. Rev. D* 100, 064024. doi:10.1103/PhysRevD.100.064024

Jani, K., Shoemaker, D., and Cutler, C. (2019). Detectability of intermediate-mass black holes in multiband gravitational wave astronomy. *Nat. Astron.* 4, 260–265. doi:10.1038/s41550-019-0932-7

Kelley, L. Z., Blecha, L., Hernquist, L., Sesana, A., and Taylor, S. R. (2018). Single sources in the low-frequency gravitational wave sky: properties and time to detection by pulsar timing arrays. *Mon. Notices Royal Astron. Soc.* 477, 964–976. doi:10.1093/mnras/sty689

Kerr, M., Reardon, D. J., Hobbs, G., Shannon, R. M., Manchester, R. N., Dai, S., et al. (2020). The Parkes Pulsar Timing Array project: second data release. *Publ. Astron. Soc. Aust.* 37, e020. doi:10.1017/pasa.2020.11

Khan, S., Chatziioannou, K., Hannam, M., and Ohme, F. (2018). Phenomenological model for the gravitational-wave signal from precessing binary black holes with two-spin effects. e-prints: arXiv:1809.10113.

Khlopov, M. Y. (2010). Primordial black holes. *Res. Astron. Astrophys.* 10, 495–528. doi:10.1088/1674-4527/10/6/001

King, A. R., Lubow, S. H., Ogilvie, G. I., and Pringle, J. E. (2005). Aligning spinning black holes and accretion discs. *Mon. Notices Royal Astron. Soc.* 363, 49–56. doi:10.1111/j.1365-2966.2005.09378.x

Klein, A., Barausse, E., Sesana, A., Petiteau, A., Berti, E., Babak, S., et al. (2016). Science with the space-based interferometer eLISA: supermassive black hole binaries. *Phys. Rev. D* 93, 024003. doi:10.1103/PhysRevD.93.024003

Kocsis, B., Yunes, N., and Loeb, A. (2011). Observable signatures of extreme mass-ratio inspiral black hole binaries embedded in thin accretion disks. *Phys. Rev. D* 84, 024032. doi:10.1103/PhysRevD.84.024032

Kowalska, I., Bulik, T., Belczynski, K., Dominik, M., and Gondek-Rosinska, D. (2011). The eccentricity distribution of compact binaries. *A&A* 527, A70. doi:10.1051/0004-6361/201015777

Kyutoku, K., and Seto, N. (2016). Concise estimate of the expected number of detections for stellar-mass binary black holes by eLISA. *Mon. Notices Royal Astron. Soc.* 462, 2177–2183. doi:10.1093/mnras/stw1767

Kyutoku, K., and Seto, N. (2017). Gravitational-wave cosmography with LISA and the Hubble tension. *Phys. Rev. D* 95, 083525. doi:10.1103/PhysRevD.95.083525

Lau, M. Y. M., Mandel, I., Vigna-Gómez, A., Neijssel, C. J., Stevenson, S., and Sesana, A. (2020). Detecting double neutron stars with LISA. *Mon. Notices Royal Astron. Soc.* 492, 3061–3072. doi:10.1093/mnras/staa002

Levin, Y. (2007). Starbursts near supermassive black holes: young stars in the Galactic Centre, and gravitational waves in LISA band. *Mon. Notices Royal Astron. Soc.* 374, 515–524. doi:10.1111/j.1365-2966.2006.11155.x

MacLeod, C. L., and Hogan, C. J. (2008). Precision of Hubble constant derived using black hole binary absolute distances and statistical redshift information. *Phys. Rev. D* 77, 043512. doi:10.1103/PhysRevD.77.043512

Madau, P., and Rees, M. J. (2001). Massive black holes as population III remnants. *Astrophys. J. Lett.* 551, L27–L30. doi:10.1086/319848

Mangiagli, A., Klein, A., Bonetti, M., Katz, M. L., Sesana, A., Volonteri, M., et al. (2020). On the inspiral of coalescing massive black hole binaries with LISA in the era of Multi-Messenger Astrophysics. e-prints: arXiv:2006.12513.

McGee, S., Sesana, A., and Vecchio, A. (2020). Linking gravitational waves and X-ray phenomena with joint LISA and Athena observations. *Nat. Astron.* 4, 26–31. doi:10.1038/s41550-019-0969-7

McWilliams, S. T., Thorpe, J. I., Baker, J. G., and Kelly, B. J. (2010). Impact of mergers on LISA parameter estimation for nonspinning black hole binaries. *Phys. Rev. D* 81, 064014. doi:10.1103/PhysRevD.81.064014

Milosavljević, M., and Phinney, E. S. (2005). The afterglow of massive black hole coalescence. *Astrophys. J. Lett.* 622, L93–L96. doi:10.1086/429618

Miyoshi, M., Moran, J., Herrnstein, J., Greenhill, L., Nakai, N., Diamond, P., et al. (1995). Evidence for a black hole from high rotation velocities in a sub-parsec region of NGC4258. *Nature* 373, 127–129. doi:10.1038/373127a0

Nelemans, G., Yungelson, L. R., and Portegies Zwart, S. F. (2001). The gravitational wave signal from the Galactic disk population of binaries containing two compact objects. *A&A* 375, 890–898. doi:10.1051/0004-6361:20010683

Nishizawa, A., Berti, E., Klein, A., and Sesana, A. (2016). eLISA eccentricity measurements as tracers of binary black hole formation. *Phys. Rev. D* 94, 064020. doi:10.1103/PhysRevD.94.064020

Nishizawa, A., Sesana, A., Berti, E., and Klein, A. (2017). Constraining stellar binary black hole formation scenarios witheLISAeccentricity measurements. *Mon. Notices Royal Astron. Soc.* 465, 4375–4380. doi:10.1093/mnras/stw2993

Nissanke, S., Vallisneri, M., Nelemans, G., and Prince, T. A. (2012). Gravitational-wave emission from compact galactic binaries. *Astrophys. J.* 758, 131. doi:10.1088/0004-637X/758/2/131

Palenzuela, C., Lehner, L., and Liebling, S. L. (2010). Dual jets from binary black holes. *Science* 329, 927–930. doi:10.1126/science.1191766

Perego, A., Dotti, M., Colpi, M., and Volonteri, M. (2009). Mass and spin co-evolution during the alignment of a black hole in a warped accretion disc. *Mon. Notices Royal Astron Soc.* 399, 2249–2263. doi:10.1111/j.1365-2966.2009.15427.x

Punturo, M., Abernathy, M., Acernese, F., Allen, B., Andersson, N., Arun, K., et al. (2010). The Einstein Telescope: a third-generation gravitational wave observatory. *Class. Quantum Grav.* 27, 194002. doi:10.1088/0264-9381/27/19/194002

Ravi, V., Wyithe, J. S. B., Hobbs, G., Shannon, R. M., Manchester, R. N., Yardley, D. R. B., et al. (2012). Does a "stochastic" background of gravitational waves exist in the pulsar timing band? *Astrophys. J.* 761, 84. doi:10.1088/0004-637X/761/2/84

Reitze, D., Adhikari, R. X., Ballmer, S., Barish, B., Barsotti, L., Billingsley, G., et al. (2019). Cosmic explorer: the U.S. Contribution to gravitational-wave astronomy beyond LIGO. *Bull. Am. Astron. Soc.* 51, 35.

Reynolds, C. S. (2014). Measuring black hole spin using X-ray reflection spectroscopy. *Space Sci. Rev.* 183, 277–294. doi:10.1007/s11214-013-0006-6

Roedig, C., Krolik, J. H., and Miller, M. C. (2014). Observational signatures of binary supermassive black holes. *Astrophys. J.* 785, 115. doi:10.1088/0004-637X/785/2/115

Rossi, E. M., Lodato, G., Armitage, P. J., Pringle, J. E., and King, A. R. (2010). Black hole mergers: the first light. *Mon. Notices Royal Astron Soc.* 401, 2021–2035. doi:10.1111/j.1365-2966.2009.15802.x

Samsing, J., and D'Orazio, D. J. (2018). Black hole mergers from globular clusters observable by LISA I: eccentric sources originating from relativistic N-body dynamics. *Mon. Notices Royal Astron Soc.* 481, 5445–5450. doi:10.1093/mnras/sty2334

Sesana, A. (2013). "Detecting massive black hole binaries and unveiling their cosmic history with gravitational wave observations," in 9th LISA Symposium, Paris, May 21–25, 2012 Editors G. Auger, P. Binétruy, and E. Plagnol, Vol. 467. 103. *Astron. Soc. Pac. Conf. Ser.*

Sesana, A., Gair, J., Berti, E., and Volonteri, M. (2011). Reconstructing the massive black hole cosmic history through gravitational waves. *Phys. Rev. D* 83, 044036. doi:10.1103/PhysRevD.83.044036

Sesana, A., Lamberts, A., and Petiteau, A. (2020). Finding binary black holes in the Milky Way with LISA. *Mon. Notices Royal Astron Soc.* 494, L75–L80. doi:10.1093/mnrasl/slaa039

Sesana, A. (2017). Multi-band gravitational wave astronomy: science with joint space- and ground-based observations of black hole binaries. *J. Phys. Conf. Ser.* 840, 012018. doi:10.1088/1742-6596/840/1/012018

Sesana, A. (2016). Prospects for multiband gravitational-wave astronomy after GW150914. *Phys. Rev. Lett.* 116, 231102. doi:10.1103/PhysRevLett.116.231102

Sesana, A., Roedig, C., Reynolds, M. T., and Dotti, M. (2012). Multimessenger astronomy with pulsar timing and X-ray observations of massive black hole binaries. *Mon. Notices Royal Astron Soc.* 420, 860–877. doi:10.1111/j.1365-2966.2011.20097.x

Sesana, A., Vecchio, A., and Colacino, C. N. (2008). The stochastic gravitational-wave background from massive black hole binary systems: implications for observations with Pulsar Timing Arrays. *Mon. Notices Royal Astron Soc.* 390, 192–209. doi:10.1111/j.1365-2966.2008.13682.x

Sesana, A., Vecchio, A., and Volonteri, M. (2009). Gravitational waves from resolvable massive black hole binary systems and observations with Pulsar Timing Arrays. *Mon. Notices Royal Astron Soc.* 394, 2255–2265. doi:10.1111/j.1365-2966.2009.14499.x

Seto, N. (2016). Prospects of eLISA for detecting Galactic binary black holes similar to GW150914. *Mon. Notices Royal Astron. Soc. Lett.* 460, slw060. doi:10.1093/mnrasl/slw060

Shapiro, C., Bacon, D. J., Hendry, M., and Hoyle, B. (2010). Delensing gravitational wave standard sirens with shear and flexion maps. *Mon. Notices Royal Astron Soc.* 404, 858–866. doi:10.1111/j.1365-2966.2010.16317.x

Tamanini, N., Caprini, C., Barausse, E., Sesana, A., Klein, A., and Petiteau, A. (2016). Science with the space-based interferometer eLISA. III: probing the expansion of the universe using gravitational wave standard sirens. *J. Cosmol. Astropart. Phys.* 2016, 002. doi:10.1088/1475-7516/2016/04/002

Tamanini, N., and Danielski, C. (2019). The gravitational-wave detection of exoplanets orbiting white dwarf binaries using LISA. *Nat. Astron.* 3, 858–866. doi:10.1038/s41550-019-0807-y

Tanaka, T., Menou, K., and Haiman, Z. (2012). Electromagnetic counterparts of supermassive black hole binaries resolved by pulsar timing arrays. *Mon. Notices Royal Astron Soc.* 420, 705–719. doi:10.1111/j.1365-2966.2011.20083.x

Tang, Y., Haiman, Z., and MacFadyen, A. (2018). The late inspiral of supermassive black hole binaries with circumbinary gas discs in the LISA band. *Mon. Notices Royal Astron. Soc.* 476, 2249–2257. doi:10.1093/mnras/sty423

Thorne, K. S. (1974). Disk-accretion onto a black hole. II. Evolution of the hole. *Astrophys. J.* 191, 507–520. doi:10.1086/152991

Tso, R., Gerosa, D., and Chen, Y. (2018). Optimizing LIGO with LISA forewarnings to improve black-hole spectroscopy. arXiv e-prints.

Van Den Broeck, C. (2014). Astrophysics, cosmology, and fundamental physics with compact binary coalescence and the Einstein Telescope. *J. Phys. Conf. Ser.* 484, 012008. doi:10.1088/1742-6596/484/1/012008

Verbiest, J. P. W., Lentati, L., Hobbs, G., van Haasteren, R., Demorest, P. B., Janssen, G. H., et al. (2016). The international pulsar timing array: first data release. *Mon. Notices Royal Astron. Soc.* 458, 1267–1288. doi:10.1093/mnras/stw347

Volonteri, M., Haardt, F., and Madau, P. (2003). The assembly and merging history of supermassive black holes in hierarchical models of galaxy formation. *Astrophys. J.* 582, 559–573. doi:10.1086/344675

Woods, T. E., Agarwal, B., Bromm, V., Bunker, A., Chen, K.-J., Chon, S., et al. (2018). Titans of the early universe: the prato statement on the origin of the first supermassive black holes. arXiv e-prints: arXiv:1810.12310.

Conflict of Interest: The author declares that the research was conducted in the absence of any commercial or financial relationships that could be construed as a potential conflict of interest.

Advantages of publishing in Frontiers

OPEN ACCESS
Articles are free to read for greatest visibility and readership

FAST PUBLICATION
Around 90 days from submission to decision

HIGH QUALITY PEER-REVIEW
Rigorous, collaborative, and constructive peer-review

TRANSPARENT PEER-REVIEW
Editors and reviewers acknowledged by name on published articles

Frontiers
Avenue du Tribunal-Fédéral 34
1005 Lausanne | Switzerland

Visit us: www.frontiersin.org
Contact us: frontiersin.org/about/contact

REPRODUCIBILITY OF RESEARCH
Support open data and methods to enhance research reproducibility

DIGITAL PUBLISHING
Articles designed for optimal readership across devices

FOLLOW US
@frontiersin

IMPACT METRICS
Advanced article metrics track visibility across digital media

EXTENSIVE PROMOTION
Marketing and promotion of impactful research

LOOP RESEARCH NETWORK
Our network increases your article's readership